PERTURBATION METHODS IN FLUID MECHANICS

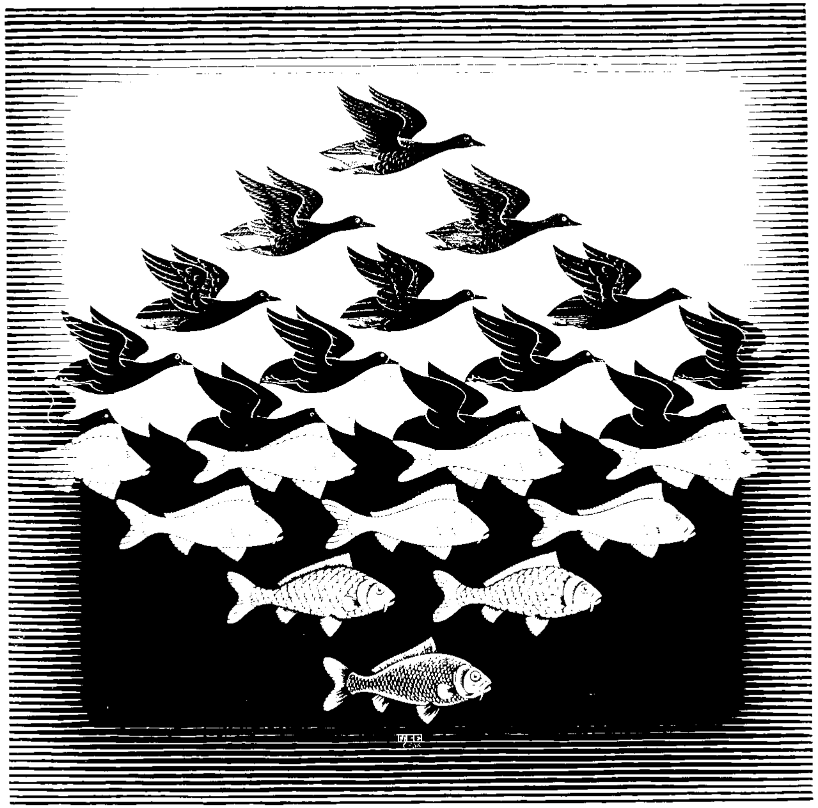

SKY AND WATER I, 1938
by M. C. Escher

Courtesy of Vorpal Galleries, San Francisco, Laguna Beach, New York, and Chicago, and the Escher Foundation, Haags Gemeentemuseum, The Hague

This woodcut by the Dutch artist gives a graphic impression of the "imperceptibly smooth blending" of one flow into another (p. 89) that is the heart of the method of matched asymptotic expansions discussed in Chapter 5.

PERTURBATION METHODS IN FLUID MECHANICS

By Milton Van Dyke

DEPARTMENT OF AERONAUTICS AND ASTRONAUTICS
STANFORD UNIVERSITY
STANFORD, CALIFORNIA

Annotated Edition

1975
THE PARABOLIC PRESS
Stanford, California

THE PARABOLIC PRESS
Post Office Box 3032
Stanford, California 94305

International Standard Book Number: ISBN 0-915760-01-0
Library of Congress Catalog Card Number: 75-15072

Originally published 1964 by Academic Press
Annotated Edition 1975

Printed in the United States of America

CONTENTS

IV. SOME SINGULAR PERTURBATION PROBLEMS IN AIRFOIL THEORY

V. THE METHOD OF MATCHED ASYMPTOTIC EXPANSIONS

VI. THE METHOD OF STRAINED COORDINATES

VII. VISCOUS FLOW AT HIGH REYNOLDS NUMBER

VIII. VISCOUS FLOW AT LOW REYNOLDS NUMBER

IX. SOME INVISCID SINGULAR PERTURBATION PROBLEMS

X. OTHER ASPECTS OF PERTURBATION THEORY

NOTES

PREFACE TO THE ANNOTATED EDITION

The technical literature devoted to perturbation methods in mechanics has burgeoned since this book appeared in 1964. Techniques for treating singular perturbation problems, then unfamiliar and esoteric, are now part of the analytical apparatus of anyone interested in research. Applications in continuum mechanics, first limited mainly to classical fluid dynamics and linear elasticity, have spread over a wide range of fields, and new techniques are being developed while older ones are refined. The resulting research papers, even if restricted to fluid mechanics, number in the thousands.

Other books have meanwhile appeared to codify and guide this body of work. Those of an applied character similar to this one are the books of Bellman (1964), Cole (1968), and Nayfeh (1973). More mathematically oriented treatments include O'Malley (1968, 1974) and Eckhaus (1973).

Despite that competition, and a limited scope, the present book has apparently remained useful. Its modest sales continued until its even more modest price made it unprofitable for the original publisher to keep it in print. Rather than let the price increase, I have elected to republish it myself.

In so doing, I have taken the opportunity to correct a number of error in the text, and to bring it more up to date by adding a section of Notes at the end. These are keyed to the main text, where an indicator in the margin of the page, of the form shown here, directs the reader to a discussion of subsequent developments and further references. Of course only a small fraction of the papers published in the past decade have been mentioned, even though the list of References at the end has been doubled. However, an attempt has been made to include any reference that provides a significant new idea or result, as well as any of close relevance to the original text.

See Note 1

The most common criticism from reviewers and readers (aside from the restriction to fluid mechanics) is that this book is somewhat too concise for self study or use as a text. It has, nevertheless, been used as the textbook for more college courses than I could have anticipated. For that purpose, the Exercises posed at the end of each chapter are in some cases rather too demanding (and in a few cases practically insoluble). I have tried to improve this situation in Note 3. On request, I should be glad to provide colleagues with my versions of the solutions, together with additional exercises I have used in recent years.

This Annotated Edition, like the original, derives from a one-quarter graduate course that I have continued to teach in the Department of Aeronautics and Astronautics at Stanford University since 1959. Like the original, it draws on my research and that of my students, which has been supported for many years by the Air Force Office of Scientific Research.

I am indebted to a number of colleagues who answered my plea for help with the Notes, or otherwise contributed corrections, suggestions, and references. Of course I could not do justice to all their suggestions, but for valuable assistance I thank A. Acrivos, S. A. Berger, P. A. Bois, S. N. Brown, S. Corrsin, R. T. Davis, C. Domb, J. Ellinwood, L. E. Fraenkel, C. François, P. Germain, C. R. Illingworth, K. P. Kerney, P. A. Lagerstrom, R. E. Melnik, A. Messiter, R. Medan, J. W. Miles, N. Riley, O. S. Ryzhov, V. V. Sychev, and H. Viviand.

The fraternity of typographers, printers, publishers, and booksellers is a friendly one, and I have found them all remarkably generous in helping a neophyte. I could not have undertaken to republish this book myself without the advice of Sharon Hawkes, Jack McLean, Eva Nyquist, Dorothy Riedel, and especially my friends John McNeil and William Kauffman at Annual Reviews Inc. Like the original, this revision could not have been written without the help and encouragement of my wife Sylvia, and I rededicate it to her as a gift of love.

MILTON VAN DYKE

Stanford, California
June, 1975

PREFACE TO THE ORIGINAL EDITION

This book is devoted primarily to the treatment of singular perturbation problems as they arise in fluid mechanics. In particular, it gives a unified exposition of two rather general techniques that have been developed during the last fifteen years, and which are associated with the names of Lagerstrom, Kaplun, and Cole, and of Lighthill and Whitham. This emphasis on what might to the uninitiated appear to be the pathological aspects of perturbation theory is justified not so much by the novelty of these techniques as by the fact that singular perturbations seem to be the rule rather than the exception in fluid mechanics, and are being increasingly encountered in current research. However, the book begins with general methods applicable to regular as well as singular perturbations, because no connected account of them is available.

The exposition is largely by means of examples, and these are—except for a few mathematical models—drawn solely from fluid mechanics. It is true that the techniques discussed are rapidly finding application in other branches of applied mechanics, and I hope the book will prove useful to workers in those fields. However, both of the general techniques mentioned above were invented to handle problems in fluid flow, and have been largely developed and applied within that field. In fact, the examples are largely confined to what might at mid-century be characterized as classical aerodynamics. It is evident, however, that singular perturbation problems abound in such new subjects as non-equilibrium and radiating flows, magnetohydrodynamics, plasma dynamics, and rarefied-gas dynamics. The techniques discussed will certainly find fruitful application there, as well as in oceanography, meteorology, and other domains of the great world of fluid motion.

This book is the outgrowth of a succession of notes prepared for a graduate course that I have taught since 1959 in the Department of Aeronautics and Astronautics at Stanford University. It naturally draws heavily on my own research and that of my students, much of which has been supported by the Air Force Office of Scientific Research.

The heart of the book is the study, in Chapter IV, of incompressible potential flow past a symmetrical thin airfoil. This problem, though conceptually simple and involving only the two-dimensional Laplace equation, embodies most of the features of both regular and singular perturbations. In particular, it serves to introduce the two standard methods of treating singular perturbation problems. References to this basic problem therefore recur throughout the subsequent chapters.

I would urge the reader not to ignore the exercises. They provide in concise form many additional details, further references, and generalizations and extensions of the material in the text.

My first debt is to P. A. Lagerstrom, who has been my teacher, colleague, and friend as well as the co-developer of one of the two main techniques described here for handling singular perturbation problems. Many of the ideas presented also bear the imprint of my years of collaboration with R. T. Jones, M. A. Heaslet, and their colleagues at Ames Laboratory. I am indebted to a number of other colleagues for helpful comments and criticism, including in particular O. Burggraf, I-Dee Chang, G. Emanuel, S. Kaplun, S. Nadir, B. Perry, and A. F. Pillow. This book would not have been written without the help and encouragement of my wife Sylvia, and I dedicate it to her as a gift of love.

MILTON VAN DYKE

Stanford, California
May, 1964

Chapter I

THE NATURE OF PERTURBATION THEORY

1.1. Approximations in Fluid Mechanics

Fluid mechanics has pioneered in the solution of nonlinear partial differential equations. In contrast with the basic equations in many other branches of mathematical physics, those governing fluid motion are essentially nonlinear (more precisely, quasi-linear); and this is true whether or not viscosity and compressibility are included. The only important exception is the well explored case of irrotational motion of an incompressible inviscid fluid, which leads to Laplace's equation, the nonlinearity then appearing only algebraically in the Bernoulli equation, provided there are no free boundaries.

Because of this basic nonlinearity, exact solutions are rare in any branch of fluid mechanics. They are usually *self-similar* solutions, for which the partial differential equations reduce, by virtue of a high degree of symmetry, to ordinary differential equations. So great is the need that a solution is loosely termed "exact" even when an ordinary differential equation must be integrated numerically. Lighthill (1948) has given a more or less exhaustive list of such solutions for inviscid compressible flow:

(a) steady supersonic flow past a concave corner,
(b) steady supersonic flow past a convex corner,
(c) steady supersonic flow past an unyawed circular cone,
(d) infinite plane wall moved impulsively into still air,
(e) infinite plane wall moved impulsively away from still air,
(f) circular cylinder expanding uniformly into still air,
(g) sphere expanding uniformly into still air.

Again, from Schlichting (1960) one can construct a partial list for incompressible viscous flow:

(a) steady flow between infinite parallel plates, through a circular pipe, or between concentric circular pipes,

(b) steady flow between a fixed and a sliding parallel plate or concentric circular pipe,
(c) steady flow between concentric rotating cylinders,
(d) plane or axisymmetric flow against an infinite plate,
(e) steady rotation of an infinite flat disk,
(f) steady plane flow between divergent plates,
(g) impulsive or sinusoidal motion of an infinite flat plate in its own plane.

It is typical of these self-similar flows that they involve idealized geometries far from most shapes of practical interest.

To proceed further, one must usually approximate. (A recent alternative is to launch an electronic computing program!) Approximation is an art, and famous names are usually associated with successful approximations:

Prandtl wing theory,
Kármán-Tsien method for airfoils in subsonic flow,
Prandtl-Glauert approximation for subsonic flow,
Janzen-Rayleigh expansion for subsonic flow,
Stokes and Oseen approximations for viscous flow,
Prandtl boundary-layer theory,
Kármán-Pohlhausen boundary-layer approximation,
Newton-Busemann theory of hypersonic flow.

In some important fields an altogether successful approximation is yet to be found. Examples are separated viscous flow, and hypersonic flow past a blunt body.

1.2. Rational and Irrational Approximations

Most useful approximations are valid when one or more of the parameters or variables in the problem is small (or large). This *perturbation quantity* is often one of the dimensionless parameters:

Janzen-Rayleigh expansion:	Mach number	$\ll 1$
Thin-airfoil theory:	Thickness ratio	$\ll 1$
Lifting-line theory:	Aspect ratio	$\gg 1$
Stokes, Oseen flow:	Reynolds number	$\ll 1$
Boundary-layer theory:	Reynolds number	$\gg 1$
Newton-Busemann theory:	Mach number $\gg 1$, $(\gamma - 1)$	$\ll 1$
Quasi-steady theory:	Reduced frequency	$\ll 1$
Free-molecule theory:	Knudsen number	$\gg 1$

An unusual example is Garabedian's (1956) analysis of axisymmetric free-streamline flow, which is based upon the approximation that the number of space dimensions differs only slightly from two. In all these cases one speaks of a *parameter perturbation.* The perturbation quantity may also be one of the independent variables (in dimensionless form):

Blasius series for boundary layer:	Distance	$\ll 1$
Impulsive motion in viscous or compressible fluid:	Time	$\ll 1$

In such cases one speaks of a *coordinate perturbation.*

An approximation of this sort becomes increasingly accurate as the perturbation quantity tends to zero (or infinity). It is therefore an *asymptotic solution.* In principle, one can improve the result by embedding it as the first step in a systematic scheme of successive approximations. The resulting series, though not necessarily convergent, is by construction an *asymptotic expansion.* In practice, one usually calculates only the first approximation, sometimes the second. The chief virtue of a second approximation is often that it helps to understand the first. Only rarely does one proceed as far as the fifth or sixth approximation; but the possibility of continuing indefinitely is of fundamental significance. We shall call an approximation of this sort a *rational approximation.*

On the other hand, some very useful approximations do not become exact in any known limit. Examples are:

Kármán-Tsien method for airfoils in subsonic flow (Liepmann and Puckett, 1947, p. 176),
Shock-expansion theory, and its extension to axisymmetric and three-dimensional flows (Hayes and Probstein, 1959, p. 265),
Spreiter's local linearization in transonic flow (Spreiter, 1959),
Chester-Chisnell theory of shock dynamics (Chester, 1960),
Mott-Smith theory of shock structure (Mott-Smith, 1951).

We shall call such a method an *irrational approximation.* Unless further study should reveal its asymptotic nature, an irrational approximation represents a dead end. One must accept whatever error it involves, with no possibility of improving the accuracy by successive approximations.

Only rational approximations are considered in this book. Thus we are concerned with asymptotic expansions, for small or large values of some parameter or independent variable, of the solutions of the equations of fluid motion.

We will often find it convenient to denote the perturbation quantity by ε, and to define it so that it is small. For example, in boundary-layer theory ε can be taken as the reciprocal of the Reynolds number, or of its square root.

As ε tends to zero, the flow must be assumed to approach a limit, which may be termed the *basic solution*. For example, at high Reynolds numbers the viscous flow past most semi-infinite bodies approaches the corresponding inviscid motion. That this approach is not uniform is clear from the ideas of boundary-layer theory. However, for bodies on which the boundary layer separates, we do not yet know the appropriate limit—or, indeed, whether a limit exists (cf. Section 7.1).

In parameter perturbations the basic solution is often a uniform parallel stream or other trivial flow. Then one usually regards it as the "zeroth approximation," and calls the leading perturbation therefrom the *first approximation* or *first-order solution*. In most coordinate perturbations, on the other hand, the basic solution is a nontrivial solution of the full equations—for example, one of the self-similar flows discussed previously—and is itself usually regarded as the first approximation.

1.3. Examples of Perturbation Expansions

These general remarks may be illustrated by exhibiting some typical perturbation expansions for which a number of terms have been calculated by assiduous researchers. In the Janzen-Rayleigh or M^2-expansion method, the effects of compressibility at subsonic speeds are studied by perturbing the basic solution for incompressible flow. The first-order correction is proportional to the square of the free-stream Mach number M, and higher approximations proceed by successive powers of M^2. Simasaki (1956) has calculated six terms of the series for subsonic flow past a circular cylinder without circulation. For the maximum speed q_{max}—which occurs on the surface at the ends of the cross-stream diameter—referred to the free-stream speed U, he finds, with the adiabatic index γ equal to 1.405:

See Note 2

$$\frac{q_{max}}{U} = 2.00000 + 1.16667M^2 + 2.58129M^4 + 7.53386M^6 + 25.69342M^8 + 96.79287M^{10} + \cdots \qquad (1.1)$$

This method is believed to yield a series that converges if the flow is purely subsonic. (A proof of convergence for sufficiently small M^2 was reported by Wendt (1948), but never published.) Indeed, it appears from the behavior of the above coefficients that the convergence becomes suspect when M approaches its critical value of about 0.40, at which q_{max} becomes sonic (cf. Exercise 10.6).

In thin-airfoil or slender-body theory, the solution for an elongated object is found as the perturbation of a uniform stream. Hantzsche (1943) has calculated the thin-airfoil expansion for an elliptic airfoil of thickness ratio ε at zero incidence in a subsonic compressible stream. For the maximum speed he finds

$$\frac{q_{max}}{U} = 1 + \frac{1}{\beta}\varepsilon + \frac{M^2}{2\beta^2}(1 + \Gamma)\varepsilon^2 + \frac{M^2}{\beta^3}\left\{\frac{\pi}{4}[1 + \tfrac{1}{2}\Gamma(1 + \Gamma)(8 - M^2)] - \tfrac{1}{2} - \tfrac{3}{2}\Gamma - \tfrac{4}{3}\Gamma^2\right\}\varepsilon^3 + \frac{M^2}{2\beta^2}[1 + \tfrac{1}{2}\Gamma(1 + \Gamma)(8 - M^2)]\varepsilon^4 \log\varepsilon + O(\varepsilon^4) \qquad (1.2a)$$

where

$$\beta = \sqrt{1 - M^2}, \qquad \Gamma = \frac{\gamma + 1}{4}\frac{M^2}{\beta^2} \qquad (1.2b)$$

Here, and throughout this book, *log* denotes the natural logarithm. In (1.2 a) as in many perturbation problems, logarithms of the perturbation quantity appear unexpectedly. For reasons discussed in Section 10.5, the unknown next term, which is indicated to be of order ε^4, ought to be included with the term in $\varepsilon^4 \log \varepsilon$ as the fourth approximation.

At low Reynolds numbers the viscous flow past a three-dimensional body is described by the Stokes approximation. For bodies with fore-and-aft symmetry a better estimate of the drag is given by the Oseen approximation. Goldstein (1929) has calculated six terms of a series for the Oseen drag of a sphere. In terms of the Reynolds number $R = Ua/\nu$ based upon the radius a, his result for the drag coefficient is

See Note 2

$$C_D = \frac{D}{\rho U^2 a^2} = \frac{6\pi}{R}\left(1 + \frac{3}{8}R - \frac{19}{320}R^2 + \frac{71}{2560}R^3 - \frac{30{,}179}{2{,}150{,}400}R^4 + \frac{122{,}519}{17{,}203{,}200}R^5 + \cdots\right) \qquad (1.3)$$

Here the last coefficient has been corrected by Shanks (1955). The solution of the full Navier-Stokes equations departs from the Oseen approximation after the second term. According to the work of Proudman and Pearson (1957) it gives instead

See Note 10

$$C_D = \frac{6\pi}{R}\left[1 + \frac{3}{8}R + \frac{9}{40}R^2 \log R + O(R^2)\right] \qquad (1.4)$$

At high Reynolds numbers the viscous flow very close to a body is described by Prandtl's boundary-layer equations. Because they are nonlinear, additional approximations are usually required. A coordinate perturbation for small distances from the stagnation point of any smooth symmetrical plane shape, initiated by Blasius, has been carried to six terms by Tifford (1954). For the coefficient of local skin friction on a parabola this gives (Van Dyke, 1964a) See Note 12

$$c_f = \frac{\tau}{\frac{1}{2}\rho U^2} = \frac{2}{\sqrt{R}}\Big[1.23259\frac{x}{a} - 1.93186\left(\frac{x}{a}\right)^3 + 3.11051\left(\frac{x}{a}\right)^5 - 5.02892\left(\frac{x}{a}\right)^7 + 8.14109\left(\frac{x}{a}\right)^9 - 13.18662\left(\frac{x}{a}\right)^{11} + \cdots\Big] \quad (1.5)$$

Here x is the distance along the surface, and R again the Reynolds number based upon the nose radius a.

Incompressible flow past a thin wing of high aspect ratio A is described approximately by Prandtl's lifting-line theory. The calculation of higher approximations is discussed in Chapter 9. For an elliptical wing the lift-curve slope is found to be (Van Dyke, 1964b) See Note 13

$$\frac{dC_L}{d\alpha} = 2\pi\Big[1 - \frac{2}{A} - \frac{16}{\pi^2}\frac{\log A}{A^2} - \frac{4}{\pi^2}\left(\frac{7}{2} + \pi^2 - 4\log\pi\right)\frac{1}{A^2} + \cdots\Big] \quad (1.6)$$

The notoriously difficult problem of hypersonic flow past a blunt body has been attacked, in the Newton-Busemann approximation, by expanding in powers of $1/M^2$ and $(\gamma-1)/(\gamma+1)$. Chester (1956b) has carried the series farthest for the body of revolution that produces a paraboloidal shock wave. At $M = \infty$ he finds the ratio of the stand-off distance Δ of the shock wave to its nose radius b to be

$$\frac{\Delta}{b} = \frac{\gamma-1}{\gamma+1} - \sqrt{\frac{8}{3}}\left(\frac{\gamma-1}{\gamma+1}\right)^{3/2} + \frac{13}{5}\left(\frac{\gamma-1}{\gamma+1}\right)^2 - \frac{463}{168}\sqrt{\frac{8}{3}}\left(\frac{\gamma-1}{\gamma+1}\right)^{5/2} + \cdots \quad (1.7)$$

In later chapters we shall have something further to say about each of these examples.

1.4. Regular and Singular Perturbation Problems

Under the happiest circumstances, a perturbation solution leads to altogether satisfactory results. The series cannot often be presumed to

converge, particularly for parameter perturbations. Nevertheless, its asymptotic nature means that a few terms may yield ample accuracy, for reasonably small ε, everywhere in the flow field. Such uniform validity appears to be true, for example, of the Janzen-Rayleigh expansion below the critical Mach number. One speaks then of a *regular perturbation problem*.

On the other hand, one may find that the straightforward perturbation solution is not uniformly valid throughout the flow field. The best known example is unseparated viscous flow at high Reynolds numbers, where a perturbation of the basic inviscid motion fails near the surface, and must be supplemented by the boundary-layer approximation. Not only does the first approximation break down locally in such cases, but the difficulty is compounded in higher approximations—if they can be calculated at all—so that in the region of non-uniformity the solution grows worse rather than better. One then speaks of a *singular perturbation problem*.

Singular perturbation problems arise frequently in fluid mechanics. They have been studied increasingly in the recent literature as the requisite mathematical techniques were developed. Fresh insight is gained into even some classical problems by recognizing their singular nature. For these reasons this book is largely devoted to singular perturbation problems.

Two more or less general methods have recently been developed for treating singular perturbation problems. One is a generalization of the notions of boundary-layer theory, which we call the *method of matched asymptotic expansions*. The other is the extension of an idea due to Poincaré, which we call the *method of strained coordinates*. Mathematical justification of these two procedures is in its infancy. Therefore no precise statements can be made as to when either of them can be applied, as to which is preferable in a given problem, or as to how the two methods are related. Nevertheless, we will attempt to gain some insight into these questions by studying a variety of illustrative examples. In some cases, ordinary differential equations will be adopted as simple models to demonstrate the essential points. Whenever possible, however, we draw our examples from the recent literature in fluid mechanics, so that partial differential equations are usually encountered.

Because we are concerned with techniques having some generality of application, our examples will—as in the results already quoted—be taken from the theories of both inviscid and viscous flows, and for speeds ranging from incompressible to hypersonic. The reader is assumed to understand the physical bases of those problems, which will often illuminate the mathematics. He is also expected to be familiar with the elementary processes of analysis, the basic theory of partial differential equations, and the fundamental notions of complex-variable theory, including in particular the grand concept of the complete description of an analytic function that results from the process of analytic continuation.

Chapter II

SOME REGULAR PERTURBATION PROBLEMS

2.1. Introduction; Basic Flow past a Circle

We illustrate some of the techniques of perturbation theory by considering first several related regular perturbation problems. These techniques will be systematized in the next chapter. The complications associated with singular perturbations are deferred to later chapters.

Because exact solutions are rare, one cherishes them, and seeks to exploit them as fully as possible. Thus a single exact solution is often perturbed in a number of ways, to explore different effects. In the usual aerodynamic problem of unbounded flow past a body, one may perturb

(i) the distant boundary conditions, far upstream,
(ii) the near boundary conditions, at the body surface,
(iii) the equations of motion,

and each of these possibilities may in turn be carried out in a variety of ways. For example, the exact inviscid solution for supersonic flow past a circular cone has been perturbed as in (i) to study the effects of

(a) angle of attack (Stone, 1948),
(b) pitching motion (Kawamura and Tsien, 1964),

as in (ii) for the effects of

(c) initial curvature of an ogival tip (Cabannes, 1951),
(d) departure from circular cross section (Ferri *et al.*, 1953),
(e) slight blunting (Yakura, 1962),

and as in (iii) for the effects of

(f) slight viscosity (Hantzsche and Wendt, 1941).

To illustrate these possibilities without excessive calculation, we adopt as our basic solution the steady plane motion of an incompressible inviscid fluid past a circle without circulation (Fig. 2.1). It is convenient to work with the stream function as well as the velocity potential, because we later consider rotational flow, for which no potential exists.

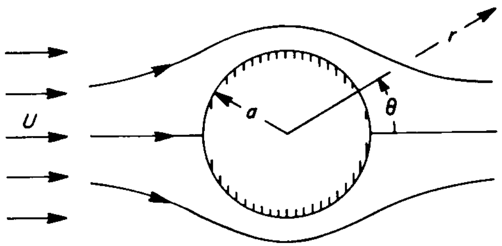

Fig. 2.1. Basic incompressible flow past a circle.

For plane incompressible flow the stream function is defined in Cartesian coordinates by

$$d\psi = u\,dy - v\,dx \tag{2.1}$$

In inviscid motion it satisfies the differential equation

$$\nabla^2\psi = -\omega(\psi) \tag{2.2}$$

which expresses the physical fact that vorticity is constant along streamlines in the absence of viscosity. This is a nonlinear equation unless the vorticity $\omega(\psi)$ is a linear function of ψ. For uniform flow far upstream the vorticity vanishes, leaving Laplace's equation

$$\psi_{rr} + \frac{\psi_r}{r} + \frac{\psi_{\theta\theta}}{r^2} = 0 \tag{2.3a}$$

Here, and throughout this book, subscripts are used to indicate partial derivatives. The boundary conditions are

upstream: $\psi(r, \theta) \to Ur \sin\theta \quad \text{as} \quad r \to \infty$ (2.3b)

surface: $\psi(a, \theta) = 0$ (2.3c)

together with some condition to rule out circulation, such as a requirement that the flow be symmetric about the line $\theta = 0$:

$$\psi(r, \theta) = -\psi(r, -\theta) \tag{2.3d}$$

The solution is given by the uniform stream plus a dipole at the center of the circle:

$$\psi_0 = U\left(r - \frac{a^2}{r}\right) \sin\theta \tag{2.4a}$$

The corresponding velocity potential is

$$\phi_0 = U\left(r + \frac{a^2}{r}\right) \cos\theta \tag{2.4b}$$

and these can of course be combined in the complex expression

$$\phi_0 + i\psi_0 = U\left(z + \frac{a^2}{z}\right), \qquad z = re^{i\theta} \tag{2.4c}$$

2.2. Circle in Slight Shear Flow

Consider first a slight perturbation of the boundary conditions far upstream. Let the oncoming stream be a parallel flow with small constant vorticity (Fig. 2.2), its speed being

$$\psi_{\infty y} = U\left(1 + \varepsilon\frac{y}{a}\right) = U\left(1 + \varepsilon\frac{r}{a}\sin\theta\right) \tag{2.5a}$$

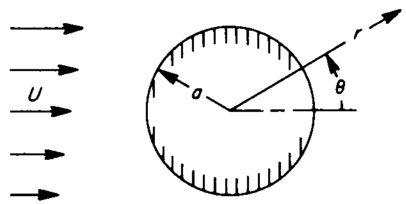

Fig. 2.2. Slight shear flow past a circle.

so that its stream function is, to within a constant,

$$\psi_\infty = U\left(y + \tfrac{1}{2}\varepsilon\frac{y^2}{a}\right) = U\left[r\sin\theta + \tfrac{1}{4}\varepsilon\frac{r^2}{a}(1 - \cos 2\theta)\right] \tag{2.5b}$$

with the vorticity

$$\omega_\infty = -\nabla^2\psi_\infty = -\varepsilon\frac{U}{a} \tag{2.5c}$$

The full problem is therefore

$$\psi_{rr} + \frac{\psi_r}{r} + \frac{\psi_{\theta\theta}}{r^2} = \varepsilon\frac{U}{a} \tag{2.6a}$$

$$\psi \to U\left[r\sin\theta + \tfrac{1}{4}\varepsilon\frac{r^2}{a}(1 - \cos 2\theta)\right] \quad \text{as} \quad r \to \infty \tag{2.6b}$$

$$\psi(a, \theta) = 0 \tag{2.6c}$$

To obtain a unique solution we must add, for example, the requirement that no *additional* circulation is induced by the body.

If the dimensionless "vorticity number" ε is small, it seems likely that the flow will depart only slightly from our previous solution for irrotational motion. On that assumption we tentatively set

$$\psi(r, \theta; \varepsilon) = \psi_0(r, \theta) + \varepsilon\psi_1(r, \theta) + \cdots \tag{2.7}$$

where ψ_0 is the basic solution (2.4a). Substituting into the full problem (2.6) and equating like powers of ε yields for the first-order perturbation ψ_1 the problem

$$\psi_{1rr} + \frac{\psi_{1r}}{r} + \frac{\psi_{1\theta\theta}}{r^2} = \frac{U}{a} \tag{2.8a}$$

$$\psi_1 \to \tfrac{1}{4}\frac{U}{a} r^2(1 - \cos 2\theta) \qquad \text{as} \quad r \to \infty \tag{2.8b}$$

$$\psi_1(a, \theta) = 0 \tag{2.8c}$$

In this simple problem a *particular integral* that accounts for the nonhomogeneous terms on the right-hand side of the differential equation (2.8a) is given by the rotational part of the flow far upstream. Thus it is convenient to express the solution as

$$\psi_1 = \tfrac{1}{4}\frac{U}{a} r^2(1 - \cos 2\theta) + \chi_1(r, \theta) \tag{2.9}$$

Discovery of a particular integral has reduced the differential equation to homogeneous form—the Laplace rather than the Poisson equation—so that the *complementary solution* χ_1 satisfies the problem

$$\chi_{1rr} + \frac{\chi_{1r}}{r} + \frac{\chi_{1\theta\theta}}{r^2} = 0 \tag{2.10a}$$

$$\chi_1 \to \text{const} \qquad \text{as} \quad r \to \infty \tag{2.10b}$$

$$\chi_1(a, \theta) = -\tfrac{1}{4} Ua(1 - \cos 2\theta) \tag{2.10c}$$

This is as readily solved by separation of variables as was the basic problem (2.3), there being again a unique solution that is free of circulation. Then collecting results gives as the complete first-order solution

$$\psi = U\left(r - \frac{a^2}{r}\right)\sin\theta + \tfrac{1}{4}\varepsilon U\left[\frac{r^2}{a}(1 - \cos 2\theta) + \frac{a^3}{r^2}\cos 2\theta - a\right] \tag{2.11}$$

The basic solution consists of the uniform stream—a dipole at infinity—plus its image in the circle—a dipole at the origin. Similarly, the first-order perturbation consists of the rotational part of the free stream, its image in the circle, and a constant to adjust the stream function to zero on the surface.

Ordinarily one would write "$+ \ldots$" or "$+ O(\varepsilon^2)$" at the end of this equation, to emphasize that the result is correct only to first order for small ε. However, in this untypical case the perturbation expansion terminates; the solution is exact [cf. Lamb, 1932, p. 235, Eq. (23)]. For any other upstream profile, however, the problem would be nonlinear, and the perturbation solution would be an infinite series in powers of ε (see Exercise 2.4).

This solution has been considered by Hall (1956) as a model for the effect of shear upon the reading of a pitot tube in a wake or boundary layer. It is easily shown that the stagnation streamline $\psi = 0$ originates upstream at $y \approx \frac{1}{4}\varepsilon a$. Hence the measured stagnation pressure is greater than that directly upstream; the impact tube reads too high a value. This effect has been observed experimentally. Hall treats the same problem for a sphere, which is a great deal more complicated.

2.3. Slightly Distorted Circle

Consider next a perturbation of the boundary conditions at the surface of the body. This introduces some features of perturbation theory that did not appear in the preceding example. Let the body (Fig. 2.3) be described by

$$r = a(1 - \varepsilon \sin^2\theta) \tag{2.12}$$

This may be regarded either as the first approximation for an ellipse, or the exact description of a more complicated curve.

As before, we tentatively assume a perturbation expansion in powers of ε:

$$\psi(r, \theta; \varepsilon) = \psi_0(r, \theta) + \varepsilon\psi_1(r, \theta) + \cdots \tag{2.13}$$

and substitute into the full problem. In the equation of motion (2.3a)

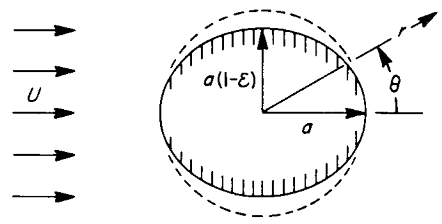

Fig. 2.3. Uniform flow past a slightly distorted circle.

and upstream boundary condition (2.3b) we can again equate like powers of ε to obtain for the first two terms

$$\nabla^2\psi_0 = 0, \qquad \psi_0 \to Ur \sin\theta \qquad \text{as} \quad r \to \infty \tag{2.14a}$$

$$\nabla^2\psi_1 = 0, \qquad \psi_1 \to 0 \qquad \text{as} \quad r \to \infty \tag{2.14b}$$

However, there is a complication in the condition of tangent flow at the surface of the body. Written out precisely it is

$$\psi_0[a(1 - \varepsilon \sin^2\theta), \theta] + \varepsilon\psi_1[a(1 - \varepsilon \sin^2\theta), \theta] + \cdots = 0 \tag{2.15a}$$

Here the perturbation parameter ε appears implicitly, in the first argument of the functions, as well as explicitly, so that it is not possible directly to equate like powers of ε to zero. This can be achieved only by expanding the functions to exhibit explicitly their dependence on ε. If we assume that ψ_1, like ψ_0, is analytic in its dependence upon r, we can expand in Taylor series about $r = a$. Keeping only linear terms in ε gives

$$\psi_0(a, \theta) - \varepsilon a \sin^2\theta\, \psi_{0r}(a, \theta) + \varepsilon\psi_1(a, \theta) + \cdots = 0 \tag{2.15b}$$

It is now possible to equate like powers of ε, giving

$$\psi_0(a, \theta) = 0 \tag{2.16a}$$

$$\psi_1(a, \theta) = a \sin^2\theta\, \psi_{0r}(a, \theta) = \tfrac{1}{2}Ua(3 \sin\theta - \sin 3\theta) \tag{2.16b}$$

The last form is obtained by using the basic solution (2.4a) for ψ_0.

The perturbation problem (2.14b), (2.16b) now has the form of the basic problem, and is just as easily solved. Thus the complete first-order approximation is found to be

$$\psi = U\left(r - \frac{a^2}{r}\right) \sin\theta + \tfrac{1}{2}\varepsilon U\left(3\frac{a^2}{r} \sin\theta - \frac{a^4}{r^3} \sin 3\theta\right) + O(\varepsilon^2) \tag{2.17}$$

Values at the surface of the body, which are usually those of most interest, could be obtained simply by setting r equal to its surface value (2.12). However, it is consistent with the approximation already introduced to simplify the results by dropping higher-order terms, which have no significance. This is accomplished by again expanding in Taylor series about the basic value $r = a$. Thus, for example, one finds for the surface speed

$$q_s = U(2 \sin\theta + \varepsilon \sin 3\theta + \cdots) \tag{2.18}$$

2.4. Circle in Slightly Compressible Flow

Consider now a perturbation of the equations of motion. Let the fluid be slightly compressible, the free-stream Mach number being small. It is convenient to work with the velocity potential, because the connection between the stream function and the velocity is complicated by variations of density. Let the velocity vector be given by $\mathbf{q} = U \operatorname{grad} \phi$. Then for plane flow of a perfect gas the full potential equation is (Oswatitsch, 1956, p. 328)

$$\begin{aligned}\phi_{xx} + \phi_{yy} = M^2\Big[&\phi_x^2\phi_{xx} + 2\phi_x\phi_y\phi_{xy} + \phi_y^2\phi_{yy} \\ &+ \frac{\gamma - 1}{2}(\phi_x^2 + \phi_y^2 - 1)(\phi_{xx} + \phi_{yy})\Big]\end{aligned} \tag{2.19a}$$

where M is the free-stream Mach number. Transforming this to polar coordinates gives

$$\begin{aligned}\phi_{rr} + \frac{\phi_r}{r} + \frac{\phi_{\theta\theta}}{r^2} = \tfrac{1}{2}M^2\Big[&\left(\phi_r \frac{\partial}{\partial r} + \frac{\phi_\theta}{r^2}\frac{\partial}{\partial\theta}\right)\left(\phi_r^2 + \frac{\phi_\theta^2}{r^2}\right) \\ &+ (\gamma - 1)\left(\phi_r^2 + \frac{\phi_\theta^2}{r^2} - 1\right)\left(\phi_{rr} + \frac{\phi_r}{r} + \frac{\phi_{\theta\theta}}{r^2}\right)\Big]\end{aligned} \tag{2.19b}$$

It is convenient to choose the length scale such that the radius of the circle is unity. Then the boundary conditions are

$$\text{upstream:} \qquad \phi \to r \cos\theta \quad \text{as} \quad r \to \infty \tag{2.20a}$$

$$\text{surface:} \qquad \phi_r(1, \theta) = 0 \tag{2.20b}$$

plus a requirement of symmetry to rule out circulation.

Rather than assume a perturbation expansion as before, we take this opportunity to illustrate *iteration* as an alternative way of finding successive approximations. To this end, all terms representing the effects of compressibility have been written on the right-hand side of the differential equation. Neglecting them altogether leads to the basic incompressible solution, given by (2.4b) with $U = a = 1$. To calculate the first-order effects of compressibility, we use that basic solution to evaluate the nonlinear right-hand side, and solve again. The differential equation becomes

$$\phi_{1rr} + \frac{\phi_{1r}}{r} + \frac{\phi_{1\theta\theta}}{r^2} = 2M^2\left[\left(\frac{1}{r^7} - \frac{2}{r^5}\right) \cos\theta + \frac{1}{r^3} \cos 3\theta\right] \tag{2.21}$$

In iterating it is convenient to calculate the complete solution at each stage, rather than only a small correction to the previous result. Then the full boundary conditions (2.20) are to be imposed at each stage. To indicate this change, we denote the successive approximations by Roman-numeral rather than Arabic subscripts. The term in $(\gamma - 1)$ in the differential equation is seen to have no effect upon the first approximation ϕ_I. The first-order effect of compressibility is independent of the thermodynamic properties of the gas.

Following Rayleigh (1916), we find by separation of variables a particular integral of the iteration equation (2.21) that vanishes at infinity:

$$\phi_{Ip} = M^2\left[\left(\frac{1}{12}\frac{1}{r^5} - \frac{1}{2}\frac{1}{r^3}\right)\cos\theta - \frac{1}{4}\frac{1}{r}\cos 3\theta\right] \qquad (2.22)$$

To this must be added a solution of the homogeneous equation—the Laplace equation—that restores the boundary conditions. The final result is

$$\phi_I = \left(r + \frac{1}{r}\right)\cos\theta - M^2\left[\left(\frac{13}{12}\frac{1}{r} - \frac{1}{2}\frac{1}{r^3} - \frac{1}{12}\frac{1}{r^5}\right)\cos\theta - \left(\frac{1}{12}\frac{1}{r^3} - \frac{1}{4}\frac{1}{r}\right)\cos 3\theta\right] \qquad (2.23)$$

Calculating from this the maximum surface speed reproduces the first two terms of Simasaki's series (1.1) quoted in Chapter I.

See Note 2 Higher approximations can be found by repeating the iteration procedure, the only complication being that the computational labor involved grows at a staggering rate. It can be minimized by using complex-variable theory and by systematizing the procedure.

2.5. Effect of Slight Viscosity

One might attempt to treat viscosity in the same way as compressibility. It is convenient to work with the stream function, which in plane incompressible flow satisfies the equation

$$\left(\psi_y \frac{\partial}{\partial x} - \psi_x \frac{\partial}{\partial y}\right)\nabla^2\psi = \nu\nabla^4\psi \qquad (2.24)$$

Here ν is the kinematic viscosity. If we again introduce dimensionless variables such that $U = a = 1$, ν can be replaced by R^{-1}, where $R = Ua/\nu$ is the Reynolds number based on radius. This equation expresses the physical fact that vorticity is convected with the local velocity (the left-hand side) and simultaneously diffused by viscosity (the right-hand side).

At infinite Reynolds number the right-hand side of the equation vanishes, leading to Eq. (2.2) for ψ. Thus the basic inviscid solution (2.4a) becomes exact in that limit. Suppose that we try to iterate to obtain a perturbation solution for large Reynolds numbers. The equation should be transformed to polar coordinates, and the condition of no slip at the surface added. However, it is clear without carrying out these details that the iteration attempt will fail. The right-hand side vanishes when evaluated in terms of the basic solution, so that the Reynolds number does not enter into the problem.

The resolution of this dilemma is of course provided by Prandtl's boundary-layer theory. Despite their superficial resemblance, the problems of slight compressibility and slight viscosity are essentially different. For the first, the basic solution is a valid approximation everywhere in the flow field, whereas for the second it is invalid in a neighborhood of the surface no matter how large the Reynolds number. For this reason the effect of slight compressibility is a regular perturbation, whereas the effect of slight viscosity is a singular perturbation.

2.6. Boundary Layer by Coordinate Expansion

Singular perturbation problems and the basic ideas of boundary-layer theory will be discussed in later chapters. For the present, it is informative simply to recall the well-known results of Prandtl. At high Reynolds numbers, viscosity is significant only within a thin layer near the surface of a body, where Eq. (2.24) for ψ may be approximated by

$$\psi_y\psi_{xy} - \psi_x\psi_{yy} = \nu\psi_{yyy} + q\frac{dq}{dx} \qquad (2.25a)$$

Here x and y are curvilinear coordinates along and normal to the body surface (Fig. 2.4). Evidently one integration has been performed with respect to y to reduce the equation from fourth to third order. The last term is the function of integration, q being the inviscid surface speed.

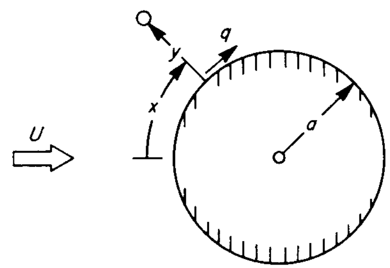

Fig. 2.4. Boundary-layer coordinates for a circle.

Two boundary conditions are provided by the requirement of zero velocity at the surface:

$$\psi(x, 0) = \psi_y(x, 0) = 0 \tag{2.25b}$$

The third condition, that the inviscid surface speed be attained at the outer edge of the boundary layer, may be written

$$\lim_{y\to\infty} \psi_y(x, y) = q \tag{2.25c}$$

with the understanding that here $y \to \infty$ means far from the surface only on the small scale of the boundary-layer thickness.

The previous examples were all parameter perturbations. We now consider a coordinate perturbation for the boundary layer on a circle. Within the framework of Prandtl's theory, this is again a regular perturbation.

Suppose that the distance x from the stagnation point is small compared with the radius a of the circle. Then the stream function can be expanded in powers of x/a, and it is clear from symmetry that only odd powers will appear. It is convenient to write the expansion as

$$\psi = \sqrt{2Ua\nu}\left[\frac{x}{a} f_1(\eta) - \frac{2}{3}\left(\frac{x}{a}\right)^3 f_3(\eta) + \cdots\right], \qquad \eta = y\sqrt{\frac{2U}{\nu a}} \tag{2.26}$$

which is the standard form of the Blasius series (Schlichting, 1960, p. 146). We take the inviscid surface speed from the basic solution

$$q = 2U \sin\frac{x}{a} = 2U\left[\frac{x}{a} - \frac{1}{6}\left(\frac{x}{a}\right)^3 + \cdots\right] \tag{2.27}$$

and substitute into the boundary-layer problem (2.25). Upon equating like powers of x/a, we obtain a sequence of problems involving ordinary differential equations:

$$f_1''' + f_1 f_1'' - f_1'^2 + 1 = 0, \qquad f_1(0) = f_1'(0) = 0, \qquad f_1'(\infty) = 1 \tag{2.28a}$$

$$f_3''' + f_1 f_3'' - 4f_1'f_3' + 3f_1''f_3 + 1 = 0, \qquad f_3(0) = f_3'(0) = 0, \qquad f_3'(\infty) = \tfrac{1}{4} \tag{2.28b}$$

The first of these is Hiemenz' classical problem of viscous flow at a plane stagnation point, and the remainder are linear perturbations thereof.

Numerical integration (Tifford, 1954) gives $f_1''(0) = 1.2325877$ and $f_3''(0) = 0.7244473$. Hence the expansion for the coefficient of skin friction is found to be

$$c_f \equiv \frac{\tau}{\frac{1}{2}\rho U^2} = \frac{1}{\sqrt{R}}\left[6.973\,\frac{x}{a} - 2.732\left(\frac{x}{a}\right)^3 + \cdots\right] \tag{2.29}$$

This vanishes at $x/a = 1.6$, suggesting that the boundary layer separates from a circle at about 92° from the stagnation point. Although this estimate has been refined to 109° by calculating four more terms in the series (Schlichting, 1960, p. 154), the occurrence of separation invalidates the whole analysis. The resulting broad wake drastically alters the flow over the front of the body. Therefore although Prandtl's Eq. (2.25a) is valid there, the inviscid surface speed q is not given correctly by (2.27) but is unknown (see Fig. 7.1). Experiments show that separation actually occurs at about 81°.

The Blasius series is self-consistent only for bodies where the solution shows no separation. An example is the parabola in a uniform stream, for which the 6-term counterpart of (2.29) was shown in Eq. (1.5) of Chapter I.

EXERCISES

2.1. *Pulsating circle.* Consider uniform plane flow of an incompressible inviscid liquid past a circular cylinder whose radius varies slightly with time according to $a[1 + \varepsilon f(t)]$. Calculate the velocity potential to first order in ε. Find the stream function, and show that it does not vanish on the surface.

See Note 3

2.2. *Slightly porous circle.* A uniform stream of incompressible inviscid liquid flows past a hollow circular cylinder whose surface is made porous by drilling many tiny holes normal to the surface. Assume that the normal velocity at the surface is some small parameter ε times the difference in pressure coefficient between the outer surface and the interior (which is assumed to be at constant pressure throughout), and that the net flux through the surface is zero. Calculate the stream function of the external flow approximately to order ε, and the interior pressure. Check the signs of these results by physical reasoning. What is the corresponding result for a slightly compressible flow, if only linear terms in ε and M^2 are retained?

See Note 3

2.3. *Corrugated quasi cylinder.* Consider an infinitely long body of revolution (Fig. 2.5) of radius $a[1 + \varepsilon \sin(z/b)]$. Calculate approximately the three-dimensional velocity potential for uniform incompressible flow (without circulation) normal to the axis, keeping only linear terms in ε. Using expansions for the Bessel functions, simplify your solution for the case of wavelength so great that only linear terms in a/b are retained, and interpret the result as a quasi-two-dimensional one. Show that in the opposite extreme of very large a/b the perturbation is a plane harmonic function near the surface, with θ appearing only as a parameter; and justify this by physical arguments.

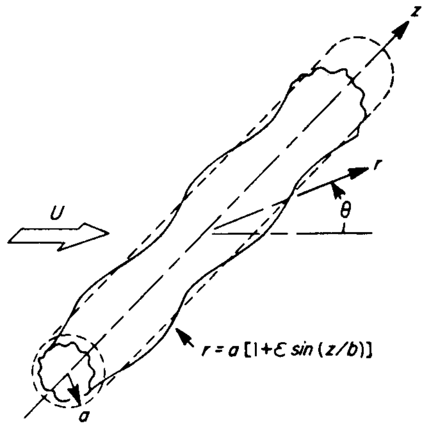

Fig. 2.5. Infinite corrugated cylinder.

See Note 3

2.4. *Circle in parabolic shear.* A circular cylinder of radius a is symmetrically placed in a parallel stream of incompressible inviscid fluid having the parabolic velocity profile $u = U(1 - \frac{1}{2}\varepsilon y^2/a^2)$. Find an exact implicit expression for the vorticity $\omega(\psi)$, and expand to give ω as a series, keeping terms of order ε^2. Carry out a perturbation solution for the flow, showing that a difficulty arises in the term of order ε because no solution can be found for which the velocity disturbances produced by the body disappear far upstream.

Chapter III

THE TECHNIQUES OF PERTURBATION THEORY

3.1. Introduction; Limit Processes

The examples in the preceding chapter have served to introduce various techniques for handling perturbation problems. We now seek to classify and generalize those that are of common utility. We begin with some matters of notation, definitions, and relevant processes of analysis.

We are concerned with finding approximate solutions of the equations of fluid motion that are close to the exact solutions in some useful sense. This involves various kinds of equality, which in decreasing degree of identification will be expressed by the following symbols:

$$\begin{aligned}
&\equiv \text{ identical with}\\
&= \text{ equal to}\\
&\sim \text{ asymptotically equal to (in some given limit)}\\
&\approx \text{ approximately equal to (in any useful sense)}\\
&\propto \text{ proportional to}
\end{aligned} \tag{3.1}$$

As discussed in Chapter I, we consider approximations that depend upon a *limit process*, the result becoming exact as a perturbation quantity approaches zero or some other critical value. One often encounters a *double* or *multiple limit process*, in which two or more perturbation quantities approach their limits simultaneously. Because the order of carrying out several limits cannot in general be interchanged, one must frequently specify the relative rates of approach. This specification provides a *similarity parameter* for the problem. The following are some familiar examples:

(a) Plane transonic small-disturbance theory for a wing of thickness ratio ε (von Kármán, 1947):

$$\left.\begin{array}{l}\varepsilon \to 0\\ M \to 1\end{array}\right\} \qquad \frac{M-1}{\varepsilon^{2/3}} = O(1)$$

(b) Hypersonic small-disturbance theory for a body of thickness ratio ε (Hayes and Probstein, 1959, p. 36):

$$\left.\begin{array}{l}\varepsilon \to 0\\ M \to \infty\end{array}\right\} \quad \frac{1}{M\varepsilon} = O(1)$$

(c) Newton-Busemann approximation for hypersonic flow past a blunt body (Cole, 1957):

$$\left.\begin{array}{l}M \to \infty\\ \gamma \to 1\end{array}\right\} \quad \frac{1}{(\gamma - 1)M^2} = O(1)$$

(d) Hypersonic small-disturbance form of Newton-Busemann approximation for a slender body of thickness ratio ε (Cole, 1957):

$$\left.\begin{array}{l}\varepsilon \to 0\\ M \to \infty\\ \gamma \to 1\end{array}\right\} \quad \frac{1}{(\gamma - 1)M^2\varepsilon^2} = O(1)$$

In the last example one might have anticipated two similarity parameters, but only one is found to be significant.

A perturbation quantity is never uniquely defined. For example, the thickness parameter for a slender body may be taken as its thickness ratio, maximum slope, mean slope, etc. Of course it may also be changed by a constant multiplier, as in referring Reynolds number to radius rather than diameter for a sphere. One should be alert to the possibility of exploiting this freedom by replacing the obvious choice by an alternative that is superior to it in some respect. The possibilities are too diverse to be subject to rules. They can only be suggested here by listing a number of cases where an ingenious choice of the perturbation quantity, usually suggested by extraneous considerations, leads to simplification or improvement of the results:

(a) $(M^2 - 1)$ instead of $(M - 1)$ in transonic small-disturbance theory, so that the result is valid also in the adjacent regimes of subsonic and supersonic flow (Spreiter, 1953),

(b) $1/\sqrt{M^2 - 1}$ instead of $1/M$ in hypersonic small-disturbance theory, so that the result is valid also in the adjacent regime of supersonic flow (Van Dyke, 1951),

(c) $(\gamma - 1)/(\gamma + 1)$ instead of $(\gamma - 1)$ in the Newton-Busemann approximation for hypersonic flow, because it can be identified with the density ratio across a strong shock wave (Hayes and Probstein, 1959, p. 7),

(d) $(\log R/4 + \gamma - \frac{1}{2})$ instead of $\log R$ in viscous flow past a circle at low Reynolds number (γ being Euler's constant), because the first two terms of the Stokes expansion are thereby combined into one (Kaplun, 1957; see Section 8.7),

(e) $\varepsilon/(1 - \varepsilon)$ instead of ε, ε being the density ratio across a normal shock, in the Newton-Busemann approximation for the standoff distance of the detached shock wave on a blunt body in supersonic flow, because it then becomes infinite for $M \to 1$, as it should (Serbin, 1958),

(f) $(A + BR^{-1/2} + \cdots)^2$ instead of $(A^2 + 2ABR^{-1/2} + \cdots)$ for the drag of a bluff body in laminar flow at high Reynolds numbers, which is suggested by theory and agrees better with known results (Imai, 1957b),

(g) $2\pi/(1 + 2/A + \cdots)$ instead of $2\pi(1 - 2/A + \cdots)$ for the lift-curve slope of an elliptic wing of high aspect ratio A, because it then vanishes for $A \to 0$, as it should (see Chapter IX),

(h) $\xi\sqrt{1 - \xi^2}$, ξ being a parabolic coordinate, instead of x in the Blasius series for the boundary layer on a parabola, because the radius of convergence is thereby extended to infinity (see Chapter X),

(i) $\varepsilon/(2 - \varepsilon)$ instead of ε in free-streamline theory (Garabedian, 1956), where $2 + \varepsilon$ is the number of space dimensions, because the radius of convergence is thereby increased.

3.2. Gauge Functions and Order Symbols

The solution of a problem in fluid mechanics will depend upon the coordinates, say x, y, z, t, and also upon various parameters. One or more of these quantities may, by appropriate redefinition, be regarded as vanishingly small in a perturbation solution. We consider the behavior of the solution as it depends upon one such perturbation quantity, with the other coordinates and parameters fixed. Thus we seek to describe the way in which a function $f(\varepsilon)$ behaves as ε approaches zero. An analogous situation has already arisen in the upstream boundary conditions (2.3b), (2.6b), etc., where it was necessary to describe the behavior of the solution far from the body.

There are a number of possible descriptions, of varying degrees of precision. We discuss six of them, in increasing order of refinement. First, one may simply state whether or not a limit *exists*. For example, $\sin 2\varepsilon$ has a limit as $\varepsilon \to 0$, whereas $\sin 2/\varepsilon$ has not. However, we are concerned only with problems where a limit is believed to exist.

Second, one may describe the limiting value *qualitatively*. There are three possibilities: the function may be

$$\left.\begin{array}{lll}\text{(a) vanishing:} & f(\varepsilon) \to 0 \\ \text{(b) bounded:} & f(\varepsilon) < \infty \\ \text{(c) infinite:} & f(\varepsilon) \to \infty\end{array}\right\} \quad \text{as} \quad \varepsilon \to 0$$

It is a peculiarity of this mode of description that the first case is included in the second; a function that vanishes is also bounded. However, one would naturally use the first description when possible, because it is more precise.

Third, one may describe the limiting value *quantitatively*. There are again three possibilities, only the second having been refined:

$$\left.\begin{array}{lll}\text{(a)} \lim f(\varepsilon) = 0 & \\ \text{(b)} \lim f(\varepsilon) = c, & \text{a constant} \\ \text{(c)} \lim f(\varepsilon) = \infty & \end{array}\right\} \quad \text{as} \quad \varepsilon \to 0$$

Fourth, one may describe *qualitatively* the *rate* at which the limit is approached. Only cases (a) and (c) above are thus refined. This can be done by comparing with a set of *gauge functions*. These are functions that are so familiar that their limiting behavior can be regarded as known intuitively. The comparison is made using the order symbols O ("big oh") and o ("little oh"). They provide an indispensible means for keeping account of the degree of approximation in a perturbation solution.

The symbol O is used if comparing $f(\varepsilon)$ with some gauge function $\delta(\varepsilon)$ shows that the ratio $f(\varepsilon)/\delta(\varepsilon)$ remains bounded as $\varepsilon \to 0$. One writes

$$f(\varepsilon) = O[\delta(\varepsilon)] \quad \text{as} \quad \varepsilon \to 0 \quad \text{if} \quad \lim_{\varepsilon \to 0} \frac{f(\varepsilon)}{\delta(\varepsilon)} < \infty \tag{3.2}$$

The symbol o is used instead if the ratio tends to zero. One writes

$$f(\varepsilon) = o[\delta(\varepsilon)] \quad \text{as} \quad \varepsilon \to 0 \quad \text{if} \quad \lim_{\varepsilon \to 0} \frac{f(\varepsilon)}{\delta(\varepsilon)} = 0 \tag{3.3}$$

Some examples are

$$\begin{array}{rlrl} \sin 2\varepsilon = O(\varepsilon), & & 1 - \cos \varepsilon & = O(\varepsilon^2) = o(\varepsilon) \\ \sqrt{1 - \varepsilon^2} = O(1), & & \operatorname{sec}^{-1}(1 + \varepsilon) & = O(\varepsilon^{1/2}) = o(1) \\ \cot \varepsilon = O\left(\dfrac{1}{\varepsilon}\right), & & \exp(-1/\varepsilon) & = o(\varepsilon^m) \quad \text{for all } m \end{array} \tag{3.4}$$

Like the perturbation quantity ε itself, the gauge functions are not unique, and a choice other than the obvious one may occasionally be advantageous. For example, it might under some circumstances prove useful to replace the first case in (3.4) by the equivalents

$$\sin 2\varepsilon = O(2\varepsilon), \qquad O(\tan \varepsilon), \qquad O\left(\frac{\varepsilon}{1+\varepsilon}\right), \qquad \text{etc.}$$

One ordinarily chooses the real powers of ε as gauge functions, because they have the most familiar properties. However, this set is not complete. It fails, for example, to describe $\log 1/\varepsilon$, which becomes infinite as ε tends to zero, but more slowly than any power of ε. The powers of ε must therefore be supplemented, when necessary, by its logarithm, exponential, log log, etc., or their equivalents. Examples are

$$\begin{array}{rlrl} \operatorname{sech}^{-1} \varepsilon = O\left(\log \dfrac{1}{\varepsilon}\right), & & \cosh^{-1} K_0(\varepsilon) & = O\left(\log \log \dfrac{1}{\varepsilon}\right) \\ \cosh \dfrac{1}{\varepsilon} = O(e^{1/\varepsilon}), & & \exp\left(-\cosh \dfrac{1}{\varepsilon}\right) & = O(\exp[-\tfrac{1}{2}e^{1/\varepsilon}]) \end{array} \tag{3.5}$$

Often, as in (1.4), one writes $\log \varepsilon$ where $\log 1/\varepsilon$ would be more appropriate.

Neither order symbol necessarily describes the actual rate of approach to the limit, but provides only an upper bound. Thus it is formally correct to replace the first example in (3.4) by

$$\sin 2\varepsilon = O(1), \quad o(1), \quad O(\varepsilon^{1/2}), \quad o(\varepsilon^{1/2}), \quad \text{etc.} \tag{3.6}$$

However, we assume that the sharpest possible estimate is always given. This means, for example, choosing the largest possible power of ε as the gauge function, and using o only when one has insufficient knowledge to use O. Of course the result may still be only an upper bound for lack of sufficient information.

The *mathematical order* expressed by the symbols O and o is formally distinct from *physical order of magnitude*, because no account is kept of constants of proportionality. Therefore $K\varepsilon$ is $O(\varepsilon)$ even if K is ten thousand. In physical problems, however, one has at least a mystical hope, almost invariably realized, that the two concepts are related. Thus if the error in a physical theory is $O(\varepsilon)$ and ε has been sensibly chosen, one can expect that the numerical error will not exceed some moderate multiple of ε: possibly 2ε or even $2\pi\varepsilon$, but almost certainly not 10ε.

The rules for simple operations with order symbols are evident from this physical connection. For example, the order of a product (or ratio) is the product (or ratio) of the orders; the order of a sum or difference is that of the dominant term—i.e., the term of order ε^m having the smallest value of m—etc. Order symbols may be integrated with respect to either ε or another variable. It is not in general permissible to differentiate order relations. Nevertheless, in physical problems one commonly assumes that differentiation with respect to another variable is legitimate, so that the derivative has the same order as its antecedent. For other properties of order symbols see the first chapter of Erdélyi (1956).

3.3. Asymptotic Representations; Asymptotic Series

A fifth scheme is to describe *quantitatively* the rate at which a function approaches its limit. This constitutes a refinement of the fourth scheme—the use of order symbols—just as the third scheme does of the second. We simply restore the constant of proportionality, and write

$$f(\varepsilon) \sim c\delta(\varepsilon) \qquad \text{as} \quad \varepsilon \to 0 \tag{3.7a}$$

if

$$\lim_{\varepsilon\to 0} \frac{f(\varepsilon)}{\delta(\varepsilon)} = c \tag{3.7b}$$

that is, if

$$f(\varepsilon) = c\delta(\varepsilon) + o[\delta(\varepsilon)] \tag{3.7c}$$

This is the *asymptotic form* or *asymptotic representation* of the function, and constitutes the leading term in the asymptotic expansion discussed below. Some examples are

$$\begin{aligned} &\sin 2\varepsilon \sim 2\varepsilon, && \operatorname{sech}^{-1} \varepsilon \sim \log \frac{2}{\varepsilon} \\ &\sqrt{1-\varepsilon^2} \sim 1, && K_0\Big(\frac{1}{\varepsilon}\Big) \sim \sqrt{\frac{\pi}{2}}\,\varepsilon^{1/2} e^{-1/\varepsilon} \\ &\cot \varepsilon \sim \frac{1}{\varepsilon}, && \int_0^\infty \frac{e^{-t}\,dt}{1+\varepsilon t} \sim 1 \end{aligned} \tag{3.8}$$

Sixth, the preceding description—which is the most precise one possible using only one gauge function—can be refined by adding further terms. Consider the *difference* between the function in question and its asymptotic form as a new function, and determine its asymptotic form. The result can be written

$$f(\varepsilon) \sim c_1\delta_1(\varepsilon) + c_2\delta_2(\varepsilon) \qquad \text{as} \quad \varepsilon \to 0 \tag{3.9a}$$

where the second gauge function $\delta_2(\varepsilon)$ is necessarily of smaller order than the first:

$$\delta_2(\varepsilon) = o[\delta_1(\varepsilon)] \qquad \text{or} \qquad \lim_{\varepsilon\to 0} \frac{\delta_2(\varepsilon)}{\delta_1(\varepsilon)} = 0 \tag{3.9b}$$

and the error is of still smaller order:

$$f(\varepsilon) = c_1\delta_1(\varepsilon) + c_2\delta_2(\varepsilon) + o[\delta_2(\varepsilon)] \tag{3.9c}$$

Further terms can be added by repeating this process. Thus one constructs the *asymptotic expansion* or *asymptotic series* to N terms, written as

$$\begin{aligned} f(\varepsilon) &\sim c_1\delta_1(\varepsilon) + c_2\delta_2(\varepsilon) + \cdots + c_N\delta_N(\varepsilon) \\ &= \sum_{n=1}^{N} c_n\delta_n(\varepsilon) \qquad \text{as} \quad \varepsilon \to 0 \end{aligned} \tag{3.10a}$$

and defined by

$$f(\varepsilon) = \sum_{n=1}^{N} c_n\delta_n(\varepsilon) + o[\delta_N(\varepsilon)] \qquad \text{as} \quad \varepsilon \to 0 \tag{3.10b}$$

If the function $f(\varepsilon)$ were known, together with the gauge functions $\delta_n(\varepsilon)$, the coefficients c_n of the asymptotic expansion could be computed in succession from

$$c_m = \lim_{\varepsilon\to 0} \frac{f(\varepsilon) - \sum_{n=1}^{m-1} c_n\delta_n(\varepsilon)}{\delta_m(\varepsilon)} \tag{3.11}$$

If the gauge functions are all integral positive powers of ε, one speaks of an *asymptotic power series*. As the number N of terms increases without limit, one obtains an *infinite asymptotic series*, which may be either convergent or divergent.

Some examples of asymptotic expansions are

$$\begin{aligned} &\sin 2\varepsilon \sim 2\varepsilon - \frac{4}{3}\varepsilon^3 + \frac{4}{15}\varepsilon^5 + \cdots \\ &\operatorname{sech}^{-1} \varepsilon \sim \log \frac{2}{\varepsilon} - \frac{1}{4}\varepsilon^2 - \frac{3}{32}\varepsilon^4 + \cdots \\ &K_0\Big(\frac{1}{\varepsilon}\Big) \sim \sqrt{\frac{\pi}{2}}\,\varepsilon^{1/2} e^{-1/\varepsilon}\Big(1 - \frac{1}{8}\varepsilon + \frac{9}{128}\varepsilon^2 + \cdots\Big) \\ &\int_0^\infty \frac{e^{-t}\,dt}{1+\varepsilon t} \sim 1 - \varepsilon + 2\varepsilon^2 - 6\varepsilon^3 + \cdots = \sum_{n=0}^{\infty} (-1)^n n!\,\varepsilon^n \\ &\log n! \sim (n + \tfrac{1}{2}) \log n - n + \log\sqrt{2\pi} + \cdots \end{aligned} \tag{3.12}$$

The first two of these converge if extended indefinitely; the latter three diverge.

It is proper to regard a distant boundary condition as an asymptotic relation. For example, (2.6b) will henceforth be rewritten as

$$\psi \sim U\left[\frac{1}{4}\frac{\varepsilon}{a}r^2(1 - \cos 2\theta) + r \sin\theta\right] \quad \text{as} \quad r \to \infty \tag{2.6b'}$$

It must be understood that this admits the possibility of an error of order $o(r)$. Actually, in the problem in question, the next term in this asymptotic expansion is $O(1)$; the stream function must be left unprescribed far upstream to within a constant, which corresponds physically to the displacement of the stagnation streamline.

3.4. Asymptotic Sequences

The process just described of constructing an expansion term by term is effectively that employed in perturbation solutions, such as those of Chapter II. Thus in each problem a perturbation solution generates a special sequence of gauge functions

$$\delta_1(\varepsilon), \quad \delta_2(\varepsilon), \quad \delta_3(\varepsilon), \quad \cdots \tag{3.13}$$

that are arranged in decreasing order: $\delta_{n+1} = o(\delta_n)$. This is the *asymptotic sequence* associated with the problem. It cannot be prescribed arbitrarily, because it must be sufficiently complete to describe logarithms, for example, if they appear. On the other hand, there are an unlimited number of alternatives to any particular asymptotic sequence:

$$\begin{aligned} \sin 2\varepsilon &\sim 2\varepsilon - \frac{4}{3}\varepsilon^3 + \frac{4}{15}\varepsilon^5 + \cdots \\ &\sim 2\tan\varepsilon - 2\tan^3\varepsilon - 2\tan^5\varepsilon + \cdots \\ &\sim 2\log(1+\varepsilon) + \log(1+\varepsilon^2) - 2\log(1+\varepsilon^3) + \cdots \\ &\sim 6\left(\frac{\varepsilon}{3+2\varepsilon^2}\right) - \frac{756}{5}\left(\frac{\varepsilon}{3+2\varepsilon^2}\right)^5 + \cdots \end{aligned} \tag{3.14}$$

The last two forms illustrate the fact that alternative sequences need not be equivalent: corresponding terms are not of the same order. Both the asymptotic sequence and the asymptotic expansion itself are unique if the perturbation quantity (e.g., ε) and the gauge functions (e.g., ε^m, $\log 1/\varepsilon$, $\log\log 1/\varepsilon$, etc.) are specified.

We have seen that one way of attacking a perturbation problem is to assume the form of a series solution. This requires guessing an appropriate asymptotic sequence. The simplest possibility is that, as in the

examples of Chapter II, it consists of integral powers, ε^n. Fractional powers may also occur, particularly in singular perturbation problems. Examples are:

$1, \varepsilon^{1/2}, \varepsilon, \varepsilon^{3/2}, \ldots$	Unseparated laminar flow over smooth bodies at high Reynolds number R, where $\varepsilon = 1/R$ (Van Dyke, 1962a)
$1, \varepsilon^{3/4}, \ldots$	Separated Oseen flow at high Reynolds number R, $\varepsilon = 1/R$ (Tamada and Miyagi, 1962)

Logarithms may occur at some stage, examples being

$1, \varepsilon, \varepsilon^2\log\varepsilon, \varepsilon^2, \varepsilon^3\log\varepsilon, \varepsilon^3, \ldots$	Axisymmetric flow at low Reynolds number R, $\varepsilon = R$ (Proudman and Pearson, 1957)
$1, \varepsilon^2\log\varepsilon, \varepsilon^2, \varepsilon^4\log^2\varepsilon, \varepsilon^4\log\varepsilon, \varepsilon^4, \ldots$	Supersonic axisymmetric slender-body theory, ε = thickness parameter (Broderick, 1949)
$\varepsilon\log\varepsilon, \varepsilon, \varepsilon^2\log\varepsilon, \varepsilon^2, \ldots$	Newton-Busemann approximation for plane hypersonic flow past a blunt body, $\varepsilon = (\gamma-1)/(\gamma+1)$ (Chester, 1956a)
$(\log\varepsilon)^{-1}, (\log\varepsilon)^{-2}, (\log\varepsilon)^{-3}, \ldots$	Plane viscous flow at low Reynolds number R, $\varepsilon = R$ (Kaplun, 1957; Proudman and Pearson, 1957)
$1, \varepsilon, \varepsilon^2, \varepsilon^3, \varepsilon^4\log\varepsilon, \varepsilon^4, \ldots$	Subsonic thin-airfoil theory for round-nosed profile, ε = thickness parameter (Hantzsche, 1943)
$1, \varepsilon^{1/2}, \varepsilon, \varepsilon^{3/2}\log\varepsilon, \varepsilon^{3/2}, \ldots$	Laminar flow over flat plate at high Reynolds number R, $\varepsilon = 1/R$ (Goldstein, 1956; Imai, 1957a)

In the last two examples, earlier investigators had obtained erroneous solutions because they did not suspect the presence of logarithmic terms. Other examples arising in boundary-layer theory have been discussed by Stewartson (1957), who shows that even log log's occur in the asymptotic solution far downstream on a circular cylinder.

Exponentially small terms are seldom encountered, and are difficult to deal with. The following example shows that the estimate $O(e^{-1/\varepsilon})$ has very little practical value:

$$\lim_{\varepsilon\to 0}\frac{e^{-x/\varepsilon}}{e^{-1/\varepsilon}} = \begin{cases} 0, & x > 1 \\ 1, & x = 1 \\ \infty, & x < 1 \end{cases} \tag{3.15}$$

The question naturally arises how one can be sure of guessing the proper asymptotic sequence. Apparently there are no general rules, but the following principles are of some help:

(a) When in doubt, overguess. A superfluous term will drop out by producing for its coefficient a homogeneous problem, whose solution (if unique!) is zero.

(b) Be ready to suspect the presence of logarithmic terms at the first hint of difficulty.

(c) Iteration will sometimes (but not always!) produce the proper sequence automatically.

One usually has a feeling when the solution is progressing properly; all terms match, and complicated expressions often simplify. With experience, one learns when the absence of such reassurance suggests a re-examination of the assumed form of the series. However, the only fool-proof procedure is to leave the asymptotic sequence unspecified, and to determine it term by term in the course of the solution. This technique will be illustrated in Chapters VII and VIII.

3.5. Convergence and Accuracy of Asymptotic Series

We have seen that an infinite asymptotic series may either converge for some range of ε, or diverge for all ε. In perturbation problems one often neither knows nor cares whether the series converges. This point of view has been persuasively set forth by Jeffreys (1926). It is a fallacy to think that convergence is necessarily of practical value. Mathematical convergence depends upon the behavior of terms of indefinitely high order, whereas in physical problems one can calculate only the first few terms and hope that they rapidly approach the true solution. This requirement may sometimes be better met with a divergent than a convergent series. Thus the expansion

$$J_0(\varepsilon) = 1 - \frac{1}{4}\varepsilon^2 + \frac{1}{64}\varepsilon^4 - \frac{1}{2304}\varepsilon^6 + \cdots \tag{3.16}$$

for the Bessel function has an infinite radius of convergence, but many terms are needed for accurate results unless ε is small. With $\varepsilon \geqslant 4$, for example, the first three terms actually increase in magnitude—so that the series appears to be diverging—and at least eight terms are required for three-figure accuracy. On the other hand, the asymptotic expansion

$$J_0\left(\frac{1}{\varepsilon}\right) \sim \sqrt{\frac{2\varepsilon}{\pi}}\left[\left(1 - \frac{9}{128}\varepsilon^2 + \cdots\right)\cos\left(\frac{1}{\varepsilon} - \frac{\pi}{4}\right) + \left(\frac{1}{8}\varepsilon - \frac{75}{1024}\varepsilon^3 + \cdots\right)\sin\left(\frac{1}{\varepsilon} - \frac{\pi}{4}\right)\right] \quad \text{as } \varepsilon \to 0 \tag{3.17}$$

is divergent for all ε no matter how small, but a few terms give good accuracy for moderately small ε. The first term alone is correct to three significant figures for $(1/\varepsilon) = 4$.

The utility of an asymptotic expansion lies in the fact that the error is, by definition, of the order of the first neglected term, and therefore tends rapidly to zero as ε is reduced. For a fixed value of ε, the error can also be decreased at first by adding terms; but if the series is divergent, a point is eventually reached beyond which additional terms increase the error. This behavior is indicated in Fig. 3.1. These properties are often ideal

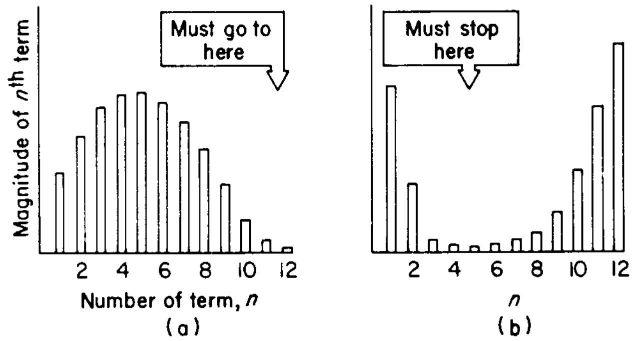

Fig. 3.1. Behavior of terms in series. (a) Slowly convergent series. (b) Divergent asymptotic series.

for practical purposes, particularly in parameter perturbations of the sort exemplified by thin-airfoil theory. Then only small values of ε are of practical interest; and only a few terms are calculated, so that the point of increasing error is not reached.

There are other problems, however, in which one attempts to make ε as large as possible. This is true of such parameter perturbations as expansions for large or small Reynolds numbers. It is almost always true of coordinate perturbations, because one intends to apply the results as far from the origin as possible. Under such circumstances, convergence may be of considerable practical interest. As discussed in Chapter X, one can sometimes improve the rate and radius of convergence, or even render a divergent series convergent.

From a physical point of view, the perturbation quantity ε assumes only positive real values. However, mathematical insight is often gained by envisioning its analytic continuation into the complex plane (Fig. 3.2). This is particularly useful when the solution is a power series in the perturbation quantity. Thus one considers the complex M^2-plane in the Janzen-Rayleigh method, the complex thickness-ratio-plane in thin-

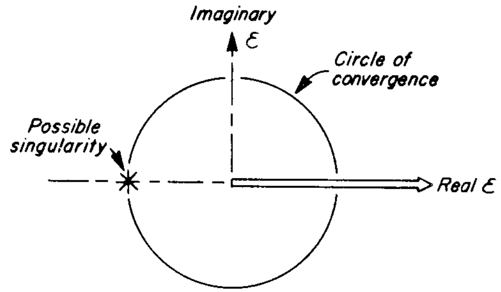

Fig. 3.2. Complex plane of perturbation quantity ε.

airfoil theory, and so on. Then one can take advantage of the powerful unifying viewpoint of complex-variable theory.

Some knowledge of—and feeling for—the principle of analytic continuation is essential. An analytic function has a power series development at every regular point. This converges within a circle that extends to the nearest singularity. A function defined in any region, or even on just a line segment, is ordinarily defined uniquely in a much larger region of the complex plane (possibly on several Riemann sheets), and can be completed by the process of analytic continuation.

See Note 15

Sometimes the first few terms of a perturbation solution suggest that the series converges, but has its radius of convergence limited for no apparent physical reason. According to the principles just outlined, this must result from a singularity in the complex plane of ε elsewhere than on the positive real axis. Several examples to be discussed in Chapter X suggest that in these circumstances the singularity ordinarily lies on the *negative* real axis, and in fact at $\varepsilon = -1$, if the most natural choice of variables has been made (Fig. 3.2). This artificial limitation can be eliminated by shifting the singularity to infinity using a simple conformal mapping, the *Euler transformation*:

$$\bar{\varepsilon} = \frac{\varepsilon}{1 - \varepsilon} \tag{3.18}$$

The radius of convergence is thereby extended to the nearest singularity in the complex plane of $\bar{\varepsilon}$, and the utility of the series often greatly improved.

3.6. Properties of Asymptotic Expansions

In substituting an assumed series solution into a perturbation problem one must carry out such operations as addition, multiplication, and

differentiation. Addition and subtraction are justified in general. Multiplication is valid if the result is an asymptotic expansion. It is not in general permissible to differentiate an asymptotic expansion with respect to either the perturbation quantity or another variable. These and other properties of asymptotic expansions are discussed by Erdélyi (1956). However, it appears that results are not available in sufficient generality to cover such commonly occuring series as those involving logarithmic terms. In practice, therefore, one ordinarily carries out formally such operations as differentiation with respect to another variable without attempting to justify them. When they are not justified, nonuniformities will arise in the solution.

In a physical problem, the coefficients in an asymptotic expansion will depend upon space or time variables other than ε. The series is said to be *uniformly valid* (in space or time) if the error is small uniformly in those variables. Examples of nonuniformity in x are

$$\begin{aligned} \frac{\varepsilon}{\sqrt{x}} &= O(\varepsilon), \qquad \text{but not uniformly near } x = 0 \\ \varepsilon \log x &= O(\varepsilon), \qquad \text{but not uniformly near } x = 0, \infty \end{aligned} \tag{3.19}$$

A *singular perturbation problem* is best defined as one in which no single asymptotic expansion is uniformly valid throughout the field of interest. The nonuniformities illustrated in (3.19) arise in practical singular perturbation problems. For example, the first will be encountered at a round leading edge in subsonic thin-airfoil theory, and the second at a sharp leading edge or in plane viscous flow at low Reynolds numbers.

We have observed that each function has a unique asymptotic expansion if the gauge functions or asymptotic sequence is prescribed. On the other hand, the statement is often made that different functions may have the same asymptotic expansion. The extent of this nonuniqueness may be understood by considering the following example:

$$\left.\begin{aligned} &\frac{1}{1+\varepsilon} \\ &\frac{1+e^{-1/\varepsilon}}{1+\varepsilon} \end{aligned}\right\} \sim 1 - \varepsilon + \varepsilon^2 - \cdots = \sum_{n=0} (-1)^n \varepsilon^n \tag{3.20a}$$

With respect to the gauge functions ε^n, these two functions have identical asymptotic expansions to any number of terms. Their difference is so small that it would become evident only if the infinite sequence of powers of ε were exhausted, for example by summing them. It happens that this is easily accomplished in this example by making the Euler transformation (3.18). With respect to powers of the new perturbation quantity $\bar{\varepsilon}$, the two functions have *different* asymptotic expansions (which happen to terminate):

$$\frac{1}{1+\varepsilon} \sim 1 - \bar{\varepsilon}$$
$$\frac{1+e^{-1/\varepsilon}}{1+\varepsilon} \sim 1 - \bar{\varepsilon} + e \cdot e^{-1/\bar{\varepsilon}} - e\bar{\varepsilon}e^{-1/\bar{\varepsilon}} \tag{3.20b}$$

One speaks of $e^{-1/\varepsilon}$ as being *transcendentally small* compared with the sequence of powers of ε, because it is $o(\varepsilon^m)$ for any m no matter how large. Similarly, on a different level of magnitude, ε itself is transcendentally small compared with the sequence $(\log \varepsilon)^{-m}$, which arises, for example, in plane viscous flow at low Reynolds numbers. The possibility of dealing with transcendentally small terms will be discussed in Chapter VIII in connection with that problem.

See Note 11

3.7. Successive Approximations

The perturbation problems encountered in fluid mechanics usually involve a system of ordinary or partial differential equations together with appropriate initial and boundary conditions. Integro-differential equations may also arise, as in problems involving thermal radiation. There are two systematic procedures for finding a solution by successive approximations, both of which were illustrated in the previous chapter:

(i) substitution of an assumed series,
(ii) iteration upon a basic approximate solution.

In the first method—which is somewhat more common—the guiding principle is that since the expansion must hold, at least in an asymptotic sense, for arbitrary values of the perturbation quantity ε, terms of like order in ε must separately satisfy each equality. That is, one can equate like powers of ε, terms in $\varepsilon^m \log^n \varepsilon$ having the same values of both m and n, etc.

Each method has its advantages and disadvantages, which can sometimes be exploited by working with a combination of the two. The most important of these differences can be summarized as follows:

(a) Iteration can be started only if an appropriate initial approximation is known. Series expansion is more automatic, because it can generate the basic approximation if one substitutes a series with the asymptotic sequence left unspecified. An example is given in Chapter VII.

(b) Iteration eliminates the need to guess the asymptotic sequence. It is therefore safer than assuming an expansion, unless one leaves the asymptotic sequence unspecified. For example, it will often though not always, in singular perturbation problems produce logarithms in higher-order terms that are missed if a power series is assumed.
(c) Beyond the second term the series expansion is more systematic because it produces only significant results, whereas iteration will, in nonlinear problems, generate some higher-order terms, to which no significance can be attached because others of equal order are missing. For example, in the Janzen-Rayleigh solution for a circle (Section 2.4), the next iteration step would clearly produce not only terms in M^4, which are correct and identical with those given by series expansion, but also some terms in M^6 and M^8 that should be disregarded because they are incomplete.
(d) Iteration will yield in a single step groups of terms of nearly the same order that require several steps in a series expansion. For example, in axisymmetric slender-body theory, each iteration adds one more of the following groups of terms:

$$[1], \quad [\varepsilon^2 \log \varepsilon, \varepsilon^2], \quad [\varepsilon^4 \log^2 \varepsilon, \varepsilon^4 \log \varepsilon, \varepsilon^4], \ldots$$

Whichever method is used, there are certain features common to all perturbation solutions. The basic solution may be linear or nonlinear, but all higher approximations are governed by linear equations with linear boundary conditions. An exception arises in the case of transonic and hypersonic small-disturbance theory, where the double limit process is specifically designed to retain in the perturbation the essential nonlinearity of the problem. In those special cases only the third and subsequent terms in the series satisfy linear problems. Otherwise, because first-order perturbations are linearly independent, they may be superimposed. For example, the three perturbations studied separately in Sections 2.2, 2.3, and 2.4 may be added to give the first-order solution for slightly compressible flow past a slightly distorted circle in a slight shear flow. Higher approximations, however, will be coupled through cross products of the various ε's.

Although the equations governing higher approximations are linear, they ordinarily contain nonconstant coefficients that depend upon the previous approximations. It is often possible to simplify the computation dramatically by taking advantage of known relations for those earlier results. A simple example will appear in Chapter IV in thin-airfoil theory, where both the differential equations and the boundary conditions are used to simplify their counterparts in subsequent approximations.

As in the Janzen-Rayleigh solution of Section 2.4, higher-order problems typically differ from one another only in the appearance of successively more complicated nonhomogeneous terms (depending upon previous approximations) in the differential equations. These are accounted for by finding a particular integral. Usually the best way of seeking a particular integral is to guess it. Only after that attempt has failed should one apply more sophisticated processes of analysis.

One should also be on the alert for the occasional problem in which a *general particular integral* can be found in terms of previous approximations. We illustrate this possibility by two examples from the small-disturbance theory of axisymmetric compressible flow. First, in an approximate linearized theory of supersonic propellers the second-order velocity potential is found to satisfy the nonhomogeneous wave equation

$$\square^2\phi_2 = (1 - M^2)\phi_{2xx} + \phi_{2rr} + \frac{\phi_{2r}}{r} + \frac{\phi_{2\theta\theta}}{r^2} = 2M\phi_{1x\theta} \tag{3.21a}$$

where the first approximation is a solution of the homogeneous equation $\square^2\phi_1 = 0$. Burns (1951) has noticed that a particular integral is always given in terms of the first-order solution by

$$\phi_{2p} = \frac{M}{1 - M^2}\, x\phi_{1\theta} \tag{3.21b}$$

Second, if one seeks to improve the linearized theory of subsonic or supersonic flow past a body of revolution by considering nonlinear terms, the second-order potential satisfies

$$\square^2\phi_2 = M^2\{[2 + (\gamma - 1)M^2]\phi_{1x}\phi_{1xx} + 2\phi_{1r}\phi_{1xr} + \phi_{1r}^2\phi_{1rr}\} \tag{3.22a}$$

where again $\square^2\phi_1 = 0$. Van Dyke (1952) has found that to within third-order terms a particular integral is given by

$$\phi_{2p} = M^2\left[\phi_{1x}\left(\phi_1 - \frac{\gamma + 1}{2}\frac{M^2}{1 - M^2} r\phi_{1r}\right) - \tfrac{1}{4} r\phi_{1r}^3\right] \tag{3.22b}$$

Particular integrals of this sort are also ordinarily found by trial rather than by systematic analysis. Analogous solutions of some homogeneous equations were discovered by Lin and Schaaf (1951) for viscous flow.

3.8. Transfer of Boundary Conditions

Often a boundary condition is imposed at a surface whose position varies slightly with the perturbation quantity ε. The surface may be that of a solid body (as for the slightly distorted circle of Section 2.3), a free streamline, a shock wave, etc. (Fig. 3.3). In order to carry out a systematic expansion scheme, the boundary condition must in each case be expressed in terms of quantitites evaluated at the basic position of the surface, corresponding to $\varepsilon = 0$. Otherwise ε will appear implicitly as well as

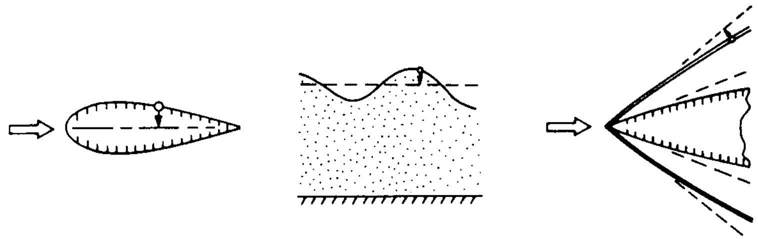

Fig. 3.3. Examples of transfer of boundary conditions.

explicitly in the perturbation expansion, so that the result is unnecessarily complicated, the series is not an asymptotic expansion, and it is not possible to equate like functions of ε.

The transfer of a boundary condition is effected by using a knowledge of the way in which the solution varies in the vicinity of the basic surface. Often the solution is known to be analytic in the coordinates, in which case the transfer is accomplished by expanding in Taylor series about the values at the basic surface. In the first approximation this usually means that the condition is simply shifted from the disturbed to the basic surface. In axisymmetric slender-body theory, on the other hand, the solution is singular on the axis, but the transfer can be carried out using the fact that the velocity potential varies near the axis like $\log r$ or the radial velocity like $1/r$.

After the solution is calculated, values of flow quantities are often required at the body or other surface. These can be found in simplest form by repeating the transfer process, expressing them in terms of values at the basic surface. Both of these transfer processes are illustrated in Chapter IV; see also Exercises 2.1, 2.3, and 3.2.

3.9. Direct Coordinate Expansions

Perturbation problems in which the small quantity is a dimensionless combination involving the coordinates (space or time) rather than the parameters alone have certain special features. A useful discussion of the distinction between parameter and coordinate expansions is given by Chang (1961). The essential point is that no derivatives with respect to a parameter occur, and it is therefore possible to calculate the solution for one value of the parameter without considering other values. Ordinarily one seeks an approximation for either small or large values of one of the coordinates. It is useful to designate these respectively as *direct* and *inverse coordinate expansions.*

A direct coordinate expansion is natural to a problem governed by parabolic or hyperbolic differential equations. One expands the solution for small values of a time-like variable, which can of course be a space coordinate rather than actual time. The perturbation quantity must increase in the positive sense of that variable, following time's arrow. Then there is no backward influence, so that each term in the perturbation series is independent of later ones, and can be calculated in its turn. The result is a perturbation expansion that describes the early stages of the evolution of the solution from a known basic initial state.

The following are typical examples of direct coordinate expansions. Goldstein and Rosenhead (1936) have calculated the growth of the boundary layer on a cylinder set impulsively into motion by expanding in powers of the time, the governing equations being parabolic. Near the stagnation point of a circle, for example, they find the skin friction to be given by

$$\tau \sim \rho\nu^{1/2}U_1^{3/2}x\,\frac{1}{\sqrt{\pi U_1 t}}\,[1 + 1.42442(U_1 t) - 0.21987(U_1 t)^2 + \cdots] \qquad (3.23)$$

where U_1 is the gradient of inviscid surface speed at the nose and x the distance along the surface. As shown in Fig. 3.4, this series obviously

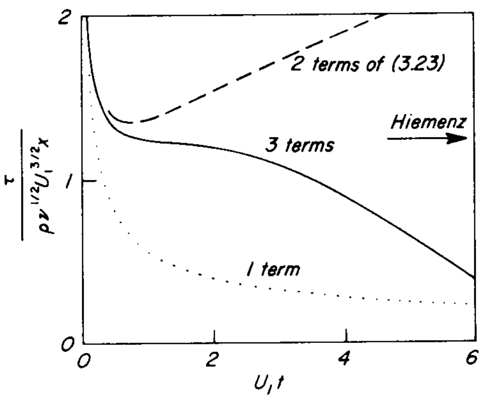

Fig. 3.4. Growth of skin friction near a stagnation point.

diverges for large time, where it should approach Hiemenz' result for steady flow. Such nonuniformity usually arises in direct coordinate expansions (but see Sections 10.6 to 10.8).

A case where a space coordinate assumes the time-like role is Blasius' expansion of the steady boundary layer on a cylinder in powers of the distance x from the stagnation point, the boundary-layer equation (2.25a) being parabolic for steady as well as unsteady motion. The result (1.5) for the parabola is believed to converge only for $x/a < \pi/4$ (Van Dyke, 1964a). Another such case, involving hyperbolic equations, is the axisymmetric Crocco problem: a perturbation of the self-similar solution for supersonic flow past a circular cone yields the initial flow gradients at the tip of an ogive of revolution (Cabannes, 1951).

For elliptic equations, coordinate expansions usually provide only qualitative results. One ordinarily encounters a boundary-value rather than an initial-value problem. Then because of backward influence any local solution depends on remote boundary conditions, and it is not possible to calculate successive terms of an expansion for small values of a coordinate. All that can be achieved is to find the *form* of the expansion, each term being indeterminate by one or more constants. For example, Carrier and Lin (1948) have examined the nature of viscous flow near the leading edge of a flat plate by expanding for small radius. Their series for the stream function is, after correction

See Note 8

$$\psi = 2Ar^{3/2}\left(\cos\frac{\theta}{2} - \cos\frac{3}{2}\theta\right) - Br^{5/2}\left(\cos\frac{\theta}{2} - \cos\frac{5}{2}\theta\right)$$
$$- \frac{A^2}{4\nu}\,r^3\{2\sin^2\theta[\log r\sin\theta + (\theta - \pi)\cos\theta]$$
$$+ \frac{8}{5}(\sin 2\theta - 2\sin\theta) + \frac{4}{3}C\sin^3\theta\} + \cdots \qquad (3.24)$$

where $\theta = 0$ on the plate. The constants $A, B, C, \ldots$ depend upon boundary conditions far outside the range of validity of the expansion, and are therefore undeterminable within the framework of the analysis.

An exception is the unconventional case of an initial-value problem for an elliptic equation. In the inverse problem of supersonic flow past a blunt body (Fig. 3.5), the detached shock wave is prescribed, and one seeks the body that produces it. Although the flow is subsonic near the axis, the stream function can be expanded in powers of the distance downstream of the shock wave, and the coefficients found in succession. Cabannes (1956) has calculated seven terms of the series when $M = 2$.

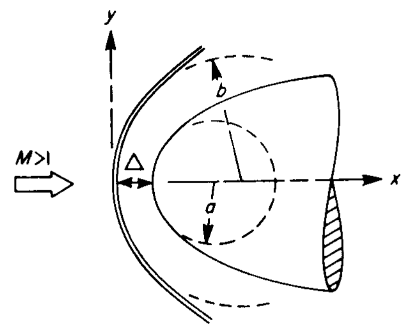

Fig. 3.5. Supersonic flow past a blunt body.

For a paraboloidal shock wave, the stream function is described near the axis by

$$\frac{\psi}{y^2} = \frac{1}{2} - \frac{5}{3}\frac{x}{a} - \frac{85}{18}\left(\frac{x}{a}\right)^2 - \frac{215}{27}\left(\frac{x}{a}\right)^3 - \frac{11{,}945}{324}\left(\frac{x}{a}\right)^4$$
$$- \frac{7051}{243}\left(\frac{x}{a}\right)^5 - \frac{1{,}817{,}909}{2916}\left(\frac{x}{a}\right)^6 - \cdots \tag{3.25}$$

Aside from such rare exceptions, direct coordinate expansions can be effectively applied to elliptic equations only by treating them as if they were parabolic and truncating the series at a finite number of terms.

The blunt-body problem is so intractable that several investigators have been willing to introduce another independent variable in order to render the equations parabolic or hyperbolic. Thus Cabannes (1953) considers an impulsive start, and expands the unsteady flow field in powers of the time. He suggests that the accuracy will increase with Mach number; at $M = \infty$ and for $\gamma = 7/5$ he finds as the ratio of shock-wave standoff distance Δ to nose radius a for any smooth body:

$$\frac{\Delta}{a} = \frac{1}{5}\left(\frac{Ut}{a}\right) - (n-1)\frac{7}{75}\left(\frac{Ut}{a}\right)^2 + \cdots \tag{3.26}$$

Here n is the number of space dimensions: $n = 2$ for plane flow and $n = 3$ for axisymmetric flow. We can expect the result to be the more accurate for plane motion, because it is exact for the one-dimensional piston problem $n = 1$. The series evidently diverges for large time, but Cabannes attempts to estimate its limit as the maximum given by the two known terms. This yields $\Delta/a = 0.107$ for plane flow, compared with accurate numerical calculations of 0.377 for the circular cylinder. We reconsider this discrepancy in Section 10.7.

3.10. Inverse Coordinate Expansions

In contrast to direct expansions, which usually possess a finite radius of convergence, inverse expansions for large values of a coordinate ordinarily appear to be divergent asymptotic series. They also suffer from indeterminacy irrespective of the type of the governing equations. For elliptic equations the situation is the same as that discussed above for a direct expansion. However, the undetermined constants can sometimes be related to simple integral properties of the solution. Thus the first few constants in the expansion for subsonic flow far from a finite body can be identified with its lift, drag, moment, etc. (Imai, 1953; Chang, 1961). For parabolic and hyperbolic equations, indeterminacy arises because the expansion runs contrary to the direction of the time-like variable. Eigensolutions therefore appear at an early stage, whose constant multipliers depend upon certain details of the previous history. Occasionally a few of these can be supplied without detailed knowledge of past events by invoking some global conservation principle (cf. Section 4.5). More often a sequence of constants remains undetermined.

The form of an inverse coordinate expansion varies widely with the type of the equations, the number of space dimensions, and the extent of the body. In some problems the leading term of the expansion is obvious; for example, it is evidently the undisturbed stream for the steady flow far from a finite body, the conical motion for flow far downstream on a blunted cone, and the corresponding steady motion for the flow long after an impulsive start. Then one perturbs that basic solution to find how it is approached. The approach is sometimes algebraic, in inverse powers of the large coordinate, as for noncirculatory potential flow far from a finite body (Imai, 1953). It very often involves logarithmic as well as algebraic terms, as for circulatory potential motion or viscous flow far from a body (Chang, 1961). In time-dependent problems it is often exponential, as for unsteady viscous or free-streamline flows (Kelly, 1962; Curle, 1956).

We quote one example. The Blasius series for the boundary layer (Section 2.6) is a direct coordinate expansion for small distances from the stagnation point. On a parabolic cylinder we can supplement that approximation by an inverse expansion for large distances. It is evident that the leading term is the solution for the flat plate, because far downstream the nose radius is negligible compared with the dimensions of interest. Perturbing that basic solution yields as the complement to (1.5) for the coefficient of skin friction

$$c_f \sim 0.6641\sqrt{\frac{\nu}{Ux}}\left[1 + 0.3006\,\frac{\log(2x/a)}{x/a} + \frac{C_1 - 1}{2x/a} + \cdots\right] \tag{3.27}$$

Here x is the abscissa, and C_1 is an undetermined constant multiplying the first of an infinite sequence of eigensolutions for the flat-plate solution (Section 7.6).

Sometimes the leading term is by no means obvious. Free-streamline motion provides an example of the complications that may appear. In plane flow the width of the deadwater region increases far downstream like $x^{1/2}$, but in axisymmetric flow it has the unlikely growth of $x^{1/2}(\log x)^{-1/4}$ (Levinson, 1946).

3.11. Change of Type and of Characteristics

A curious feature of perturbation methods is that they may spuriously change the type of the governing partial differential equations. A striking example is Prandtl's boundary-layer approximation. Although the Navier-Stokes equations are elliptic, they are replaced by parabolic equations inside the boundary layer, and by elliptic or hyperbolic ones outside, according as the flow is subsonic or supersonic. Again, in the theory of surface waves the elliptic Laplace equation is replaced by a nonlinear hyperbolic equation in the shallow-water approximation (Stoker, 1957). Conversely, the hyperbolic equations of inviscid supersonic motion become elliptic in the slender-body approximation (Ward, 1955).

These changes of type imply significant changes in the regions of influence and dependence, and in the boundary conditions required. Thus Prandtl's boundary-layer equations, because they are parabolic, can be integrated step-by-step downstream. The backward influence of their elliptic antecedents has been suppressed, but will reassert itself in higher approximations (cf. Chapter VII). Similarly, the Kutta-Joukowski condition must be abandoned at a subsonic trailing edge in thin-wing theory, because its upstream influence has been lost.

Some assumption of smoothness underlies any such change of type. The true type of the equations must be recognized wherever that assumption is violated. Otherwise the perturbation solution will break down at least locally. Thus boundary-layer theory is invalid near a corner, as are the shallow-water and slender-body approximations. These thus become singular perturbation problems as the result of discontinuities in the boundary conditions.

Often the tendency toward change of type is incomplete; the perturbation equations merely become "less hyperbolic" or "more elliptic." For hyperbolic equations this means that the characteristic surfaces are changed. An example is supersonic small-disturbance theory, where at each stage the true characteristics are approximated in the perturbation equations by the free-stream Mach cones. Again this defect is inconsequential if the body is sufficiently smooth, but otherwise leads to nonuniformities (cf. Chapter VI and Exercise 3.4).

EXERCISES

3.1. *Modified hypersonic similarity rule.* According to hypersonic small-disturbance theory the pressure coefficient on a slender wedge or cone of semivertex angle ε has the form

$$C_{p_s} \approx \varepsilon^2 f(M\varepsilon)$$

Devise an alternative form that can be expected to be superior for thick bodies in view of Newtonian impact theory, according to which the pressure coefficient at any point on a body in hypersonic flight is twice the square of the sine of the angle of the surface with the stream. Exhibit the degree of improvement realized by making numerical comparison with the full solutions at $M = \infty$. Investigate whether the result can be extended further to thick bodies at lower speeds if one is guided by the supersonic similarity rule

$$C_{p_s} \approx \frac{1}{M^2 - 1} F(\sqrt{M^2 - 1}\,\varepsilon)$$

3.2. *Transfer of tangency condition.* A small sphere pulsates in still air, its radius varying with time as $\varepsilon f(t)$, and thereby produces weak outgoing waves whose velocity potential satisfies the acoustic equation $\phi_{tt} = c^2 \nabla^2 \phi$. Show that if the function f is sufficiently smooth the tangency condition can approximately be transferred to the origin as

$$\lim_{r \to 0} r^2 \phi_r = \frac{1}{3} \frac{d}{dt} [\varepsilon f(t)]^3$$

Calculate ϕ using this condition. How smooth must f be? What happens to the solution if that restriction is violated?

3.3. *Estimate of ultimate value from coordinate expansion.* Test Cabannes' idea for estimating the value of (3.26) at infinite time by applying it to (3.23) and (1.5), where the answers are known. Should one choose the value at the inflection point when no extremum exists? Try to devise a better or more rational scheme of this sort.

3.4. *Effect of change of characteristics.* The following problem is a mathematical model of steady supersonic flow over the upper surface of a thin airfoil:

$$\phi_{yy} - \phi_{xx} = \varepsilon \phi_{xx}, \qquad \phi(0, y) = \phi_x(0, y) = 0 \quad \text{for} \quad y > 0$$

$$\phi_y(x, 0) = \varepsilon f'(x), \qquad \text{where} \quad f(x) = 0 \quad \text{for} \quad x < 0$$

Solve it by first neglecting the right-hand side of the differential equation, and then iterating to find the second approximation. Compare with the exact solution to deduce under what restrictions on the function f the nth approximation is valid near the surface. Discuss what happens at great distances.

Chapter IV

SOME SINGULAR PERTURBATION PROBLEMS IN AIRFOIL THEORY

4.1. Introduction

We proceed now to consider problems in which the straightforward perturbation schemes used heretofore break down in some region of the flow field. There the ratio of successive terms is not small, as was assumed, so that locally the approximation ceases to be an asymptotic expansion. As a consequence of this nonuniformity, one may miscalculate or even lose essential results, such as the skin friction and heat transfer in viscous flow at high Reynolds numbers, or the drag of a thin airfoil. Moreover, at some early stage it usually becomes impossible to proceed even formally to higher approximations. These are singular perturbation problems. An excellent survey by Friedrichs (1955) discusses their occurrence in branches of mathematical physics other than fluid mechanics.

The prototype of a singular perturbation problem is Prandtl's boundary-layer theory. However, we introduce the subject instead by studying the simpler problem of incompressible flow past a thin airfoil. Because the motion is governed by the two-dimensional Laplace equation, which is linear, it is possible to exhibit the results in analytic form, and so display the main ideas more clearly. This problem is also admirably suited for introducing two well-known methods that have been devised for treating singular perturbation problems. Thus the present chapter forms the cornerstone of the book. The subsequent chapters are simply devoted to amplifying and extending the ideas set forth here in connection with our standard problem of the thin airfoil.

The plan of attack is the following. We first calculate formally the thin-airfoil expansion for a general symmetric profile. Then for several specific shapes we exhibit the nonuniformities and nonuniquenesses that arise because we violate the assumption of small disturbances at stagnation points. Finally, we correct those defects, first by using an intuitive physical argument, second by matching with a local solution in the spirit of boundary-layer theory, and third by straining the coordinates in the case of a round edge.

4.2. Formal Thin-Airfoil Expansion

We consider uniform plane flow of an incompressible inviscid fluid past a thin airfoil. For simplicity, we restrict attention to symmetric flow, because it embodies all the essential features. However, asymmetric effects due to camber and incidence can be treated similarly. For details the reader can see the modern expositions of thin-airfoil theory given by Lighthill (1951), Jones and Cohen (1960), and Thwaites (1960).

We use Cartesian coordinates, with the chord of the airfoil spanning any convenient segment of the x-axis, whose length may be assumed to be of order unity. Then let the airfoil be described by $y = \pm\varepsilon T(x)$, where ε is some thickness parameter, and $T(x)$ a function of order unity that gives the thickness distribution (Fig. 4.1). Varying ε produces a family of affinely related profiles.

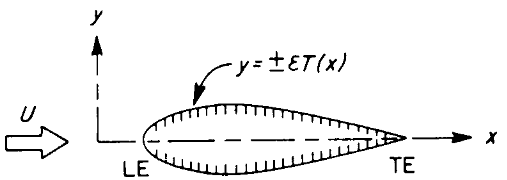

Fig. 4.1. Symmetric flow past thin airfoil.

The flow is irrotational, and it is convenient—with extension to three dimensional flows in view—to work with a velocity potential ϕ. Let it be normalized such that the velocity vector is given by $\mathbf{q} = U \operatorname{grad}\phi$ where U is the free-stream speed. Then the full problem is

$$\text{differential equation:}\quad \phi_{xx} + \phi_{yy} = 0 \tag{4.1a}$$

$$\text{upstream condition:}\quad \phi \sim x + o(1) \quad \text{as} \quad x^2 + y^2 \to \infty \tag{4.1b}$$

$$\text{tangency condition:}\quad \frac{\phi_y}{\phi_x} = \pm\varepsilon T'(x) \quad \text{at} \quad y = \pm\varepsilon T(x) \tag{4.1c}$$

The second term in the asymptotic condition (4.1b) merely requires that the perturbation potential vanish at infinity, although it is actually $O(1/r)$ for a closed body. This requirement ensures a unique solution by ruling out circulation.

This innocuous-looking problem, involving only the simplest linear elliptic partial differential equation, is difficult to solve with acceptable accuracy. The standard numerical method of conformal mapping due to Theodorsen (Abbott and von Doenhoff, 1959) is tedious and inaccurate. Hence the thin-airfoil approximation is of practical utility as well as theoretical interest. It is even more useful in subsonic compressible flow, where the equation of motion is nonlinear, and in three dimensions, where conformal mapping is inapplicable.

We seek the asymptotic expansion of the solution as the thickness parameter ε tends to zero. In the limit, the airfoil degenerates to a line which causes no disturbance of the free stream, so the basic solution is the uniform parallel flow. We tentatively assume that the asymptotic series has, for a given thickness function T, the form

$$\phi(x, y; \varepsilon) \sim x + \varepsilon\phi_1(x, y) + \varepsilon^2\phi_2(x, y) + \varepsilon^3\phi_3(x, y) + \cdots \tag{4.2}$$

It is implied here that the expansion proceeds indefinitely in integral powers of ε. This appears to be true for incompressible flow unless the airfoil is extremely blunt; see Exercise 4.3. For subsonic compressible flow past a round-nosed profile, however, our example (1.2) illustrates that logarithms of ε appear beginning with $\varepsilon^4 \log \varepsilon$.

In order to substitute this expansion into the full problem and equate like powers of ε, we must transfer the tangency condition (4.1c) to the axis $y = 0$. If we assume that the $\phi_n(x, y)$ are analytic in y at $y = 0$, we can expand in Taylor series to obtain

$$\begin{aligned}\phi_y(x, \pm\varepsilon T) = {} & \varepsilon\phi_{1y}(x, 0\pm) + \varepsilon^2[\phi_{2y}(x, 0\pm) \\ & \pm T(x)\phi_{1yy}(x, 0\pm)] + \varepsilon^3[\phi_{3y}(x, 0\pm) \\ & \pm T\phi_{2yy}(x, 0\pm) + \tfrac{1}{2}T^2\phi_{1yyy}(x, 0\pm)] + \cdots\end{aligned} \tag{4.3}$$

and similarly for ϕ_x. Here $y = 0\pm$ refers to the top and bottom sides of the slit to which the airfoil degenerates in the limit as $\varepsilon \to 0$, and across which ϕ_y is discontinuous (whereas ϕ_x is continuous). This expansion, though essential to obtaining a series of the desired form (see Section 3.8), is one source of the nonuniformities that we encounter later. We might anticipate difficulties because of the successively higher derivatives that appear.

Thus we obtain a sequence of problems that are linear in the tangency condition as well as the differential equation, the first being that of conventional linearized thin-airfoil theory:

$$\phi_{1xx} + \phi_{1yy} = 0 \tag{4.4a}$$

$$\phi_1 = o(1) \quad \text{as} \quad x^2 + y^2 \to \infty \tag{4.4b}$$

$$\phi_{1y}(x, 0\pm) = \pm T'(x) \tag{4.4c}$$

$$\phi_{2xx} + \phi_{2yy} = 0 \tag{4.5a}$$
$$\phi_2 = o(1) \quad \text{as} \quad x^2 + y^2 \to \infty \tag{4.5b}$$
$$\begin{aligned}\phi_{2y}(x, 0 \pm) &= \pm T'(x)\phi_{1x}(x, 0) \mp T(x)\phi_{1yy}(x, 0) \\ &= \pm [T(x)\phi_{1x}(x, 0)]'\end{aligned} \tag{4.5c}$$

$$\phi_{3xx} + \phi_{3yy} = 0 \tag{4.6a}$$
$$\phi_3 = o(1) \quad \text{as} \quad x^2 + y^2 \to \infty \tag{4.6b}$$
$$\begin{aligned}\phi_{3y}(x, 0 \pm) &= \pm T'(x)\phi_{2x}(x, 0) + T(x)T'(x)\phi_{1xy}(x, 0) \\ &\mp T(x)\phi_{2yy}(x, 0) - \tfrac{1}{2}T^2(x)\phi_{1yyy}(x, 0) \\ &= \pm [T(x)\{\phi_{2x}(x, 0) + \tfrac{1}{2}T(x)T''(x)\}]'\end{aligned} \tag{4.6c}$$

The simpler alternative forms given for the second- and third-order tangency conditions (4.5c) and 4.6c) are obtained by making use of both the differential equations and the tangency conditions from previous approximations. As a result of this modification, each problem is formally the same as the first. Any higher approximation can be regarded as the first approximation for some fictitious airfoil whose thickness function $T_n(x)$ is the last square bracket in the tangency condition.

Flow quantities at the surface of the airfoil can be expressed as power series in ε by relating them, again through Taylor series expansion, to the velocity components on the axis. Because ϕ_{ny} is given there by the tangency condition, one needs only $\phi_{nx}(x, 0)$. Thus, for example, the surface speed q is found to be given by

$$\frac{q}{U} = 1 + \varepsilon\phi_{1x}(x, 0) + \varepsilon^2[\phi_{2x}(x, 0) + T(x)T''(x) + \tfrac{1}{2}T'^2(x)] + \cdots \tag{4.7}$$

Of course this process represents another possible source of nonuniformities.

4.3. Solution of the Thin-Airfoil Problem

We have reduced each higher-order thin-airfoil problem to the form of the first. This crucial problem can be solved in various ways. It is usually simplest to use complex-variable theory, the best method often being to guess $(\phi_x - i\phi_y)$ as a function of the complex variable $z = x + iy$ that satisfies the boundary conditions. A useful table of such solutions is given by Jones and Cohen (1960).

Methods based upon the complex variable have the disadvantage, however, that they cannot be generalized to three-dimensional flows. An alternative method that is capable of such generalization is the

representation of the body by a distribution of singularities. Sources, dipoles, and so on, can be placed either on the surface or inside the body. In thin-airfoil theory they are naturally distributed along the axis between the leading and trailing edges. Only sources and sinks are required in our symmetrical problem, an equal quantity of each being needed for a closed body.

A point source of unit strength at the origin gives

$$\phi = \frac{1}{2\pi} \log \sqrt{x^2 + y^2} = \frac{1}{2\pi} \operatorname{Re} \log z \tag{4.8a}$$
$$\phi_x = \frac{1}{2\pi} \frac{x}{x^2 + y^2} \tag{4.8b}$$
$$\phi_y = \frac{1}{2\pi} \frac{y}{x^2 + y^2} \tag{4.8c}$$

For a sufficiently smooth airfoil, considerations of continuity show that the local source strength must be twice the airfoil slope. This approximation is, in fact, justified to precisely the same extent as our transfer of the tangency condition to the axis. Hence the solution of any one of the thin-airfoil problems (4.4), (4.5), etc., is given by

$$\phi_{nx}(x, y) = \frac{1}{\pi} \int_{\text{LE}}^{\text{TE}} \frac{(x - \xi)\phi_{ny}(\xi, 0+)}{(x - \xi)^2 + y^2}\, d\xi \tag{4.9a}$$
$$\phi_{ny}(x, y) = \frac{1}{\pi} \int_{\text{LE}}^{\text{TE}} \frac{y\phi_{ny}(\xi, 0+)}{(x - \xi)^2 + y^2}\, d\xi \tag{4.9b}$$

as can be verified by direct substitution, or in complex form

$$\phi_{nx} - i\phi_{ny} = \frac{1}{\pi} \int_{\text{LE}}^{\text{TE}} \frac{\phi_{ny}(\xi, 0+)}{x + iy - \xi}\, d\xi \tag{4.9c}$$

In order to calculate surface values, as in (4.7), we need only

$$\phi_{nx}(x, 0) = \frac{1}{\pi} \oint_{\text{LE}}^{\text{TE}} \frac{\phi_{ny}(\xi, 0+)}{x - \xi}\, d\xi = \frac{1}{\pi} \oint_{\text{LE}}^{\text{TE}} \frac{T_n'(\xi)}{x - \xi}\, d\xi \tag{4.10}$$

Here the Cauchy principal value of the divergent integral is indicated if x lies between the leading and trailing edges. A table of the *airfoil integral* (4.10) for a number of thickness functions $T(x)$ is given by Van Dyke (1956).

4.4. Nonuniformity for Elliptic Airfoil

Most subsonic airfoils have round leading edges. The simplest finite round-nosed profile is the ellipse, which we will investigate in considerable detail. Let the thickness function be $T(x) = \sqrt{1 - x^2}$, which describes an ellipse of thickness ratio ε extending over $-1 \leqslant x \leqslant 1$ (Fig. 4.2). The radius of the leading and trailing edges is ε^2.

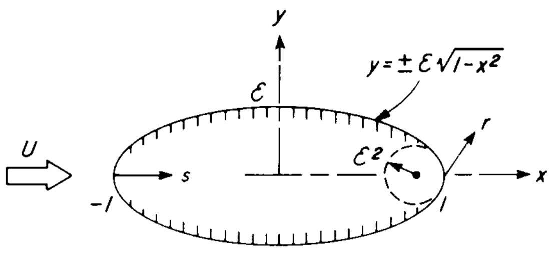

Fig. 4.2. Elliptic airfoil.

Substituting into (4.10) yields as the solution of the first-order problem (4.4) for ϕ_{1x} on the axis

$$\phi_{1x}(x, 0) = -\frac{1}{\pi}\oint_{-1}^{1} \frac{\xi \, d\xi}{\sqrt{1-\xi^2}\,(x-\xi)} = \begin{cases} 1, & x^2 < 1 \\ 1 - \sqrt{\dfrac{x^2}{x^2-1}}, & x^2 > 1 \end{cases} \tag{4.11}$$

More generally, the complex perturbation velocity throughout the flow field is, from the table of Jones and Cohen:

$$\phi_{1x} - i\phi_{1y} = 1 - \frac{z}{\sqrt{z^2-1}} \tag{4.12}$$

With proper attention to principal values at branch cuts, this reproduces (4.11) on the axis. Then (4.7) gives the familiar result of linearized thin-airfoil theory that the surface speed is constant on an ellipse, with $q/U = 1 + \varepsilon$. This value happens to be exact at the middle of the ellipse, where the maximum occurs (Fig. 4.3).

It is a misleading circumstance that the first-order surface speed is finite even at the ends of the airfoil. According to (4.12) the perturbation velocity itself is singular at the leading and trailing edges. The assumption of small disturbances has been violated at the stagnation points, and as a consequence the solution has broken down locally. The thin-airfoil solution is not uniformly valid near the edges.

The perturbation velocity is singular like a multiple of $\varepsilon/r^{1/2}$, where r is the distance from the stagnation point. Hence the region of nonuniformity is a circular neighborhood whose radius is of order ε^2. As

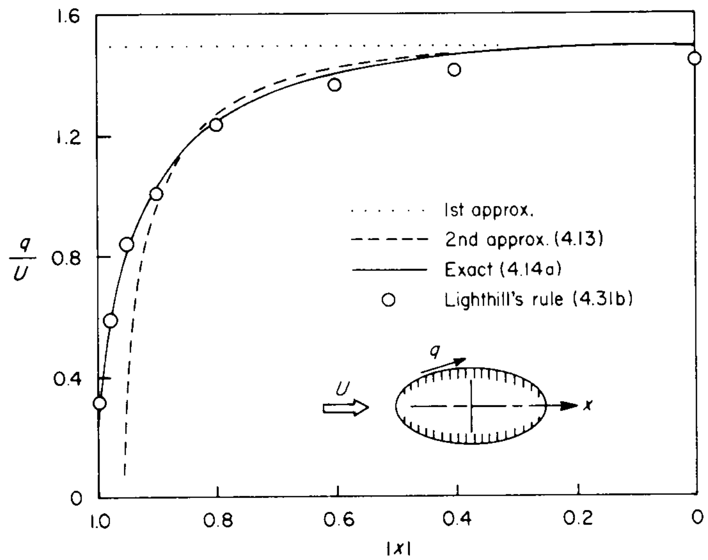

Fig. 4.3. Surface speed on ellipse with $\varepsilon = 0.5$.

might have been anticipated on physical grounds, this is of the order of the leading-edge radius.

The failure of the perturbation solution is compounded in higher approximations. The problem (4.5) for ϕ_2 is seen to be identical with that for ϕ_1. Hence the second approximation for surface speed is found from (4.7) as

$$\frac{q}{U} \sim 1 + \varepsilon - \frac{1}{2}\varepsilon^2 \frac{x^2}{1-x^2} \tag{4.13}$$

and this is singular like the square of $\varepsilon/r^{1/2}$. The first and second approximations for the case $\varepsilon = 0.5$ are compared with the exact result in Fig. 4.3, where the divergence of the series near the stagnation point is evident. Further terms can be calculated indefinitely, and the $2n$th approximation found to be singular like $(\varepsilon/r^{1/2})^{2n}$, with the signs alternating in a futile attempt to attain zero speed at the stagnation point by superposing successively stronger singularities. (As in the first approximation, velocity components of odd order are also singular, but contribute only regular terms to the surface speed.) Thus the solution is improved at each stage except within a distance of order ε^2 from either edge, where it becomes worse.

The formal thin-airfoil expansion can be verified by comparison with the full solution, which is readily calculated by conformal mapping or separation of variables in elliptic coordinates. The exact result for surface speed is

$$\frac{q}{U} = \frac{1 + \varepsilon}{\sqrt{1 + \varepsilon^2[x^2/(1 - x^2)]}} \tag{4.14a}$$

Expanding this formally for small ε yields

$$\frac{q}{U} = 1 + \varepsilon - \frac{1}{2}\varepsilon^2 \frac{x^2}{1 - x^2} - \frac{1}{2}\varepsilon^3 \frac{x^2}{1 - x^2} + \frac{3}{8}\varepsilon^4 \frac{x^4}{(1 - x^2)^2} + \cdots \tag{4.14b}$$

which confirms and extends our result (4.13). Moreover, it makes evident the source of the nonuniformity. The singular terms arise from expanding the denominator by the binomial theorem, which is justified only if

$$(1 - x^2) > \frac{\varepsilon^2}{1 + \varepsilon^2} \tag{4.15}$$

and hence not uniformly near the stagnation points $x = \pm 1$.

4.5. Nonuniqueness; Eigensolutions

The verification just given is important, because for a round nose the solution of the thin-airfoil problem is not mathematically unique. The tangency conditions (4.4c), (4.5c), etc., are singular at a round edge. Therefore one is entitled to add to the solution any harmonic function that is singular there but does not otherwise affect the boundary conditions. In the present problem one such function is given by a point source located at one edge and a sink of equal strength at the other:

$$\phi = \frac{C}{2\pi}\left[\log\sqrt{(x + 1)^2 + y^2} - \log\sqrt{(x - 1)^2 + y^2}\right] \tag{4.16a}$$

$$\phi_x = \frac{C}{2\pi}\left[\frac{x + 1}{(x + 1)^2 + y^2} - \frac{x - 1}{(x - 1)^2 + y^2}\right] \tag{4.16b}$$

$$\phi_y = \frac{C}{2\pi}\left[\frac{y}{(x + 1)^2 + y^2} - \frac{y}{(x - 1)^2 + y^2}\right] \tag{4.16c}$$

It is evident that this leaves each of the problems (4.4), (4.5), etc., unaffected except at the leading and trailing edges, where the solution for the ellipse is singular anyhow.

This is our first example of an *eigensolution*. The role of eigensolutions in inverse coordinate expansions was discussed in Section 3.10. Although the present example is manifestly a parameter expansion, it can—because it is a singular perturbation problem—be regarded also as an inverse coordinate expansion. That is, the thin-airfoil solution becomes accurate for distances from the edges large compared with their radius ε^2. The eigensolution (4.16) represents ignorance of the details of the flow near the edges.

The x-derivative of (4.16) is also an eigensolution for the elliptic airfoil. It consists of dipoles at the leading and trailing edges (whose strengths need no longer be equal in order to satisfy the upstream condition). Similarly, an infinite sequence of successively more singular eigensolutions—consisting of quadrupoles, octupoles, etc.—is formed by repeated differentiation with respect to x.

In order to make the solution unique, the constant multiplying each possible eigensolution must be determined. This can be attempted in the following successively more sophisticated ways:

(i) *Principle of minimum singularity*. A very reliable bit of mysticism asserts that in any case of nonuniqueness the correct solution involves the weakest possible singularity. For the elliptic airfoil, this principle serves to rule out all eigensolutions in the first-order solution, all except sources in the second and third approximations, all except sources and dipoles in the fourth and fifth, and so on. A justification of the principle will appear later in Section 5.6 when we discuss matching with a local solution of boundary-layer type.

(ii) *Global conservation principle*. It is sometimes possible to find a conservation law that will serve to determine an eigensolution. For the elliptic airfoil, the principle of conservation of mass serves to rule out the source eigensolution (4.16). A convenient way of accomplishing this is to work not with the velocity potential but with the stream function, which assures that mass is conserved globally. Then the weakest admissible eigensolution is a dipole rather than a source (see Exercise 4.1). Together with the first method, this defers the indeterminacy to the fourth approximation for the elliptic airfoil.

(iii) *Matching with supplementary expansion*. Later in this chapter we generalize Prandtl's idea of examining in detail the region of nonuniformity. An essential feature of that procedure is the possibility of matching with a supplementary asymptotic expansion valid in that region. This process serves to rule out all eigensolutions in the thin-airfoil expansion for the ellipse.

In the preceding section we used none of these methods, but simply compared with the known exact solution.

All these methods may fail in more complicated problems. An example is the third approximation for the boundary layer on a semi-infinite flat plate, which is discussed in Chapter VII. In that case it is perhaps impossible, even in principle, to determine even the first eigensolution short of solving the full problem. In such difficult problems, attempts have been made to determine the first eigensolution by patching at an arbitrary point with a different approximate solution (Imai, 1957a) or by comparing with a numerical solution (Traugott, 1962).

4.6. Joukowski Airfoil; Leading-Edge Drag

The failure of the thin-airfoil expansion at a round edge means that one cannot calculate the drag by integrating surface pressures. Indeed, divergent integrals appear beyond the first approximation. The elliptic airfoil obscures this matter because the effects of the leading and trailing edges cancel by symmetry. We therefore consider instead a simple profile with only one round edge.

To second order a symmetrical Joukowski airfoil (Fig. 4.4a) is described

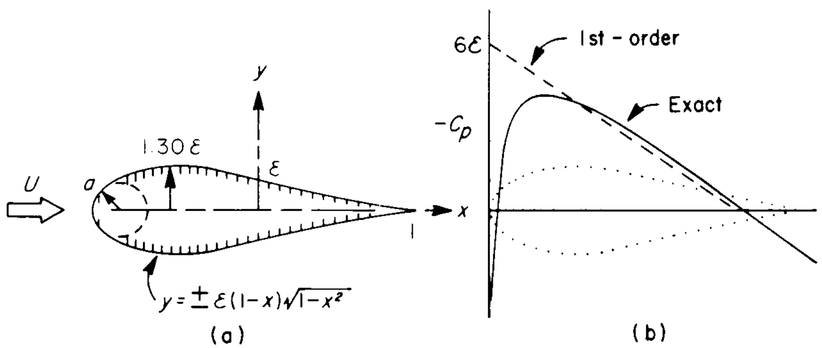

Fig. 4.4. Symmetrical Joukowski airfoil. (a) Geometry. (b) Surface pressure.

by the thickness function $T(x) = (1-x)\sqrt{1-x^2}$. The thickness ratio is ε at midchord, and $(3\sqrt{3}/4)\varepsilon = 1.30\varepsilon$ at the thickest point. For the first-order streamwise velocity perturbation on the axis (4.10) gives

$$\phi_{1x}(x, 0) = -\frac{1}{\pi}\oint_{-1}^{1} \frac{1+\xi-2\xi^2}{\sqrt{1-\xi^2}\,(x-\xi)}\,d\xi = 1-2x, \qquad x^2 < 1 \tag{4.17}$$

By continuing with the second approximation we obtain for the surface speed

$$\frac{q}{U} = 1 + \varepsilon(1-2x) - \frac{1}{2}\varepsilon^2\frac{1-x}{1+x}(1+2x)^2 + \cdots \tag{4.18}$$

and, from Bernoulli's equation, for the surface pressure coefficient

$$C_p = \frac{p-p_\infty}{\frac{1}{2}\rho U^2} = -2\varepsilon(1-2x) - 2\varepsilon^2 x\,\frac{4x^2-3}{1+x} + \cdots \tag{4.19}$$

The drag coefficient can be calculated by integrating the pressure over the surface of the airfoil according to

$$C_d = \frac{1}{\frac{1}{2}\rho U^2}\int p\,dy = \varepsilon\int_{-1}^{1} C_p(x)T'(x)\,dx \tag{4.20}$$

However, substituting the thin-airfoil expansion (4.19) shows that the second-order term is divergent at the leading edge. Keeping only first-order terms gives a negative drag:

$$C_d \approx 2\varepsilon^2\int_{-1}^{1}(1-2x^2)\sqrt{\frac{1-x}{1+x}}\,dx = -2\pi\varepsilon^2 \tag{4.21}$$

This result is obviously wrong, for the drag must vanish according to d'Alembert's principle. Because first-order thin-airfoil theory fails to predict the pressure rise near the stagnation point (Fig. 4.4b), it misses a positive contribution to drag that would exactly cancel the thrust of the remainder of the airfoil that we have just calculated.

Jones (1950) has shown that this *leading-edge drag* can be recovered by calculating the drag not from surface pressures but with a momentum contour that avoids the region of invalidity near the leading edge. It can also be recovered by correcting the surface pressure near the edge using methods discussed later; and only this method is successful in the second and higher approximations.

Thus one finds that the leading-edge drag to be added to the integral of surface pressure in linearized theory is the same for any round-nosed airfoil as for our Joukowski profile. It is given in general terms by

$$D_{\mathrm{LE}} = \tfrac{1}{2}\pi\rho U^2 a \tag{4.22}$$

where a is the leading-edge radius, equal to $4\varepsilon^2$ for the Joukowski airfoil of Fig. 4.4. This is just the drag of an infinite parabola of the same nose radius, defined—following Prandtl and Tietjens (1934)—as the drag of a nose section separated by a cut into which the ambient pressure penetrates, in the limit as the cut moves downstream to infinity (Fig. 4.5). That this should be the case is clear from the fact that as its thickness vanishes any round-nosed airfoil is approximated by a parabola to an increasing number of radii downstream from the leading edge. This rolе of the osculating parabola will be exploited further in Section 4.8.

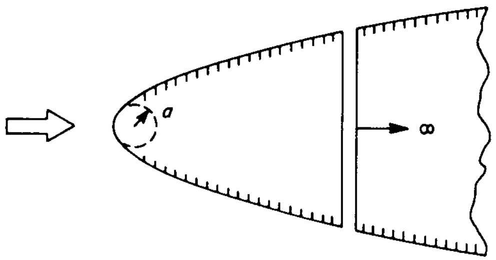

Fig. 4.5. Scheme defining drag of parabola.

A similar violation of d'Alembert's principle occurs for lifting airfoils of zero thickness. In that case, however, integration of the surface pressures predicted by linearized theory yields a spurious drag rather than a thrust. Thus for an inclined flat plate it evidently gives a resultant normal force, which has a downstream component. The resolution of this paradox is again associated with a singularity at the leading edge. The additional *leading-edge thrust* required to restore the drag to zero can be found by the methods just described for the symmetrical airfoil (von Kármán and Burgers, 1935, pp. 51-52).

4.7. Biconvex Airfoil; Rectangular Airfoil

We consider two other shapes, involving stagnation edges that are respectively sharper and blunter than those of the elliptic airfoil. First, the thickness function $T(x) = 1 - x^2$ describes a biconvex airfoil formed of two parabolic arcs (Fig. 4.6).

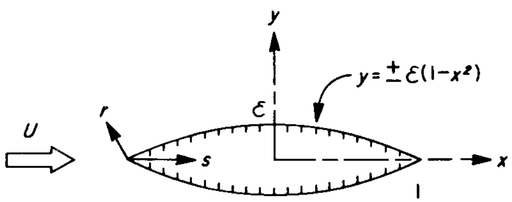

Fig. 4.6. Biconvex airfoil.

Proceeding as before gives for the first approximation

$$\phi_{1x} - i\phi_{1y} = \frac{2}{\pi}\Big(2 - z \log \frac{z+1}{z-1}\Big) \tag{4.23}$$

At the sharp stagnation edges the perturbation velocity is logarithmically infinite, behaving like $\varepsilon \log r$ even on the surface. Again this failure is compounded in higher approximations. Thus to second order the surface speed is found to be

$$\frac{q}{U} \sim 1 + \frac{2}{\pi}\varepsilon\Big(2 - x \log \frac{1+x}{1-x}\Big) + \varepsilon^2\Big[\frac{3}{\pi^2}\Big(2 - x \log \frac{1+x}{1-x}\Big)^2 - \frac{1}{\pi^2}\log^2 \frac{1+x}{1-x} - (1 - x^2)\Big] \tag{4.24}$$

This is singular like $(\varepsilon \log r)^2$ at the stagnation points, and the nth term is found to be singular like $(\varepsilon \log r)^n$. Hence the expansion is invalid within a distance of either edge of order $e^{-1/\varepsilon}$. Because this is smaller than any power of ε, it is usually negligible in practice; and at the trailing edge the nonuniformity would be swamped by viscous effects. However, it is of fundamental interest to understand and correct this minor defect as well as the more serious one at a round edge.

The singularities are so weak in this example that no practical difficulties arise. All eigensolutions can be excluded by invoking the principle of minimum singularity, because even the weakest of them—the source eigensolution (4.16)—is more singular at the stagnation points than any term in the thin-airfoil expansion. Furthermore, the integral (4.20) for the drag coefficient is convergent. Thus the formal thin-airfoil solution can be calculated to indefinitely high order for a sharp-edged airfoil.

Second, consider the rather extreme case of a thin rectangular airfoil (Fig. 4.7), which can be described by the thickness function $T(x) = H(1 - x^2) = H(x + 1) - H(x - 1)$. Here H is the Heaviside unit step function, which is zero for negative values of its argument and unity

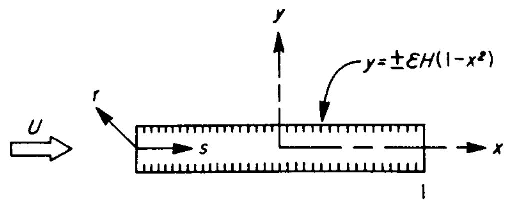

Fig. 4.7. Rectangular airfoil.

down within a distance from the leading edge of the order of the nose radius a, which is proportional to ε^2. In that vicinity the airfoil can be approximated by a parabola having the same nose radius. Moreover, the approximation becomes better as the thickness is decreased, in that it holds to a given accuracy over an increasing number of nose radii.

The exact surface speed on the parabola is easily calculated, or extracted through a limit process from the result (4.14a) for the ellipse, as

$$q = U_i \sqrt{\frac{s}{s + a/2}} \tag{4.28}$$

Here s is the distance into the edge, and U_i the maximum speed on the parabola. The latter is obviously nearly equal to the free-stream speed U, but its value will not be needed. Expanding this expression formally for small values of the nose radius a (more precisely, for small values of the ratio a/s) yields the series

$$\text{“}q\text{”} = U_i\left(1 - \frac{a}{4s} + \cdots\right) \tag{4.29}$$

The quotation marks indicate that this is only a formal result. This must be the result that would be given by thin-airfoil theory. It can in fact be extracted from the second-order solution (4.13) for the ellipse. The two terms shown here constitute the second approximation, because the nose radius is of order ε^2. There is no term of order ε because the first-order perturbation happens to vanish at the surface of a parabola.

We now claim that the ratio of these two expressions serves as a multiplicative correction factor that converts the formal thin-airfoil solution "q" for the speed on any airfoil of nose radius a into a uniformly valid approximation $\bar{q}$:

$$\bar{q} = \frac{\sqrt{\dfrac{s}{s + a/2}}}{1 - \dfrac{a}{4s} + \cdots}\,\text{“}q\text{”} \tag{4.30a}$$

The reason is that near the leading edge, where the disturbances are large, the exact speed on the airfoil is nearly that on the osculating parabola. Far from the edge, on the other hand, the correction factor approaches unity, so that the thin-airfoil solution for the airfoil is recovered where it is valid.

It is possible to simplify this rule. The denominator has already been expanded formally, so that no damage results from further expansion; and the same is true of the thin-airfoil solution "q" for the airfoil. Then

if we recall that "q"$/U$ is of the form $1 + O(\varepsilon)$, and retain only terms of order ε^2, we obtain the simpler rule

$$\frac{\bar{q}_2}{U} = \sqrt{\frac{s}{s + a/2}}\left(\frac{\text{“}q_2\text{”}}{U} + \frac{a}{4s}\right) \tag{4.30b}$$

Here the subscripts indicate that the formal second-order solution "q_2" is rendered uniformly valid to second order. This is to be understood in the sense that both leading and secondary terms—of relative order ε—are given correctly everywhere on the airfoil for the *perturbation* in speed, or the pressure coefficient.

This rule was first deduced by Lighthill (1951) by quite different reasoning that is described later in Section 4.12. He shows that it applies also at angle of attack, and to cambered airfoils. In the latter case, however, the perturbation is correct only to first order near the nose. Henceforth we refer to (4.30b) as *Lighthill's rule.*

As an example, we apply the rule to the leading edge of the elliptic airfoil, for which "q_2"$/U$ is given by (4.13). With $s = x + 1$ and $a = \varepsilon^2$ we find

$$\frac{\bar{q}_2}{U} = \sqrt{\frac{1 + x}{1 + x + \frac{1}{2}\varepsilon^2}}\left(1 + \varepsilon + \tfrac{1}{4}\varepsilon^2\,\frac{1 - 2x}{1 - x}\right) \tag{4.31a}$$

The singularity at the leading edge has been removed, and replaced by the proper zero. Of course a singularity remains at the trailing edge, so that the solution is not symmetrical in x; but that too can be eliminated by applying Lighthill's rule again with $s = 1 - x$. This yields, after further simplification, the fully uniform result

$$\frac{\bar{q}_2}{U} = \sqrt{\frac{1 - x^2}{1 - x^2 + \varepsilon^2 + \frac{1}{4}\varepsilon^4}}\,(1 + \varepsilon + \tfrac{1}{2}\varepsilon^2) \tag{4.31b}$$

The result is shown in Fig. 4.3 in comparison with the exact and the thin-airfoil solutions, which displays its uniform validity.

It is instructive to interpret the above derivation of Lighthill's rule in the light of conformal mapping. If we seek to map a uniform stream into the flow past an airfoil, the thin-airfoil approximation cannot cope with the rapid changes near a round nose. However, we can use the product of two mappings—from the uniform stream to the osculating parabola, and from that parabola to the airfoil—and thin-airfoil theory is adequate for the latter, although the former must be performed exactly. The two terms in (4.30b) correspond to these two mappings.

4.9. Local Solution near a Round Edge

We now reconsider the round-nosed airfoil from the point of view of Prandtl's boundary-layer theory. That is, we examine the details of the flow in the region of nonuniformity by introducing magnified variables. We thereby obtain a local solution that complements the thin-airfoil series, and will be matched with it in the next section. The relationship between this formal procedure and the preceding intuitive argument will become clear in the course of the analysis.

For definiteness we consider the ellipse; it will be evident how the results apply to other round-nosed airfoils. We study only the nonuniformity at the leading edge; the trailing edge is treated in exactly the same way. For simplicity we again discuss only the surface speed, but the method can obviously be applied to the entire flow field. We examine the second approximation and, in order to exhibit the effectiveness of the method, suppose that it contains an unknown multiple of the source eigensolution (4.16) in each term. According to (4.13) and (4.16) the formal thin-airfoil series for the surface speed is then

$$\frac{q}{U} = 1 + \varepsilon\Big(1 + \frac{C_1}{1 - x^2}\Big) - \frac{1}{2}\varepsilon^2\Big(\frac{x^2}{1 - x^2} + \frac{C_2}{1 - x^2}\Big) + \cdots \qquad (4.32a)$$

Of course conservation of mass can be used, as discussed in Section 4.5, to show that $C_1 = C_2 = 0$. However, we want to show that this follows from matching with the local solution, as is necessary in more difficult problems.

Because the nonuniformity under consideration occurs at the leading edge, it is convenient to shift the origin there (Fig. 4.2) by setting $s = x + 1$. Then the ellipse is described by

$$y = \pm\varepsilon\sqrt{2s - s^2} \qquad (4.33a)$$

and the thin-airfoil series (4.32a) for the surface speed may be written as

$$\frac{q}{U} \sim 1 + \varepsilon\Big[1 + \frac{C_1}{s(2 - s)}\Big] - \frac{1}{2}\varepsilon^2\Big[\frac{(1 - s)^2}{s(2 - s)} + \frac{C_2}{s(2 - s)}\Big]$$

$$\text{as } \varepsilon \to 0 \quad \text{with} \quad \frac{1}{s} = O(1) \qquad (4.32b)$$

This asymptotic expansion is invalid in the region where $s = O(\varepsilon^2)$, because there the third term is of order unity rather than small as was assumed.

We aim to introduce new independent and dependent variables—

denoted by capital letters—that are of order unity in the region of nonuniformity. Evidently s is to be magnified by a factor $1/\varepsilon^2$, and the other Cartesian coordinate y is treated similarly, because the region of nonuniformity was seen to be circular. Thus we introduce the new coordinates

$$S = \frac{s}{\varepsilon^2}, \qquad Y = \frac{y}{\varepsilon^2} \qquad (4.34)$$

In these variables the ellipse is described by

$$Y = \pm\sqrt{2S - \varepsilon^2 S^2} \qquad (4.33b)$$

The dependent variable ϕ should be correspondingly magnified by introducing $\Phi = \phi/\varepsilon^2$. However, this modification cancels out of the present problem because both the differential equation and boundary conditions are linear in ϕ.

We now consider the result of letting ε tend to zero with the magnified variables fixed. That is, as the thickness ratio vanishes we continually magnify the vicinity of the leading edge in such a way that the nose radius remains finite. In the limit the airfoil shape becomes

$$Y \sim \pm\sqrt{2S} \qquad \text{as } \varepsilon \to 0 \text{ with } S = O(1) \qquad (4.33c)$$

which is an infinite parabolic cylinder of unit nose radius. Laplace's equation is unchanged by our magnification of coordinates. Hence the local problem is again that of potential flow past the osculating parabola (Fig. 4.9).

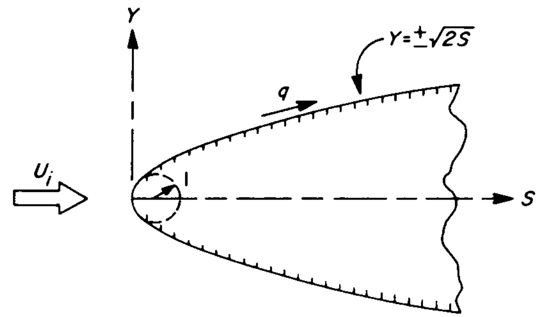

Fig. 4.9. Local flow past osculating parabola.

Additional boundary conditions are required to make the solution unique. Clearly the flow should be symmetrical about the S-axis. On the other hand, it is not obvious that the flow far upstream should be uniform. However, any other possibility involves a stronger singularity at infinity, and can therefore be ruled out by the principle of minimum singularity (Section 4.5). We cannot conclude, however, that the speed of the oncoming stream is the original free-stream speed U; we therefore denote it again by U_i and determine it by matching with the thin-airfoil solution. Note that the value of U_i was not required for deriving Lighthill's rule in the last section, because it canceled out.

The boundary-value problem for $\phi(S, Y)$ can readily be solved for the surface speed. However, the result is available from (4.28) as

$$q \sim U_i \sqrt{\frac{2S}{1+2S}} \quad \text{as} \quad \varepsilon \to 0 \quad \text{with} \quad S = O(1) \tag{4.35}$$

Thus we have two different asymptotic approximations to the solution for small ε. The thin-airfoil expansion (4.32b) is valid except near the leading edge, where the local solution (4.35) applies.

It is helpful to introduce now some terminology that will be extended in the next chapter. Following Kaplun (1954) and Lagerstrom and Cole (1955) we call the thin-airfoil series the *outer expansion*. It is the result of letting ε tend to zero with the *outer variables* s and y (or x and y) fixed. Similarly, the local solution is the first term of the *inner expansion*, which is the result of letting ε tend to zero with the *inner variables* S and Y fixed. (The subscript on U_i is now recognized as standing for "inner.")

4.10. Matching with Solution near Round Edge

In general, as in this example, the inner and outer expansions complement each other, one being valid in the region where the other fails. An important feature of this complementarity is that one can *match* the two expansions. Matching is essential to the success of the method, and will be discussed in detail in the next chapter. For the present we simply assert that here, as in many problems, we can apply what we will call (Section 5.7) the *asymptotic matching principle*:

See Note 4

The m-term inner expansion of (the n-term outer expansion)
= the n-term outer expansion of (the m-term inner expansion). (4.36)

Here m and n may be taken as any two integers, equal or unequal. By definition, the m-term inner expansion of the n-term outer expansion is found by rewriting it in inner variables, expanding asymptotically for small ε, and truncating the result to m terms; and conversely for the right-hand side of (4.36).

We now apply this principle to find the unknown constants C_1 and C_2 in the outer expansion (4.32) and U_i in the inner solution (4.35). At the outset, we know only the first term of the outer expansion, representing the undisturbed stream, and no terms of the inner expansion. We therefore choose $m = n = 1$, in order to find a first approximation to the effective free-stream speed U_i in the inner problem. It is convenient to systematize the procedure as follows:

1-*term outer expansion*:	$q \sim U$	(4.37a)
rewritten in inner variables:	$= U$	(4.37b)
expanded for small ε:	$= U$	(4.37c)
1-term inner expansion:	$= U$	(4.37d)

1-*term inner expansion*:	$q \sim U_i\sqrt{\dfrac{2S}{1+2S}}$	(4.38a)
rewritten in outer variables:	$= U_i\sqrt{\dfrac{2s}{2s+\varepsilon^2}}$	(4.38b)
expanded for small ε:	$= U_i\left(1 - \dfrac{1}{4}\dfrac{\varepsilon^2}{s} + \cdots\right)$	(4.38c)
1-term outer expansion:	$= U_i$	(4.38d)

By equating (4.37d) and (4.38d) according to the matching principle (4.36) we obtain

$$U_i = U \tag{4.39}$$

That is, to first order the effective free-stream speed for the inner solution is the actual free-stream speed, which is plausible physically. Exercise 4.2 shows that this matching cannot be carried out if the inner solution is singular at infinity, which justifies our appeal to the principle of minimum singularity.

We now reverse the process to find the second term in the outer expansion. Taking $m = 1$ and $n = 2$ we have

1-*term inner expansion*:	$q \sim U\sqrt{\dfrac{2S}{1+2S}}$	(4.40a)
rewritten in outer variables:	$= U\sqrt{\dfrac{2s}{2s+\varepsilon^2}}$	(4.40b)
expanded for small ε:	$= U\left(1 - \dfrac{1}{4}\dfrac{\varepsilon^2}{s} + \cdots\right)$	(4.40c)
2-term outer expansion:	$= U$	(4.40d)

2-*term outer expansion*: $$q \sim U\left\{1 + \varepsilon\left[1 + \frac{C_1}{s(2-s)}\right]\right\} \tag{4.41a}$$

rewritten in inner variables: $$= U\left\{1 + \varepsilon\left[1 + \frac{C_1}{\varepsilon^2 S(2-\varepsilon^2 S)}\right]\right\} \tag{4.41b}$$

expanded for small ε: $$= U\left(\frac{C_1}{2\varepsilon S} + 1 + \cdots\right) \tag{4.41c}$$

1-term inner expansion: $$= U\begin{cases}\dfrac{C_1}{2\varepsilon S} & \text{if} \quad C_1 \neq 0\\ 1 & \text{if} \quad C_1 = 0\end{cases} \tag{4.41d}$$

By comparing (4.40d) and (4.41d), we find that they match only if C_1 vanishes; there can be no source eigensolution in the first-order thin-airfoil solution.

We now reverse the process once more to find the second term in the inner expansion. With $m = n = 2$ we have

2-*term outer expansion*: $$q \sim U(1 + \varepsilon) \tag{4.42a}$$

rewritten in inner variables: $$= U(1 + \varepsilon) \tag{4.42b}$$

expanded for small ε: $$= U(1 + \varepsilon) \tag{4.42c}$$

2-term inner expansion: $$= U(1 + \varepsilon) \tag{4.42d}$$

This last result indicates that the second term in the inner expansion must be of order ε. Now it is clear from (4.33b) that the error in approximating the nose of the ellipse by the osculating parabola (4.33c) is only of order ε^2. Hence the inner solution is that for a parabola to second as well as first order, provided that U_i is refined. We find

2-*term inner expansion*: $$q \sim U_i\sqrt{\frac{2S}{1+2S}} \tag{4.43a}$$

rewritten in outer variables: $$= U_i\sqrt{\frac{2s}{2s+\varepsilon^2}} \tag{4.43b}$$

expanded for small ε: $$= U_i\left(1 - \frac{1}{4}\frac{\varepsilon^2}{s} + \cdots\right) \tag{4.43c}$$

2-term outer expansion $$= U_i \tag{4.43d}$$

and matching shows that to second order

$$U_i = U(1 + \varepsilon) \tag{4.44}$$

Physically, this means that although the nature of the flow near the leading edge depends upon only the local airfoil shape, and is to second

order that for the osculating parabola, the effective free-stream speed for that parabola differs slightly from the actual free-stream speed. It is increased by the effects of relatively remote parts of the airfoil, which may be regarded as formed by adding sinks to the parabola. Thus the parabolic nose is flying in a stream that has been speeded up in order to flow past the rest of the airfoil.

We could now return again to the outer expansion by choosing $m = 2$ and $n = 3$, and show that matching requires C_2 to vanish; there are no source eigensolutions in the second-order thin-airfoil solution. Dipole and higher-order eigensolutions would be ruled out by the same process.

This process could in principle be continued indefinitely. Beginning with the next step, however, it must be recognized that the inner problem is no longer that for a parabola, but for the more complicated shape obtained by expanding (4.33b):

$$Y \sim \sqrt{2S}\left(1 - \frac{1}{4}\varepsilon^2 S - \frac{1}{32}\varepsilon^4 S^2 - \cdots\right)$$
$$\text{as} \quad \varepsilon \to 0 \quad \text{with} \quad S = O(1) \tag{4.45}$$

and retaining the required number of terms (Fig. 4.10). The solution can be found by making a coordinate perturbation of the basic flow past the

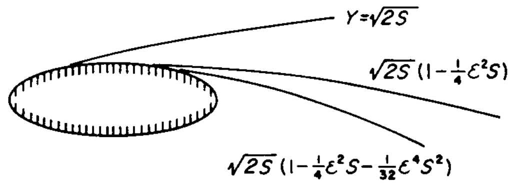

Fig. 4.10. Successive inner expansions for shape of ellipse.

osculating parabola. Of course the inner expansion (4.45) for the airfoil shape diverges for large S, in fact for $S > 2\ \varepsilon^2$. Hence the inner expansion will be nonuniform at $S = \infty$. It can be extracted from the known exact solution by introducing inner variables and expanding, which yields

$$\frac{q}{U} = \frac{1+\varepsilon}{\sqrt{1 + \dfrac{(1-\varepsilon^2 S)^2}{S(2-\varepsilon^2 S)}}} \sim \sqrt{\frac{2S}{1+2S}}\left[1 + \varepsilon + \frac{3}{4}\varepsilon^2\frac{S}{1+2S}\right.$$
$$\left. + \frac{3}{4}\varepsilon^3\frac{S}{1+2S} - \varepsilon^4\frac{S^2(8S-23)}{32(1+2S)^2} + \cdots\right] \tag{4.46}$$

Singularities at $S = \infty$ are seen to appear beginning with the fifth term of the inner expansion. This divergence is of no concern, because the inner expansion is used at nowhere near such great distances.

4.11. Matching with Solution near Sharp Edge

We now apply the same technique to a sharp edge. The example of the biconvex airfoil (Section 4.7) shows that sharp edges lead to logarithmic singularities in the thin-airfoil expansion. These are so weak that without devoting any special attention to them one can calculate an unlimited number of terms in the series. However, it is of interest to understand the source of the logarithms by examining the flow in the immediate vicinity of the edge.

For simplicity we consider only the leading edge of the biconvex airfoil, the extension to any sharp edge being evident. With the origin shifted to the leading edge (Fig. 4.6) the airfoil is described by

$$y = \pm\, \varepsilon(2s - s^2) \tag{4.47a}$$

The thin-airfoil expansion (4.24) was seen in Section 4.7 to fail within a distance $s = O(e^{-1/\varepsilon})$ of the leading edge. Hence appropriate magnified inner variables are

$$S = s e^{1/\varepsilon}, \qquad Y = y e^{1/\varepsilon} \tag{4.48}$$

in terms of which airfoil is described by

$$Y = \pm\, \varepsilon(2S - e^{-1/\varepsilon} S^2) \tag{4.47b}$$

As ε tends to zero the second term vanishes faster than any power of ε. Hence whereas a round edge is locally parabolic only to second order, a sharp edge is approximated *to any order* by a wedge (Fig. 4.11). The wedge angle is vanishingly small, our airfoil being approximated by

$$Y \sim \pm\, 2\varepsilon S \qquad \text{as} \quad \varepsilon \to 0 \quad \text{with} \quad S = O(1) \tag{4.47c}$$

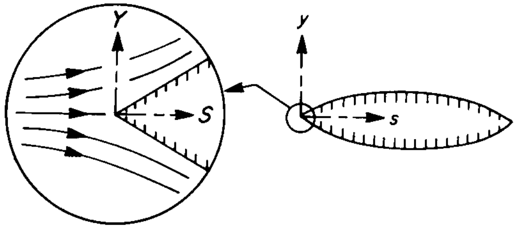

Fig. 4.11. Inner solution for sharp-edged airfoil.

The appropriate inner solution is a symmetric potential flow past this wedge with the weakest possible singularity at infinity. It can be found, as indicated in Fig. 4.12, by a familiar elementary conformal transforma-

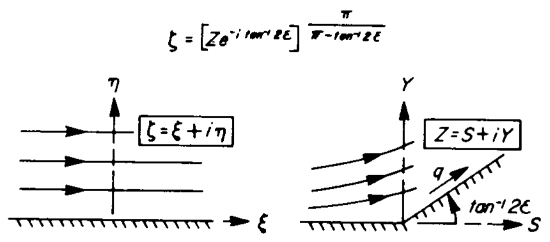

Fig. 4.12. Conformal mapping for flow past wedge.

tion of uniform parallel flow. It can equally well be found by separation of variables in polar coordinates, which is a method that can be extended to three-dimensional problems. Thus the inner solution for surface speed is found to be

$$q \sim U_i S^{\tan^{-1}2\varepsilon/(\pi - \tan^{-1}2\varepsilon)} \qquad \text{as} \quad \varepsilon \to 0 \quad \text{with} \quad S = O(1) \tag{4.49}$$

Here, in contrast to the round nose, even the first term of the inner expansion diverges at infinity. It gives unbounded velocities as $S \to \infty$, so that the factor U_i cannot be interpreted as an equivalent free-stream speed, but merely as the surface speed at $S = 1$. As for the round nose, U_i can be found by matching with the outer expansion of thin-airfoil theory.

In order to match, we need the outer expansion of the inner solution (4.49). This requires forcing a small fractional power into a formal series in powers of the exponent, and is accomplished using the rule that

$$s^\varepsilon = \exp(\log s^\varepsilon) = \exp(\varepsilon \log s) = 1 + \varepsilon \log s + \tfrac{1}{2}\varepsilon^2 \log^2 s + \cdots \tag{4.50}$$

which is not uniformly valid for small s. It fails where $\varepsilon \log s = O(1)$, so that $s = O(e^{-1/\varepsilon})$. This result explains the mysterious occurrence of logarithms in the thin-airfoil expansion for a sharp edge.

In matching the two expansions we need not, as in the case of the round nose, work up from one approximation to the next, but can at once treat any desired approximation. Let us consider the second approximation.

Then the matching principle (4.36) is to be applied with $m = n = 2$, for which we find

2-term outer expansion:
$$q \sim U\left\{1 + \frac{2}{\pi}\varepsilon\left[2 + (1-s)\log\frac{s}{2-s}\right]\right\} \qquad (4.51a)$$

rewritten in inner variables:
$$= U\left\{1 + \frac{2}{\pi}\varepsilon\left[2 + (1 - e^{-1/\varepsilon}S)\log\frac{e^{-1/\varepsilon}S}{2 - e^{-1/\varepsilon}S}\right]\right\} \qquad (4.51b)$$

expanded for small ε:
$$= U\left[\left(1 - \frac{2}{\pi}\right) + \frac{2}{\pi}\varepsilon(2 + \log S - \log 2) + \cdots\right] \qquad (4.51c)$$

2-term inner expansion:
$$= U\left[\left(1 - \frac{2}{\pi}\right) + \frac{2}{\pi}\varepsilon(2 + \log S - \log 2)\right] \qquad (4.51d)$$

rewritten in outer variables:
$$= U\left[1 + \frac{2}{\pi}\varepsilon\left(2 + \log\frac{s}{2}\right)\right] \qquad (4.51e)$$

2-term inner expansion:
$$q \sim U_i S^{\tan^{-1} 2\varepsilon/(\pi - \tan^{-1} 2\varepsilon)} \qquad (4.52a)$$

rewritten in outer variables:
$$= U_i(e^{1/\varepsilon}s)^{\tan^{-1} 2\varepsilon/(\pi - \tan^{-1} 2\varepsilon)} \qquad (4.52b)$$

expanded for small ε:
$$= e^{2/\pi}U_i\left[1 + \frac{2}{\pi}\varepsilon\left(\log s + \frac{2}{\pi}\right) + \cdots\right] \qquad (4.52c)$$

2-term outer expansion:
$$= e^{2/\pi}U_i\left[1 + \frac{2}{\pi}\varepsilon\left(\log s - \frac{2}{\pi}\right)\right] \qquad (4.52d)$$

rewritten in inner variables:
$$= e^{2/\pi}U_i\left[\left(1 - \frac{2}{\pi}\right) + \frac{2}{\pi}\varepsilon\left(\log S + \frac{2}{\pi}\right)\right] \qquad (4.52e)$$

The rule (4.50) has been used in obtaining (4.52c). The additional last step (4.51e) or (4.52e) is required because the comparison of the two results must be made in terms of either outer or inner variables alone. Then equating (4.51e) and (4.52d) yields (but see exercise 4.5)

See Note 4

$$U_i = e^{-2/\pi}U\left[1 + \frac{2}{\pi}\varepsilon\left(2 - \log 2 - \frac{2}{\pi}\right) + \cdots\right] \qquad (4.53)$$

This completes the inner expansion (4.49) to second order. The reader can, using (4.24), find the next term in (4.53) by matching with $m = n = 3$.

4.12. A Shifting Correction for Round Edges

We return to the singularity at a round edge, and describe an alternative way of correcting it. This serves to introduce a second general method of handling singular perturbation problems, which is discussed in detail in Chapter VI.

Consider the simplest round-nosed shape, the parabola. We must examine the complete velocity field, because the surface speed suffers distortion through transfer of the boundary conditions. For the parabola $y = \pm\varepsilon\sqrt{2x}$ of nose radius ε^2 the first-order complex velocity can be extracted from that (4.12) for the ellipse as

$$\phi_x - i\phi_y = 1 - \frac{i\varepsilon}{\sqrt{2z}} + O(\varepsilon^2), \qquad z = x + iy \qquad (4.54)$$

We compare with the corresponding exact result which, by conformal mapping or separation of variables in parabolic coordinates, is found to be

$$\phi_x - i\phi_y = 1 - \frac{i\varepsilon}{\sqrt{2(z - \frac{1}{2}\varepsilon^2)}} \qquad (4.55)$$

We see that the first approximation (4.54) becomes exact if the origin of coordinates is simply shifted by $\frac{1}{2}\varepsilon^2$. This removes the square-root singularity from the vertex and places it inside the parabola at the focus, which is the singular point of the conformal mapping. Thus thin-airfoil theory is seen to give the exact source distribution for a parabola, but displaced by half its nose radius.

This remarkable property must hold approximately for any round-nosed airfoil. For that reason Munk (1922) advocated modifying the abscissae to shift the leading edge of any profile by half its radius. It is clear that a simple translation is not correct for a finite airfoil, because that would leave the trailing edge misplaced. For the ellipse of Fig. 4.2, a uniform contraction of the x-coordinate evidently provides the required shift at both ends, as do an unlimited number of more complicated strainings. To retain the benefits of complex-variable theory, we strain instead the single variable $z = x + iy$.

Lighthill (1949a) has proposed the following principle for finding strained coordinates that restore uniform validity in a wide class of singular perturbation problems:

> Higher approximations shall be no more singular than the first. (4.56)

We illustrate this principle by application to the thin-airfoil expansion for the ellipse. It is necessary to examine the third approximation, because the second is already no more singular than the first. For this reason the straining is of order ε^2 rather than ε.

Extending the first approximation (4.12) yields the thin-airfoil expansion as

$$\phi_x - i\phi_y = 1 + (\varepsilon + \varepsilon^2 + \varepsilon^3)\left(1 - \sqrt{\frac{z^2}{z^2 - 1}}\right) + \frac{1}{2}\varepsilon^3\sqrt{\frac{z^2}{(z^2 - 1)^3}} + O(\varepsilon^4) \tag{4.57}$$

Now suppose that, as in the case of the parabola, this result becomes uniformly valid if z is replaced by a slightly strained coordinate ζ. Set

$$z = \zeta + \varepsilon^2 z_2(\zeta) + \cdots \tag{4.58}$$

where the straining function z_2, which was $-\frac{1}{2}$ for the parabola, is to be determined. Making this substitution in (4.57) and expanding again in powers of ε yields

$$\phi_x - i\phi_y = 1 + (\varepsilon + \varepsilon^2 + \varepsilon^3)\left(1 - \sqrt{\frac{\zeta^2}{\zeta^2 - 1}}\right) + \frac{1}{2}\varepsilon^3\sqrt{\frac{\zeta^2}{\zeta^2 - 1}}\left(\frac{1 - 2\zeta z_2}{\zeta^2 - 1} - 2\frac{z_2}{\zeta}\right) + \cdots \tag{4.59}$$

Now the third term will be no more singular than the second at $\zeta = \pm 1$ (and also at $\zeta = 0$) if we set

$$z_2(\zeta) = -\tfrac{1}{2}\zeta \quad \text{or} \quad -\tfrac{1}{2}\zeta^3 \quad \text{or} \quad \cdots \tag{4.60}$$

Consider for simplicity the first of these possibilities, which provides the uniform contraction of abscissae already proposed. Then the first-order solution becomes

$$\phi_x - i\phi_y = 1 + \varepsilon\left(1 - \sqrt{\frac{\zeta^2}{\zeta^2 - 1}}\right) \tag{4.61a}$$

where

$$z = \zeta - \tfrac{1}{2}\varepsilon^2\zeta + \cdots \tag{4.61b}$$

Although one can eliminate ζ here to obtain an explicit solution, that is not possible with any other choice of z_2. In general, one must be content with an implicit representation of the solution in terms of ζ as a parameter. This approximation is uniformly valid to first order, as can be verified by comparing with the exact solution:

$$\phi_x - i\phi_y = 1 + \frac{\varepsilon}{1 - \varepsilon}\left(1 - \sqrt{\frac{z^2}{z^2 - 1 + \varepsilon^2}}\right) \tag{4.62}$$

Because we have manipulated the solution, rather than introducing the straining into the original problem, the above procedure is really a modification of Lighthill's technique suggested by Pritulo (1962); see Exercise 6.4.

Applying his technique to a general profile led **Lighthill (1951)** to the rule (4.30b) for correcting thin-airfoil theory at round edges. However, in contrast to our previous derivation of that rule, Lighthill's method is not successful for edges that are sharp, square, or in fact of any shape other than round.

EXERCISES

4.1. *Thin-airfoil theory using stream function.* Reproduce the analysis of Sections 4.2 and 4.3 using the stream function instead of the velocity potential. Carry out the solution for the elliptic airfoil, and verify that indeterminate source eigensolutions are automatically excluded.

4.2. *Matching and the principle of minimum singularity.* The local problem of symmetric flow past an osculating parabola (Fig. 4.9) has eigensolutions that are singular at infinity. Show that the least singular of them adds to the surface speed a multiple of $[S^3/(1 - 2S)]^{1/2}$. This can be done, for example, by introducing parabolic coordinates ξ and η and seeking a solution of the potential problem as a polynomial in $(\xi - i\eta)$. Then show that matching with the thin-airfoil solution for any round-nosed profile excludes this eigensolution, in accord with the principle of minimum singularity.

4.3. *Matching with local solution for square edge.* Introduce inner variables appropriate to the leading edge of the rectangular airfoil of Fig. 4.7. Show that the inner solution is that for flow past a semi-infinite rectangular slab of thickness 2, on whose sides the surface speed is given in terms of a parameter t (Milne-Thompson 1960, Section 10.6) by

$$q = U_i\sqrt{\frac{t + 1}{t - 1}} \qquad \text{where} \qquad \pi S = \sqrt{t^2 - 1} - \cosh^{-1} t$$

Match with the outer solution (4.27) to show that the coefficient of the eigensolution is $C = \frac{1}{2} - \log(4\pi/\varepsilon)$, so that the asymptotic sequence for the thin-airfoil expansion (4.2) contains logarithms beginning with $\varepsilon^2 \log \varepsilon$.

4.4. *Correction rule for sharp edges.* Devise a multiplicative correction rule for sharp edges, analogous to Lighthill's rule (4.30b) for round edges. Discuss the prospects for treating square edges similarly, and also sharp tips on slender axisymmetric bodies.

See Note 3

4.5. *Exact solution for biconvex airfoil.* Milne-Thompson (1960, Section 6.51) gives the exact solution for symmetrical potential flow past a biconvex profile formed by two circular arcs. To what order can these be replaced by parabolic arcs in thin-airfoil theory? In the coordinates of Fig. 4.6 the exact surface speed is

$$\frac{q}{U} = \frac{4}{n^2}\,\frac{\cosh\eta - \cos n\pi/2}{1 + \cosh 2\eta/n}$$

where

$$x = \frac{\sinh\eta}{\cosh\eta - \cos n\pi/2}, \qquad n = \frac{4}{\pi}\cot^{-1}\varepsilon$$

See Note 4

Extract from this the outer and inner expansions, and compare with the results of Sections 4.7 and 4.11. Show that equating (4.51d) and (4.52e) instead of (4.51e) and (4.52d) does not give (4.53). Explain the reason for the difference, and discuss its implications.

4.6. *Block matching for elliptic airfoil.* Show that instead of matching step by step as in Section 4.10, one can at once match the 3-term outer expansion (4.32) with the 2-term inner expansion (4.35).

4.7. *Nose-correction rules for bodies of revolution.* Devise a rule analogous to (4.30b) for round-nosed bodies of revolution in axisymmetric incompressible flow. Use the fact that the surface speed on a paraboloid of revolution is the same as on a parabolic cylinder. Apply the rule to the ellipsoid of revolution formed by rotating Fig. 4.2 about the x-axis, for which slender-body theory (Van Dyke, 1959) gives the surface speed as

$$\frac{q}{U} = 1 + \varepsilon^2\left[\log\frac{2}{\varepsilon} - \frac{1}{2}\left(1 + \frac{1}{1 - x^2}\right)\right] + O(\varepsilon^4\log^2\varepsilon)$$

Compare with the exact result

$$\frac{q}{U} = \frac{1 + \varepsilon^2(\operatorname{sech}^{-1}\varepsilon - \sqrt{1-\varepsilon^2})/(\sqrt{1-\varepsilon^2} - \varepsilon^2\operatorname{sech}^{-1}\varepsilon)}{\left(1 + \varepsilon^2\dfrac{x^2}{1 - x^2}\right)^{1/2}}$$

In the same way devise a rule for treating sharp-nosed bodies of revolution, and apply it to the spindle formed by rotating Fig. 4.6, for which slender-body theory gives

$$\frac{q}{U} = 1 + \varepsilon^2\left[2(1 - 3x^2)\log\frac{2}{\varepsilon\sqrt{1 - x^2}} - 3 + 11x^2\right] + O(\varepsilon^4\log^2\varepsilon)$$

4.8. *Small-disturbance theory for paraboloid of revolution.* Consider axisymmetric incompressible flow past the paraboloid of revolution $r = \sqrt{2\varepsilon^2 x}$. Derive the counterpart of (4.4) for the first perturbation, but do not transfer the tangency condition to the axis. Solve by separating variables in paraboloidal coordinates, showing that the disturbances are of order ε^2 rather than ε, and that

$$\phi \sim x + \tfrac{1}{2}\varepsilon^2\log\frac{\sqrt{x^2 + r^2} - x}{\varepsilon^2} + O(\varepsilon^4\log\varepsilon)$$

Verify that this result becomes exact if the origin is shifted downstream by half the nose radius.

Expand the above approximation formally for r small, of order ε, to obtain the slender-body solution, and verify that it satisfies the approximate equation $\phi_{rr} + \phi_r/r = 0$ of slender-body theory. Improve this result by iterating upon the full Laplace equation to find the second-order slender-body solution as

$$\phi \sim x - \tfrac{1}{2}\varepsilon^2\log\frac{r^2}{2\varepsilon^2 x} + \tfrac{1}{2}\varepsilon^2\left[\varepsilon^2 f(x) - \frac{r^2}{4x^2}\right]$$

Deduce the form of the function f by dimensional reasoning, using the fact that ε^2 is the only characteristic length in the problem, thus completing the solution except for an unknown multiple of an eigensolution. Interpret this as the slender-body form of a particular solution of Laplace's equation. Find its constant by comparison with the exact solution. [See Chang (1961) for a discussion of the role played here by the *artificial parameter* ε, and application of the method of matched asymptotic expansions. For the paraboloid in subsonic compressible flow, see Van Dyke (1958c).]

4.9. *Subsonic thin-airfoil theory.* Deduce the first- and second-order problems, corresponding to (4.4) and (4.5), for symmetric subsonic compressible flow, where the Laplace equation (4.1a) is replaced by (2.19a). Show that a change in vertical scale (the Prandtl-Glauert transformation) reduces the first to an equivalent incompressible problem. Verify that a general particular integral (Section 3.7) for the second-order equation is given by (Van Dyke, 1952)

$$M^2\left[\left(1 + \frac{\gamma+1}{4}\,\frac{M^2}{1 - M^2}\right)\phi_1 - \frac{\gamma+1}{4}\,\frac{M^2}{1 - M^2}\,y\phi_{1y}\right]\phi_{1x}$$

Calculate the second-order solution for the wavy wall $y = \varepsilon\sin x$. Calculate the surface pressure coefficient from

$$C_p = 2\varepsilon\phi_{1x} - \varepsilon^2\left[(1 - M^2)\phi_{1x}^2 + \phi_{1y}^2 + 2\phi_{2x}\right] + \ldots$$

and check that it satisfies the second-order similarity rule for airfoils (Hayes, 1955):

If at

$$M = 0, \qquad C_p = \qquad \varepsilon C_{p1}(x) + \varepsilon^2 C_{p2}(x) + \cdots$$

then for

$$M \geqslant 0, \qquad C_p = \frac{\varepsilon}{\sqrt{1 - M^2}} C_{p1}(x) + \varepsilon^2 \frac{(\gamma + 1)M^4 + 4(1 - M^2)}{4(1 - M^2)^2} C_{p2}(x) + \cdots$$

Chapter V

THE METHOD OF MATCHED ASYMPTOTIC EXPANSIONS

5.1. Historical Introduction

We introduced in the preceding chapter a method for treating singular perturbation problems that is a generalization of the boundary-layer theory of Prandtl (1905). This has in the past been called the method of "inner and outer expansions" or of "double asymptotic expansions." We prefer to follow Bretherton (1962) in speaking of the *method of matched asymptotic expansions*.

The ideas underlying the method have grown through the years. It was being used in the 1950's by Friedrichs (1953, p. 126; 1954, p. B-184) and his students. It was systematically developed and applied to viscous flows at the California Institute of Technology. Kaplun (1954) introduced the formal inner and outer limit processes for boundary-layer theory, and the corresponding inner and outer expansions. Later, in studying flows at low Reynolds number, Kaplun and Lagerstrom (1957) made a penetrating analysis of the matching process (see also Lagerstrom, 1957). Kaplun (1957) used those ideas to gain deeper insight into the resolution of the Stokes paradox for plane flow at low Reynolds number. Lagerstrom and Cole (1955) evaluated the method in comparison with new exact solutions of the Navier-Stokes equations for a sliding and expanding circular cylinder. Coles (1957) applied it to some special solutions for the compressible boundary layer.

Proudman and Pearson (1957) applied this expansion method to treat flow past a sphere and circular cylinder at low Reynolds number. Goldstein (1956, 1960) and Imai (1957a) gave the first correct extension of Blasius' boundary-layer solution for the semi-infinite flat plate. Ting (1959) solved the riddle of the course of the viscous shear layer between two streams of different speeds. See Note 16

Following this developmental period, the method of matched asymptotic expansions was applied to a variety of problems in fluid mechanics. Most of the earlier applications were to viscous flows. For example, Germain and Guiraud (1960, 1962) and Chow and Ting (1961) calculated the effect of curvature upon the structure of a shock wave. Murray (1961) and Ting (1960) found the effect of external vorticity upon the boundary layer near and far from the leading edge of a flat plate. Chang (1961) clarified the behavior of viscous flow far from a finite body. Flows at low Reynolds numbers have been analyzed for ellipsoids by Breach (1961), for a spinning sphere by Rubinow and Keller (1961), for a circle in shear flow by Bretherton (1962), and so on.

The method is equally successful for inviscid flows. The preceding chapter gives examples in incompressible flow. Cole and Messiter (1957) have studied transonic flow past slender bodies. Although the method appears to be less popular in the Soviet Union, Bulakh (1961) has used it to correct linearized supersonic conical flow and its higher approximations in the vicinity of the bow shock wave. Similarly, Fraenkel and Watson (1964) have attacked the "pseudotransonic" flow past a triangular wing that occurs when the bow wave lies close to the leading edge. Yakura (1962) has analyzed the entropy layer produced by slightly blunting the tip of a body in hypersonic flow.

Since 1960, applications of the method have proliferated in many fields of fluid mechanics, as well as in other branches of applied mathematics. Some recent examples are discussed in later chapters of this book.

5.2. Nonuniformity of Straightforward Expansion

Before we discuss the details of the method of matched asymptotic expansions, it is useful to inquire how singular perturbation problems arise. What is the source of the nonuniformity? Can we predict whether a given physical problem will lead to regular or singular perturbations?

The classical warning of singular behavior is familiar from Prandtl's boundary-layer theory. A small parameter multiplies one of the highest derivatives in the differential equations. Then in a straightforward perturbation scheme that derivative is lost in the first approximation so that the order of the equations is reduced. One or more boundary conditions must be abandoned, and the approximation breaks down near where they were to be imposed. This happens except in the unlikely circumstance that the original boundary conditions are consistent with the reduced equations.

It is often helpful to examine linear ordinary differential equations as mathematical models that illustrate the essential features of more complicated problems. A simple model that illustrates loss of the highest

derivative in boundary-layer theory is given by Friedrichs (1942) as

$$\varepsilon \frac{d^2f}{dx^2} + \frac{df}{dx} = a, \qquad f(0) = 0, \qquad f(1) = 1 \tag{5.1}$$

The exact solution is

$$f(x;\ \varepsilon) = (1 - a)\frac{1 - e^{-x/\varepsilon}}{1 - e^{-1/\varepsilon}} + ax \tag{5.2}$$

However, setting $\varepsilon = 0$ reduces the differential equation to first order, so that both boundary conditions cannot be satisfied unless it happens that $a = 1$. The exact solution shows that the condition at $x = 0$ must be dropped. Then the approximate solution for small ε is

$$f(x;\varepsilon) \sim (1 - a) + ax \tag{5.3}$$

As indicated in Fig. 5.1, this is a good approximation except within the "boundary layer" where $x = O(\varepsilon)$. Introduction of a magnified inner coordinate X appropriate to that region by setting

$$f(x;\varepsilon) = F(X;\varepsilon), \qquad X = \frac{x}{\varepsilon} \tag{5.4}$$

transforms the original problem (5.1) to

$$\frac{d^2F}{dX^2} + \frac{dF}{dX} = a\varepsilon, \qquad F(0) = 0, \qquad F\left(\frac{1}{\varepsilon}\right) = 1 \tag{5.5}$$

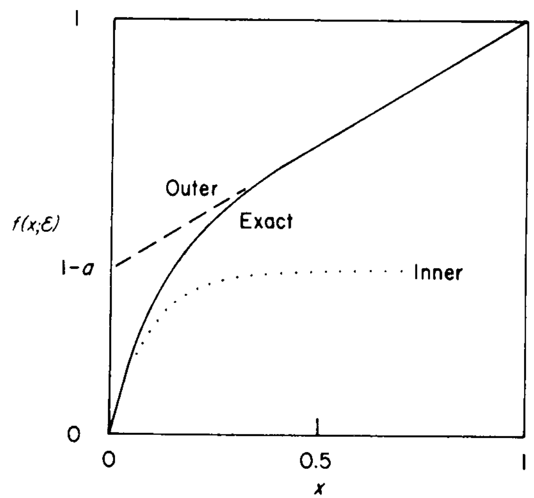

Fig. 5.1. Solution of model problem.

If we now set $\varepsilon = 0$, the solution of the differential equation that satisfies the inner boundary condition is any multiple of $(1 - e^{-X})$. Imposing the outer boundary condition would give the multiplicative factor as unity, but the exact solution shows that this is incorrect. The outer boundary condition must be abandoned for the inner solution just as the inner condition was dropped from the outer solution. Instead, the inner solution must be matched to the outer solution using the matching principle (4.36). Thus one finds the uniform first approximation for small ε:

$$f(x;\varepsilon) \sim \begin{cases} (1-a)+ax & \text{as } \varepsilon \to 0 \text{ with } x > 0 \text{ fixed} \quad (5.6a) \\ (1-a)(1-e^{-X}) & \text{as } \varepsilon \to 0 \text{ with } X = \dfrac{x}{\varepsilon} \text{ fixed} \quad (5.6b) \end{cases}$$

The warning provided by loss of a highest derivative is more often than not absent from a singular perturbation problem. In the thin-airfoil theory of Chapter IV, the nonuniformity arises not from the differential equation but from the boundary conditions. Likewise, for viscous flow at low Reynolds numbers the highest derivatives are all preserved in the approximate equations of Stokes; the nonuniformity is associated rather with the infinite extent of the fluid. Evidently it would be useful to have a more reliable indication of nonuniformity.

5.3. A Physical Criterion for Uniformity

In physical problems a more general warning of singular behavior can be based upon dimensional reasoning. We have seen that inherent nonuniformity will be suppressed by exceptional boundary conditions, so that one can give only necessary and not sufficient conditions for nonuniformity. We therefore state the following rule instead as a positive test for uniformity:

> A perturbation solution is uniformly valid in the space and time coordinates unless the perturbation quantity ε is the ratio of two lengths or two times. (5.7)

This criterion may be understood by considering first a parameter perturbation. The geometry of the problem will be characterized by a typical major dimension that we may call the *primary reference length*. Examples are the radius of the circular cylinder in Chapter II, and the chord length of the thin airfoil in Chapter IV. This length is the natural basis for forming dimensionless coordinates—a characteristic speed also being required in unsteady flows—and these constitute the straightfor-

ward outer variables. Nonuniform behavior is possible only if the parameters in the problem provide another *secondary reference length* whose ratio to the first tends to zero or infinity as ε vanishes. This second length, if properly chosen, is the basis for the inner variables.

A familiar problem involving two disparate lengths is potential flow past a thin round-nosed airfoil. The geometry is characterized by the chord length except close to the leading edge, where it is dominated by the nose radius. Since the ratio of these two lengths vanishes with the square of the thickness ratio, our criterion (5.7) suggests that the thin-airfoil solution could be singular. In Chapter IV this possibility was seen to be realized, outer variables being based on the chord and inner variables on the nose radius.

Our criterion shows that a coordinate perturbation is never safe from nonuniformity in the remaining coordinates. The latter may be made dimensionless using either the primary reference length or the perturbation coordinate; and because the ratio of these two lengths tends to zero or infinity, they provide the scales for an inner and an outer expansion.

The following are examples of parameter perturbations that involve only one characteristic length scale, and are therefore necessarily regular according to our criterion. Slightly compressible flow past a circle (Section 2.4) contains the radius as the only characteristic length, the perturbation parameter being formed from a ratio of speeds or energies rather than lengths. The slightly distorted circle in potential flow (Section 2.3) involves two lengths, but they are of the same order of magnitude, their ratio approaching unity rather than zero or infinity in the limit $\varepsilon \to 0$.

The following parameter perturbations involve two disparate lengths, and do as a consequence exhibit singular behavior (Fig. 5.2). A lifting wing is characterized by its chord and its span, and their ratio vanishes

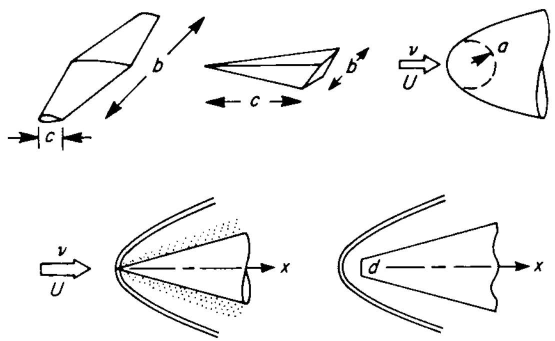

Fig. 5.2. Singular perturbation problems involving two disparate lengths.

in Prandtl's lifting-line theory (cf. Section 9.2) and becomes infinite in the slender-wing approximation. A body in viscous flow is characterized by not only a geometric dimension, but also the viscous length ν/U; and their ratio is the Reynolds number, which vanishes in Stokes flow (Chapter VIII) and becomes infinite in boundary-layer theory (Chapter VII). This example illustrates that the secondary reference length is not always a geometric dimension.

The following are some coordinate perturbations that are singular (Fig. 5.2). Viscous supersonic flow over a cone or a wedge (including the flat plate) can be solved approximately for distances from the vertex large compared with the viscous length ν/U. Flow of a gas undergoing vibrational or chemical reactions can be treated similarly using a characteristic relaxation length, as can the effect of slight blunting. The impulsive start of a body through viscous fluid can be expanded in powers of time, referred to a characteristic length and speed. Viscous flow far from a body can be expanded in inverse powers of the radius, referred to a typical dimension.

Although the following examples involve two disparate lengths, they are nevertheless regular perturbation problems. Potential flow past a wavy wall, a cusp-nosed airfoil, or any thin shape free of stagnation points is a regular perturbation in the thickness parameter. Uniform shear flow past a circle (Section 2.2) shows the superficial symptoms of nonuniformity at infinity, in that the ratio of the perturbation to the basic solution in (2.11) grows like εr; but the result is exact and therefore uniformly valid. However, any other shear distribution would lead to a singular perturbation problem (Exercises 2.4 and 5.7). In an inviscid fluid the expansion for flow far from a body is regular, as is that for an impulsive start. Even the archetypical nonuniformity of Prandtl's boundary-layer theory disappears if in place of a fixed solid surface one prescribes a distensible skin moving at just the speed of the potential flow.

A problem may involve more than two disparate lengths, associated with a multiple limit process; then multiple nonuniformities are possible. In the case of three layers one may speak of the *outer*, *middle*, and *inner expansions*. An example is viscous flow at high Reynolds number and high or low Prandtl number, where the thermal boundary layer is much thicker or thinner than the viscous layer. An inviscid example is analyzed in Section 9.9.

A coordinate perturbation may sometimes be replaced by a parameter perturbation. For example, the expansion for distances far from the tip of a blunted wedge (Fig. 5.2) may be regarded instead as the solution for a wedge of finite length whose nose thickness tends to zero (Section 9.9). Thus in conical geometry an angle plays the role of a length. Consequently, nonuniformity is possible in conical flows if the perturbation parameter is the ratio of two angles. Examples are a flat elliptic cone, where the straightforward perturbation solution evidently fails at the leading edges just as in thin-airfoil theory, and a circular cone at infinitesimal angle of attack, which exhibits near its surface the vortical layer of Ferri (1950).

5.4. The Role of Composite and Inner Expansions

We have seen that a singular perturbation flow problem typically involves two disparate lengths. As a result, the straightforward perturbation solution with coordinates referred to the primary reference length fails in regions where the secondary reference length is the relevant dimension. The secondary reference length is not always the obvious one. It is clearly the chord for a wing of high aspect ratio, the thickness for a flat-nosed airfoil, and the viscous length ν/U for flow at low Reynolds number. However, at high Reynolds number it is the square root of the product of the viscous and geometric lengths. For a round-nosed airfoil it is not the thickness but the nose radius, which is proportional to the square of the thickness divided by the chord. For a thin airfoil in supersonic flow (Section 6.4) it is the mean radius of curvature of the profile, which is proportional to the square of the chord divided by the thickness. The sharp-nosed airfoil in subsonic flow is a delicate borderline case between uniformity and nonuniformity in which the region of non-uniformity, being exponentially small, is not directly related to any physical dimension. A similar observation applies to the vortical layer on an inclined cone in supersonic flow.

The straightforward perturbation solution yields an asymptotic expansion of the form

$$f(x, y, z; \varepsilon) \sim \sum \delta_n(\varepsilon) f_n(x, y, z) \quad \text{as} \quad \varepsilon \to 0 \quad \text{with} \quad x, y, z \text{ fixed} \tag{5.8}$$

Here the $\delta_n(\varepsilon)$ are an appropriate asymptotic sequence, and x, y, z are the coordinates made dimensionless using the primary reference length. This expansion is valid wherever the functions f_n are regular. They will become singular at any point within the flow field where phenomena are dominated by the secondary rather than the primary reference length. This point lies at infinity if the secondary length is the larger. A modified expansion, in order to be uniformly valid, must depend also upon the coordinates made dimensionless by the secondary reference length. Because the ratio of primary and secondary lengths is a function of ε, this amounts to depending also upon ε. Thus a uniformly valid expansion must have the more complicated form

$$f(x, y, z; \varepsilon) \approx \sum \delta_n(\varepsilon) g_n(x, y, z; \varepsilon) \qquad \text{uniformly as} \quad \varepsilon \to 0 \tag{5.9}$$

Because the perturbation parameter ε now appears implicitly in the function g_n as well as explicitly in the asymptotic sequence δ_n, this is not an asymptotic expansion in the usual sense. We call it a *composite expansion*. Such expansions have been discussed in connection with singular perturbation problems by Erdélyi (1961), who calls them "generalized asymptotic expansions." There are two objections to working with composite expansions. First, they are difficult to manipulate; evidently such familiar operations as equating like powers of ε must be reconsidered and, as will be seen later, a composite series is not uniquely determined. Second, they unnecessarily combine the complications of both the straightforward expansion and the region of nonuniformity (see, however, Sections 10.3 and 10.4).

It is simpler to isolate the difficulties associated with the nonuniformity by constructing a supplementary *inner expansion* valid in its vicinity. This is accomplished by introducing new *inner coordinates* that are of order unity in the region of nonuniformity. Then the inner expansion has the form

$$f(x, y, z; \varepsilon) \sim \sum \Delta_n(\varepsilon) F_n(X, Y, Z) \qquad \text{as} \quad \varepsilon \to 0 \quad \text{with} \quad X, Y, Z \text{ fixed} \tag{5.10}$$

We always denote inner variables by capital letters. Here the asymptotic sequence $\Delta_n(\varepsilon)$ must be allowed to differ from the asymptotic sequence $\delta_n(\varepsilon)$ for the outer expansion; often they are identical, but Section 6.3 gives an example in which they are different. If the region of nonuniformity is the neighborhood of a point in the finite plane, the inner coordinates X, Y, Z are ordinarily the coordinates made dimensionless using the secondary reference length. If the nonuniformity occurs along a line, as in boundary-layer theory, only the normal coordinate is changed. If it occurs at infinity, the coordinates must sometimes be stretched by different functions of ε in different directions. Like the outer expansion, the inner expansion is a conventional asymptotic series, so that the usual operations are valid.

It is often a useful preliminary to introduce dependent as well as independent variables that are of order unity in the inner and outer regions, so that the leading terms in the asymptotic sequences δ_n and Δ_n are unity. The degree of stretching is in general different for the independent and dependent variables. Following Kaplun (1954) and Lagerstrom and Cole (1955), we may formalize the procedure by defining:

Outer variables: Dimensionless independent and dependent variables based upon the primary reference quantities in the problem.

Outer limit: The limit as the perturbation parameter ε tends to zero with the outer variables fixed.

Outer expansion: The asymptotic expansion for $\varepsilon \to 0$ with outer variables fixed. Obtained in principle from the exact result by successive application of the outer limit process in conjunction with an appropriate outer asymptotic sequence.

Inner variables: Dimensionless independent and dependent variables stretched by appropriate functions of ε so as to be of order unity in the region of nonuniformity of the outer expansion.

Inner limit: The limit as $\varepsilon \to 0$ with inner variables fixed.

Inner expansion: The asymptotic expansion for $\varepsilon \to 0$ with inner variables fixed. Obtained in principle from the exact result by successive application of the inner limit process in conjunction with an appropriate inner asymptotic sequence.

Composite expansion: Any series that reduces to the outer expansion when expanded asymptotically for $\varepsilon \to 0$ in outer variables, and to the inner expansion in inner variables.

The technique of matching two complementary asymptotic expansions reduces a singular perturbation problem to its simplest possible elements. If the first inner problem is nevertheless found to be "impossible," then one may suppose that the problem itself is intractable. For example, it is clear that extending the thin-airfoil theory of Chapter IV to subsonic compressible flow leads, in the case of a round-nosed airfoil, to the inner problem of subsonic flow past a parabolic cylinder, for which no complete solution is known. Again, viscous flow past a cusp-nosed airfoil at high Reynolds number leads to the inner problem of viscous flow past a semi-infinite flat plate, for which only partial solutions exist. An advantage of the technique is that even in these "impossible" situations one can make use of numerical solutions or even of experimental measurements for the inner solution. Thus in his lifting-line theory Prandtl advocates the use of experimental airfoil-section data for what will be seen in Section 9.2 to be the inner solution.

5.5. Choice of Inner Variables

A crucial step in the method of matched asymptotic expansions is the choice of inner variables. One faces the questions:

(a) Which independent variables should be stretched?
(b) How should they be stretched?
(c) How should the dependent variables be stretched?

Answering the first question depends upon recognizing the singular nature of the problem, including the location of the nonuniformity and its "shape"—that is, whether it is the neighborhood of a point, line, or surface.

The degree of stretching required is usually evident when it is possible to calculate several terms of the outer expansion. For example, the formal thin-airfoil solution for an ellipse was seen in Section 4.4 to be invalid within a distance of order ε^2 from the leading edge, and the inner coordinates were magnified accordingly. Physical insight may suggest or confirm the proper stretching as the scale of the secondary reference length in the problem.

Otherwise, the stretching can be sought by trial. The guiding principles are that the inner problem shall have the least possible degeneracy, that it must include in the first approximation any essential elements omitted in the first outer solution, and that the inner and outer solutions shall match. As an example, consider the model problem (5.1). Trying an arbitrary stretching of the independent variable only, we set

$$f(x;\varepsilon) = F(X;\varepsilon), \qquad X = \frac{x}{\sigma(\varepsilon)} \tag{5.11}$$

The problem becomes

$$\frac{d^2F}{dX^2} - \frac{\sigma(\varepsilon)}{\varepsilon}\frac{dF}{dX} = \frac{\sigma^2(\varepsilon)}{\varepsilon}a, \qquad F(0) = 0, \qquad F\left(\frac{1}{\sigma}\right) = 1 \tag{5.12}$$

Because the highest derivative was lost in the outer limit, d^2F/dX^2 must now be preserved in the inner limit. This means that the factor $\sigma(\varepsilon)/\varepsilon$ multiplying dF/dX must not become infinite as $\varepsilon \to 0$. If it vanishes, the solution satisfying the inner boundary condition (which must also be preserved) is simply a multiple of X; but this cannot be matched with the outer solution (5.3). The remaining possibility is that $\sigma(\varepsilon)/\varepsilon$ approaches a constant; this also yields the least degenerate differential equation. Taking the constant as unity without loss of generality gives the previous results (5.4) and (5.5). It was unnecessary to stretch the dependent variable in this example because the first inner problem is homogeneous; but in general one must admit separate stretching of each dependent as well as each independent variable.

The inner variables are almost always, as in the preceding examples, formed by linear stretching. An exception arises in the problem of the vortical layer on an inclined cone (Munson, 1964). This is illustrated by the following model problem:

$$x^m \frac{df}{dx} - \varepsilon f = 0, \qquad f(1) = 1 \tag{5.13}$$

Iterating or substituting a series in powers of ε yields the straightforward (outer) perturbation solution:

$$f(x;\varepsilon) \sim 1 + \frac{\varepsilon}{1-m}(x^{1-m} - 1) + O(\varepsilon)^2, \qquad m \neq 1 \tag{5.14a}$$

$$\sim 1 + \varepsilon \log x + O(\varepsilon^2), \qquad m = 1 \tag{5.14b}$$

This is singular at $x = 0$ for $m \geqslant 1$ and at $x = \infty$ for $m \leqslant 1$. It seems likely that for $m \neq 1$ an appropriate inner coordinate is

$$X = x\varepsilon^{-1/(m-1)} \tag{5.15}$$

and this is confirmed by examining either the resulting inner equation

$$X^m \frac{df}{dX} - f = 0 \tag{5.16}$$

or the exact solution

$$f(x;\varepsilon) = \exp\left(-\frac{\varepsilon}{1-m}\right)\exp\left(\frac{\varepsilon x^{1-m}}{1-m}\right), \qquad m \neq 1 \tag{5.17a}$$

$$= x^\varepsilon, \qquad m = 1 \tag{5.17b}$$

In the special case $m = 1$, (5.14b) indicates that the region of nonuniformity near the origin is exponentially small: $x = O(e^{-1/\varepsilon})$. One might suppose that, just as for the sharp-nosed airfoil of Section 4.7, an appropriate inner variable would therefore be given by the corresponding linear stretching:

$$X = xe^{1/\varepsilon} \tag{5.18}$$

However, this leaves the transformed differential equation

$$X\frac{df}{dX} - \varepsilon f = 0 \tag{5.19}$$

unchanged, so that simple stretching is ineffective. Instead, the exact solution (5.17b) shows that the proper inner coordinate is given by the nonlinear distortion

$$X = x^\varepsilon \tag{5.20}$$

which transforms the differential equation to

$$X \frac{df}{dX} - f = 0 \tag{5.21}$$

Thus it appears that a fractional-power transformation is required when nonuniformity in an exponentially small region arises not from the boundary conditions but from a homogeneous operator of the form $x\,\partial/\partial x$ in the differential equation.

5.6. The Role of Matching

The method of matched asymptotic expansions involves loss of boundary conditions. An outer expansion cannot be expected to satisfy conditions that are imposed in the inner region; conversely, the inner expansion will not in general satisfy distant conditions. Thus it is an exceptional circumstance that the inner solution for the elliptic airfoil (Section 4.10) happens to satisfy the upstream boundary condition; the inner solution for a sharp edge does not (Section 4.11). Hence insufficient boundary conditions are generally available for either the outer or inner expansion. The missing conditions are supplied by matching the two expansions.

For partial differential equations a useful preliminary to matching is application of the principle of minimum singularity (Section 4.5). Experience has shown that of the admissible solutions only the one that is least singular in its region of nonuniformity can be matched to the complementary expansion. For example, the inner solution for a round-nosed thin airfoil was seen in Section 4.9 to be a symmetric flow past the osculating parabola. Figure 5.3 shows the first two of an unlimited

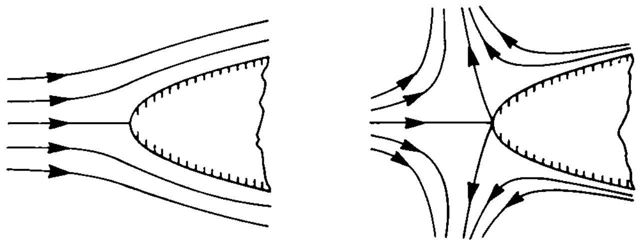

Fig. 5.3. Alternative symmetric flows past parabola.

number of possibilities. All but the first give unbounded speeds at infinity, and consequently cannot be matched with the thin-airfoil expansion (Exercise 4.2).

Although the principle of minimum singularity often reduces the number of possibilities, it cannot always single out a unique flow pattern. For example, it rules out source eigensolutions in the linearized solution for a round-nosed airfoil, but not in the second approximation. This is as it should be, because a source eigensolution must actually occur in the second-order outer solution for a smooth profile that differs from an ellipse only in the vicinity of the leading and trailing edges (Fig. 5.4).

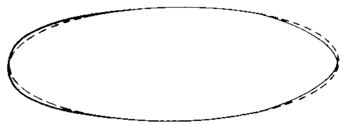

Fig. 5.4. Airfoil having same linearized solution as ellipse.

Matching is the crucial feature of the method. The possibility of matching rests on the existence of an *overlap domain* where both the inner and outer expansions are valid. By virtue of the overlap, one can obtain exact relations between finite partial sums. This remarkable achievement is possible only for a parameter perturbation that is nonuniform in the coordinates, or for a coordinate perturbation that is nonuniform in the other coordinates. One cannot match two different parameter perturbations, such as expansions for large and small values of Reynolds number or of Mach number. Neither can one match two different coordinate expansions, such as for small and large time or distance. Such series may overlap in the sense that they have a common region of convergence, but the process of analytical continuation yields only approximate relations from any finite number of terms (cf. Section 10.9).

Matching may also be contrasted with what we shall call numerical *patching*. This consists in joining two series by forcing their values and perhaps several derivatives to agree at an arbitrary intermediate boundary. Although the result may be of practical utility—or even numerically indistinguishable from that of matching—patching is esthetically displeasing, and ordinarily no simpler. Also, matching is more systematic than patching in higher approximations. Our view is that patching should be avoided whenever it can be replaced by matching, which provides an imperceptibly smooth blending of the two solutions.

5.7. Matching Principles

The existence of an overlap domain implies that the inner expansion of the outer expansion should, to appropriate orders, agree with the outer expansion of the inner expansion (Lagerstrom, 1957). This general matching principle can be given various specific formulations. The literature shows that the choice of matching principle is somewhat a matter of the investigator's taste.

See Note 5

In matching his boundary-layer approximation to the outer inviscid flow, Prandtl tacitly applied what we may call the *limit matching principle:*

$$\begin{aligned}&\text{The inner limit of (the outer limit)}\\ &= \text{the outer limit of (the inner limit).}\end{aligned} \qquad (5.22)$$

Whether this primitive rule is correct, or adequate, depends not only on the problem, but also on the choice of independent variables being matched. It is evidently valid for the tangential velocity in the boundary layer, which must for large values of its argument approach the inviscid surface speed. However, it is invalid for the normal velocity or stream function, where the first repeated limit in (5.22) is zero but the second is infinite. The same difficulty arises in plane flow at low Reynolds number (Chapter VIII).

We can improve this simple rule by describing more precisely the limiting behavior of the quantity being matched (cf. Sections 3.2 and 3.3). Instead of mere limits we use asymptotic representations. This gives the matching principle

$$\begin{aligned}&\text{Inner representation of (outer representation)}\\ &= \text{outer representation of (inner representation).}\end{aligned} \qquad (5.23)$$

Here the outer (or inner) representation means the first *nonzero* term in the asymptotic expansion in outer (or inner) variables. This rule provides matching in cases where the limit principle (5.22) gives only a trivial result. For example, we shall see in Section 8.7 that it suffices for plane flow at low Reynolds number.

The principle is extended to higher approximations by retaining further terms in the asymptotic expansions. We must permit the number of terms to be different in the inner and outer expansions, because the normal matching order (Section 5.9) requires a difference of one in the even-numbered steps. Thus we obtain the *asymptotic matching principle* introduced in Chapter IV: See Note 4

$$\begin{aligned}&\text{The } m\text{-term inner expansion of (the } n\text{-term outer expansion)}\\ &= \text{the } n\text{-term outer expansion of (the } m\text{-term inner expansion).}\end{aligned} \qquad (5.24)$$

Here m and n are any two integers; in practice m is usually chosen as either n or $n + 1$.

This matching principle appears to suffice for any problem to which the method of matched asymptotic expansions can successfully be applied. It will be used throughout this book. In the following section, however, we describe an alternative principle that provides deeper insight into the nature of the overlap domain.

5.8. Intermediate Matching

In the outer limit process of thin-airfoil theory (Chapter IV) a point remains a fixed distance from the leading edge as the thickness ratio ε tends to zero, whereas in the inner limit process for the elliptic airfoil the distance decreases like ε^2. It is by no means obvious that the two limit processes can be interchanged, because there is a gap between the inner and outer regions. That a gap exists is clarified by considering a point whose distance from the nose decreases only like ε (Fig. 5.5). This point ultimately emerges from any vicinity of the leading edge, and is at the same time excluded from the region of validity of the outer solution.

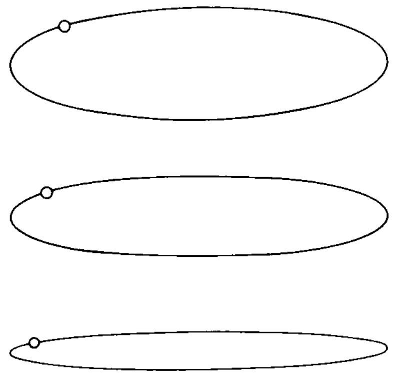

Fig. 5.5. Intermediate limit process for elliptic airfoil.

To bridge this gap, Kaplun (1957) has introduced the concept of a continuum of *intermediate limits*, lying between the inner and outer limits. Although he considers a very general class of limits, it will suffice for purposes of illustration to consider only those associated with powers of the small parameter. If s is the outer variable associated with a nonuniformity at $s = 0$, we introduce an *intermediate variable* See Note 5

$$\tilde{s} = \frac{s}{\varepsilon^{\alpha}}, \qquad 0 < \alpha < \alpha_i \qquad (5.25)$$

Here $\alpha = 0$ gives the outer and $\alpha = \alpha_i$ the inner limit; for example, $\alpha_i = 2$ for the elliptic airfoil. The limit as $\varepsilon \to 0$ with $\tilde{s}$ fixed is called the intermediate limit; and its repeated application in conjunction with an appropriate asymptotic sequence yields the *intermediate expansion*.

Carrying out the intermediate limit in the differential equations and boundary conditions yields the *intermediate problem*. Although we have introduced very many limit processes, they lead to only a few different problems. All intermediate limits yield essentially a single intermediate problem, which is often the same as the inner problem. For example, setting $\tilde{s} = s/\varepsilon^{\alpha}$ and $\tilde{y} = y/\varepsilon^{\alpha}$ in Eq. (4.33a) for the elliptic airfoil and letting $\varepsilon \to 0$ gives

$$\tilde{y} \sim \pm \varepsilon^{1-\alpha/2}\sqrt{2\tilde{s}} \qquad (5.26)$$

Thus the intermediate problem is that of symmetric flow past a parabola of nose radius $\varepsilon^{2-\alpha}$.

The *intermediate solution* is the solution of the intermediate problem. Its difference from the full solution must vanish uniformly in the intermediate limit. Thus for the elliptic airfoil the intermediate solution for surface speed is, from (4.28),

$$q \sim U_i \sqrt{\frac{\tilde{s}}{\tilde{s} - \frac{1}{2}\varepsilon^{2-\alpha}}} \tag{5.27}$$

The denominator cannot be expanded, because the result would not be uniform near the stagnation point. This example illustrates that the intermediate solution is not necessarily the intermediate limit of the full solution—which is here simply U_i—but may have a more complex structure.

Although the gap between inner and outer limits has been bridged by the intermediate solution, it is not yet apparent that there exists an overlap domain. This is assured by Kaplun's *extension theorem*, which asserts that the range of validity of the inner or outer limit extends at least slightly into the intermediate range. We forego the proof of this theorem, whose truth will be evident in specific examples. Thus we can match the intermediate expansion with the outer expansion at one end of the range and with the inner expansion at the other end. Often the intermediate expansion is identical with the inner expansion—as in our example of the elliptic airfoil—or is contained in it as a special case. Then we can simply match the inner and outer expansions in the outer overlap domain.

Matching requires that in the overlap domain the difference between the outer (or inner) and intermediate solutions vanish in the intermediate limit. Thus for the elliptic airfoil we match the intermediate solution (5.27) to the outer uniform stream by considering

$$\lim_{\varepsilon \to 0,\ \tilde{s}\ \text{fixed}} \left[U - U_i \sqrt{\frac{\tilde{s}}{\tilde{s} - \frac{1}{2}\varepsilon^{2-\alpha}}} \right] = \lim_{\varepsilon \to 0} \left[U - U_i + O(\varepsilon^{2-\alpha}) \right] \tag{5.28}$$

This vanishes if $U_i = U$, and $\alpha < 2$. Hence the outer overlap domain is $0 \leqslant \alpha \leqslant 2$.

We may call the extension of this rule to higher approximations the *intermediate matching principle*:

> In some overlap domain the intermediate expansion of the difference between the outer (or inner) expansion and the intermediate expansion must vanish to the appropriate order. (5.29)

For example, consider two terms each of the intermediate and outer expansions for the speed on an elliptic airfoil, where in the latter we

admit the source eigensolution of (4.32a). The difference between the two expansions is, in intermediate variables

$$D = U\left[1 + \varepsilon + \frac{\varepsilon C_1}{2\varepsilon^{\alpha}\tilde{s} - \varepsilon^{2\alpha}\tilde{s}^2}\right] - U_i \sqrt{\frac{\tilde{s}}{\tilde{s} + \frac{1}{2}\varepsilon^{2-\alpha}}} \tag{5.30}$$

and expanding gives

$$D \sim U(1 + \varepsilon) - U_i + C_1 U\left(\frac{\varepsilon^{1-\alpha}}{2s} + \frac{\varepsilon}{4}\right) + O(\varepsilon^{1+\alpha}, \varepsilon^{2-\alpha}) \tag{5.31}$$

This vanishes to order ε—that is, to second order in powers of ε—if $U_i = U(1 + \varepsilon)$, $C_1 = 0$, and $0 < \alpha < 1$. The first two of these results were found by asymptotic matching in Chapter IV. The third means that the outer overlap domain has shrunk to half its previous width.

5.9. Matching Order

All our previous discussion suggests complete symmetry between the inner and outer limits, so that the two terms could be interchanged throughout. However, we have heretofore used "outer" always to denote the straightforward or basic approximation, and we insist on adhering to this convention. More precisely, we assign the terms so that the outer solution is, to first order, independent of the inner. The test is to consider a first-order change in each, and see whether the other is affected. For example, in thin-airfoil theory the free stream is disturbed only slightly by doubling the nose radius, whereas the flow near the nose is drastically altered by doubling the free-stream speed.

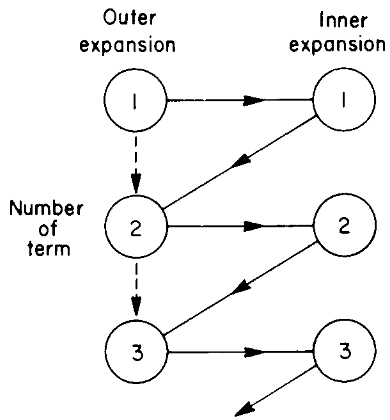

Fig. 5.6. Matching order for inner and outer expansions.

In general, matching must proceed step by step as indicated by the solid arrows in Fig. 5.6. The basic solution dominates the inner solution, which in turn exerts a secondary influence on the outer expansion, and so on. This order is inviolable in the direct problem of boundary-layer theory, for example.

One can sometimes short-circuit the standard matching order. An obvious case is an initial-value problem, where all the boundary conditions are imposed in the outer region. Then one can calculate an unlimited number of terms of the outer expansion, as indicated by dotted arrows in Fig. 5.6, and subsequently match with the inner expansion to complete the solution. This situation can arise in fluid mechanics from inverse formulation of a problem, an example being given in Section 9.9.

The same bypassing of the inner expansion occurs in a more subtle case, when the nonuniformity is so weak that it does not affect the outer flow. An example is the biconvex airfoil of Sections 4.7 and 4.11. For a round-nosed airfoil, on the other hand, the example of Fig. 5.4 shows that only two terms can be calculated before one must resort to matching with the inner expansion.

When the standard order is followed, matching will indicate each new term in the asymptotic sequence, which therefore need not be guessed in advance. For example, rewriting any number of terms of the thin-airfoil expansion (4.14b) for the ellipse in inner variables and expanding for small ε shows at each stage that the next term in the inner expansion is of the order of the next higher power of ε. An example where the asymptotic sequences are different for the inner and outer expansions is discussed in Section 6.3.

5.10. Construction of Composite Expansions

Representing the solution of a singular perturbation problem by an inner and an outer expansion may raise awkward practical questions of where to shift from one to the other. A crude device would be to change where the two curves cross, but the result would have spurious corners. Moreover, for the elliptic airfoil, for example, the first-order inner and outer solutions for surface speed do not meet (Fig. 5.7).

Fortunately, since the two expansions have a common region of validity, it is easy to construct from them a single uniformly valid expansion. The result is necessarily more complex than either of its constituents, and is in fact a composite expansion in the sense of Section 5.4. The construction can in principle be carried out in a variety of ways. The results may be different, because a composite expansion is not unique; but they will all be equivalent to the order of accuracy retained.

Two essentially different methods have been used in practice. The first may be called *additive composition*. The sum of the inner and outer expansions is corrected by subtracting the part they have in common, so that it is not counted twice. The common part can sometimes be

found by inspection. Otherwise, it may be calculated as the inner expansion of the outer expansion, or vice versa. Thus, in an obvious

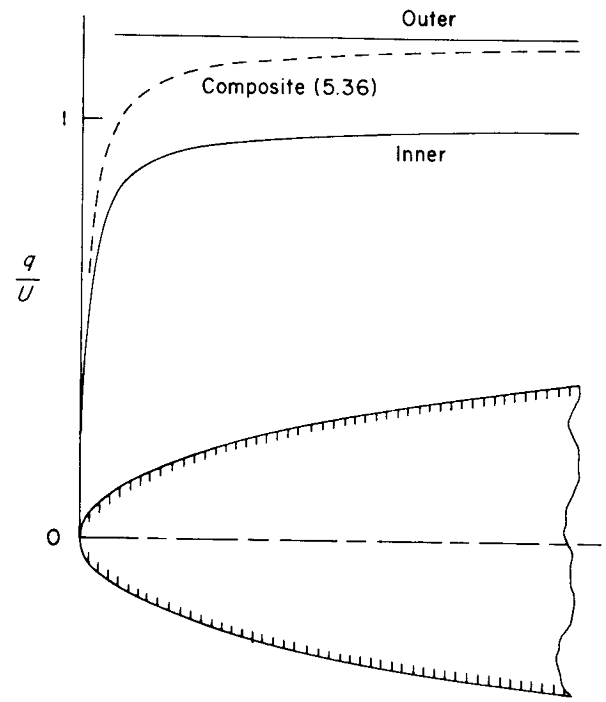

Fig. 5.7. First-order inner and outer solutions for speed on thin ellipse.

notation, where $f_i^{(m)}$ means the m-term inner expansion, and so on, the rule for additive composition is

$$f_c^{(m,n)} = \begin{cases} f_i^{(m)} + f_o^{(n)} - [f_o^{(n)}]_i^{(m)} \\ f_o^{(n)} + f_i^{(m)} - [f_i^{(m)}]_o^{(n)} \end{cases} \tag{5.32}$$

One can verify this rule by taking the m-term inner and n-term outer expansions of both sides. Using the asymptotic matching principle (5.24) shows that the inner and outer expansions are reproduced in their respective regions.

Working with differences, though conceptually somewhat different, yields the same rule. The outer expansion is made uniformly valid by adding to it the solution of the inner problem for the *difference* between the exact solution and its outer expansion, or the inner expansion is corrected analogously. This may be written symbolically

$$f_c^{(m,n)} = \begin{cases} f_o^{(n)} + [f - f_o^{(n)}]_i^{(m)} \\ f_i^{(m)} + [f - f_i^{(m)}]_o^{(n)} \end{cases} \tag{5.33}$$

The asymptotic matching principle shows that these are equivalent to the additive rule (5.32).

The second method may be called *multiplicative composition.* The outer expansion is multiplied by a correction factor consisting of the ratio of the inner expansion to its outer expansion, or the inner expansion is treated similarly. This gives

$$f_c^{(m,n)} = f_o^{(n)} \frac{f_i^{(m)}}{[f_i^{(m)}]_o^{(n)}} = f_i^{(m)} \frac{f_o^{(n)}}{[f_o^{(n)}]_i^{(m)}}$$

$$= \frac{f_o^{(n)} f_i^{(m)}}{[f_o^{(n)}]_i^{(m)} = [f_i^{(m)}]_o^{(n)}} \tag{5.34}$$

The first form is recognized as providing the multiplicative correction factor that was applied to round-nosed airfoils in Section 4.8. The last form exhibits the inherent symmetry between the inner and outer limit processes.

The additive and multiplicative rules of composition are related by the fact that the ratio of two quantities near unity can be expanded into a sum using the binomial theorem. The additive rule is usually simpler to apply; the multiplicative one sometimes gives simpler results. Either can be used even when the inner problem cannot be solved analytically, the solution being known only from numerical computation or experiment.

See Note 6

We illustrate these two methods for the surface speed on a thin elliptic airfoil. From two terms of the outer expansion (4.13) and one term of the inner expansion (4.46) we obtain as the uniform first-order perturbation solution, by additive composition (5.32)

$$\frac{q}{U} \sim \sqrt{\frac{2s}{2s + \varepsilon^2}} + \varepsilon \tag{5.35}$$

and by multiplicative composition (5.34)

$$\frac{q}{U} \sim (1 + \varepsilon) \sqrt{\frac{2s}{2s + \varepsilon^2}} \tag{5.36}$$

Here $s = 1 + x$ or $1 - x$ according as we correct the nonuniformity at the leading or trailing edge; a truly uniform solution is obtained by treating each edge in turn (Exercise 5.3). Other kinds of multiple nonuniformity (cf. Section 9.13) can likewise be handled by repeated application of the rules for composition.

A composite expansion has at least the accuracy of each of its constituents. Thus (5.35) and (5.36) are in error by no more than $O(\varepsilon^2)$ away from the edge and $O(\varepsilon)$ near the edge. In fact the additive result (5.35) is evidently in error by precisely ε at the stagnation point. The multiplicative result (5.36) has the advantage of being exact there. Extending the composite result by using two terms of the inner as well as the outer expansion leads again to (5.36) for either addition or multiplication. This means that by coincidence the error in (5.36) is actually no greater than $O(\varepsilon^2)$ everywhere. Figure 5.7 shows the improvement resulting from use of the composite expansion.

EXERCISES

5.1. *Uniform approximation for Friedrichs' model.* Form in two different ways a composite expansion from the solution (5.6). Discuss the difference, and compare with the exact solution. Consider higher approximations.

5.2. *Uniform approximation for biconvex airfoil.* Construct an approximation for the surface speed on a thin biconvex airfoil in incompressible flow that is uniformly valid to order ε except at the trailing edge.

5.3. *Composite rules for two nonuniformities.* Devise rules, analogous to (5.32) and (5.34), for constructing composite expansions in the case of two separated nonuniformities—as for a thin airfoil with stagnation leading and trailing edges. Apply your results to the surface speed on an elliptic airfoil, and compare with the exact solution.

5.4. *Outer, middle, and inner expansions.* Show that a perturbation solution of the problem

$$x^3 \frac{dy}{dx} = \varepsilon[(1 + \varepsilon)x + 2\varepsilon^2]y^2, \qquad y(1) = 1 - \varepsilon$$

for $0 \leqslant x \leqslant 1$ requires three matched expansions. Calculate in succession two terms of the straightforward (outer) expansion, two terms of the middle expansion, and one term of the inner expansion. Choose new magnified variables as suggested by the preceding expansion, and match at each step.

5.5. *Model with nonvanishing highest derivative.* Calculate three terms of an approximate solution in powers of ε for

$$(1+\varepsilon)x^2\frac{dy}{dx} = \varepsilon[(1-\varepsilon)xy^2 - (1+\varepsilon)x + y^3 + 2\varepsilon y^2], \qquad y(1) = 1$$

Deduce the location of any nonuniformity for $0 \leqslant x \leqslant 1$, and the size of the region involved. Calculate the leading term in the inner expansion, finding the constant by matching. Calculate the second term, and form a uniformly valid second approximation.

5.6. *Impulsive motion of light mass on spring.* A small mass hangs from a weightless spring with internal damping proportional to velocity. A vertical impulse I is imparted to the mass by striking it with a hammer. Show that appropriate choice of variables reduces the problem to

$$\varepsilon\ddot{y} + \dot{y} + y = 0, \qquad y(0) = 0, \qquad \varepsilon\dot{y}(0) = 1$$

Show how a straightforward approximation for small ε breaks down. Calculate an inner expansion, and a composite approximation. Discuss the applicability of the method when damping is absent, the canonical equation being $\varepsilon\ddot{y} + y = 0$.

See Note 3 **5.7.** *Circle in parabolic shear.* Complete the solution of Exercise 2.4 to order ε by introducing a supplementary expansion valid far from the circle. Construct a uniformly valid composite approximation.

Chapter VI

THE METHOD OF STRAINED COORDINATES

6.1. Historical Introduction

In the late 1940's Whitham and Lighthill were concerned at Manchester University with problems involving the locations of bow shock waves in supersonic flow. As an outgrowth of that work, Lighthill (1949a) described a general technique for removing nonuniformities from perturbation solutions of nonlinear problems. The method has subsequently been applied to a variety of problems in fluid mechanics. Thus it constitutes an important alternative to the method of matched asymptotic expansions.

The basic idea of Lighthill's technique is that the linearized solution may have the right form, but not quite at the right place. The remedy is to slightly strain the coordinates, by expanding one of them as well as the dependent variables in asymptotic series. The first approximation—which becomes the same function of the strained variables as it was of the unstrained ones—is thereby rendered uniformly valid. One can proceed similarly to higher approximations. The straining of coordinates is initially unknown, and must be determined term-by-term as the solution progresses.

The straining is determined by the principle already introduced in Section 4.12:

Higher approximations shall be
no more singular than the first. (6.1)

This halts the disastrous compounding of singularities that invalidates a straightforward perturbation expansion in a region of nonuniformity. Lighthill notes that sometimes a weak increase in singularity can actually be tolerated (Exercise 6.1), but it is simplest to adopt the above principle.

This principle does not by any means determine the straining uniquely; but the nonuniqueness can often be used to advantage. Because both independent and dependent variables are expanded, the solution is found in implicit form, with the strained coordinate appearing as a parameter. This implicitness, far from being undesirable, is essential in most problems. Often one requires only a uniform first approximation. Then the second-order equations need not be solved, but merely inspected to determine the straining.

An analogous straining of the independent variable was used by Poincaré (1892) to obtain periodic solutions of nonlinear ordinary differential equations. For this reason Tsien (1956), in a survey article, has dubbed it the "PLK method," the K standing for an application to viscous flows undertaken by Kuo (1953, 1956). We prefer to speak of Lighthill's technique, or of the *method of strained coordinates*, which describes its essential feature.

The technique has proved altogether successful for treating hyperbolic differential equations—particularly in problems with waves traveling primarily in one direction, which is the sort of problem for which it was invented. Lighthill himself (1949b) applied it immediately to conical shock waves in steady supersonic flow. Whitham applied it to the pattern of shock waves on an axisymmetric projectile in steady supersonic flight (1952) and to the propagation of spherical shocks in stars (1953). Legras (1951, 1953) treated supersonic airfoils, and Rao (1956) sonic booms.

An important generalization of the method has been advanced by Lin (1954) for hyperbolic equations in two variables. The strained coordinate of Lighthill may then be interpreted as one of the characteristics. Lin adopts characteristic parameters as the basis for a perturbation theory, which amounts to straining both families of characteristics. This permits treatment of waves traveling in both directions.

Because of the flexibility of Lighthill's method, it represents a philosophy of approach rather than a definite set of rules. For this reason it is difficult ever to say that the method has failed. Nevertheless, it appears that the method is inappropriate for elliptic equations, despite Lighthill's (1951) treatment of round-nosed airfoils in incompressible flow which we outlined in Section 4.12. Likewise, despite Kuo's attempts, the method appears to be unsuitable for parabolic equations, where it has even led to erroneous results (Wu, 1956; Levey, 1959). Thus in a later survey bearing the same title as his original paper, Lighthill (1961) advises that his method be used only for hyperbolic partial differential equations.

See Note 7

It is illuminating to compare the method of strained coordinates with that of matched asymptotic expansions. It is a strength as well as a weakness of the former that only one asymptotic expansion is used for the dependent variables. The analysis is simpler as a result, and one

avoids the possibility of encountering an "impossible" nonlinear problem for the first term of the inner expansion. On the other hand, the principle used for determining the straining of coordinates is so crude in comparison with the detailed description of the region of nonuniformity provided by an inner expansion that it is scarcely surprising that Lighthill's technique is not universally sucessful.

6.2. A Model Ordinary Differential Equation

Because of our devotion to fluid mechanics, we have emphasized application of the method of strained coordinates to partial differential equations. However, it is useful also for many ordinary differential equations. Indeed, Lighthill introduces his method by considering equations of the form

$$(x + \varepsilon f)\frac{df}{dx} + q(x)f = r(x) \tag{6.2}$$

and Wasow (1955) has proved convergence under mild restrictions on the functions q and r (with corrections by Lighthill, 1961). We make a simple choice for these functions, and consider the model problem

$$(x + \varepsilon f)\frac{df}{dx} + f = 1, \qquad f(1) = 2 \tag{6.3}$$

A straightforward perturbation expansion in powers of the parameter ε yields the formal solution

$$f \sim \frac{1+x}{x} - \varepsilon\,\frac{(1+x)(1+3x)}{2x^3} + \varepsilon^2\,\frac{(1+x)(1-x)(1+3x)}{2x^5} + \cdots \tag{6.4}$$

This is a familiar situation arising from a singular perturbation problem. The series converges, but the radius of convergence vanishes as x approaches zero; the expansion is not uniformly valid near $x = 0$. The exact solution is

$$f = \sqrt{\left(\frac{x}{\varepsilon}\right)^2 + 2\,\frac{1+x}{\varepsilon} + 4} - \frac{x}{\varepsilon} \tag{6.5}$$

and this is finite at $x = 0$. The full equation is singular along the line $x = -\varepsilon f$ (Fig. 6.1), but linearization transfers the singularity to $x = 0$; and in higher approximations it is spuriously intensified rather than being corrected.

The method of strained coordinates permits the singularity in the linearized solution to shift toward its true position by straining the coordinate x. We expand both x and f in powers of ε with coefficients that are functions of a new auxiliary coordinate, say s. Since the straining is slight, the leading term in the expansion for x may be taken as s itself.

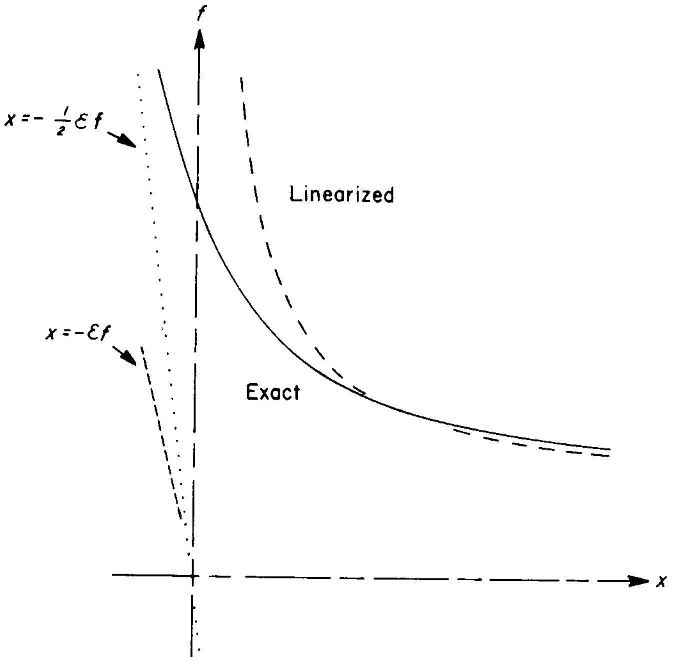

Fig. 6.1. Integral curves for (6.3).

Thus we set

$$f(x;\varepsilon) \sim f_1(s) + \varepsilon f_2(s) + \varepsilon^2 f_3(s) + \cdots \tag{6.6a}$$

where

$$x \sim s + \varepsilon x_2(s) + \varepsilon^2 x_3(s) + \cdots \tag{6.6b}$$

Substituting into Eq. (6.3) and equating like powers of ε yields

$$(sf_1)' = 1 \tag{6.7a}$$

$$(sf_2)' = f_1'(sx_2' - x_2 - f_1) = [x_2(1 - f_1) - \tfrac{1}{2}f_1^2]' \tag{6.7b}$$

and so on. The solution for f_1 that satisfies the boundary condition is

$$f_1(s) = \frac{1+s}{s} \tag{6.8}$$

Then the equation for f_2 becomes

$$(sf_2)' = -\left[\frac{1+2s}{2s^2} + \frac{x_2(s)}{s}\right]' \tag{6.9}$$

and the solution is

$$f_2(s) = \frac{c}{s} - \frac{1}{s^2}\left[x_2(s) + \frac{1+2s}{2s}\right] \tag{6.10}$$

However, this last solution is not required if we seek only a uniformly valid first approximation. The straining x_2 can be found simply by examining the equation for f_2 without solving it.

The straining is to be chosen in accord with the principle (6.1) that f_2 shall be no more singular than f_1. Evidently the simplest way of accomplishing this is to annihilate the nonhomogeneous right-hand side of the equation (6.9) for f_2, setting

$$\frac{1+2s}{2s^2} + \frac{x_2(s)}{s} = \text{const} \tag{6.11}$$

although the constant could be replaced by any regular function of s.

It is characteristic of the method that a further choice of straining is open. The most obvious choice, $x_2 = -(1+2s)/2s$, gives as a uniform first approximation

$$f(x;\varepsilon) \sim \frac{1+s}{s} + \cdots \tag{6.12a}$$

$$x \sim s - \varepsilon\frac{1+2s}{2s} + \cdots \tag{6.12b}$$

In this simple problem it happens that the parameter s can be eliminated to give the explicit first approximation

$$f(x;\varepsilon) \sim \sqrt{\left(\frac{x}{\varepsilon}\right)^2 + 2\,\frac{1+x}{\varepsilon} + 1} - \frac{x}{\varepsilon} \tag{6.12c}$$

Alternatively, it may be convenient to make the straining vanish at $x = 1$, where the boundary condition is imposed. Then we choose $x_2 = (3s^2 - 1 - 2s)/2s$, and the uniform first approximation is

$$f(x;\varepsilon) \sim \frac{1+s}{s} \tag{6.13a}$$

$$x \sim s + \varepsilon\frac{3s^2 - 1 - 2s}{2s} \tag{6.13b}$$

In this case eliminating s shows that the first approximation is the exact solution (6.5), so that the series (6.13) terminate.

At $x = 0$, where the formal expansion (6.4) diverges, the exact solution (6.5) or (6.13) gives $f(0; \varepsilon) = (2/\varepsilon + 4)^{1/2}$. The result (6.12) from the first choice of straining gives instead $f(0; \varepsilon) \sim (2/\varepsilon + 1)^{1/2}$, which agrees with the exact solution to first order in ε.

6.3. Comparison with Method of Matched Expansions

It is natural to inquire as to the relative applicability and merits of the method of strained coordinates and the method of matched asymptotic expansions. We therefore seek in this example an inner expansion to supplement the straightforward outer expansion (6.4) in its region of nonuniformity.

The outer expansion fails when x^2 is as small as ε, because then successive terms do not decrease in magnitude as was assumed. This indicates that the region of nonuniformity is where $x = O(\varepsilon^{1/2})$. There the outer expansion suggests that f is of order $\varepsilon^{-1/2}$. We therefore introduce inner variables X and F, which are of order unity in the region of nonuniformity, by setting

$$X = \frac{x}{\varepsilon^{1/2}}, \qquad F = f\varepsilon^{1/2} \tag{6.14}$$

Rewritten in inner variables, Eq. (6.3) becomes

$$(X + F)\frac{dF}{dX} + F = \varepsilon^{1/2} \tag{6.15}$$

As suggested by the term $\varepsilon^{1/2}$, this is a case where the asymptotic sequences are essentially different for the inner and outer expansions. Whereas the outer expansion (6.4) proceeds in integral powers of ε, the inner expansion proceeds by half powers, having the form

$$f(x; \varepsilon) \sim \varepsilon^{-1/2}[F_1(X) + \varepsilon^{1/2}F_2(X) + \varepsilon F_3(X) + \cdots] \tag{6.16}$$

By substituting into the differential equation (6.15) we obtain

$$(X + F_1)F_1' + F_1 = 0 \tag{6.17a}$$

$$(X + F_1)F_2' + (1 + F_1')F_2 = 1 \tag{6.17b}$$

and so on. The general solution for F_1 is

$$F_1(X) = \sqrt{X^2 + 2C_1} - X \tag{6.18}$$

It is clear that the boundary condition is an outer one, which should be disregarded and replaced by matching with the outer expansion. We apply the asymptotic matching principle (5.24) with $m = n = 1$. Following the format introduced in Chapter IV, we have

1-term outer expansion:	$f \sim \dfrac{1+x}{x}$	(6.19a)
rewritten in inner variables:	$= 1 + \dfrac{1}{\varepsilon^{1/2}X}$	(6.19b)
expanded for small ε:	$= \dfrac{1}{\varepsilon^{1/2}X} + 1$	(6.19c)
1-term inner expansion:	$= \dfrac{1}{\varepsilon^{1/2}X} = \dfrac{1}{x}$	(6.19d)
1-term inner expansion:	$f \sim \dfrac{1}{\varepsilon^{1/2}}[\sqrt{X^2 + 2C_1} - X]$	(6.20a)
rewritten in outer variables:	$= \dfrac{x}{\varepsilon}\left[\sqrt{1 + 2C_1\dfrac{\varepsilon}{x^2}} - 1\right]$	(6.20b)
expanded for small ε:	$= \dfrac{C_1}{x} + \cdots$	(6.20c)
1-term outer expansion:	$= \dfrac{C_1}{x}$	(6.20d)

By equating (6.19d) and (6.20d), we obtain $C_1 = 1$. Hence the first-order solution by the method of matched asymptotic expansions is

$$f(x; \varepsilon) \sim \begin{cases} \dfrac{1+x}{x} & \text{as } \varepsilon \to 0 \text{ with } x \text{ fixed} \quad (6.21\text{a}) \\[2ex] \sqrt{\left(\dfrac{x}{\varepsilon}\right)^2 + \dfrac{2}{\varepsilon}} - \dfrac{x}{\varepsilon} & \text{as } \varepsilon \to 0 \text{ with } \dfrac{x}{\varepsilon^{1/2}} \text{ fixed} \quad (6.21\text{b}) \end{cases}$$

A uniformly valid composite approximation can be constructed by either of the methods described in Section 5.10, which give

$$f(x; \varepsilon) \sim \begin{cases} \sqrt{\left(\dfrac{x}{\varepsilon}\right)^2 + \dfrac{2}{\varepsilon}} - \dfrac{x}{\varepsilon} + 1, & \text{additive} \quad (6.21\text{c}) \\[2ex] (1 + x)\left[\sqrt{\left(\dfrac{x}{\varepsilon}\right)^2 + \dfrac{2}{\varepsilon}} - \dfrac{x}{\varepsilon}\right], & \text{multiplicative} \quad (6.21\text{d}) \end{cases}$$

Further terms in the inner expansion can be found by continuing the process.

It appears that in this example the method of strained coordinates is by far the simpler of the two. We defer more detailed comparison to Section 6.8.

6.4. Nonuniformity in Supersonic Airfoil Theory

A simple flow problem in which the method of strained coordinates proves efficacious is that of supersonic flow past a thin airfoil. The classical linearized solution of Ackeret is based upon the approximate equation

$$\varphi_{yy} - B^2\varphi_{xx} = 0, \qquad B^2 \equiv M^2 - 1 \tag{6.22}$$

Here φ is the perturbation velocity potential; we take it to be normalized such that the velocity vector is $\mathbf{q} = U\,\mathrm{grad}(x + \varphi)$. Although Ackeret's solution is a proper first approximation at and near the surface, it fails at great distances from the airfoil. It predicts disturbances propagating undiminished along the free-stream Mach lines to infinity (Fig. 6.2),

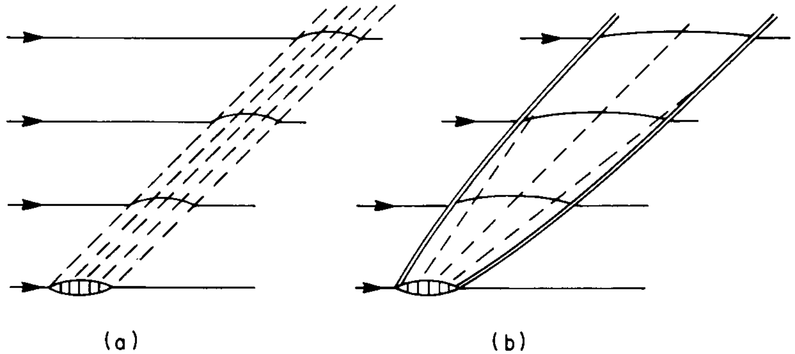

Fig. 6.2. Flow pattern above supersonic airfoil. (a) Linearized. (b) Nonlinear.

whereas in reality the Mach lines are not straight or parallel, and shock waves are formed and decay.

This nonuniformity at large distances is somewhat more delicate than that arising, for example, in Stokes' approximation for viscous flow at low Reynolds numbers (Chapter VIII). There one can use the first approximation to estimate the magnitude of the terms neglected in the equation of motion, showing that they ultimately dominate those retained. However, in the present problem the nonlinear terms are actually small everywhere compared with the linear ones; it is only their *contribution* that becomes dominant. They have what Hayes (1954) calls a *cumulative effect*, meaning that over a long stretch their influence grows

to first order. To see this it is necessary to actually calculate the second approximation. This means solving the nonlinear potential equation (2.19) by successive approximations, starting with Ackeret's linear solution. Setting $\phi = x - \varphi$ in (2.19) and grouping linear terms on the left-hand side puts it into the appropriate form:

$$\varphi_{yy} - B^2\varphi_{xx} = M^2\Big[\frac{\gamma - 1}{2}(2\varphi_x + \varphi_x^2 + \varphi_y^2)(\varphi_{xx} + \varphi_{yy}) + (2\varphi_x + \varphi_x^2)\varphi_{xx} + 2(1 + \varphi_x)\varphi_y\varphi_{xy} + \varphi_y^2\varphi_{yy}\Big] \tag{6.23}$$

Let the upper surface of the airfoil be described as before (Fig. 4.1) by $y = \varepsilon\,T(x)$. Then the formal second approximation for the streamwise velocity component above the airfoil is found, by iterating upon (6.23), to be (Van Dyke, 1952)

$$\frac{u}{U} = 1 - \varepsilon\frac{T'(\xi)}{B} + \varepsilon^2\Big[\frac{1}{B^2}\Big(1 - \frac{\gamma + 1}{4}\frac{M^4}{B^2}\Big)T'^2(\xi) - \frac{\gamma + 1}{2}\frac{M^4}{B^3}\,yT'(\xi)T''(\xi) - T(\xi)T''(\xi)\Big] + O(\varepsilon^3) \tag{6.24}$$

where $\xi \equiv x - By$. At the surface this reproduces the well-known, second-order solution of Busemann. Far from the airfoil however, the second term is not small compared with the first—as was assumed in the iteration process—because it grows linearly with y along any free-stream Mach line $x - By =$ constant. Evidently the expansion is invalid in the distant region where $y = O(\varepsilon^{-1})$.

The troublesome term in y is proportional to $(\gamma + 1)$. This is an indication of the fact that the nonuniformity arises only from the "pseudo-transonic" term $(\gamma + 1)M^4\varphi_x\varphi_{xx}$ that is inherent in the nonlinear right-hand side of the differential equation (6.23). That term can be exhibited explicitly by transforming to the oblique coordinates introduced later (see also Hayes, 1954). The contribution of all other nonlinear terms is uniformly of second order. Although the pseudo-transonic term is small, it has a first-order cumulative effect. It must therefore be retained in addition to the linear terms in seeking a uniformly valid first approximation. To that order the tangency condition may be imposed on the axis, as discussed in Sections 3.8 and 4.2. Thus the problem for the first approximation is

$$\varphi_{yy} - B^2\varphi_{xx} = (\gamma + 1)M^4\varphi_x\varphi_{xx} \tag{6.25a}$$

$$\varphi_y(x, 0) = \varepsilon T'(x) \tag{6.25b}$$

$$\varphi(x, y) = 0 \qquad \text{upstream} \tag{6.25c}$$

It is convenient to make a preliminary transformation of coordinates. There are two distinguished directions in the problem: that of the free stream, and that of the outgoing free-stream Mach lines either above or below the airfoil (Fig. 6.3). The airfoil lies nearly along the first, and the

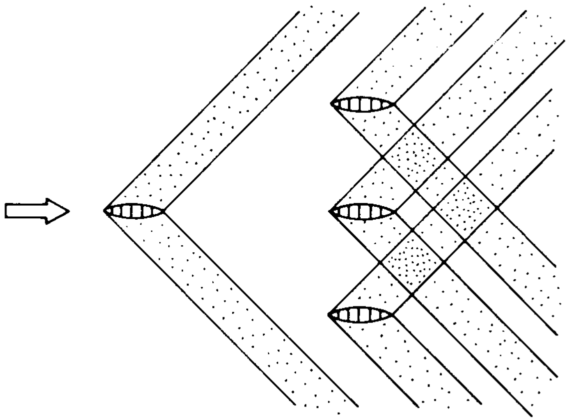

Fig. 6.3. Wave patterns in supersonic flow.

wave pattern nearly along the second. The other family of Mach lines plays only a secondary role. This is true if we restrict consideration to, say, the upper surface of a single airfoil; for multiple bodies both families of Mach waves are of primary importance, and intersect, forming a Scotch-plaid pattern. For this reason the second-order solution (6.24) can be expressed more naturally in terms of the normalized distances

$$\xi = x - By \tag{6.26a}$$
$$\eta = By \tag{6.26b}$$

perpendicular to the two distinguished directions. We therefore adopt henceforth, following Hayes (1954), these "semicharacteristic" coordinates. If both families of waves were present, one would use instead the characteristic coordinates $x - By$ and $x + By$, and in the next section Lighthill's technique would have to be replaced by the generalization of Lin (1954) mentioned previously.

Rewritten in these oblique coordinates, the problem (6.25) becomes

$$\varphi_{\xi\eta} + \frac{\gamma - 1}{2}\,\frac{M^4}{B^2}\,\varphi_\xi\varphi_{\xi\xi} = \tfrac{1}{2}\varphi_{\eta\eta} \tag{6.27a}$$
$$\varphi_\xi = -\,\varepsilon\,\frac{T'(\xi)}{B} - \varphi_\eta \qquad \text{at} \quad \eta = 0 \tag{6.27b}$$
$$\varphi = 0 \qquad \text{upstream} \tag{6.27c}$$

The linearized solution is $\varphi = -\,\varepsilon T(\xi)/B$, so that $\varphi_\eta = \varphi_{\eta\eta} = 0$. Although this is not true in the nonlinear solution, because the waves depart slightly from the free-stream Mach lines, Hayes points out that the terms φ_η and $\varphi_{\eta\eta}$ appearing here represent truly second-order effects, like others already neglected. Hence they may be discarded, and the problem for a uniform first approximation becomes simply

$$\varphi_{\xi\eta} + \frac{\gamma - 1}{2}\,\frac{M^4}{B^2}\,\varphi_\xi\varphi_{\xi\xi} = 0 \tag{6.28a}$$
$$\varphi_\xi(\xi, 0) = -\,\varepsilon\,\frac{T'(\xi)}{B} \tag{6.28b}$$
$$\varphi = 0 \qquad \text{upstream} \tag{6.28c}$$

We are now in the fortunate position of having a well-posed problem for the dimensionless streamwise velocity perturbation u', given by

$$u' \equiv \frac{\Delta u}{U} = \varphi_x = \varphi_\xi \tag{6.29}$$

We prefer to work with this, because it has more physical significance than the velocity potential φ. Thus the problem to be solved becomes finally, with the prime deleted henceforth from u',

$$u_\eta + \frac{\gamma - 1}{2}\,\frac{M^4}{B^2}\,uu_\xi = 0 \tag{6.30a}$$
$$u(\xi, 0) = -\,\varepsilon\,\frac{T'(\xi)}{B} \tag{6.30b}$$
$$u = 0 \qquad \text{upstream} \tag{6.30c}$$

6.5. First Approximation by Strained Coordinates

We apply to this problem the method of strained coordinates. It is clear physically (cf. Fig. 6.2) as well as mathematically that the coordinate ξ describing the Mach lines is to be strained. We therefore introduce a slightly strained variable s in place of ξ, and set

$$u(\xi, \eta; \varepsilon) \sim \varepsilon u_1(s, t) + \varepsilon^2 u_2(s, t) + \cdots \tag{6.31a}$$
$$\xi \sim s + \varepsilon\xi_2(s, t) + \cdots, \qquad \eta = t \tag{6.31b}$$

The transformation of derivatives is found from

$$\frac{\partial}{\partial s} = (1 + \varepsilon\xi_{2s} + \cdots)\,\frac{\partial}{\partial \xi}, \qquad \frac{\partial}{\partial t} = (\varepsilon\xi_{2t} + \cdots)\,\frac{\partial}{\partial \xi} + \frac{\partial}{\partial \eta} \tag{6.32a}$$
$$\frac{\partial}{\partial \xi} = (1 - \varepsilon\xi_{2s} + \cdots)\,\frac{\partial}{\partial s}, \qquad \frac{\partial}{\partial \eta} = \frac{\partial}{\partial t} - (\varepsilon\xi_{2t} + \cdots)\,\frac{\partial}{\partial s} \tag{6.32b}$$

By substituting the expansions (6.31) into the problem (6.30) for u and equating like powers of ε, we find

$$u_{1t} = 0, \qquad u_1(s, 0) = -\frac{T'(s)}{B}, \qquad u_1 = 0 \quad \text{upstream} \tag{6.33a}$$

and

$$u_{2t} = \left(\xi_{2t} - \frac{\gamma+1}{2}\frac{M^4}{B^2}u_1\right)u_{1s} \tag{6.33b}$$

Clearly u_1 is the same function of the strained variable s that it was in linearized theory of the unstrained variable ξ:

$$u_1(s, t) = -\frac{T'(s)}{B} \tag{6.34}$$

The straining function ξ_2 is now to be chosen according to the principle (6.1) that u_2 be no more singular than u_1 as $By = \eta = t$ becomes infinite. The simplest way of assuring this is again to annihilate the right-hand side of the equation (6.33b) for u_2 by setting

$$\xi_{2t} = \frac{\gamma+1}{2}\frac{M^4}{B^2}u_1 = -\frac{\gamma+1}{2}\frac{M^4}{B^3}T'(s) \tag{6.35}$$

so that

$$\xi_2(s, t) = f(s) - \frac{\gamma+1}{2}\frac{M^4}{B^3}tT'(s) \tag{6.36}$$

For the present it suffices to make the straining vanish at the axis $y = 0$ by taking the arbitrary function $f(s) = 0$. It is easily seen from continuity that to first order the vertical velocity is also the same function of s that it was of ξ in linearized theory. Hence, with the original Cartesian coordinates restored, a uniformly valid first approximation for the two velocity components is given by

$$u' \equiv \frac{\Delta u}{U} \sim -\varepsilon\frac{T'(s)}{B} + \cdots, \qquad v' = \frac{v}{U} \sim \varepsilon T'(s) + \cdots \tag{6.37a}$$

where the parametric variable s is given implicitly by

$$x - By \sim s - \frac{\gamma+1}{2}\frac{M^4}{B^2}\varepsilon y T'(s) + \cdots \tag{6.37b}$$

This solution has a simple physical interpretation. The lines $s =$ constant are actually the revised Mach lines, calculated using the first-order velocities. For it can be shown (Van Dyke, 1952) that the slope of the outgoing family of characteristics is

$$\frac{dy}{dx} = \frac{1}{B}\left(1 - \frac{\gamma+1}{2}\frac{M^4}{B^2}\frac{\Delta u}{U} + \cdots\right) \tag{6.38}$$

and inverting and integrating gives

$$x - By = \frac{\gamma+1}{2}\frac{M^4}{B}\frac{\Delta u}{U}y + \text{const} \tag{6.39}$$

which corresponds to (6.37b), the constant being s.

Thus the solution obtained by straining coordinates gives velocity components that are constant along the revised Mach lines, and have the values given by linearized theory on the airfoil. This is in contrast to linearized theory, according to which the velocity at any point equals that at the foot of the free-stream Mach line passing through it (Fig. 6.4). Formal second-order theory (6.24) attempts to improve the estimate

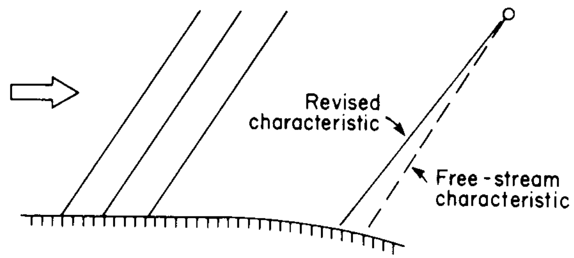

Fig. 6.4. Revision of Mach lines.

by relating values at the foot of the revised Mach line to those at the foot of the free-stream Mach line by Taylor series expansion; of course this breaks down as $y \to \infty$. The uniformly valid first approximation obtained by straining coordinates is thus seen to consist of a simple wave (Prandtl-Meyer expansion fan), and may be compared with the solution obtained on that basis by Friedrichs (1948).

Whitham (1952) has taken the above physical interpretation as the basis for a more heuristic derivation of the uniform first approximation. He introduces "the fundamental hypothesis that linearized theory gives a valid first approximation to the flow *everywhere* provided that in it the approximate characteristics are replaced by the exact ones, or at least by a sufficiently good approximation to the exact ones." The revision (6.39) gives in fact a sufficiently good approximation to the characteristics, and then Whitham's hypothesis leads at once to the solution (6.37) that we have derived more formally by the method of strained coordinates. Whitham is more concerned with applying his method to bodies of revolution; and his result is the basis for calculating sonic booms.

The implicit nature of the straining is evidently essential to the uniform validity of the solution. In sufficiently simple cases, however, the dependence can be inverted to give an explicit solution. For example, consider the smooth convex wall shown in Fig. 6.5, with $T(x) = -\frac{1}{2}x^2$ for $x > 0$. Equation (6.37b) becomes

$$x - By = s\left(1 + \varepsilon \frac{\gamma+1}{2} \frac{M^4}{B^2} y\right) \tag{6.40a}$$

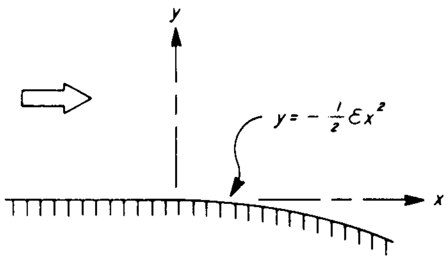

Fig. 6.5. Simple smooth convex wall.

which can be inverted to give

$$s = \frac{x - By}{1 + \varepsilon \dfrac{\gamma+1}{2} \dfrac{M^4}{B^2} y} \tag{6.40b}$$

Then (6.37a) gives the velocity components at any point

$$B\frac{\Delta u}{U} = -\frac{v}{U} = \varepsilon s = \varepsilon \frac{x - By}{1 + \varepsilon \dfrac{\gamma+1}{2} \dfrac{M^4}{B^2} y} \tag{6.41}$$

In this example one sees clearly the source of the nonuniformity in the formal thin-airfoil expansion. For any given y the solution can be expanded in powers of ε, but the result is not uniformly valid near $y = \infty$.

6.6. Modifications for Corners and Shock Waves

It may happen that removal of a glaring nonuniformity from a perturbation problem brings to light additional difficulties, which must be

treated in their turn to obtain a truly uniform solution. This is the case in the present problem if the airfoil involves corners or shock waves. Although these details are not essential to our main exposition, we digress for the sake of completeness to indicate the additional modifications that are required.

The preceding result is uniformly valid for a convex wall whose slope is continuous and slowly changing (T'' of order unity). However, it is clear physically (Fig. 6.6) that the result is invalid even on the surface

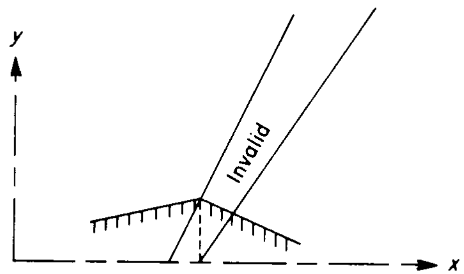

Fig. 6.6. Region of invalidity behind corner.

for a distance of order ε downstream of a corner, unless the corner lies on the axis $y = 0$, because the solution singles out the surface slope ahead of rather than behind the corner. The same is true of any region where the curvature is so great (T'' of order ε^{-1}) that the slope changes by an appreciable fraction of its total variation over a distance of the order of the thickness of the airfoil.

This difficulty arises from having imposed the tangency condition on the axis rather than precisely on the surface, and correspondingly having made the straining vanish on the axis. It can be remedied simply by choosing the function of integration $f(s)$ in (6.36) such that the straining vanishes precisely at the surface, so that $s = x$ on the airfoil. This gives

$$f(s) = \frac{\gamma+1}{2} \frac{M^4}{B^2} \varepsilon T(s)T'(s) - BT(s) \tag{6.42}$$

Thus a solution that is uniformly valid on the surface even with rapid changes in curvature, or corners, is given by (6.37a) with (6.37b) replaced by

$$x - By = s - \varepsilon BT(s) - \frac{\gamma+1}{2} \frac{M^4}{B^2} [y - \varepsilon T(s)]\varepsilon T'(s) \tag{6.43}$$

This is equivalent to the result of Eqs. (92) and (93) of Whitham (1952), though somewhat simpler.

The solution is now uniformly valid for any smooth convex wall, though shock waves have yet to be inserted for a concave wall. This is true no matter how rapidly the curvature changes. However, in the limit as the curvature becomes discontinuous (Fig. 6.7), tracing characteristics

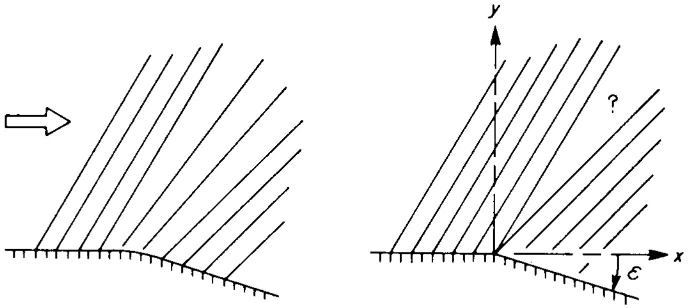

Fig. 6.7. Corner as limit of smooth wall.

shows that the solution is undefined in the Prandtl-Meyer fan from the corner. For example, taking $T(x) = -xH(x)$, where H is the Heaviside unit step function, gives the convex corner shown in Fig. 6.7. Substituting into (6.37b) or (6.43) and solving for s gives, to first order in ε

$$s = \begin{cases} x - By & \text{for } x - By < 0 \\ x - By - \dfrac{\gamma+1}{2}\dfrac{M^4}{B^2}\varepsilon y & \text{for } x - By > \dfrac{\gamma+1}{2}\dfrac{M^4}{B^2}\varepsilon y \end{cases} \tag{6.44}$$

However, s is undefined for $0 < x - By < [(\gamma+1)/2](M^4/B^2)\varepsilon y$, which is just the region of the Prandtl-Meyer fan.

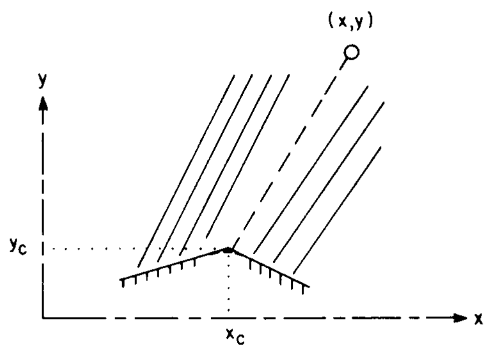

Fig. 6.8. Smoothing of convex corner.

This difficulty is easily remedied by temporarily smoothing the corner slightly, so that the revised characteristic through every point again strikes the surface at a point with a definite slope, as indicated in Fig. 6.8. Clearly s is approximately x_c everywhere in the fan, if the corner lies at (x_c, y_c). Hence $T(s)$ is constant in the fan with value $T(x_c)$, whereas T' varies from $T'(x_c-)$ to $T'(x_c+)$. The value of T' associated with any point (x, y) in the fan is found from (6.43), which gives

$$x - By = x_c - By_c - \frac{\gamma+1}{2}\frac{M^4}{B^2}\varepsilon(y - y_c)T' \tag{6.45}$$

so that

$$T' = -\frac{(x - By) - (x_c - By_c)}{\dfrac{\gamma+1}{2}\dfrac{M^4}{B^2}\varepsilon(y - y_c)} \tag{6.46}$$

Then substituting into (6.37a) gives the velocity components in the fan as

$$B\frac{\Delta u}{U} = -\frac{v}{U} = \varepsilon\frac{(x - By) - (x_c - By_c)}{\dfrac{\gamma+1}{2}\dfrac{M^4}{B^2}\varepsilon(y - y_c)} \tag{6.47}$$

This holds only in the fan, where the value of (6.46) lies between $T'(x_c-)$ and $T'(x_c+)$.

Finally, if the wall is concave the revised characteristics converge, and they overlap at sufficiently great distances—immediately for a concave corner—so that the solution is not unique. For example, changing the sign of the deflection in Fig. 6.7 leads to two values of s at each point in the fan. This multivaluedness must be eliminated by introducing a shock wave to cut off the Mach lines before they can overlap (Fig. 6.9). The shock wave is inserted according to the well-known principle that to

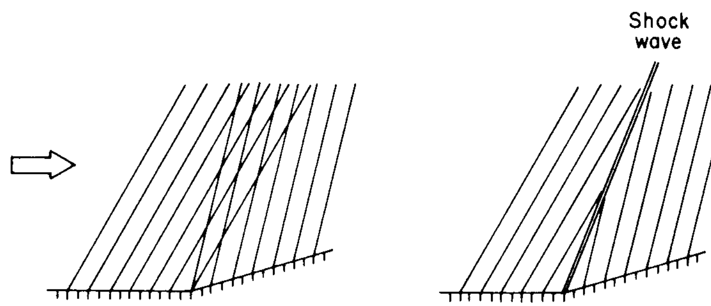

Fig. 6.9. Treatment of overlapping characteristics.

first order a shock wave bisects the Mach directions ahead and behind. Whitham (1952) gives an ingenious graphical construction of the shock pattern for axisymmetric flow based on this principle, which can be adapted to plane flow.

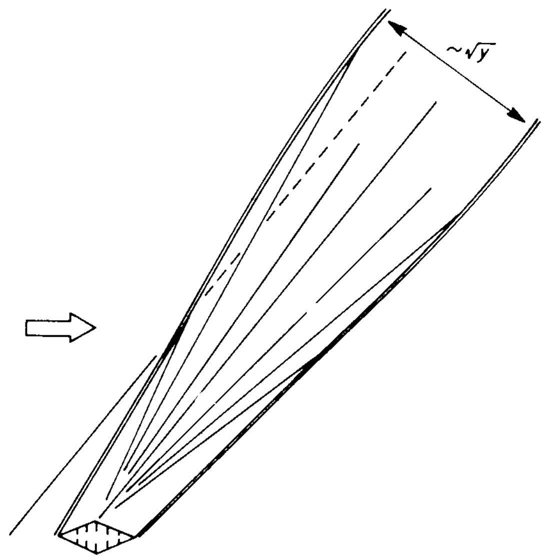

Fig. 6.10. Shock pattern for double-wedge airfoil.

For simple shapes the resulting form of the shock waves can be reasoned out. For example, for a double-wedge profile the bow and stern shock waves must, beyond their straight sections, be portions of a parabola with the corner as focus and a free-stream Mach line as axis, in view of the focussing property of a parabolic mirror (Fig. 6.10). More generally, at such remote distances that the airfoil appears simply as a point, this is true for any profile. Hence the shock pattern grows asymptotically in width like $y^{1/2}$.

6.7. First Approximation by Matched Expansions

It is of interest again to solve the problem (6.30) by the alternative method of matched asymptotic expansions. Substituting the assumed series

$$u(\xi, \eta; \varepsilon) \sim \varepsilon u_1(\xi, \eta) + \varepsilon^2 u_2(\xi, \eta) + \cdots \qquad (6.48)$$

leads without difficulty to the straightforward expansion

$$u \sim -\varepsilon \frac{T'(\xi)}{B} - \varepsilon^2 \frac{\gamma+1}{2} \frac{M^4}{B^4} \eta T'(\xi) T''(\xi) + \cdots \qquad (6.49)$$

This is an approximate form of the full second-order result (6.24). In accord with our convention, discussed in Section 5.9, we call this the outer expansion even though its region of nonuniformity is the vicinity of the point at infinity.

The outer expansion is invalid where $\eta = O(\varepsilon^{-1})$, and in that region u is of order ε. This suggests introducing inner variables such that the inner expansion is

$$u(\xi, \eta; \varepsilon) \sim \varepsilon U_1(\xi, H) + \varepsilon^2 U_2(\xi, H) + \cdots, \qquad H = \varepsilon\eta \qquad (6.50)$$

Substituting into the differential equation (6.30a) gives for the first approximation

$$\frac{\partial U_1}{\partial H} + \frac{\gamma+1}{2} \frac{M^4}{B^2} U_1 \frac{\partial U_1}{\partial \xi} = 0 \qquad (6.51)$$

This is a nonlinear partial differential equation. However, it happens that it can be linearized by interchanging the roles of the independent and dependent variables, and seeking a solution for $\xi(U_1, H)$. The equation becomes

$$\frac{\partial \xi}{\partial H} = \frac{\gamma+1}{2} \frac{M^4}{B^2} U_1 \qquad (6.52)$$

and its general solution is

$$\xi(U_1, H) = g(U_1) + \frac{\gamma+1}{2} \frac{M^4}{B^2} U_1 H \qquad (6.53a)$$

The function of integration g is found by matching with the outer solution (6.49). It is clear, despite the implicit form of the inner solution, that this gives

$$g(U_1) = T'^{-1}(-BU_1) \qquad (6.53b)$$

where T'^{-1} is the function inverse to T'. For example, in the case shown in Fig. 6.5 we have $T'(x) = -x$, so that $T'^{-1}(-BU_1) = BU_1$, and then solving (6.53a) for U_1 yields the result (6.41) obtained previously by the method of strained coordinates.

This inner solution is uniformly valid, because the inner equation (6.51) is in fact the full equation (6.30a). In this simple example no simplification is introduced by the inner expansion, which accordingly terminates at one term.

6.8. Utility of the Method of Strained Coordinates

The particular merits of the method of strained coordinates are emphasized by contrasting it with the alternative method of matched asymptotic expansions. It appears that, as in the foregoing two examples, the latter method is applicable whenever the former is. The converse is unfortunately not true. Thus the method of matched expansions is the more reliable and perhaps the more fundamental of the two.

See Note 7

However, in cases where the method of strained coordinates applies, it is often strikingly simple. This is well illustrated by the preceding examples, which demonstrate two advantages of Lighthill's technique:

(i) It requires solving only the straightforward (outer) perturbation equations, which are linear.

(ii) It gives directly a single uniformly valid expansion.

The second of these is less important, because we have seen in Chapter V that an inner and an outer expansion can easily be combined in several ways to form a single uniformly valid composite expansion. On the other hand, the first is often a substantial advantage, because in nonlinear problems the equation for the leading term of the inner expansion may be difficult or even impossible to solve. Thus in both our examples the first inner problem is nonlinear, whereas the method of strained coordinates involves only linear equations. It is the glory of Lighthill's technique that it attains its goal while avoiding any detailed examination of the region of nonuniformity.

For the same reason, however, it is not always successful. What is worse, it may appear to succeed while giving an incorrect result. The crucial question is, therefore, when is it safe to apply the method of strained coordinates? At present, no general rules can be set forth, but only some indications.

One definite rule is that it is useless to strain the coordinates in a perturbation problem that is singular because the highest derivative is multiplied by a small parameter. Thus Lighthill's technique cannot be used to treat Prandtl's boundary layer. Attempting to do so usually leads to a null result, as can be seen by considering the model problem of Section 5.2. Under special circumstances, however, it leads to a definite but erroneous result. This situation has been analyzed by Levey (1959), who provides a mathematical model illustrating the essential difficulty.

The method of strained coordinates succeeds when the singularity predicted by the straightforward first approximation actually exists, but at a slightly different location. It fails when the actual singularity is of a different type, or nonexistent. The former situation appears to arise with hyperbolic equations, the latter usually with elliptic ones. An example

arising from an elliptic equation is the logarithmic singularity of incompressible thin-airfoil theory at a sharp edge. This was seen in Section 4.11 to correspond in reality to a small fractional power. Hence straining of coordinates fails, whereas the method of matched asymptotic expansions was successful.

The round-nosed airfoil in incompressible flow is an exception, because the square-root singularity of thin-airfoil theory exists, being merely shifted from the leading edge to approximately the focus of the osculating parabola (Section 4.12). For this reason Lighthill (1951) was able to use his technique to find a uniform second approximation for round-nosed airfoils. That this is an exceptional case, however, is indicated by the fact that all attempts have failed to extend his solution to higher order, to subsonic compressible flow, or to other nose shapes. All these problems have been successfully treated by the method of matched asymptotic expansions (Van Dyke, 1954).

See Note 7

This situation has forced Lighthill (1961) to recommend that his technique be restricted to hyperbolic partial differential equations. This is an unfortunate limitation on a powerful method. It is to be hoped that further study will not only clarify the conditions under which the existing method of strained coordinates applies, but also disclose a refinement that can be applied with confidence to other problems, particularly those involving elliptic and parabolic partial differential equations.

EXERCISES

6.1. *Weaker straining principle.* Show that a uniformly valid solution of the problem (6.3) on page 101 is obtained by the method of strained coordinates if the straining principle (6.1) is relaxed to require only that the second approximation shall be no more singular than the square of the first.

6.2. *A problem of Carrier* (1954). Apply the method of strained coordinates to the problem

See Note 3

$$(x^2 + \varepsilon f)\frac{df}{dx} + f = 0, \qquad f(1) = e$$

showing that a uniformly valid first approximation has the form

$$f \sim ae^{b/s}, \quad x \sim s - \varepsilon c\,(1 + ds + gs^2)e^{b/s}$$

with appropriate values of the constants $a, b, c, d,\ g$. Calculate the value of $f(0)$.

6.3. *Delayed straining.* Show that in application of the method of strained coordinates to the problem

$$2x^2 \frac{df}{dx} = \varepsilon f^3, \qquad f(1) = 1$$

the first straining is determined only by the third-order problem. Compare the solution with that obtained by the method of matched asymptotic expansions.

See Note 3

6.4. *Pritulo's method.* Pritulo (1962) points out that if one has calculated a straightforward perturbation solution and found it to be nonuniform, the straining of coordinates required to render it uniformly valid can be found directly therefrom by solving only algebraic rather than differential equations. Illustrate this by substituting (6.6b) into (6.4) and determining the straining to order ε^2.

6.5. *Cylindrical wave propagation.* Consider the nonlinear model problem

$$\frac{\partial v}{\partial y} + \frac{v}{y} + v\frac{\partial v}{\partial x} = 0, \qquad v(x, 1) = \varepsilon f(x)$$

Find the region of nonuniformity of the straightforward expansion for small ε and $y \geqslant 1$. Show that the method of strained coordinates produces the exact solution.

Chapter VII

VISCOUS FLOW AT HIGH REYNOLDS NUMBER

7.1. Introduction

We turn now to the prototype of singular perturbation problems, that of viscous flow past a body at high Reynolds number. Prandtl's boundary-layer theory was invented to treat this problem. It was realized for some time thereafter that boundary-layer theory provides the leading term in an asymptotic expansion for high Reynolds number. However, attempts to calculate further terms in the expansion led at first to considerable confusion, controversy, and error. The problem became straightforward with systematic application of the method of matched asymptotic expansions. Here, using that method, we show how Prandtl's theory can be embedded as the first step in a scheme of successive approximations. The practical utility of such refinement is suggested by an estimate of Lagerstrom and Cole (1955) that the second approximation may predict the skin friction accurately down to Reynolds numbers of 10 or even 5.

For simplicity we consider only plane steady laminar flow of an incompressible fluid past a solid body in a uniform parallel stream. To commence the analysis we need the basic solution for infinite Reynolds number. Of course the actual flow becomes unsteady and turbulent above a certain Reynolds number, but that is irrelevant because our objective is an approximation for moderate values. Unfortunately, the proper limiting solution is unknown for finite bodies, where flow separation presumably occurs. For example, Fig. 7.1 shows three conjectures as to the relevant solution of the inviscid (Euler) equations for a circle, and there are many other possibilities. Until this important question is settled, it is impossible to treat flows with separation, because the wake would exert a first-order influence even in the flow upstream. This means that the body must be semi-infinite, with the exception of the finite flat plate and perhaps some very thin airfoils. For further discussion of these matters see Goldstein (1960).

See Note 8

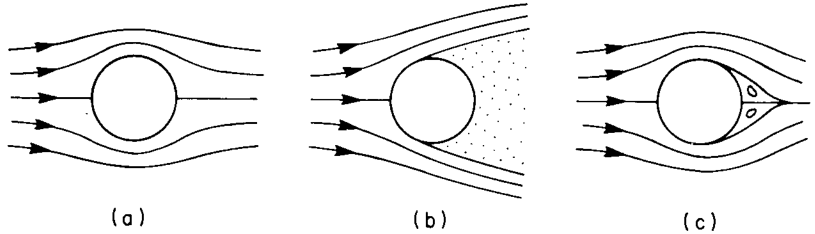

Fig. 7.1. Inviscid flow past circle. (a) Continuous potential flow. (b) Infinite dead-water region. (c) Finite cusped wake (Batchelor 1956).

Serious difficulties arise from corners and other discontinuities, so that it would be preferable to restrict attention to analytic bodies. On the other hand, Prandtl's equations are readily solved only for certain self-similar flows, most of which correspond to sharp-nosed bodies. In the face of this dilemma, we choose to accept the difficulties arising from sharp edges for the sake of reducing the partial differential equations to ordinary ones. We shall in fact make specific application to the finite or semi-infinite flat plate, while indicating the modifications that arise for other shapes.

The reader is assumed to be familiar with the elements of classical boundary-layer theory—in particular, with the Prandtl-Blasius solution for the flat plate as given, for example, by Prandtl (1935), Goldstein (1938), or Rosenhead (1963).

7.2. Alternative Interpretations of Flat-Plate Solution

The Blasius solution for the flat plate plays a variety of roles in boundary-layer theory. We describe here three essentially different

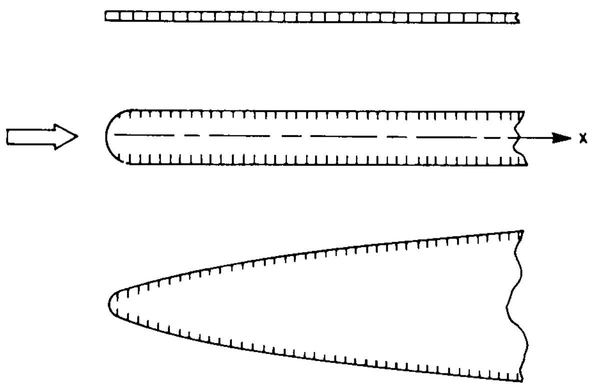

Fig. 7.2. Bodies with Blasius solution valid far downstream.

interpretations. First, it applies to a semi-infinite flat plate. It then represents a coordinate perturbation for large x. More precisely, since the problem contains only the viscous length ν/U, it represents the asymptotic solution for large values of the running Reynolds number Ux/ν. In this sense it applies also to a round-nosed thick plate, or even to such a growing shape as the parabola (Fig. 7.2).

Second, the Blasius solution applies to a cusp-nosed plate (Fig. 7.3).

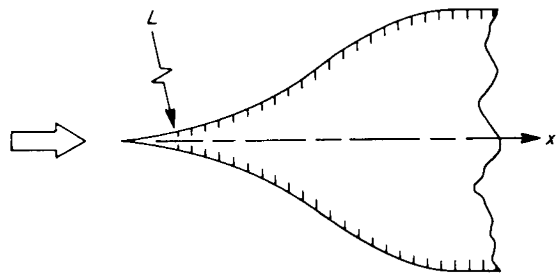

Fig. 7.3. Body with Blasius solution valid near leading edge.

In this case, oddly enough, it represents a coordinate perturbation for *small* x. More precisely, it is the asymptotic solution for small x/L, where L is a characteristic length such as the initial radius of curvature of the profile. The approximation could be improved by calculating additional terms in a series in powers of x/L. To be sure, the result is not valid in the immediate vicinity of the leading edge, where $x = O(\nu/U)$. Thus we encounter a situation that arises occasionally in other branches of fluid mechanics—for example, for power-law bodies in hypersonic small-disturbance theory (Hayes and Probstein, 1959, Section 2.6)—where a coordinate perturbation is valid for small (or large) distances, but not *too* small (or large). One might suppose that the nonuniformity at the leading edge could be removed by constructing a third expansion for that region. However, the limiting problem is evidently just that of the semi-infinite plate itself. Of course the flow very near the edge is given by the approximation of Carrier and Lin described in Section 3.9. However, that is not an inner solution in the sense of Chapter V; it has no overlap with the Blasius solution and so cannot be matched with it (Section 10.9).

Third, Blasius' solution applies over a finite flat plate (Fig. 7.4). It then represents a parameter perturbation, being the asymptotic solution for large Reynolds number UL/ν based on plate length. This situation arises only because the basic inviscid solution is the same for a finite and a semi-infinite plate, and because the equations are parabolic, so that the boundary layer on the plate is not affected by the wake downstream of the trailing edge. Of course the result is not uniformly valid, but breaks down at both edges. The nonuniformity at the leading edge has just been discussed; that at the trailing edge is probably even more complicated.

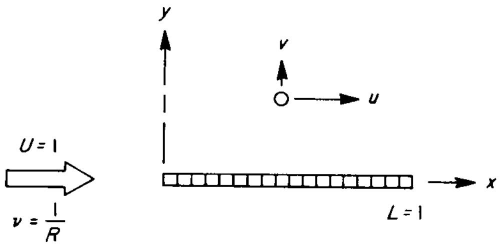

Fig. 7.4. Notation for finite flat plate.

The distinction between these three interpretations of the Blasius solution appears in higher approximations. We consider concurrently the first and third viewpoints, for the finite and semi-infinite flat plate. For the second, see Van Dyke (1962b).

7.3. Outer Expansion for Flat Plate; Basic Inviscid Flow

Let L be the length of the finite plate, or an arbitrary reference length for the semi-infinite plate (say the distance from the leading edge to a red line painted on the plate!). The solution must actually be independent of L in the latter case, and will be so to first order in the former.

It is convenient to introduce dimensionless variables by referring all lengths to L and velocities to U. This is equivalent to choosing units such that $L = U = 1$ (Fig. 7.4). Then in Cartesian coordinates the Navier-Stokes equations are equivalent to Eq. (2.24) for the dimensionless stream function ψ, with ν replaced by the inverse of the Reynolds number R based on the length L:

$$R = \frac{UL}{\nu} \tag{7.1}$$

Adding the boundary conditions of zero velocity on the plate and a uniform oncoming stream gives as the full problem

$$\left(\psi_y \frac{\partial}{\partial x} - \psi_x \frac{\partial}{\partial y} - \frac{1}{R}\nabla^2\right)\nabla^2\psi = 0 \tag{7.2a}$$

$$\psi(x, 0) = 0 \tag{7.2b}$$

$$\psi_y(x, 0) = 0 \quad \text{for} \quad 0 < x < \begin{cases} 1, & \text{finite plate} \\ \infty, & \text{semi-infinite} \end{cases} \tag{7.2c}$$

$$\psi(x, y) \sim y \quad \text{upstream} \tag{7.2d}$$

We seek an asymptotic solution of this problem as the Reynolds number R becomes infinite. Because the perturbation parameter appears in the problem only as $1/R$, one might be tempted to assume that the appropriate asymptotic sequence consists of powers of $1/R$. However, Prandtl's theory shows that this is incorrect. We therefore adopt the safer course of leaving the sequence unspecified, and assume a straightforward (outer) expansion in the form

$$\psi(x, y; R) \sim \delta_1(R)\psi_1(x, y) + \delta_2(R)\psi_2(x, y) + \cdots$$

$$\text{as} \quad R \to \infty \quad \text{with} \quad x, y > 0 \quad \text{fixed} \tag{7.3}$$

By substituting into the full problem and taking the limit as $R \to \infty$, we obtain for the upstream condition (7.2d)

$$\psi_1(x, y) \sim \lim_{R\to\infty}\left[\frac{1}{\delta_1(R)}\right] y \quad \text{upstream} \tag{7.4}$$

The limit appearing here may be zero, infinite, or finite. If it is zero, the problem is homogeneous and the solution (if unique) is $\psi_1 = 0$. If the limit is infinite, the problem is meaningless. Hence a significant result is obtained only if the limit is finite. Without loss of generality we take

$$\delta_1(R) = 1 \tag{7.5}$$

The equation for the first approximation then becomes that for inviscid flow:

$$\left(\psi_{1y}\frac{\partial}{\partial x} - \psi_{1x}\frac{\partial}{\partial y}\right)\nabla^2\psi_1 = 0 \tag{7.6a}$$

according to which vorticity is simply convected, its viscous diffusion being negligible to this approximation. A first integral was given in Section 2.1 as

$$\nabla^2\psi_1 = -\omega_1(\psi_1) \tag{7.6b}$$

That is, the vorticity $-\nabla^2\psi_1$ is some function ω_1 of the stream function only, and therefore constant along streamlines. The form of this function is determined by the flow far upstream. It vanishes in the present problem, as it does whenever the oncoming stream is irrotational. Hence the problem for the first term of the outer expansion becomes

$$\nabla^2\psi_1 = 0 \tag{7.7a}$$

$$\psi_1(x, 0) = 0 \tag{7.7b}$$

$$\psi_1(x, y) \sim y \qquad \text{upstream} \tag{7.7c}$$

Here the no-slip condition $\psi_{1y}(x, 0) = 0$ has been dropped because it is unenforceable. The order of the differential equation is reduced by one with neglect of the viscous term, and one boundary condition must consequently be given up. The question of which boundary condition to abandon can, in simple problems, be settled mathematically; here one must be guided by experience and physical insight.

The solution of this problem is

$$\psi_1(x, y) = y \tag{7.8}$$

which represents simply the uniform parallel stream. At infinite Reynolds number a flat plate causes no disturbance. The corresponding solution for any other plane body free of separation is the inviscid potential flow.

7.4. Inner Expansion; Boundary-Layer Equations; Matching

Loss of the highest derivative is the classical hallmark of a singular perturbation problem (Section 5.2); and we know that the basic inviscid solution is not valid near the surface, where the no-slip condition had to be abandoned. Thus the region of nonuniformity is the neighborhood of a line, rather than of a point as in the thin-airfoil problems of Chapter IV. Coordinates of order unity in that region will be obtained by magnifying the normal coordinate y, leaving x unaltered.

Prandtl was led to the proper magnification by physical intuition and comparison with simple exact solutions. To some extent, however, one can proceed formally. Let the width of the region of nonuniformity (the boundary layer) be of order $\Delta_1(R)$, where Δ_1 is a function that vanishes as its argument becomes infinite. Then an appropriate magnified (inner) normal coordinate is given by $Y = y/\Delta_1(R)$, where the stretching factor $1/\Delta_1(R)$ is still to be determined. As for the dependent variable, it is clear at least physically that $u = \psi_y$ must be of order unity inside as well as outside the boundary layer, so that

$$\psi = O(y) = O(\Delta_1)$$

That is, ψ must be magnified by the same factor as y.

Generalizing to higher approximations, we assume an inner expansion, valid within the boundary layer, of the form

$$\psi(x, y; R) \sim \Delta_1(R)\Psi_1(x, Y) + \Delta_2(R)\Psi_2(x, Y) + \Delta_3(R)\Psi_3(x, Y) + \cdots \quad \text{as} \quad R \to \infty \quad \text{with} \quad x, Y \text{ fixed} \tag{7.9a}$$

where

$$Y = \frac{y}{\Delta_1(R)} \tag{7.9b}$$

The Δ_n are an asymptotic sequence such that the Ψ_n are all of order unity in the boundary layer, where $Y = O(1)$. We determine Δ_1 by substituting this expansion into the Navier-Stokes equation (7.2a), multiplying by Δ_1, and letting R tend to infinity. This gives

$$\left(\Psi_{1Y}\frac{\partial}{\partial x} - \Psi_{1x}\frac{\partial}{\partial Y}\right)\Psi_{1YY} = \lim_{R\to\infty}\left[\frac{1}{R\,\Delta_1^2(R)}\right]\Psi_{1YYYY} \tag{7.10}$$

Again the limit appearing here may be zero, infinite, or finite. The first two possibilities lead to degenerate solutions that cannot satisfy the inner boundary conditions and match the outer flow. Hence we choose the third possibility. That is, we apply again as in the previous section the *principle of least degeneracy* (cf. Section 5.5). Without loss of generality we take the constant limit to be unity, giving

$$\Delta_1(R) = R^{-1/2}, \qquad Y = R^{1/2}y \tag{7.11}$$

Thus we recover the familiar result that the boundary-layer thickness is proportional to $R^{-1/2}$.

Equation (7.10) for the first term of the inner expansion now becomes

$$\left(\frac{\partial^2}{\partial Y^2} - \Psi_{1Y}\frac{\partial}{\partial x} + \Psi_{1x}\frac{\partial}{\partial Y}\right)\Psi_{1YY} = 0 \tag{7.12a}$$

This is a perfect differential, and can be written as

$$\frac{\partial}{\partial Y}(\Psi_{1YYY} + \Psi_{1x}\Psi_{1YY} - \Psi_{1Y}\Psi_{1xY}) = 0 \tag{7.12b}$$

so that integrating yields a third-order equation:

$$\Psi_{1YYY} + \Psi_{1x}\Psi_{1YY} - \Psi_{1Y}\Psi_{1xY} = f(x) \tag{7.12c}$$

The function of integration $f(x)$ is proportional to the inviscid surface pressure gradient. This will be shown by matching with the basic inviscid flow, which determines $f(x)$ and also provides an outer boundary condition.

We apply the asymptotic matching principle (5.24) with $m = n = 1$. It is sufficient, and more convenient at this stage, to match ψ_y, which has the physical interpretation of tangential velocity, rather than ψ itself. Using the previous results (7.3), (7.5), (7.8), (7.9), and (7.11) we obtain for any plane body:

1-*term outer expansion*: $\psi_y \sim \psi_{1y}(x, y)$ (7.13a)

rewritten in inner variables: $= \psi_{1y}\left(x, \frac{Y}{\sqrt{R}}\right)$ (7.13b)

expanded for large R: $= \psi_{1y}(x, 0) + \frac{Y}{\sqrt{R}}\psi_{1yy}(x, 0) + \cdots$ (7.13c)

1-term inner expansion: $= \psi_{1y}(x, 0)$ (7.13d)

1-*term inner expansion*: $\psi_y \sim \Psi_{1Y}(x, Y)$ (7.14a)

rewritten in outer variables: $= \Psi_{1Y}(x, \sqrt{R}\, y)$ (7.14b)

expanded for large R: $= \Psi_{1Y}(x, \infty) + \cdots$ (7.14c)

1-term outer expansion: $= \Psi_{1Y}(x, \infty)$ (7.14d)

Here we have used certain properties of the functions ψ_1 and Ψ_1: we take advantage in (7.13c) of the fact that $\psi_1(x, y)$ is analytic in y at $y = 0$, and in (7.14c) we assume that Ψ_1 has a limit as Y approaches infinity. Equating the two final results gives the required matching condition:

$$\Psi_{1Y}(x, \infty) = \psi_{1y}(x, 0) \tag{7.15a}$$

This is recognized as the familiar requirement that the tangential velocity approach at the outer edge of the boundary layer ($Y = \infty$) the inviscid speed $\psi_{1y}(x, 0)$. If we had matched ψ itself, the result would have been

$$\Psi_1(x, Y) \sim Y\psi_{1y}(x, 0) + o(Y) \quad \text{as} \quad Y \to \infty \tag{7.15b}$$

This is obtainable from (7.15a) by integration; and it is in this sense, as the first term of an asymptotic expansion for large Y, that the matching condition is properly understood.

The matching condition can be used to find the function of integration $f(x)$, by evaluating the boundary-layer equation (7.12c) at $Y = \infty$. The result is the conventional boundary-layer equation of Prandtl:

$$\Psi_{1YYY} + \Psi_{1x}\Psi_{1YY} - \Psi_{1Y}\Psi_{1xY} = -\psi_{1y}(x, 0)\psi_{1xy}(x, 0) \tag{7.16a}$$

The right-hand side is the (dimensionless) surface pressure gradient in the inviscid flow according to Bernoulli's equation. This equation actually applies to any plane body, where x is the distance along the surface and y that normal to it, because curvature of the surface affects only the second approximation of boundary-layer theory. The relevant boundary conditions are those of zero velocity at a solid surface, which give, if ψ is normalized to vanish on the body,

$$\Psi_1(x, 0) = \Psi_{1Y}(x, 0) = 0 \tag{7.16b}$$

together with the matching condition (7.15). The latter is retained despite its already having been used to evaluate the function of integration; it does double duty because $Y = \infty$ is a singular point.

The boundary-layer equation (7.16a) is parabolic—with x as time-like variable—although the original Navier-Stokes equation (7.2a) is elliptic. This change of type (cf. Section 3.11) means that upstream influence is suppressed. For this reason the first-order boundary layer on a flat plate is quite unaffected by the trailing edge and the subsequent wake.

7.5. Boundary-Layer Solution for Flat Plate

For the flat plate the inviscid solution (7.8) gives no pressure gradient, and the boundary-layer problem becomes

$$\Psi_{1YYY} + \Psi_{1x}\Psi_{1YY} - \Psi_{1Y}\Psi_{1xY} = 0 \tag{7.17a}$$

$$\Psi_1(x, 0) = 0 \tag{7.17b}$$

$$\Psi_{1Y}(x, 0) = 0 \quad \text{for} \quad 0 < x < \begin{cases} 1, & \text{finite plate} \\ \infty, & \text{semi-infinite} \end{cases} \tag{7.17c}$$

$$\Psi_{1Y}(x, \infty) = 1 \tag{7.17d}$$

For the finite plate the boundary layers on the top and bottom surfaces merge at the trailing edge and leave the plate as a wake without separating (Fig. 7.5). Evidently the boundary-layer approximation continues to be

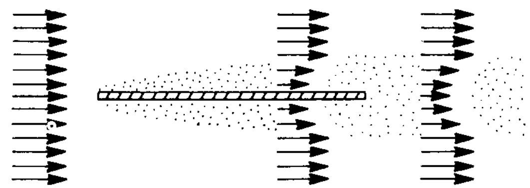

Fig. 7.5. Boundary layer and wake on finite plate.

valid in the wake, and the pressure gradient still vanishes. The only change required is to replace the no-slip condition (7.17c) by a requirement of symmetry

$$\Psi_{1YY}(x, 0) = 0 \qquad \text{for} \quad 1 < x \tag{7.17c'}$$

We shall, however, follow the boundary layer in detail only back to the trailing edge, because thereafter the flow is not self-similar.

A self-similar solution exists on the plate because the problem has a certain *group property* that permits its reduction to an ordinary differential equation. This property is expressed by the fact that the problem (7.17) is invariant* under the transformation

$$\Psi_1 \to c\Psi_1, \qquad x \to c^2 x, \qquad Y \to cY \tag{7.18}$$

As in dimensional analysis—where invariance under changes of scale is a physical necessity rather than, as here, a mathematical circumstance—this means that the solution (if unique) cannot involve the variables Ψ_1, x, and Y separately, but only in combinations that are invariant under the transformation. Some alternatives are

$$\left.\begin{matrix} \dfrac{\Psi_1}{Y} \\ \dfrac{\Psi_1}{\sqrt{x}} \end{matrix}\right\} = \text{function of} \left\{\begin{matrix} \dfrac{x}{Y^2} \\ \dfrac{Y}{\sqrt{x}} \end{matrix}\right. \tag{7.19}$$

We choose the latter forms, inserting factors of 2 in accord with the standard Falkner-Skan notation (Schlichting, 1960, p. 143; Rosenhead, 1963, p. 222):

$$\Psi_1(x, Y) = \sqrt{2x} f_1(\eta), \qquad \eta = \frac{Y}{\sqrt{2x}} \tag{7.20}$$

Reintroducing the original dimensional variables at this point shows that the length L disappears from f_1 and η, in accord with the facts that it is arbitrary for the semi-infinite plate and irrelevant for the boundary layer on a finite plate. This is another way of motivating the group transformation.

Substituting (7.20) into the boundary-layer problem (7.17) gives

$$f_1''' + f_1 f_1'' = 0 \tag{7.21a}$$

$$f_1(0) = f_1'(0) = 0 \tag{7.21b}$$

$$f_1'(\infty) = 1 \tag{7.21c}$$

This is the Prandtl-Blasius problem, free of factors of 2 that appear in

* In the case of the finite flat plate, the length changes from 1 to c^2 under this transformation. Hence it is essential to recognize that the boundary layer on the plate is unaffected by the wake in order to appreciate the invariance.

earlier references. It must be integrated numerically. Blasius originally patched a series solution for small η to an asymptotic expansion for large η. However, Weyl (1942) points out that this is a dangerous business, because the first series has only a modest radius of convergence (and the second probably none). It is safer, and now simpler with electronic computers, to integrate numerically from $\eta = 0$ to some reasonably large value, say $\eta = 5$ or 10.

This is a two-point boundary-value problem, which would ordinarily require repeated guessing of $f_1''(0)$ to satisfy the condition (7.21c) for large η. In the present problem, however, this complication can be avoided by exploiting another group property of the solution. The differential equation (7.21a) and initial conditions (7.21b) are invariant under the transformation

$$f_1 \to cf_1, \qquad \eta \to \frac{1}{c}\eta \tag{7.22}$$

One can therefore integrate the problem (7.21) with (7.21c) replaced by $f_1''(0) = 1$, and subsequently pick the constant c to satisfy the condition at infinity (Goldstein, 1938, p. 135; Rosenhead, 1963, p. 223).

For our purposes the essential results of the numerical solution are contained in the expansions for small and large η:

$$f_1(\eta) = \tfrac{1}{2}\alpha_1\eta^2 + O(\eta^5), \qquad \alpha_1 = 0.469600 \tag{7.23a}$$

$$\sim \eta - \beta_1 + \text{exp}, \qquad \beta_1 = 1.21678 \tag{7.23b}$$

Here "exp" stands for terms that are exponentially small for large η. This means that the vorticity generated by shear at the wall decays through the boundary layer faster than any power of η. That this must be true for any boundary layer is suggested by the analogy with diffusion of heat (Rosenhead, 1963, p. 216) and by certain mathematical arguments (Stewartson, 1957; Chang, 1961). We shall see later that the condition of exponential decay of vorticity must be enforced in cases where it is not automatically satisfied.

7.6. Uniqueness of the Blasius Solution

The above solution of the problem (7.17) is not unique from a mathematical viewpoint. To it may be added any one of an infinite discrete set of eigensolutions, each of which satisfies a linear perturbation equation derived from (7.17a), together with the zero initial conditions (7.17b,c), and exhibits exponential decay at infinity (Stewartson, 1957; Libby and Fox, 1963). These have the form

$$\Psi_1^{(m)}(x, Y) = C_m x^{\frac{1}{2}-\lambda_m} e_m(\eta) \tag{7.24a}$$

where the C_m are arbitrary constants, and (Libby, 1965)

$$\lambda_m = 1, \quad 1.887, \quad 2.814, \quad 3.758, \quad 4.704, \ldots \tag{7.24b}$$

The first of these eigensolutions is the x-derivative of the Blasius solution (7.20):

$$\Psi_1^{(1)} = C_1 x^{-1/2}[f_1(\eta) - \eta f_1'(\eta)] \tag{7.25}$$

It represents physically a slight uncertainty in the effective location of the origin of abscissae. Similarly, the higher eigensolutions represent further uncertainty about the details of the flow near the leading edge. However, they have no such simple interpretation as the first. Stewartson (1957) has discussed how indeterminacy arises in any downstream expansion for a boundary layer, because the initial conditions are not imposed (cf. Section 3.10).

We can properly dismiss all eigensolutions at this stage by invoking the principle of minimum singularity (Section 4.5). It is more illuminating, however, to understand why the principle applies. The reference length and the associated parameter R are artificial; hence the dimensionless variables must occur only as $R\psi$, Rx, and Ry in order that L will disappear from the result. The Blasius solution has this property. The first eigensolution (7.25) has it only if the constant C_1 is of order R^{-1}. But this means it belongs to the third approximation (Section 7.11) rather than the first. In the same way the higher eigensolutions are relegated to higher approximations. This is a typical argument involving an *artificial parameter*; for further discussion see Lagerstrom and Cole (1955), Chang (1961), and Exercise 4.8.

This argument would not apply to a blunt-nosed flat plate (Fig. 7.2), which has a real geometric length L. Indeed, all the eigensolutions must be retained there in the asymptotic expansion of the first-order boundary-layer solution. They are not excluded by the principle of minimum singularity, because more singular terms appear. For example, for the parabola the expansion contains a term in $x^{-1/2}\log x$ between the Blasius solution and the first eigensolution. The resulting expression for skin friction was given as equation (3.27) in Chapter III; and we show in Section 10.9 how the constant C_1 can be found approximately by joining with another expansion from the nose or patching with a numerical solution.

7.7. Flow due to Displacement Thickness

It was observed in Section 5.9 that the normal matching order of Fig. 5.6 must be followed in the direct problem of boundary-layer

theory. We therefore proceed to the second term in the outer expansion (7.3).

The nature of the factor $\delta_2(R)$, together with the matching conditions, is found by matching with the boundary-layer solution. At this stage, matching ψ_y does not suffice; one must match ψ itself, or ψ_x as well as ψ_y. Using all previous results, we find

1-*term inner expansion*:	$\psi \sim \dfrac{1}{\sqrt{R}}\sqrt{2x}f_1(\eta)$	(7.26a)
rewritten in outer variables:	$= \dfrac{1}{\sqrt{R}}\sqrt{2x}f_1\Big(\dfrac{\sqrt{R}y}{\sqrt{2x}}\Big)$	(7.26b)
expanded for large R:	$= \dfrac{1}{\sqrt{R}}\sqrt{2x}\Big(\dfrac{\sqrt{R}y}{\sqrt{2x}} - \beta_1 + \exp\Big)$	(7.26c)
2-term outer expansion:	$= y - \dfrac{1}{\sqrt{R}}\beta_1\sqrt{2x}$	(7.26d)
rewritten in inner variables	$= \dfrac{Y}{\sqrt{R}} - \dfrac{1}{\sqrt{R}}\beta_1\sqrt{2x}$	(7.26e)
2-*term outer expansion*:	$\psi \sim y + \delta_2(R)\psi_2(x, y)$	(7.27a)
rewritten in inner variables:	$= \dfrac{Y}{\sqrt{R}} - \delta_2(R)\psi_2\Big(x, \dfrac{Y}{\sqrt{R}}\Big)$	(7.27b)
expanded for large R:	$= \dfrac{Y}{\sqrt{R}} + \delta_2(R)[\psi_2(x, 0) + \cdots]$	(7.27c)

Here we have in (7.26c) used the asymptotic expansion (7.23b) for the Blasius function f_1, and in (7.27c) the fact that ψ_2, like ψ_1, is analytic in y at $y = 0$.

We now apply the asymptotic matching principle (5.24) with $m = 1$ and $n = 2$. Comparing (7.26e) and (7.27c) shows that $\delta_2(R)$ must be some multiple of $R^{-1/2}$; we choose

$$\delta_2(R) = \frac{1}{\sqrt{R}} \tag{7.28}$$

It then follows that

$$\psi_2(x, 0) = -\beta_1\sqrt{2x} \tag{7.29a}$$

This has a familiar physical interpretation in terms of the displacement thickness of the boundary layer. Substituting into (7.27) shows that the outer expansion for the stream function appears to vanish at $y = \beta_1 R^{-1/2}(2x)^{1/2}$. Thus the boundary layer displaces the outer inviscid flow like a solid parabola of nose radius β_1^2/R. The matching condition (7.29a) is the linearized thin-airfoil approximation, transferred to the axis (Section 4.2), to the tangency condition for the displacement parabola.

An alternative form, with a slightly different physical interpretation, results from differentiating (7.29a) with respect to x:

$$-\psi_{2x}(x, 0) = \frac{\beta_1}{\sqrt{2x}} \tag{7.29b}$$

This is the second-order component of normal velocity in the outer flow, evaluated at the surface, where it is required to equal the slope of the displacement parabola. From this point of view, the displacement effect of the boundary layer acts like a surface distribution of sources. This is the thin-airfoil condition of Section 4.3. A detailed discussion of various interpretations of the displacement effect is given by Lighthill (1958).

Substituting the outer expansion (7.3) into the full equation (7.2a) yields a linear equation for ψ_2:

$$\left(\psi_{1y}\frac{\partial}{\partial x} - \psi_{1x}\frac{\partial}{\partial y}\right)\nabla^2\psi_2 + \left(\psi_{2y}\frac{\partial}{\partial x} - \psi_{2x}\frac{\partial}{\partial y}\right)\nabla^2\psi_1 = 0 \tag{7.30a}$$

The nonlinear convective terms have split into two, as usual in a perturbation scheme. The two terms represent, respectively, convection of second-order vorticity along first-order streamlines and of first-order vorticity along second-order corrections to the streamlines. The latter term vanishes in our problem, and whenever the oncoming stream is irrotational. Viscosity has no effect at this stage, the flow outside the boundary layer being inviscid at least to second order, and to every order when the oncoming stream is irrotational. Then (7.30a) has the first integral

$$\nabla^2\psi_2 = -\omega_2(\psi_1) \tag{7.30b}$$

However, the second-order outer vorticity ω_2 also vanishes when the oncoming stream is irrotational, so that ψ_2 then satisfies the Laplace equation.

7.8. Second-Order Boundary Layer for Semi-Infinite Plate

For the semi-infinite flat plate, the problem for the flow due to displacement thickness is

$$\nabla^2\psi_2 = 0 \tag{7.31a}$$

$$\psi_2(x, 0) = \begin{cases} 0, & x < 0 \quad (7.31b) \\ -\beta_1\sqrt{2x}, & x > 0 \quad (7.31c) \end{cases}$$

$$\psi_2(x, y) = o(y) \quad \text{upstream} \tag{7.31d}$$

The condition (7.31b) of symmetric flow serves to rule out circulatory motion. This is the linearized thin-airfoil problem for potential flow past the displacement parabola $y = \beta_1(2x/R)^{1/2}$. We require only the surface speed, which was found in Section 4.8. However, the full solution is obvious from the viewpoint of complex-variable theory:

$$\psi_2(x, y) = -\beta_1 \operatorname{Re}\sqrt{2(x + iy)} \tag{7.32}$$

where Re indicates the real part.

The form of $\Delta_2(R)$ in (7.9a) and a matching condition for Ψ_2 are found as before by applying the matching principle with $m = n = 2$. Extending the procedure of (7.13) gives as the 2-term inner expansion of the 2-term outer expansion of ψ_y:

$$\text{2-inner (2-outer)}\ \psi_y = 1 + \frac{0}{\sqrt{R}} \tag{7.33a}$$

We exhibit the second term because its coefficient will be different from zero in any other problem, including that of the finite plate. Conversely, we have

$$\text{2-outer (2-inner)}\ \psi_y = 1 + R^{-1/2}\Delta_2(R)\Psi_{2Y}(x, \infty) \tag{7.33b}$$

Here we have assumed that the limit $\Psi_{2Y}(x, \infty)$ exists; for a case where it does not, see Exercise 7.2.

Matching suggests that we may in general choose

$$\Delta_2(R) = \frac{1}{R} \tag{7.34}$$

so that both the inner and outer expansions proceed by inverse half powers of the Reynolds number. This is true for an analytic body (Van Dyke, 1962a), but only to second order for one with corners, as we shall see in Section 7.11. Completing the matching provides, for a general body, a condition on $\Psi_{2Y}(x, \infty)$, which has the physical interpretation of the increment in tangential velocity at the edge of the boundary layer. For the plate we have

$$\Psi_{2Y}(x, \infty) = 0 \tag{7.35}$$

because the displacement speed vanishes at $y = 0$. An infinite parabolic cylinder has the unique property that in thin-airfoil theory its surface speed is just the speed of the free stream.

Substituting the inner expansion (7.9) into the full equation (7.2a) yields again a perfect differential as the equation for Ψ_2:

$$\frac{\partial}{\partial Y}\left(\Psi_{2YYY} + \Psi_{1x}\Psi_{2YY} - \Psi_{1Y}\Psi_{2xY} + \Psi_{2x}\Psi_{1YY} - \Psi_{2Y}\Psi_{1xY}\right) = 0 \tag{7.36}$$

This vanishes only for the flat plate; for any other shape the right-hand side will contain terms proportional to the local curvature of the surface (Van Dyke, 1962a).

The surface boundary conditions are $\Psi_2(x, 0) = \Psi_{2Y}(x, 0) = 0$ for any body. Hence for the semi-infinite flat plate Ψ_2 satisfies a completely homogeneous problem. The solution must vanish if it is unique. Although it could be nonunique by any of the eigensolutions (7.24), the argument of Section 7.6 shows that none can appear until the next approximation. Thus $\Psi_2(x, Y) = 0$, and the complete second approximation is

$$\psi(x, y; R) \sim \begin{cases} y - \dfrac{1}{\sqrt{R}} \beta_1 \operatorname{Re}\sqrt{2(x + iy)}, & \text{outer} \quad (7.37a) \\[2ex] \dfrac{\sqrt{2x}}{\sqrt{R}} f_1\left(\dfrac{\sqrt{R}y}{\sqrt{2x}}\right) + \dfrac{0}{R}, & \text{inner} \quad (7.37b) \end{cases}$$

7.9. Second-Order Boundary Layer for Finite Plate

See Note 8

Prandtl himself discussed (Prandtl, 1935, p. 90) how the Blasius solution could be improved by successive approximations:

> Instead of the simple parallel flow, the flow around a parabolic cylinder ... should be introduced, which would slightly alter the pressure distribution. The ... calculation would have to be repeated for this new pressure distribution and if necessary the process repeated on the basis of the new measure of displacement so obtained.

However, we have seen that because of a coincidence peculiar to the parabola, this procedure gives no second-order contribution for the semi-infinite plate.

For the finite plate, on the other hand, Prandtl's procedure gives a significant result. The details have been carried out by Kuo (1953) whose analysis is, however, subject to criticism on several points. Because the boundary-layer equations are parabolic, Blasius' solution is valid ahead of the trailing edge. Behind the trailing edge, the displacement thickness of the wake is very difficult to calculate (Rosenhead, 1963, p. 280). Kuo makes the perhaps reasonable assumption that it can be taken as constant at its value at the trailing edge (Fig. 7.6). Then in the

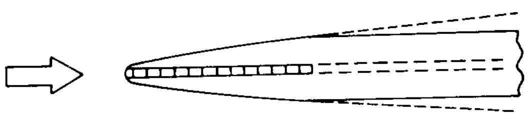

Fig. 7.6. Assumed form of displacement thickness for finite plate.

flow due to displacement thickness the surface speed is increased slightly. This is evident if one regards the difference between the displacement thickness in the wake and that for the infinite plate—which has no effect at the surface—as due to a distribution of sinks.

This thin-airfoil problem can be solved by the methods of Chapter IV. Thus the second-order matching condition (7.35) is found to be replaced by

$$\Psi_{2Y}(x, \infty) = \frac{\beta_1}{\sqrt{2}\pi} \frac{1}{\sqrt{x}} \log \frac{1 + \sqrt{x}}{1 - \sqrt{x}} = \frac{\sqrt{2}\beta_1}{\pi}\left(1 + \frac{x}{3} + \frac{x^2}{5} + \cdots\right) \tag{7.38}$$

This function is logarithmically infinite at the trailing edge, and the series expansion shown does not converge there. Nevertheless, Kuo solves the second-order boundary-layer equation (7.36) by correspondingly expanding Ψ_2 as

$$\Psi_2(x, Y) = \frac{2\beta_1}{\pi} [x^{1/2} f_1(\eta) + \tfrac{1}{3} x^{3/2} f_2(\eta) + \cdots] \tag{7.39}$$

The problems for the first nine f_n have been integrated numerically, and the remainder approximated. Thus Kuo estimates the sum of the slowly convergent series for the integrated skin friction. For one side of the plate the result is, τ being the shear,

$$c_F = \frac{\int_0^L \tau\, dx}{\frac{1}{2}\rho U^2 L} \sim \frac{1.328}{\sqrt{R}} + \frac{4.12}{R} + \cdots \tag{7.40}$$

This result is in excellent accord with experiments down to $R = 10$. However, the coefficient 4.12 will be increased by an additional effect, overlooked by Kuo, that is discussed in the next section.

7.10. Local and Integrated Skin Friction

Consider again the semi-infinite plate. From the two-term inner expansion (7.37b) we calculate the local coefficient of skin friction:

$$c_f = \frac{\tau}{\frac{1}{2}\rho U^2} \sim \frac{0.664}{\sqrt{R_x}} + \frac{0}{R_x} + \cdots \tag{7.41}$$

Here $R_x = Ux/\nu$ is the local Reynolds number, based on distance from the leading edge. The first term is integrable, and yields the classical value for the coefficient of integrated skin friction on one side of the plate:

$$c_F = \frac{\int_0^x c_f\,dx}{x} \sim \frac{1.328}{\sqrt{R_x}} + \cdots \tag{7.42}$$

The second term in (7.41) would not be integrable, except for the circumstance that its coefficient is zero, because the asymptotic expansion is not valid near the leading edge. The second term in the integrated skin friction has nevertheless been calculated in an ingenious way by Imai (1957a). He avoids the difficulty at the leading edge by considering the balance of momentum in a large contour (Fig. 7.7). This corresponds

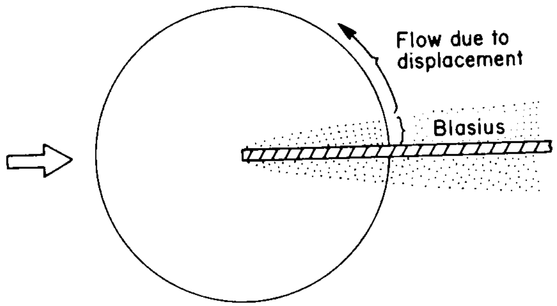

Fig. 7.7. Momentum contour for semi-infinite plate.

to Jones' treatment of leading-edge drag in thin-airfoil theory (Section 4.6). Using the Blasius solution in the boundary layer, and the flow due to displacement thickness in the outer flow, he finds

$$c_F \sim \frac{1.328}{\sqrt{R_x}} + \frac{2.326}{R_x} + \cdots \tag{7.43}$$

It is remarkable that 50 years were required to discover that one term of the boundary-layer solution provides two terms of the friction drag.

Although the details are complicated, this result is almost obvious in the light of Section 4.6. The first term in (7.43), arising from the integration across the boundary layer, is the classical result (7.42). The second term arises from integration around the rest of the contour, where the flow is inviscid. It is therefore just the leading-edge drag (4.22) for the displacement parabola of nose radius $a = \beta_1^2 R$, the constant 2.326 being $\frac{1}{2}\pi\beta_1^2$.

The second term in (7.43) thus represents a force at the leading edge. Of course it is concentrated there only on the gross scale of boundary-

layer theory. Actually, it must be the result of an increase in local skin friction above the Blasius value near the leading edge, where the local Reynolds number is of order unity. Nothing else is known about the flow in that region, except that it presumably has the form (3.24). See Note 8

Because it is a local effect, the concentrated force will appear also at the leading edge of the finite flat plate. It was, however, overlooked by Kuo. With this addition, and the revision suggested previously, the coefficient 4.12 in (7.40) is replaced by something like 5.3. The result is still in reasonable accord with experiment, while leaving some scope for third-order effects.

One may ask whether a concentrated force appears also at the trailing edge. Reflection suggests that it does, but that whereas the leading edge is exposed to the free stream, the trailing edge is sheltered by the relatively thick boundary layer. Consequently, the trailing-edge force would contribute only a third-order term, proportional to $R^{-3/2}$. Clear indications of such a difference between the leading and trailing edges are seen in the numerical solutions for a finite flat plate carried out by Janssen (1958).

7.11. Third Approximation for Semi-Infinite Plate

Third-order boundary-layer theory has been studied only for the semi-infinite plate. At this stage the difficulties arising from the nonanalytic leading edge become severe. For that and other reasons, the first attempts of Alden (1948) and others were erroneous. The correct solution was given by Goldstein (1956) and Imai (1957a), and is described in detail in the book of Goldstein (1960).

All those analyses use parabolic coordinates, but we can persevere with Cartesian coordinates. The third term in the outer expansion is seen to vanish, because it represents the displacement effect of the second term in the boundary layer, which is zero. The equation for the third approximation in the boundary layer is found to be (since $\Psi_2 = 0$).

$$\frac{\partial}{\partial Y}(\Psi_{3YYY} - \Psi_{1x}\Psi_{3YY} + \Psi_{1YY}\Psi_{3x} - \Psi_{1Y}\Psi_{3xY} - \Psi_{1xY}\Psi_{3Y})$$
$$= (\Psi_{1Y}\Psi_{1xxx} - \Psi_{1x}\Psi_{1xxY} - 2\Psi_{1xxYY}) \lim_{R\to\infty}\left[\frac{R^{-3/2}}{\Delta_3(R)}\right] \tag{7.44}$$

In order to balance the nonhomogeneous terms on the right, there must be a term in the inner expansion (7.9) with $\Delta_3(R) = 1/R^{3/2}$. This yields the problem solved by Alden. However, the resulting vorticity is found to decay only algebraically for large η, which is unacceptable (Section 7.5). This difficulty arises because of the sharp leading edge. On an analytic body, a well-defined boundary layer exists beginning at the stagnation point, and exponential decay of vorticity is automatically assured. Near the sharp edge of the plate, on the other hand, the boundary-layer approximation is invalid. Although it becomes valid far downstream, exponential decay is not assured, but must be enforced.

This is achieved by adding to Ψ_3 a term involving $\log x$. Then for the solution to be independent of L there must be a corresponding term with

$$\Delta_3'(R) = (\log R)/R^{3/2}.$$

Thus the inner expansion is found to have the form

$$\psi(x, y; R) \sim \frac{1}{\sqrt{R}}\sqrt{2x}f_1(\eta) + \frac{0}{R} + \frac{1}{R^{3/2}}\left[\log Rx\,\frac{f_{32}(\eta)}{\sqrt{2x}} + \frac{f_{31}(\eta)}{\sqrt{2x}}\right] + \cdots \tag{7.45}$$

Although the problem for f_{32} is homogeneous, the solution is not zero but is the first eigensolution (7.25). Exponential decay of vorticity in f_{31} can be achieved by proper choice of the constant C_1.

A final difficulty remains, however. The solution for f_{31} is nonunique by the first eigensolution, and no way is known of determining its constant. Thus the local coefficient of skin friction is given by

$$c_f \sim \frac{0.664}{\sqrt{R_x}} - 0.551\,\frac{\log R_x}{R_x^{3/2}} + \frac{C_1 - 1}{R_x^{3/2}} + \cdots \tag{7.46}$$

and the integrated skin friction (Imai 1957a) by

$$c_F \sim \frac{1.328}{\sqrt{R_x}} - \frac{2.326}{R_x} - 1.102\,\frac{\log R_x}{R_x^{3/2}} - \frac{0.204 + 2C_1}{R_x^{3/2}} + \cdots \tag{7.47}$$

where the constant C_1 is unknown. As discussed by Goldstein (1960), similar undetermined constants arise in higher approximations. These depend on certain details of the flow near the leading edge. Whether it is possible, even in principle, to determine them—short of solving the problem exactly—is at present a mystery. Imai (1957a) has estimated C_1 by patching (7.47) at $R_x = 1$ with the result of the approximation (3.24) for the leading edge.

See Note 8

7.12. The Effect of Changing Boundary-Layer Coordinates

The boundary-layer solution can be combined with the associated outer expansion, using the methods of Section 5.10, to form a composite result. We consider instead a significant alternative way of forming a single uniformly valid expansion. This is Kaplun's (1954) method of

optimal coordinates, in which the independent variables are altered to make the boundary-layer solution uniformly valid.

We must first discuss how the boundary-layer solution is affected by a change of coordinates. This question was implicit in the preceding section when we observed that recent investigations of the semi-infinite flat plate have been carried out in parabolic rather than the traditional Cartesian coordinates.

Suppose that the entire Prandtl boundary-layer analysis is repeated in a different coordinate system. That is, the Navier-Stokes equations are written in the new system, the stream function and coordinate normal to the surface are magnified by a factor $R^{1/2}$, the limit process $R \to \infty$ is carried out, and the resulting boundary-layer equation is solved subject to zero velocity at the surface and matching with the basic inviscid flow. One finds that although the outer expansion is invariant, the boundary-layer solution is not, so that it represents an altered flow field. Different coordinate systems yield boundary-layer solutions that are identical at the surface and differ only negligibly within the boundary layer—so that the skin friction is invariant—but may differ wildly outside the boundary layer.

For this reason, it has been customary to disregard the boundary-layer solution outside the boundary layer, where it is replaced by the matched inviscid flow. However, Kaplun's viewpoint is quite different. He takes advantage of the changes by seeking a special system of coordinates in which the boundary-layer solution approaches the outer flow as closely as possible.

It is not necessary to repeat the boundary-layer solution when the coordinates are changed. If the solution has been calculated in any convenient coordinate system, its counterpart in any other system is given by a simple rule. Suppose that the boundary-layer solution for steady plane flow past any body has been computed using coordinates (x, y), which are not necessarily orthogonal, but are for convenience chosen such that the body is described by $y = 0$. Then just as for the flat plate in Section 7.8, the classical first three steps of the boundary-layer procedure yield a solution correct to order $R^{-1/2}$ in the form

$$\psi \sim \begin{cases} \psi_1(x, y) + \dfrac{1}{\sqrt{R}}\psi_2(x, y) + \cdots & \text{as } R \to \infty \text{ with } x, y > 0 \text{ fixed} \quad (7.48\text{a}) \\ \dfrac{1}{\sqrt{R}}\Psi_1(x, \sqrt{R}y) + \cdots & \text{as } R \to \infty \text{ with } x, \sqrt{R}y \text{ fixed} \quad (7.48\text{b}) \end{cases}$$

Now suppose that a different coordinate system (ξ, η) is introduced such that again, for convenience, the body is described by $\eta = 0$. [The present η must not be confused with the Blasius variable of (7.20).] If the transformation is regular at the surface, we have by Taylor series expansion

$$x = x(\xi, \eta) = x(\xi, 0) + O(\eta) \tag{7.49a}$$

$$y = y(\xi, \eta) = \eta y_\eta(\xi, 0) + O(\eta^2) \tag{7.49b}$$

Because the outer expansion is invariant under change of coordinates, its expression in the new coordinates is found simply by introducing the transformation (7.49) into (7.48a). However, the same is not true of the boundary-layer solution. Its new form is found by introducing (7.49) into (7.48b), expanding in Taylor series, and discarding terms that are of order R^{-1} in the inner variables. Thus the solution in the new coordinate system is found to be

$$\psi \sim \begin{cases} \psi_1[x(\xi, \eta), y(\xi, \eta)] + \dfrac{1}{\sqrt{R}} \psi_2[x(\xi, \eta), y(\xi, \eta)] + \cdots & (7.50a) \\ \dfrac{1}{\sqrt{R}} \Psi_1[x(\xi, 0), \sqrt{R}\eta y_\eta(\xi, 0)] + \cdots & (7.50b) \end{cases}$$

See Note 9

The latter of these is Kaplun's *correlation theorem*.

7.13. Alternative Coordinates for Flat Plate

In Cartesian coordinates (x, y) the boundary-layer solution for the semi-infinite flat plate is given by (7.37). Let us introduce parabolic coordinates (ξ, η) by setting

$$x + iy = \tfrac{1}{2}(\xi + i\eta)^2, \qquad \begin{cases} x = \tfrac{1}{2}(\xi^2 - \eta^2) \\ y = \xi\eta \end{cases} \tag{7.51}$$

These are more natural coordinates for the problem (cf. Section 10.6) because—in contrast to Cartesian coordinates—the whole body and nothing else is described by $\eta = 0$. They are therefore preferable for this as well as other problems in mathematical physics involving a half plane. Applying the correlation theorem (7.50) gives the solution in parabolic coordinates as

$$\psi \sim \begin{cases} \xi\eta - \dfrac{1}{\sqrt{R}} \beta_1 \xi + \cdots, & \text{outer} \quad (7.52a) \\ \dfrac{1}{\sqrt{R}} \xi f_1(\sqrt{R}\eta) + \cdots, & \text{inner} \quad (7.52b) \end{cases}$$

The result has been simplified in appearance. Furthermore, whereas in Cartesian coordinates the boundary-layer vorticity is infinite along the entire vertical line $x = 0$, in parabolic coordinates it is singular only at the point at the origin. Thus parabolic coordinates are seen to be superior to Cartesian coordinates in this problem.

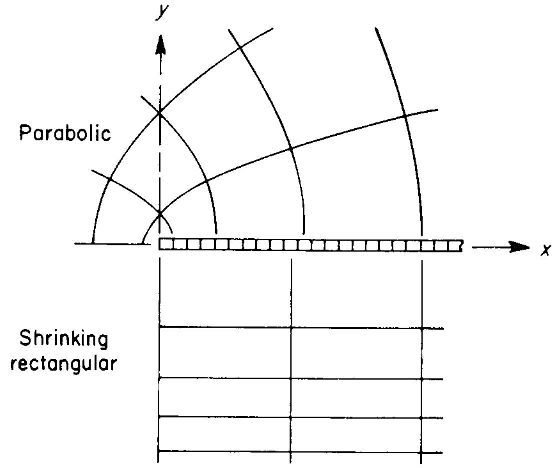

Fig. 7.8. Coordinate systems for semi-infinite plate.

It is instructive to consider a third system, which will be found to be inferior to Cartesian coordinates. What may be described as "shrinking rectangular" coordinates $(\hat{\xi}, \hat{\eta})$, indicated in the lower half of Fig. 7.8, are given by See Note 9

$$\begin{aligned} \hat{\xi} &= x, & x &= \hat{\xi} \\ \hat{\eta} &= y + y^2, & y &= \tfrac{1}{2}(\sqrt{1 + 4\hat{\eta}} - 1) \end{aligned} \tag{7.53}$$

Applying the correlation theorem gives for the boundary-layer solution in this system:

$$\psi \sim \begin{cases} \tfrac{1}{2}(\sqrt{1 + 4\hat{\eta}} - 1) - \dfrac{\beta_1}{\sqrt{R}} \operatorname{Re} \sqrt{2\hat{\xi} + i(\sqrt{1 + 4\hat{\eta}} - 1)} + \cdots & (7.54a) \\ \dfrac{1}{\sqrt{R}} \sqrt{2\hat{\xi}}\, f_1\left(\dfrac{\sqrt{R}\hat{\eta}}{\sqrt{2\hat{\xi}}}\right) + \cdots & (7.54b) \end{cases}$$

We now examine the behavior in the outer region of the boundary-layer solution in each of these coordinate systems. We form the two-term outer expansion of the one-term inner expansion. Using the asymptotic form (7.23b) for the Blasius function gives

$$\text{Cartesian:} \qquad y \sim \frac{\sqrt{2}\beta_1}{\sqrt{R}}\sqrt{x} + \cdots \tag{7.55a}$$

$$\text{parabolic:} \qquad \xi\eta \sim \frac{\beta_1}{\sqrt{R}}\xi + \cdots \tag{7.55b}$$

$$\text{shrinking rectangular:} \qquad \hat{\eta} \sim \frac{\beta_1}{\sqrt{R}}\sqrt{2\hat{\xi}} + \cdots \tag{7.55c}$$

Comparing with the corresponding outer expansions (7.37a), (7.52a), and (7.54a) shows that parabolic coordinates have reproduced two terms, Cartesian coordinates only one, and shrinking rectangular coordinates none at all. Accordingly, we say that the boundary-layer solution in parabolic coordinates *contains* not only the basic inviscid flow but also that due to displacement thickness. The boundary-layer solution is uniformly valid to order $R^{-1/2}$, so that the outer expansion is superfluous. Coordinates having this property are said to be *optimal.*

Cartesian coordinates are not optimal according to this definition. However, they lead to a boundary-layer solution that contains the basic inviscid flow, and is therefore uniformly valid to first order. We may therefore say that Cartesian coordinates are *semioptimal* in this problem. By contrast, the boundary-layer solution in shrinking rectangular coordinates is utterly useless in the outer flow; and no more than this can be anticipated in general.

7.14. Determination of Optimal Coordinates

Kaplun's search for optimal coordinates was inspired by the discovery that if the Navier-Stokes equations are approximated by the linearized Oseen equations (Chapter VIII), the boundary-layer solution is the exact solution if parabolic coordinates are used (Exercise 8.1). This, together with other considerations already mentioned, suggested that parabolic coordinates may be preferable for the flat plate also when the full Navier-Stokes equations are used; and this has been seen to be true.

The question arises: how can optimal coordinates be found for other shapes? A very simple answer has been given by Kaplun. Carry out the solution to order $R^{-1/2}$ in any convenient coordinate system (x, y); it will have the form (7.48). Then an optimal coordinate system is given by

$$\xi_{\text{opt}}(x, y) = \psi_2(x, y), \qquad \eta_{\text{opt}}(x, y) = \psi_1(x, y) \tag{7.56a}$$

Optimal coordinates are not unique, but the most general system is given by

$$\begin{aligned}\xi_{\text{opt}}(x, y) &= F_1[\psi_2(x, y)]\\ \eta_{\text{opt}}(x, y) &= \psi_1(x, y)F_2[\psi_2(x, y)]\end{aligned} \tag{7.56b}$$

where F_1 and F_2 are arbitrary functions.

As an example, consider again the semi-infinite plate, and the boundary-layer solution (7.37) in Cartesian coordinates. From (7.56a) we find, using the generality of (7.56b) only to drop irrelevant constant factors,

$$\begin{aligned}\xi_{\text{opt}} &= \operatorname{Re}\sqrt{2(x + iy)} = \xi\\ \eta_{\text{opt}} &= y \qquad\qquad\qquad = \xi\eta\end{aligned} \tag{7.57}$$

These are not orthogonal; an orthogonal system is obtained from (7.56b) by taking $F_2(\psi_2) = 1/\psi_2$, which yields the parabolic coordinates of (7.51).

Other examples are given by Kaplun (1954). An interesting case is flow normal to an infinite plane wall. Cartesian coordinates are optimal, and the boundary-layer solution satisfies the full Navier-Stokes equations.

7.15. Extension of the Idea of Optimal Coordinates

See Note 9

Optimal coordinates probably exist also for second- and higher-order boundary-layer theory, although the rules for finding them are not yet known. They could presumably be found also for three-dimensional and compressible boundary layers.

A more significant generalization would be to other kinds of singular perturbation problems. We may ask, for example, whether optimal coordinates can be found for the thin-airfoil problems of Chapter IV. As a simple test, consider the surface speed on an ellipse of thickness ratio ε (Fig. 4.2). Corresponding to (7.48), the 2-term outer and 1-term inner expansions (4.13) and (4.46) are

$$\frac{q}{U} \sim \begin{cases} 1 + \varepsilon & \text{as } \varepsilon \to 0 \text{ with } s > 0 \text{ fixed} \qquad (7.58\text{a})\\ \sqrt{\dfrac{2S}{1 + 2S}} & \text{as } \varepsilon \to 0 \text{ with } S = \dfrac{s}{\varepsilon^2} \text{ fixed} \qquad (7.58\text{b})\end{cases}$$

Replacing the abscissa s measured from the leading edge by a new coordinate σ, which vanishes when s does, transforms the inner solution (7.58b) to

$$\frac{q}{U} \sim \sqrt{\frac{2\sigma s'(0)}{\varepsilon^2 + 2\sigma s'(0)}} \tag{7.59}$$

This is the counterpart of Kaplun's correlation theorem (7.50b). The 2-term outer expansion of this is simply unity. Therefore in this example any coordinate is semioptimal, but none is optimal.

This matter deserves further study, together with the question of the connection between Kaplun's optimal coordinates and Lighthill's strained coordinates (Chapter VI). They have in common the idea of achieving uniformity by modifying the independent variables. A superficial difference is that Kaplun changes inner coordinates whereas Lighthill strains the outer ones. However, this is irrelevant insofar as there is a duality between inner and outer expansions (Section 5.9). A more significant difference appears in the way in which the modification of coordinates is determined. Whereas Kaplun requires that the inner solution be valid insofar as possible in the outer region, Lighthill imposes the cruder condition that singularities not be compounded. It is conceivable that after appropriate generalization and refinement of both methods, they may be found to represent two faces of the same coin. See also Section 10.4.

EXERCISES

7.1. *Boundary layer on a wedge.* Consider symmetric viscous flow past a semi-infinite wedge of semivertex angle $\beta\pi/2$. Calculate the potential flow, and describe how the upstream condition (7.2d) for the Navier-Stokes equations must be modified. Discuss the applicability of the boundary-layer solutions as a coordinate perturbation and as a parameter perturbation. Show, by exploiting its group property, that Prandtl's boundary-layer equation (7.16a) can be reduced to the Falkner-Skan equation

$$f''' + ff'' + \beta(1 - f'^2) = 0$$

Assuming required numerical properties of f, calculate the flow due to displacement thickness. Find orthogonal optimal coordinates. Calculate the second-order boundary-layer solution. Is there a concentrated force at the leading edge?

7.2. *Boundary layer on flat plate in shear flow.* As a model of the effect of external vorticity on a boundary layer, consider a semi-infinite flat plate at zero incidence in a parallel stream with constant vorticity, its speed being $U - \omega y$. Derive the problem for the second approximation in the boundary layer, showing that the matching condition has the form

$$\Psi_2(x, Y) \sim aY^2 + bY + O(1) \qquad \text{as} \quad Y \to \infty$$

Show that interaction between the displacement effect and the external vorticity induces a second-order pressure gradient on the boundary layer. Reduce the problem to a third-order ordinary differential equation with proper boundary conditions. [The definitive treatment of this controversial problem, together with earlier references, is given by Murray (1961).]

7.3. *Inverse boundary-layer problem.* Suppose that we solve the inverse rather than the direct problem in boundary-layer theory, in the following sense: we seek the body that produces a given inviscid flow outside the boundary layer. Explain why the asymptotic sequences for the inner and outer expansions are not the successive powers of $R^{-1/2}$ of the direct problem. Carry the solution as far as practicable for the upper surface of a body that has a uniform parallel stream outside the boundary layer.

7.4. *Second-order correlation theorem.* Show that the second-order counterpart of (7.50b) is

$$\psi \sim \frac{1}{\sqrt{R}}\, \Psi_1[x(\xi, 0), \sqrt{R}\eta y_\eta(\xi, 0)] + \frac{1}{R}\{\Psi_2[\ ]$$ See Note 9

$$+ \sqrt{R}\eta x_\eta(\xi, 0)\Psi_{1x}[\ ] + \tfrac{1}{2}R\eta^2 y_{\eta\eta}(\xi, 0)\Psi_{1Y}[\ ]\}$$

where all square brackets contain the same arguments as the first.

7.5. *Slip sublayer.* If slight slip is admitted at the surface, the second of the boundary conditions (7.16b) is replaced by

$$\Psi_{1Y}(x, 0) = \varepsilon\Psi_{1YY}(x, 0), \qquad \varepsilon \ll 1$$

Calculate the boundary-layer solution for the semi-infinite flat plate to order ε by perturbing the solution for $\varepsilon = 0$. Note that the perturbation is the Y-derivative of the basic solution (Lin and Schaaf, 1951). Show that this approximation is not valid in a thin sublayer near the surface. Construct the first term of a supplementary expansion valid in that region.

Chapter VIII

VISCOUS FLOW AT LOW REYNOLDS NUMBER

8.1. Introduction

We consider now incompressible flow past a body at low Reynolds number, as exemplified by the sphere and circular cylinder (Fig. 8.1).

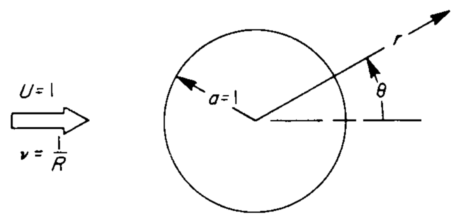

Fig. 8.1. Notation for sphere and circle.

Every high-school student learns that Millikan calculated the drag of an oil drop using the approximation developed by Stokes in 1851:

$$C_D = \frac{D}{\rho U^2 a^2} \sim \frac{6\pi}{R} \quad \text{as} \quad R \equiv \frac{Ua}{\nu} \to 0 \tag{8.1a}$$

A second approximation was found by Oseen in 1910:

$$C_D \sim \frac{6\pi}{R}\left(1 + \tfrac{3}{8}R\right) \tag{8.1b}$$

However, only in 1957 was it shown how further terms [cf. (1.4)] can be calculated using the method of matched asymptotic expansions.

The classical warning of singular behavior is absent; the highest derivatives are retained in the Navier-Stokes equations in the limit $R \to 0$. However, the problem contains two characteristic lengths: the radius a and the viscous length ν/U. Their ratio is the Reynolds number, so that in the limit $R \to 0$ the viscous length becomes vastly greater than the radius of the body. Hence singular behavior can be anticipated according to the physical criterion advanced in Section 5.3.

Viscous flows at low Reynolds number are easily observed experimentally, in contrast with those at high Reynolds number. Fig. 8.2 shows the sequence of flow patterns for a sphere or circular cylinder as

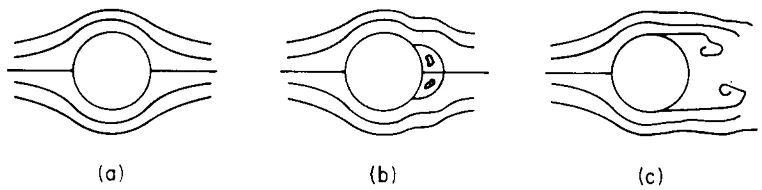

Fig. 8.2. Flow patterns for sphere or circle at low Reynolds number. (a) No eddies. (b) Standing eddies. (c) Unsteady flow.

the Reynolds number increases. At very low speeds the streamline pattern is almost symmetrical fore and aft. A closed recirculating wake or standing eddy makes its appearance at about $R = 10$ for a sphere and $R = 2.5$ for a circle (our Reynolds number being based upon radius rather than diameter). One may imagine that the eddies always exist inside the body, and at these Reynolds numbers penetrate through its surface (cf. Fig. 8.3). The flow becomes unsteady, with oscillations of

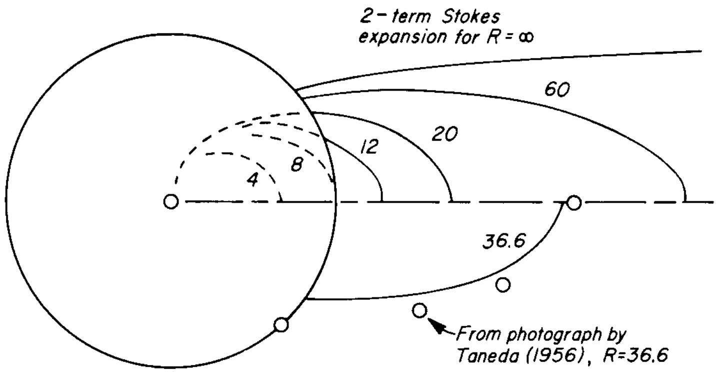

Fig. 8.3. Shape of standing eddy behind sphere.

the downstream part of the wake, at about $R = 65$ for a sphere and $R = 15$ for a circle. The flow becomes irregular, with separation of vortices from the rear of the body, above about $R = 100$ for a sphere and $R = 20$ for a circle.

8.2. Stokes' Solution for Sphere and Circle

Stokes reasoned that at low speeds the inertia forces, represented by the convective terms in the Navier-Stokes equations, are ineffective because they are quadratic in the velocity. Hence at low Reynolds number the pressure forces must be nearly balanced by viscous forces alone. As a first approximation, Stokes neglected the convective terms. In plane flow the result is the biharmonic equation for the stream function:

$$\nabla^4\psi = \left(\frac{\partial^2}{\partial r^2} + \frac{1}{r}\frac{\partial}{\partial r} + \frac{1}{r^2}\frac{\partial^2}{\partial\theta^2}\right)^2\psi = 0 \tag{8.2a}$$

This follows formally from (7.2a) by letting $R \to 0$. In axisymmetric flow, the corresponding result is

$$\left[\frac{\partial^2}{\partial r^2} + \frac{\sin\theta}{r^2}\frac{\partial}{\partial\theta}\left(\frac{1}{\sin\theta}\frac{\partial}{\partial\theta}\right)\right]^2\psi = 0 \tag{8.2b}$$

Let lengths be made dimensionless by reference to the radius a, and velocities by reference to the free-stream speed U (Fig. 8.2). Then the boundary conditions of zero velocity at the surface are

$$\psi(1,\theta) = \psi_r(1,\theta) = 0 \tag{8.3a}$$

and the condition of uniform flow upstream is

$$\psi(r,\theta) \sim \begin{cases} r\sin\theta, & \text{plane} \\ \frac{1}{2}r^2\sin^2\theta, & \text{axisymmetric} \end{cases} \quad \text{as} \quad r\to\infty \tag{8.3b}$$

For the circle a symmetry condition must be added to rule out circulation.

Consider first the sphere. The upstream condition (8.3b) suggests separating variables, seeking a solution of the form $\psi = \sin^2\theta f(r)$. This leads to

$$\psi = \sin^2\theta \left\{r^4, r^2, r, \frac{1}{r}\right\} \tag{8.4}$$

The upstream condition shows that no term in r^4 can be tolerated, and that the coefficient of the term in r^2 is $\frac{1}{2}$. Then the surface conditions (8.3a) fix the coefficients of r and $1/r$, giving Stokes' approximation:

$$\psi \sim \frac{1}{4}\left(2r^2 - 3r + \frac{1}{r}\right)\sin^2\theta \tag{8.5}$$

The first term is the uniform stream, and the third a dipole at the center of the sphere, both representing irrotational flows. The second term, which contains all the vorticity, has been dubbed a "stokeslet" by Hancock (1953), who used a linear distribution of these three elements to simulate a swimming worm. For inviscid flow the stokeslet is absent, and the coefficient of the dipole is $-\frac{1}{2}$ instead of $\frac{1}{4}$. Calculating the skin friction gives two-thirds of the drag (8.1a), the remaining third being pressure drag (Tomotika and Aoi, 1950). The flow pattern is symmetric fore and aft, and is therefore free of eddies as in Fig. 8.2a.

Consider now the circular cylinder. The upstream condition (8.3b) suggests seeking a solution of the form $\psi = \sin\theta\, f(r)$, which leads to

$$\psi = \sin\theta \left\{ r^3,\ r\log r,\ r,\ \frac{1}{r} \right\} \tag{8.6}$$

Imposing the conditions (8.3a) at the surface reduces this to

$$\psi \sim C\left[(1+2k)r\log r - \frac{1}{2}r - \frac{1+k}{2}\frac{1}{r} - \frac{k}{2}r^3\right]\sin\theta \tag{8.7}$$

We can invoke the principle of minimum singularity (Section 4.5), choosing $k = 0$ so that the stream function and velocity grow as slowly as possible with r. This leaves

$$\psi \sim C\left(r\log r - \frac{1}{2}r + \frac{1}{2}\frac{1}{r}\right)\sin\theta \tag{8.8}$$

The second term is the uniform parallel stream, the third a dipole at the origin, and the first a two-dimensional stokeslet containing the vorticity. The solution cannot be completed, however, because no choice of the constant C satisfies the upstream condition (8.3b). The difficulty is that, in contrast with the solution for the sphere, the stokeslet is now more singular at infinity than a uniform stream, and so predicts velocities that are unbounded far from the body.

8.3. The Paradoxes of Stokes and Whitehead

See Note 16

The nonexistence of a solution of Stokes' equation for unbounded plane flow past any body is known as *Stokes' paradox*. Stokes himself (1851) regarded it as an indication that no steady flow exists; a body started from rest would entrain a continually increasing quantity of fluid. However, this explanation is now believed to be incorrect, for reasons discussed in the next section.

Indeed, analogous difficulties arise with three-dimensional bodies, though they are deferred to the second approximation for finite shapes because, as usual, flow disturbances are weaker in three dimensions than two. (For semi-infinite shapes see Exercise 8.2.) Thus Whitehead (1889) failed in his attempt to improve upon Stokes' approximation for the sphere by iteration. The full Navier-Stokes equations give (Goldstein, 1938, p. 115):

$$\frac{1}{R}D^4\psi = \frac{1}{r^2\sin\theta}\left(\psi_\theta\frac{\partial}{\partial r} - \psi_r\frac{\partial}{\partial\theta} + 2\cot\theta\,\psi_r - 2\frac{\psi_\theta}{r}\right)D^2\psi \tag{8.9a}$$

where

$$D^2 = \frac{\partial^2}{\partial r^2} + \frac{\sin\theta}{r^2}\frac{\partial}{\partial\theta}\left(\frac{1}{\sin\theta}\frac{\partial}{\partial\theta}\right) \tag{8.9b}$$

Substituting the first approximation (8.5) into the convective terms on the right-hand side of (8.9a) that were neglected by Stokes yields the iteration equation

$$\left[\frac{\partial^2}{\partial r^2} + \frac{\sin\theta}{r^2}\frac{\partial}{\partial\theta}\left(\frac{1}{\sin\theta}\frac{\partial}{\partial\theta}\right)\right]^2\psi = -\frac{9}{4}R\left(\frac{2}{r^2} - \frac{3}{r^3} + \frac{1}{r^5}\right)\sin^2\theta\cos\theta \tag{8.10}$$

A particular integral that satisfies the surface conditions (8.3a) is easily found to be

$$-\frac{3}{32}R\left(2r^2 - 3r + 1 - \frac{1}{r} + \frac{1}{r^2}\right)\sin^2\theta\cos\theta \tag{8.11}$$

However, the velocity does not behave properly at infinity, and no complementary function can be added to correct it. In the next approximation the velocity would become infinite at infinity, as in the first approximation (8.8) for the circular cylinder.

The nonexistence of a second approximation to Stokes' solution for unbounded uniform flow past a three-dimensional body is known as *Whitehead's paradox*. Whitehead himself regarded it as an indication that discontinuities must arise in the flow field associated with the formation of a dead-water wake. However, this explanation too is now known to be incorrect. See Note 16

8.4. The Oseen Approximation

Just as d'Alembert's paradox was resolved by Prandtl's discovery that flow at high Reynolds number is a singular perturbation problem, so the paradoxes of Stokes and Whitehead were shown by Oseen to arise from the singular nature of flow at low Reynolds number. Whereas the region of nonuniformity is a thin layer near the surface of the body at high Reynolds number, it is the neighborhood of the point at infinity for low Reynolds number. The source of the difficulty can be undertood by examining the relative magnitude of the terms neglected in the Stokes approximation.

Far from the body the nonlinear convective terms are seen from the right-hand side of (8.10) to be of order R/r^2. A typical viscous term—the cross-product in the left-hand side of (8.10)—is, from (8.5),

$$\frac{\partial^2}{\partial r^2}\left[\frac{\sin\theta}{r^2}\frac{\partial}{\partial\theta}\left(\frac{1}{\sin\theta}\frac{\partial}{\partial\theta}\right)\right]\psi = \left(\frac{3}{r^3} - \frac{6}{r^5}\right)\sin^2\theta = O\left(\frac{1}{r^3}\right) \tag{8.12}$$

Thus the ratio of terms neglected to those retained is

$$\frac{\text{convective}}{\text{viscous}} = O(Rr) \qquad \text{as} \quad r \to \infty \tag{8.13}$$

Although this ratio is small near the body when R is small, it becomes arbitrarily large at sufficiently great distances, no matter how small R may be. Thus the Stokes approximation becomes invalid where Rr is of order unity. This occurs at distances of the order of ν/U, meaning that the viscous length is then the significant reference dimension. The same objection applies *a fortiori* to plane flow, where the incomplete Stokes approximation (8.8) for the circle suggests the estimate

$$\frac{\text{convective}}{\text{viscous}} = O(CRr\log r) \qquad \text{as} \quad r \to \infty \tag{8.14}$$

These nonuniformities are the source of the singular behavior of the Stokes approximation. In three-dimensional flow the difficulty tends to be concealed because the first approximation is sufficiently well behaved; in the region of nonuniformity where $Rr = O(1)$ the velocity has already effectively attained its free-stream value, so that it is possible to impose the upstream boundary condition. This is an exceptional circumstance, which arose previously in the inner solution for a round-nosed airfoil (cf. Section 5.6).

This explanation of the difficulties encountered by Stokes and Whitehead was given by Oseen (1910), who prescribed a cure at the same time. Rather than neglect the convective terms altogether, he approximates them by their linearized forms valid far from the body, where the difficulty arises. For example, in the x-momentum equation in Cartesian coordinates

$$uu_x + vu_y + wu_z + \frac{p_x}{\rho} = \nu(u_{xx} + u_{yy} + u_{zz}) \tag{8.15}$$

Stokes neglects the first three terms altogether, but Oseen approximates

them by Uu_x. In plane flow the dimensionless equation (7.2a) for the stream function then becomes

$$\left(\nabla^2 - R\frac{\partial}{\partial x}\right)\nabla^2\psi = 0 \tag{8.16}$$

This constitutes an *ad hoc* uniformization, of a sort to be discussed further in Section 10.2. The general principle is to identify those terms whose neglect in the straightforward perturbation solution leads to nonuniformity, and to retain them after simplifying them insofar as possible in the region of nonuniformity. If the resulting equations can be solved, the result is a uniformly valid composite approximation, of the sort discussed in Section 5.4.

Thus Oseen's equations provide a uniformly valid first approximation for either plane or three-dimensional flow at low Reynolds number. In principle, one could refine the solution by successive approximations, and the result would presumably preserve its uniformity at every stage. In practice, however, although the Oseen equations are linear, their solution is sufficiently complex that no second approximations are known. It is simpler to decompose the composite expansion into its constituent inner and outer expansions, which may subsequently be recombined. This process will be carried out in the following sections.

The Oseen equations possess a second, essentially different, interpretation. At an arbitrary Reynolds number they describe viscous flow at such great distances from a finite body that the velocity has nearly returned to its free-stream value. From this small-disturbance point of view, the Oseen approximation has been used to study the wake far behind a body (Exercises 8.1 and 8.3). In such applications, ψ in (8.16) ordinarily represents a perturbation rather than the full stream function, the distinction affecting only the form of the boundary conditions. This second interpretation of the Oseen approximation of course remains valid at low Reynolds numbers, and will be used in what follows.

The solution of the Oseen equations was given for the sphere by Oseen himself (1910) as See Note 10

$$\psi = \frac{1}{4}\left(2r^2 - \frac{1}{r}\right)\sin^2\theta - \frac{3}{2}\frac{1}{R}(1 + \cos\theta)\left[1 - e^{-\frac{1}{2}Rr(1-\cos\theta)}\right] \tag{8.17}$$

The solution for the circular cylinder was given by Lamb (1911) in terms of Cartesian velocity components. For example, the component normal to the free stream is

$$\psi_x = \frac{1}{\log(4/R) - \gamma + \frac{1}{2}}\left\{\frac{\sin 2\theta}{2r^2} + \frac{2}{R}\frac{\partial}{\partial y}\left[\log Rr + e^{\frac{1}{2}Rr\cos\theta}K_0\left(\tfrac{1}{2}Rr\right)\right]\right\} \tag{8.18}$$

Here $\gamma = 0.5772 \ldots$ is Euler's constant, and K_0 is the Bessel function.

In both these solutions the surface conditions were satisfied only approximately in a manner appropriate to the underlying assumption that the Reynolds number is small. We shall reconstruct these results later. Solutions for arbitrary Reynolds number were carried out by Goldstein (1929) and Tomotika and Aoi (1950). These more complicated results are of limited value because, contrary to Oseen's own views, the approximation is qualitatively as well as quantitatively invalid at high Reynolds number. For example, the Oseen approximation gives boundary layers whose thickness is of order R^{-1} rather than $R^{-1/2}$ as in Prandtl's correct theory. This discrepancy may be understood physically as arising from the fact that in Oseen's approximation the vorticity generated at the surface by shear is convected *through* rather than along the surface. The detailed flow patterns calculated by Tomotika and Aoi would be of some interest had not Yamada (1954) pointed out that numerical inaccuracy invalidates their qualitative nature even at low Reynolds number. For example, Tomotika and Aoi predict the standing eddies of Fig. 8.2b at arbitrarily low Reynolds number, whereas Yamada shows that they first appear behind the circular cylinder at $R = 1.51$ in the Oseen approximation.

8.5. Second Approximation Far from Sphere

See Note 10

We now improve Stokes' solution for the sphere by applying the method of matched asymptotic expansion. Our analysis follows the spirit of Kaplun and Lagerstrom (1957), but more nearly the notation of Proudman and Pearson (1957).

Let Stokes's approximation (8.5) be the leading term in an asymptotic expansion for small Reynolds number, which we call the *Stokes expansion*. We have seen that this series is invalid far from the body where r is of order R^{-1}. We therefore introduce an appropriate contracted radial coordinate ρ by setting

$$\rho = Rr \tag{8.19}$$

and envision a second asymptotic expansion valid in that distant region. We call it the *Oseen expansion*, because the flow far from the body is a small perturbation of the uniform stream. According to the convention adopted in Section 5.9, the Oseen expansion is the outer, and the Stokes expansion the inner expansion. We choose our notation accordingly except for the radial variable where, because R is not available, we use ρ for the outer and r for the inner variable.

We could, as in the last chapter, write down the two expansions with

their asymptotic sequences left unspecified. However, we prefer to show how matching automatically determines the form of each term in succession when, as in this problem, the matching proceeds according to the standard order (Section 5.9).

Writing the Stokes solution (8.5) in terms of the Oseen variable (8.19) and expanding for small R gives as its 2-term Oseen expansion:

$$\text{2-Oseen (1-Stokes) } \psi = \frac{1}{2}\frac{1}{R^2}\rho^2 \sin^2\theta - \frac{3}{4}\frac{1}{R}\rho \sin^2\theta \tag{8.20}$$

where the first term is the uniform stream. In order to match this, the Oseen expansion must have the form

$$\psi \sim \frac{1}{2}\frac{1}{R^2}\rho^2 \sin^2\theta + \frac{1}{R}\psi_2(\rho, \theta) + \cdots \quad \text{as} \quad R \to 0 \quad \text{with } \rho \text{ fixed} \tag{8.21}$$

Substituting into the full equation (8.9) yields for ψ_2 the classical linearized Oseen equation (8.16) in the form

$$\Big(\mathscr{L}^2 - \cos\theta \frac{\partial}{\partial\rho} + \frac{\sin\theta}{\rho}\frac{\partial}{\partial\theta}\Big)\mathscr{L}^2\psi_2 = 0 \tag{8.22a}$$

where

$$\mathscr{L}^2 = \frac{\partial^2}{\partial\rho^2} + \frac{\sin\theta}{\rho^2}\frac{\partial}{\partial\theta}\Big(\frac{1}{\sin\theta}\frac{\partial}{\partial\theta}\Big) \tag{8.22b}$$

Setting

$$\mathscr{L}^2\psi_2 = e^{\frac{1}{2}Rx}\phi_2 = e^{\frac{1}{2}\rho\cos\theta}\phi_2 \tag{8.23}$$

reduces Eq. (8.22) to

$$(\mathscr{L}^2 - \tfrac{1}{4})\phi_2 = 0 \tag{8.24}$$

Seeking as before a solution of the form $\phi_2 = \sin^2\theta\, f(\rho)$ gives

$$f'' - \Big(\frac{2}{\rho^2} + \frac{1}{4}\Big)f = 0 \tag{8.25}$$

The solution that vanishes at infinity is

$$f = c_2\Big(1 + \frac{2}{\rho}\Big)e^{-\frac{1}{2}\rho} \tag{8.26}$$

and any other solution of (8.24) having the proper symmetry is more singular at the origin, and can therefore be rejected as unmatchable by the principle of minimum singularity (Section 5.6).

Thus the original equation for (8.22) for ψ_2 is reduced to

$$\mathscr{D}^2\psi_2 = c_2\left(1 + \frac{2}{\rho}\right)e^{-\frac{1}{2}\rho(1-\cos\theta)} \sin^2\theta \tag{8.27}$$

A particular integral is

$$\psi_2 = -2c_2(1 + \cos\theta)[1 - e^{-\frac{1}{2}\rho(1-\cos\theta)}] \tag{8.28}$$

where the first term is a potential source at the origin, which has been added to cancel the sink in the second term, and so assure zero flux through any surface enclosing the body. Any other complementary function that possesses this property, gives no velocity at infinity, and has the proper symmetry will be more singular at the origin and hence unmatchable.

This is a fundamental solution of the Oseen equation, which describes the disturbance field produced at great distances by any finite three-dimensional nonlifting body. The constant c_2 depends upon certain details of the flow near the body. We find it by applying the asymptotic matching principle (5.24). Writing the Oseen expansion (8.21) in Stokes variables and expanding for small R yields

$$\text{1-Stokes (2-Oseen) } \psi = \tfrac{1}{2}r^2 \sin^2\theta - c_2 r \sin^2\theta \tag{8.29}$$

This matches (8.20) if $c_2 = \frac{3}{4}$.

We have thus found two terms of the Oseen expansion (8.21). When rewritten in Stokes variables this becomes

$$\psi \sim \frac{1}{2}r^2 \sin^2\theta - \frac{3}{2}\frac{1}{R}(1 + \cos\theta)[1 - e^{-\frac{1}{2}Rr(1-\cos\theta)}]$$
$$\text{as} \quad R \to 0 \quad \text{with } Rr \text{ fixed} \tag{8.30}$$

We can construct a uniformly valid composite expansion by combining this with the Stokes approximation (8.5) using the rule (5.32) for additive composition. The result gives a uniform approximation to the *perturbation* field. It is found to be just the solution (8.17) of the Oseen equations given by Oseen himself. This confirms the statement in Section 8.4 that his linearized equations yield a uniform first approximation. Near the body the last term in (8.17) reduces to the stokeslet of the Stokes approximation; it may by analogy be called an "oseenlet."

8.6. Second Approximation near Sphere

We proceed to the second term in the Stokes expansion. The 2-term Stokes expansion of the Oseen expansion (8.21) is found to be

$$\text{2-Stokes (2-Oseen) } \psi = \frac{1}{4}(2r^2 - 3r)\sin^2\theta + \frac{3}{16}Rr^2(1 - \cos\theta)\sin^2\theta \tag{8.31}$$

In order to match this, the Stokes expansion must have the form

$$\psi \sim \frac{1}{4}\left(2r^2 - 3r + \frac{1}{r}\right)\sin^2\theta + R\Psi_2(r, \theta) + \cdots \tag{8.32}$$

The equation for Ψ_2 is evidently Whitehead's (8.10) without the factor R. His particular integral (8.11) remains valid, and the original Stokes approximation (8.5) provides the only complementary function with the proper symmetry that is no more singular at infinity. Thus we set

$$\Psi_2 = C_2\left(2r^2 - 3r + \frac{1}{r}\right)\sin^2\theta - \frac{3}{32}\left(2r^2 - 3r + 1 - \frac{1}{r} - \frac{1}{r^2}\right)\sin^2\theta\cos\theta \tag{8.33}$$

The constant C_2 is found by matching. Carrying out the Oseen expansion of (8.33) yields

$$\text{2-Oseen (2-Stokes) } \psi = \frac{1}{2}\frac{1}{R^2}\rho^2\sin^2\theta$$
$$+ \frac{1}{R}\left(2C_2\rho^2 - \frac{3}{16}\rho^2\cos\theta - \frac{3}{4}\rho\right)\sin^2\theta \tag{8.34}$$

and this matches (8.31) if $C_2 = 3/32$.

Thus we have found two terms of the Stokes expansion for the stream function in the vicinity of the sphere:

$$\psi \sim \frac{1}{4}(r-1)^2\sin^2\theta\left[\left(1 + \frac{3}{8}R\right)\left(2 + \frac{1}{r}\right) - \frac{3}{8}R\left(2 + \frac{1}{r} + \frac{1}{r^2}\right)\cos\theta\right] \tag{8.35}$$

This vanishes not only on the sphere and along the axis of symmetry, but also along the curve

$$\cos\theta = \left(\frac{8}{3}\frac{1}{R} + 1\right)\frac{2r^2 + r}{2r^2 + r + 1} \tag{8.36}$$

This is the approximate description of the boundary of the standing eddy. It is plotted in Fig. 8.3. The eddy appears only at Reynolds numbers so large that one would not have expected the Stokes expansion to have any validity. Nevertheless, the lower half of Fig. 8.3 shows striking agreement with the experimental observations of Taneda (1956) at R = 36.6. The downstream end of the eddy lies at

$$r_e = \tfrac{1}{4}(\sqrt{1+3R} - 1) \tag{8.37}$$

Therefore the eddy first appears in the flow field at $R = 8$. Despite its magnitude, this agrees well with the value of 12 measured by Taneda and the value of 8.5 calculated numerically by Jenson (1959) using the full Navier-Stokes equations. Indeed, Fig. 8.4 shows that good agreement

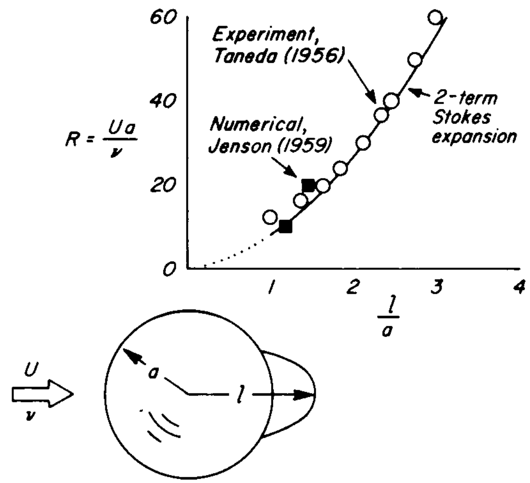

Fig. 8.4. Length of eddy behind sphere.

persists out to $R = 60$, which is about the limit for observation of steady flow. These remarkable results call for corroboration through examination of the effect of further terms in the Stokes expansion.

Higher approximations can be found by continuing the preceding
See analysis. Proudman and Pearson (1957) have carried it far enough to
Note show that the next Stokes approximation contains a term in $R^2 \log R$
10 as well as R^2, and that logarithms are thereby introduced also into the Oseen expansion beginning with $R^3 \log R$. They have calculated only the term in $R^2 \log R$ in the Stokes expansion. This provides the drag formula (1.4) of Chapter I.

According to these results, the Reynolds number at which the eddy first appears is a solution of the transcendental equation

$$1 - \frac{1}{8}R + \frac{9}{40}R^2 \log R + O(R^2) = 0 \tag{8.38}$$

Unfortunately, this has no real root if three terms are retained. The logarithmic term limits the Stokes expansion to values of R small compared with 1. Until some method is found of enlarging the range of applicability of such a series (cf. Section 10.7), we cannot say whether the striking predictions of the second Stokes approximation are more than coincidence.

Because of symmetry, the second term in square brackets in (8.35) contributes nothing to the drag, which according to the first term is then $(1 - \frac{3}{8}R)$ times the Stokes value. But the second term is the particular integral of Whitehead for the nonlinear terms. For that reason, the Oseen approximation, which neglects the nonlinear terms near the body, nevertheless gives the drag correct to second order at least for symmetric shapes (Chester, 1962).

8.7. Higher Approximations for Circle

Stokes' paradox for plane flow is more striking than Whitehead's for See
three dimensions. Its resolution by the method of matched asymptotic Note
expansions is correspondingly more dramatic, despite the practical 10
shortcoming that the solution cannot be carried to nearly as great accuracy. We treat the typical example of the circular cylinder, using a synthesis of the work of Kaplun (1957) and of Proudman and Pearson (1957).

The analysis largely parallels that for the sphere, but interesting differences appear. In particular, the matching is marginal, and the asymptotic sequence correspondingly slow. It was for this problem that Kaplun and Lagerstrom (1957) devised their sophisticated apparatus of intermediate limits and expansions, and the intermediate matching principle (Section 5.8). However, we shall see that the asymptotic matching principle (5.24) is entirely adequate, although the simple limit matching principle (5.22) does not hold.

We reconsider the solution (8.8) of the biharmonic equation as the first term in a Stokes expansion:

$$\psi \sim \Delta_1(R)\left(r \log r - \frac{1}{2}r + \frac{1}{2}\frac{1}{r}\right)\sin\theta \quad \text{as} \quad R \to 0 \quad \text{with } r \text{ fixed} \tag{8.39}$$

The multiplier Δ_1 must be allowed to depend upon Reynolds number because our asymptotic sequence is unspecified. Although this approximation cannot satisfy the condition (8.3b) of a uniform stream at infinity, it can be *matched* to the uniform stream, regarded as the first term of an Oseen expansion (Lagerstrom and Cole, 1955, Section 6.3). Again the Oseen variable is taken as $\rho = Rr$ so that lengths are referred to the viscous dimension ν/U rather than the radius a. Then the Oseen expansion begins with the free stream in the form

$$\psi \sim \frac{1}{R}\rho \sin\theta + \cdots \quad \text{as} \quad R \to 0 \quad \text{with} \quad \rho > 0 \quad \text{fixed} \tag{8.40}$$

Writing the Stokes approximation (8.39) in Oseen variables and expanding gives

$$\text{1-Oseen (1-Stokes)}\ \psi = \frac{\Delta_1(R)}{R} \log \frac{1}{R}\rho \sin\theta \tag{8.41}$$

This matches (8.40) if $\Delta_1(R) = (\log 1/R)^{-1}$, or more generally if $\Delta_1(R) = (\log 1/R + k)^{-1}$, where k is any constant; and we shall later exploit this freedom.

The overlap is so slight in this case that in order to match we have had to accept a relative error of order Δ_1, which is enormous compared with the error of order R in the Stokes approximation for the sphere. We are thereby committed to a slow expansion in powers of Δ_1, of which an infinite number of terms correspond to only the first term for the sphere.

Expanding the Stokes approximation (8.39) further in Oseen variables yields

$$\text{2-Oseen (1-Stokes)}\ \psi = \frac{1}{R}[1 + \Delta_1(R)(\log\rho - k - \tfrac{1}{2})]\rho \sin\theta \tag{8.42}$$

This requires, in order to match, that the Oseen expansion (8.40) continue as

$$\psi \sim \frac{1}{R}[\rho \sin\theta + \Delta_1(R)\psi_2(\rho, \theta) + \cdots] \tag{8.43}$$

Substituting this into the full equation (7.2a) shows, of course, that ψ_2 satisfies the linearized Oseen equation (8.16). The appropriate solution can be found by proceeding as for the sphere (Proudman and Pearson, 1957). However, the stream function is disadvantageous here because it can be written only as an infinite series, whereas the velocity components are closed expressions.

We evidently seek the plane counterpart of (8.28), the oseenlet representing the disturbances produced by an infinitesimal drag at the origin. This fundamental solution, due to Oseen (Rosenhead, 1963, p. 183), gives as Cartesian velocity components

$$u_2 = \frac{\partial\psi_2}{\partial(\rho\sin\theta)} = 2c_2\left\{\frac{\partial}{\partial(\rho\cos\theta)}[\log\rho + e^{\frac{1}{2}\rho\cos\theta}K_0(\tfrac{1}{2}\rho)] - e^{\frac{1}{2}\rho\cos\theta}K_0(\tfrac{1}{2}\rho)\right\} \tag{8.44a}$$

$$v_2 = -\frac{\partial\psi_2}{\partial(\rho\cos\theta)} = 2c_2\frac{\partial}{\partial(\rho\sin\theta)}[\log\rho + e^{\frac{1}{2}\rho\cos\theta}K_0(\tfrac{1}{2}\rho)] \tag{8.44b}$$

The term in $\log\rho$ is again a potential source at the origin that cancels the sink in the term involving the Bessel function K_0. For small ρ these are approximately

$$\frac{\partial\psi_2}{\partial(\rho\sin\theta)} \sim -c_2\left(\log\frac{4}{\rho} - \gamma + \cos^2\theta\right) + O(\rho\log\rho) \tag{8.45a}$$

$$\frac{\partial\psi_2}{\partial(\rho\cos\theta)} \sim c_2 \sin\theta\cos\theta + O(\rho\log\rho) \tag{8.45b}$$

where Euler's constant $\gamma = 0.5772 \ldots$, and integrating gives

$$\psi_2 \sim -c_2\left(\log\frac{4}{\rho} + 1 - \gamma\right)\rho\sin\theta + O(\rho^2\log\rho) \tag{8.46}$$

Using this, we find that the Oseen expansion (8.43) behaves near the body like

$$\text{1-Stokes (2-Oseen)}\ \psi = \frac{1}{R}\left[\rho\sin\theta + c_2\Delta_1(R)\left(\log\frac{\rho}{4} + \gamma - 1\right)\rho\sin\theta\right] \tag{8.47}$$

Then matching with (8.42) according to the asymptotic matching principle gives $c_2 = 1$.

The second term in the Stokes expansion—and indeed the term of any finite order—is evidently again a solution of the biharmonic equation, because the nonlinear terms of order R are transcendentally small on the scale of powers of $\Delta_1(R)$. Matching, or applying the principle of minimum singularity, shows that each is simply a multiple of the first approximation (8.8). It is convenient, following Kaplun (1957), to make the second term vanish by choosing the constant k so that (8.42) and (8.47) match perfectly: $k = \log 4 - \gamma + \frac{1}{2}$. Then the Stokes expansion assumes the form

$$\psi \sim \left(\Delta_1 + \sum_{n=3}^{\infty} a_n\Delta_1^{\,n}\right)\left(r\log r - \frac{1}{2}r + \frac{1}{2}\frac{1}{r}\right)\sin\theta \tag{8.48a}$$

where

$$\Delta_1 = \left(\log\frac{4}{R} - \gamma + \frac{1}{2}\right)^{-1} = \left(\log\frac{3.703}{R}\right)^{-1} \tag{8.48b}$$

Forming a uniformly valid two-term composite expansion by additive composition of (8.43) and (8.48) reproduces Lamb's solution (8.18) of the linearized Oseen equation.

Kaplun (1957) has carried the process through one more cycle to find the coefficient of the third term in the Stokes expansion (8.48) as $a_3 \approx -0.87$. Hence he finds for the drag coefficient

See Note 11

$$C_D = \frac{D}{\rho U^2 a} \sim \frac{4\pi}{R}[\Delta_1(R) - 0.87\Delta_1^3(R) + O(\Delta_1^4)] \qquad (8.49)$$

See Note 15

The first term is the classical result of Lamb (1911, 1932). Comparison with the measurements of Tritton (1959) in Fig. 8.5 shows the limited utility of this result. Also shown for comparison is Tomotika and Aoi's (1950) full numerical solution of the linearized Oseen equation (8.16).

From a formal mathematical point of view, we should exhaust all the

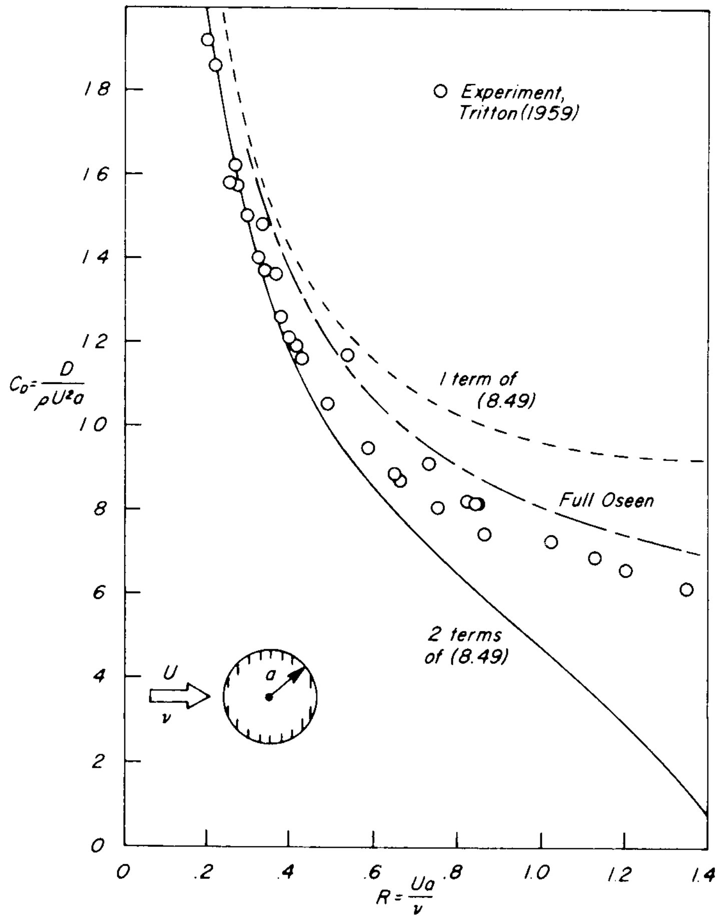

Fig. 8.5. Drag of circular cylinder at low Reynolds number.

powers of Δ_1 in (8.48) before considering nonlinear corrections to the Stokes equation, which are relatively of the transcendentally small order R. In practice, however, such terms are significant. The first such term (Exercise 8.5) is of order R, which is greater than Δ_1^4 for $R > 0.00008$. Proudman and Pearson (1957) discuss briefly how these terms could be calculated. They would be needed to show any asymmetry in the flow pattern, such as the emergence of standing eddies.

See Note 11

EXERCISES

8.1. *Oseen solution for flat plate and plane wake.* In parabolic coordinates (7.51) the Navier-Stokes equations give for the stream function in plane flow:

$$\left[\nu\left(\frac{\partial^2}{\partial\xi^2} + \frac{\partial^2}{\partial\eta^2}\right) + \psi_\xi\frac{\partial}{\partial\eta} - \psi_\eta\frac{\partial}{\partial\xi}\right]\frac{\psi_{\xi\xi} + \psi_{\eta\eta}}{\xi^2 + \eta^2} = 0$$

Derive the corresponding linearized equation (8.16) of Oseen. Find by separation of variables the Oseen solution for a semi-infinite flat plate in a uniform stream, and for the flow far from a finite nonlifting body. Show that in the first case the boundary-layer approximation in parabolic coordinates is the full Oseen solution. Compare the skin friction with the known value for the Navier-Stokes equations far downstream. In the second case express the constant multipliers for both the term representing the wake and that for potential flow in terms of the drag of the body. Relate the solution to (8.44). [The first case was originally treated in a more complicated way by Lewis and Carrier (1949); for the second, see Imai (1951) and Chang (1961).]

8.2. *Viscous flow past slender paraboloid.* In paraboloidal coordinates (cf. Exercise 8.1), the Navier-Stokes equations give for axisymmetric flow

See Note 3

$$\left[\nu(\xi^2 + \eta^2)D^2 + \frac{1}{\xi\eta}\left(\psi_\xi\frac{\partial}{\partial\eta} - \psi_\eta\frac{\partial}{\partial\xi}\right) + \frac{2}{\xi^2\eta^2}(\eta\psi_\eta - \xi\psi_\xi)\right]D^2\psi = 0$$

where

$$D^2 \equiv \frac{\xi\eta}{\xi^2 + \eta^2}\left[\frac{\partial}{\partial\xi}\left(\frac{1}{\xi\eta}\frac{\partial}{\partial\xi}\right) + \frac{\partial}{\partial\eta}\left(\frac{1}{\xi\eta}\frac{\partial}{\partial\eta}\right)\right]$$

Find the Stokes solution for the paraboloid of revolution. Show that it can be matched to the uniform stream in the same marginal way as for the circular cylinder. Calculate the second term in the Oseen expansion. Describe how the process would continue. What light does it shed on the accuracy of the known Oseen approximation for the elliptic paraboloid (Wilkinson, 1955)? How does the ratio of skin friction to pressure drag in the Oseen approximation compare with 1 : 1 for the circle and 2 : 1 for the sphere (Tomotika and Aoi, 1950)?

See Note 3

8.3. *Wake of axisymmetric body.* Calculate the leading term in the expansion of the stream function far from a finite body of revolution in viscous flow, identifying the constants with the drag of the body as in Exercise 8.1.

8.4. *Viscous flow past thin parabola.* Show that the Stokes approximation for a parabolic cylinder is unmatchable in any way with a uniform stream. Show that it appears to match the Oseen approximation for a flat plate to first order, or that for a parabola to second order; but that continuing the solution by the method of matched asymptotic expansions indicates that neither of those is the correct leading term. What is the true Oseen limit? (See Lagerstrom and Cole, 1955, p. 877.)

See Note 3

8.5. *Transcendentally small terms for circle.* Supposing that (8.48a) is known to any desired order, find the form of the "next" term, aside from undetermined constants, showing that it is of order R. With which term of the Oseen expansion would it match?

8.6. *Near success of strained coordinates.* Show that the two-term Stokes expansion (8.35) could be found using the method of strained coordinates, and straining only the radius, if one knew that the straining should vanish along the downstream axis of symmetry.

Chapter IX

SOME INVISCID SINGULAR PERTURBATION PROBLEMS

9.1. Introduction

As discussed in Chapters V and VI, the method of matched asymptotic expansions was invented to treat singular perturbation problems in viscous flow theory, whereas Lighthill's technique of strained coordinates was developed for problems in wave propagation. It is still unclear whether Lighthill's method can be generalized to handle elliptic and parabolic as well as hyperbolic equations. On the other hand, the method of matched asymptotic expansions has been successfully applied to a variety of inviscid flow problems. Indeed, we introduced it in Chapter IV for inviscid thin-airfoil theory, and applied it in Section 6.7 to the hyperbolic equations of supersonic flow.

The present chapter is devoted to three more examples of inviscid flows involving nonuniformities. These cover the gamut of speeds from subsonic through transonic to hypersonic. The first is the classical lifting-line theory of Prandtl, which is seen in a fresh light when its singular nature is revealed. The second is slightly supersonic flow past a slender cone, where the linearized solution must be corrected in order to find the position of the shock wave. The third is the entropy layer produced by slightly blunting a wedge in hypersonic flow. We treat the first and third by the method of matched asymptotic expansions, and the second by strained coordinates; but it will be useful to ask whether the alternative method could have been chosen in each case.

9.2. Lifting Wing of High Aspect Ratio

Prediction of the flow field produced by a finite lifting wing at subsonic speeds is one of the most intractable problems in aerodynamic theory. Viscosity must be neglected, except insofar as it provides the Kutta-Joukowski condition at the trailing edge; and it is almost essential to linearize, so that the effects of thickness, camber, and angle of attack can be treated separately. Then the subsonic problem is equivalent to the incompressible one according to the Göthert rule (Jones and Cohen, 1960, p. 49). However, even the remaining problem of inviscid incompressible flow past a wing of zero thickness and infinitesimal inclination to the stream is complicated. Its strict treatment by lifting-surface theory requires solution of a singular integral equation involving double integrals.

For a wing of high aspect ratio, Prandtl's lifting-line theory reduces the problem to the solution of a singular integral equation involving only one integration. It is not clear, however, how one could refine Prandtl's analysis to obtain better approximations. For example, the well-known expression for the lift-curve slope of a flat elliptic wing of aspect ratio A

$$\frac{dC_L}{d\alpha} = \frac{2\pi}{1 + (2/A)} \tag{9.1a}$$

can, to the accuracy of the approximation, be written as

$$\frac{dC_L}{d\alpha} = 2\pi\left(1 - \frac{2}{A} + \cdots\right) \tag{9.1b}$$

However, no extension of Prandtl's method will yield the next term, which we shall see is not of order A^{-2}.

Friedrichs (1953) has pointed out that this is a singular perturbation problem. There are two characteristic dimensions, the span being the primary reference length and the chord the secondary one. Their ratio tends to infinity as the aspect ratio increases. Hence according to our physical criterion (Section 5.3) it is possible for this parameter-perturbation problem to be singular. This possibility is realized for the lifting wing (and also for the nonlifting one, see Exercise 9.1). The nonuniformity can be treated by applying the method of matched asymptotic expansions. The second approximation will be found to be equivalent to Prandtl's lifting-line theory. However, application of the matching principle is seen to eliminate the occurence of integral equations, which are reduced to quadratures, so that the analysis is substantially simplified. Furthermore, continuing the process makes possible the calculation of higher approximations.

Consider for simplicity a flat wing of zero thickness, whose planform is symmetric in the streamwise as well as the spanwise direction (Fig. 9.1a). Take the free-stream speed and the semispan as units of velocity and length. Transfer of the tangency condition is avoided by letting the wing lie in the plane $y = 0$, to which the free stream is inclined at angle α. Then the planform may be described by $x = \pm A^{-1}h(z)$, where

A is the aspect ratio, and the half-chord $h(z)$ is an analytic function of order unity. At first we assume that h vanishes as smoothly as necessary at $z = \pm 1$, in order to avoid additional nonuniformities at the tips. The effects of relaxing this restriction will be faced later.

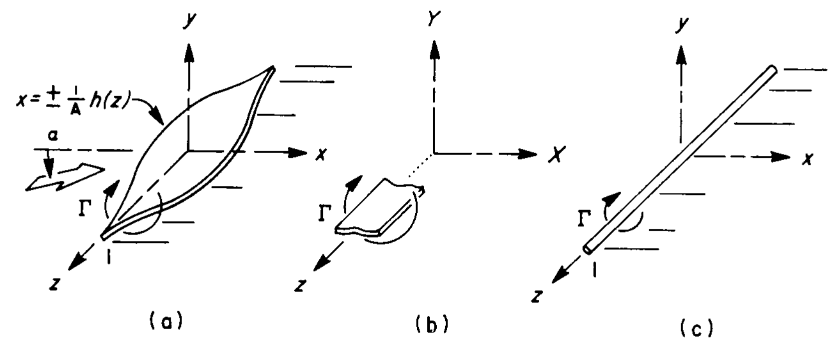

Fig. 9.1. Inner and outer limits for flat lifting wing. (a) Full problem. (b) Inner limit. (c) Outer limit.

The full problem for the dimensionless velocity potential ϕ is

equation:	$\nabla^2\phi = \phi_{xx} + \phi_{yy} + \phi_{zz} = 0$	(9.2a)
tangency:	$\phi_y = 0$ at $y = 0$, $\lvert x \rvert < A^{-1}h(z)$	(9.2b)
upstream:	$\phi \sim x \cos\alpha + y \sin\alpha$	(9.2c)
Kutta:	$\phi_x < \infty$ at $y = 0$, $x = A^{-1}h(z)$	(9.2d)

The version of the Kutta condition given here is a simple way of assuring the physical requirement that the velocity be finite at the trailing edge.

It is evident physically that as the aspect ratio A becomes infinite the flow at any spanwise station approaches plane flow past a flat plate having the local chord (Fig. 9.1b). This can be shown formally by introducing magnified inner variables that are of order unity near the wing, setting

$$\phi = A^{-1}\Phi(X, Y, z) \tag{9.3a}$$

where

$$X = Ax \tag{9.3b}$$

$$Y = Ay \tag{9.3c}$$

These are coordinates referred not to the semispan but to a typical chord, which is the relevant scale for lengths in sections normal to the span.

This transforms the full problem (9.2) to

$$\Phi_{XX} + \Phi_{YY} + A^{-2}\Phi_{zz} = 0 \tag{9.4a}$$

$$\Phi_Y = 0 \quad \text{at} \quad Y = 0, \qquad |X| < h(z) \tag{9.4b}$$

$$\Phi \sim X\cos\alpha + Y\sin\alpha \qquad \text{upstream} \tag{9.4c}$$

$$\Phi_X < \infty \quad \text{at} \quad Y = 0, \qquad X = h(z) \tag{9.4d}$$

The solution of this problem when $A = \infty$ is

$$\Phi_1 = X\cos\alpha + \operatorname{Im}\{\sqrt{(X + iY)^2 - h^2(z)} - h(z)\log[X + iY + \sqrt{(X + iY)^2 - h^2(z)}]\}\sin\alpha \tag{9.5}$$

which can be put into real form using elliptic coordinates. As it clearly should be, this is the solution for plane flow past a flat plate of chord $2h(z)$ at angle α (Fig. 9.1b). Thus to a first approximation the spanwise coordinate z plays only the role of a parameter. For present purposes we require from this solution only the circulation Γ, which is $2\pi i$ times the coefficient of $\log(x^2 + y^2)^{1/2}$ in ϕ:

$$\Gamma \sim \Gamma_1 = 2\pi\alpha A^{-1}h(z) \tag{9.6}$$

The relative error in this first approximation near the wing would, from (9.4a), appear to be of order A^{-2}. However, one cannot simply iterate to find the second approximation. Calculating Φ_{zz} from (9.5) gives an expression that behaves like $\tan^{-1} Y/X$ far from the airfoil section, corresponding to the circulatory flow. A particular integral of the iteration equation therefore behaves like $(X^2 + Y^2)$, which would overwhelm the uniform stream at distances of the order of A in the scale of the inner variables. This divergence, analogous to that encountered by Whitehead in attempting to improve Stokes flow past a sphere (Section 8.3), is indicative of a singular perturbation problem. We treat it in the following section by constructing a complementary outer expansion. Matching will be seen to force a term of relative order A^{-1} into the inner expansion, the situation being analogous to that in boundary-layer theory (Section 7.3).

9.3. Lifting-Line Theory by Matched Asymptotic Expansions

In the outer limit (Fig. 9.1c) the wing shrinks to a line of singularities, which must be solutions of (9.2a). Vortices are the first possibility that

has the proper symmetry in y. Higher multipoles can be disregarded at this stage, because they will prove to be unmatchable according to the principle of minimum singularity. The vortex strength Γ will evidently vanish as $A \to \infty$, and may therefore be tentatively expanded as

$$\Gamma(z; A) \sim A^{-1}\gamma_2(z) + A^{-2}\gamma_3(z) + \cdots \tag{9.7}$$

The bound vortices in the wing must be continued as free vortices following the streamlines downstream to infinity. Henceforth it is a considerable simplification to assume that the angle of attack is small, so that only linear terms in α need be retained. Then the trailing vortices may be taken parallel with the x-axis (Fig. 9.1c). The potential of such an assemblage of vortices is readily calculated using the Biot-Savart law. Thus the outer expansion is found to have the form

$$\phi \sim (x + \alpha y) + \frac{1}{4\pi} A^{-1}\int_{-1}^{1} \frac{y\gamma_2(\zeta)}{y^2 + (z - \zeta)^2}\left[1 + \frac{x}{\sqrt{x^2 + y^2 + (z - \zeta)^2}}\right]d\zeta$$

$$\text{as} \quad A \to \infty \quad \text{with } x, y, z \text{ fixed} \tag{9.8}$$

At this point we make a significant departure from the classical lifting-line theory of Prandtl, and so achieve an essential simplification. Prandtl finds the distribution of circulation $\gamma_2(z)$ by solving an integral equation. However, to the order of accuracy of his theory the circulation may be found directly by matching with the inner solution. This can be done formally, but the result is obvious from the fact that all curves enclosing the same vortex lines have the same circulation (Fig. 9.1). In the inner limit the circulation is given by (9.6). Because this is independent of the size of the circuit, matching with (9.7) gives

$$\gamma_2(z) = 2\pi\alpha h(z) \tag{9.9}$$

That is, to first order the bound vorticity is the circulation about a flat plate of the local chord length in plane flow at the actual angle of attack. In Prandtl's theory the circulation corresponds to a reduced "effective" angle of attack, but the difference is of higher order. Thus the two-term outer expansion (9.8) is found as

$$\phi \sim x + \alpha y + \frac{1}{2}\alpha A^{-1}\int_{-1}^{1} \frac{yh(\zeta)}{y^2 + (z - \zeta)^2}\left[1 + \frac{x}{\sqrt{x^2 + y^2 + (z - \zeta)^2}}\right]d\zeta \tag{9.10a}$$

We now return to the inner problem and seek a second approximation.

In carrying out the inner expansion of (9.10a), meaningless divergent integrals are avoided by first integrating by parts to give

$$\phi \sim x + \alpha y - \tfrac{1}{2}\alpha A^{-1} \int_{-1}^{1} h'(\zeta)\Big[\tan^{-1} \frac{y}{z-\zeta} + \tan^{-1}\frac{y}{x}\,\frac{\sqrt{x^2+y^2+(z-\zeta)^2}}{z-\zeta}\Big]\, d\zeta \tag{9.10b}$$

Then introducing inner variables (9.3) and expanding for large A gives as the two-term inner expansion of the two-term outer expansion for ϕ:

$$\text{2-inner (2-outer) } \phi = A^{-1}\Big[X + \alpha Y - \alpha h(z) \tan^{-1}\frac{Y}{X}\Big] - \tfrac{1}{2}\alpha A^{-2} Y \oint_{-1}^{1} \frac{h'(\zeta)\, d\zeta}{z-\zeta} \tag{9.11}$$

The integral must be interpreted as the Cauchy principal value. It is, remarkably enough, the integral that was encountered in Chapter IV (4.10) in treating thin symmetrical airfoils, and which arises also in other branches of fluid mechanics, including supersonic slender-body theory.

The first term in (9.11) has already been matched with the inner solution (9.5). The second term demands a correction of relative order A^{-1}, so that the inner solution (9.3a) must have the expansion

$$\phi \sim A^{-1}\Phi_1(X, Y, z) + A^{-2}\Phi_2(X, Y, z) + \cdots \quad \text{as} \quad A \to \infty \quad \text{with } X, Y, z \text{ fixed} \tag{9.12}$$

Substituting into the full equation (9.2a) shows that Φ_2 as well as Φ_1 satisfies the two-dimensional Laplace equation in X and Y. Hence (9.11) shows that Φ_2 is simply the result of reducing the angle of attack in the local flat-plate solution from its geometric value α to the effective value

$$\alpha_e(z) = \alpha\Big[1 - \tfrac{1}{2}A^{-1} \oint_{-1}^{1} \frac{h'(\zeta)\, d\zeta}{z-\zeta}\Big] \tag{9.13}$$

This is a familiar result from lifting-line theory. The trailing-vortex system induces downwash velocities in the vicinity of the wing that are constant across the chord at each spanwise station, and so act to decrease the apparent angle of attack of that section. However, we have here reduced the calculation to quadratures by recognizing that for large A the downwash angle is small compared with the geometric angle α, whereas classical lifting-line theory leads to an integral equation because that fact is not exploited. Our result can be extracted as the second step in solving Prandtl's integral equation by iteration.

From the inner solution we have used only the relation (9.6) between the circulation and angle of attack, which is equivalent to the two-dimensional lift-curve slope. Prandtl has suggested replacing the theoretical lift-curve slope by the experimental value, which would account for the effects of thickness and viscosity. This is a practical example of the fact, mentioned in Section 5.4, that the method of matched asymptotic expansions can be applied even when the inner problem is "impossible," and soluble only numerically or experimentally.

9.4. Summary of Third Approximation

The preceding analysis has been continued through one more cycle to obtain the third approximation (Van Dyke, 1964b). Here we outline the features of interest.

Carrying out the 3-term outer expansion of the 2-term inner expansion provides, by the previous physical argument, the correction γ_3 to the vortex strength (9.7). In addition, it shows the appearance at this stage of the next higher singularity in the lifting line. We call this a *divortex*, although it is a dipole with vertical axis, to emphasize its physical interpretation as the x-derivative of a vortex, representing the first moment of the distributed vorticity on the wing. Thus the 3-term outer expansion is found to be (9.10), with h modified by the factor (9.13), plus

$$\tfrac{1}{4}\alpha A^{-2} \frac{y}{x^2+y^2} \frac{\partial}{\partial z} \int_{-1}^{1} h^2(\zeta) \frac{(z-\zeta)\, d\zeta}{\sqrt{x^2+y^2+(z-\zeta)^2}} \tag{9.14}$$

The 3-term inner expansion of this result can be calculated after further integration by parts. One is surprised to find that the anticipated next term of order A^{-3} in the inner expansion (9.12) is preceded by one of order $A^{-3}\log A$. As usual (cf. Section 10.5), the logarithmic term is much the easier of the two to calculate. It requires a further change in the effective angle of attack (9.13), and also straightening by the plate of streamline curvature induced near the wing by the trailing vortex system (Fig. 9.2).

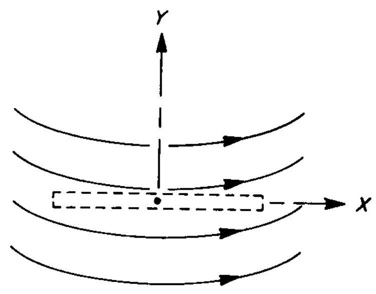

Fig. 9.2. Streamline curvature induced near wing by trailing vortex system.

The nonlogarithmic term involves these and other more complicated local flows, all of which can be found by using complex variables. Then the coefficient of all terms in $\log (x^2 + y^2)^{1/2}$ provides the distribution of circulation or spanwise lift, which is found to be

$$\frac{\Gamma}{\Gamma_\infty} = 1 - \tfrac{1}{2}A^{-1} \oint_{-1}^{1} \frac{h'(\zeta)\,d\zeta}{z-\zeta} + \tfrac{1}{4}A^{-2} \log A(2h'^2 + 3hh'')$$
$$+ \tfrac{1}{4}A^{-2}\Big\{\Big(2 \log \frac{4}{h} - \frac{3}{2}\Big)h'^2 + \Big(3 \log \frac{4}{h} + \frac{1}{2}\Big)hh''$$
$$- 2 \frac{d}{dz} \oint_{-1}^{1} \frac{[\alpha_e(\zeta)/\alpha - 1]Ah(\zeta)}{z-\zeta}\,d\zeta$$
$$+ \frac{1}{2} \frac{d^3}{dz^3} \int_{-1}^{1} h(\zeta)[h(z) + h(\zeta)] \operatorname{sgn}(z-\zeta) \log|z-\zeta|\, d\zeta\Big\} + \cdots \tag{9.15}$$

Here Γ_∞ is the two-dimensional value (9.6), and α_e is given by (9.13). Then according to the Kutta-Joukowski law the lift-curve slope is

$$\frac{dC_L}{d\alpha} = 2\pi \int_0^1 h(z) \frac{\Gamma(z)}{\Gamma_\infty(z)}\, dz \tag{9.16}$$

9.5. Application to Elliptic Wing

An elliptic wing of aspect ratio A (Fig. 9.3) has the half-chord

$$h(z) = \frac{4}{\pi} \sqrt{1 - z^2} \tag{9.17}$$

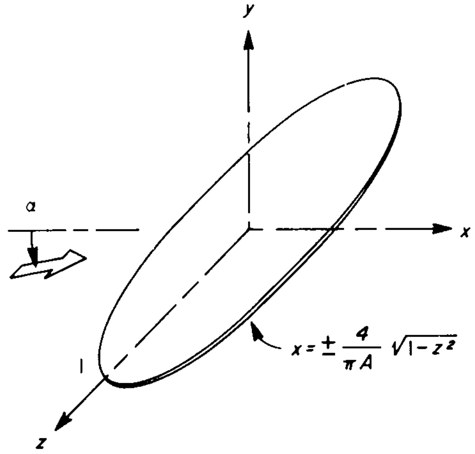

Fig. 9.3. Flat elliptic wing.

The circulation is found from (9.15) as See Note 13

$$\frac{\Gamma}{\Gamma_\infty} = 1 - \frac{2}{A} - \frac{4}{\pi^2}\frac{\log A}{A^2}\frac{3-2z^2}{1-z^2} + \frac{4}{\pi^2}\frac{1}{A^2}\Big[\frac{5}{2} + \pi^2 - \log(1-z^2)$$
$$+ \frac{\log 2}{1-z^2} - \frac{3-2z^2}{1-z^2} \log \frac{\pi}{\sqrt{1-z^2}}\Big] + \cdots \tag{9.18}$$

Integrating this across the span according to (9.16) yields the lift-curve slope quoted as (1.6) in Chapter I. The first two terms constitute our earlier modification (9.1b) of Prandtl's result (9.1a).

Fortunately, this is one of the rare cases where the lifting-surface solution has been calculated. Figure 9.4 shows that Prandtl's solution

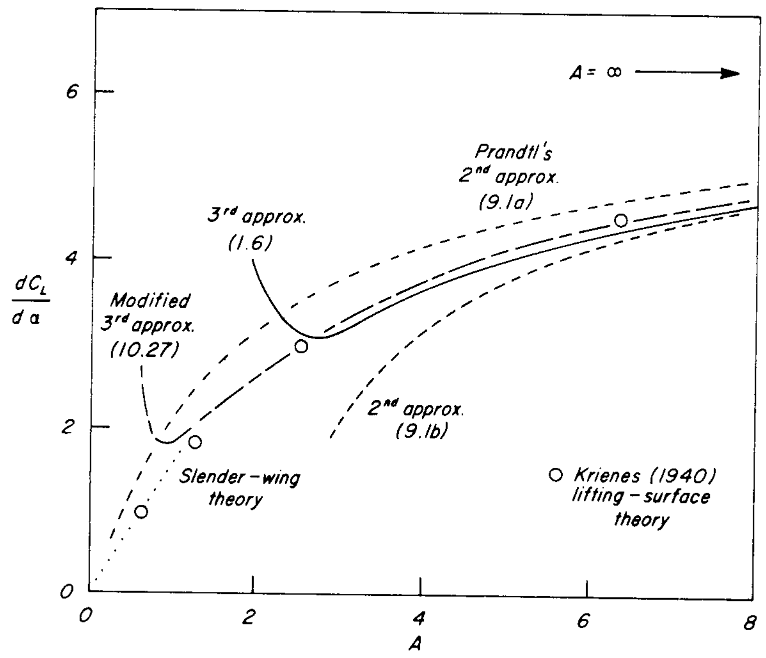

Fig. 9.4. Lift-curve slope of elliptic wing.

has the advantage of vanishing at $A = 0$, though with twice the correct slope according to slender-wing theory. However, our expanded form (9.1b) is actually the more accurate above $A = 4$. Our third approximation is seen to diverge below $A = 3$. Postponement of that catastrophe, shown by the dash-dot curve in Fig. 9.4, is discussed later in Section 10.7.

We have violated the restriction to cusped tips. Consequently, just as in the application of thin-airfoil theory to round noses (Section 4.4) or of boundary-layer theory to sharp leading edges (Chapter VII), the result is not locally valid. We see that (9.18) breaks down when $1 + z$ is

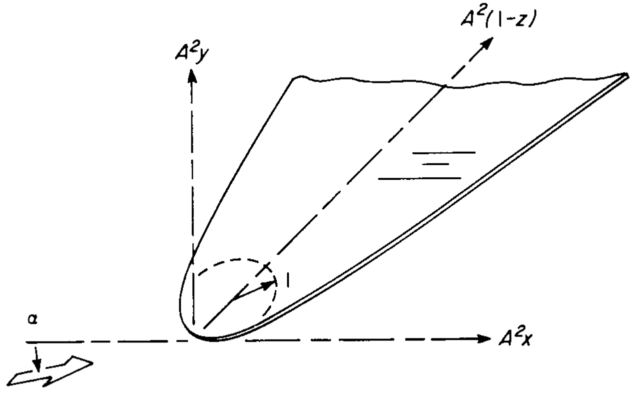

Fig. 9.5. Limiting problem for vicinity of round tip.

of order A^{-2}. At any fixed number of radii from the tip of the planform the flow fails to become plane no matter how great the aspect ratio. Clearly yet another asymptotic expansion is required for that region. The first term would represent flow past a flat semi-infinite plate of parabolic planform (Fig. 9.5), and would be applicable to the tip of any flat wing whose outline is an analytic curve. In this tip solution the original coordinates would all be magnified by a factor A^2.

Still other nonuniformities exist in this complicated problem. It is well known that a vortex sheet tends to roll up, so that our outer solution is not valid far downstream where x is of order A/α. Again, airfoil sections other than the flat plate would ordinarily be treated using thin-airfoil theory for the inner problem, which would lead to the nonuniformities at leading and trailing edges discussed in Chapter IV, and their more complicated counterparts at tips. Nonuniformities would also arise at the root juncture of a swept wing or other discontinuity in planform, at a deflected aileron, and so on. The case of a smoothly swept wing of crescent planform has been analyzed by Thurber (1961) using the method of matched asymptotic expansions. He finds that a logarithmic term then appears in the second approximation.

See Note 13

9.6. Slightly Supersonic Flow past a Slender Circular Cone

For a slender fusiform body in supersonic flow, the familiar linearized theory (e.g., Ward, 1955) provides no information about the strength

of the bow shock wave. That can be found only by retaining some nonlinear terms, and recognizing the singular nature of the perturbation solution. This problem has been treated by both the method of strained coordinates (Lighthill, 1949b) and the method of matched asymptotic expansions (Bulakh, 1961). We apply the former technique to a problem so simple that we can carry the solution one step beyond previous results.

We consider a slender circular cone of semivertex angle ε at zero incidence in a stream sufficiently supersonic that the flow is conical (Fig. 9.6). If the flow is only slightly supersonic, the essential phenomena

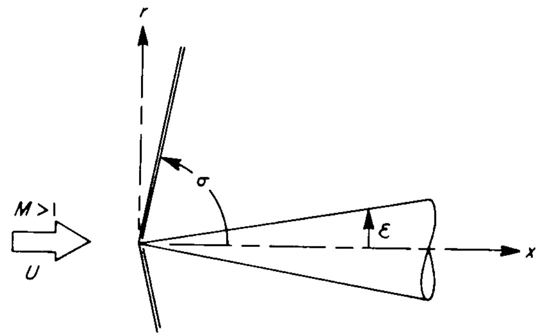

Fig. 9.6. Slightly supersonic flow past slender cone.

are described by the transonic small-disturbance equation (Oswatitsch and Berndt, 1950):

$$\varphi_{rr} + \frac{\varphi_r}{r} - (M^2 - 1)\varphi_{xx} = (\gamma + 1)\varphi_x\varphi_{xx} \tag{9.19a}$$

Here φ is the perturbation velocity potential, such that the velocity vector is U grad$(x + \varphi)$. In this approximation the tangency condition can be linearized and, because the body is smooth, transferred to the axis (Section 3.8) as

$$\lim_{r\to 0} r\varphi_r = \varepsilon^2 x \tag{9.19b}$$

The oblique shock wave relations provide two conditions to be imposed at the unknown location of the bow wave:

$$\left.\begin{aligned} \varphi &= 0 \qquad (9.19\text{c}) \\ -\varphi_x &= \frac{2}{\gamma+1}\,\frac{M^2\sin^2\sigma - 1}{M^2} \qquad (9.19\text{d}) \end{aligned}\right\} \quad \text{at} \quad \frac{r}{x} = \tan\sigma$$

On the surface of the cone the pressure coefficient is given by

$$C_p = -2\varphi_x - \varepsilon^2 \tag{9.20}$$

This problem has been solved numerically by Oswatitsch and Sjödin (1954). We instead proceed analytically, seeking an asymptotic expansion for small ε. In tacitly assuming that the Mach number is fixed, we disregard the transonic nature of the problem; and our solution will consequently be valid only in the upper portion of the transonic regime.

A straightforward perturbation expansion leads to difficulties at the free-stream Mach cone. The perturbation potential has a square-root zero there in the first approximation, which through differentiation introduces singularities into higher approximations. We accordingly introduce a strained conical variable s by setting

$$\frac{1}{x}\varphi(x, r; \varepsilon) \sim \varepsilon^2 f_1(s) + \varepsilon^4 f_2(s) + \varepsilon^6 f_3(s) + \varepsilon^8 f_4(s) + \cdots \tag{9.21a}$$

$$\sqrt{M^2 - 1}\,\frac{r}{x} \sim s - \varepsilon^4 r_3(s) + \varepsilon^6 r_4(s) + \cdots \tag{9.21b}$$

No term of order ε^2 appears in (9.21b), because we shall find that the straining vanishes to that order. For the same reason, the description of the shock wave is taken in the form

$$\sqrt{M^2 - 1}\tan\sigma \sim 1 + k_3\varepsilon^4 + k_4\varepsilon^6 + \cdots \tag{9.22}$$

9.7. Second Approximation and Shock Position

When the expansions (9.21) are substituted into the differential equation (9.19a), terms in ε^2 yield the conventional linearized equation for f_1:

$$(1 - s^2)f_1'' + \frac{f_1'}{s} = 0 \tag{9.23}$$

The solution satisfying the tangency condition (9.19b) and the first shock-wave condition (9.19c) is

$$f_1(s) = -(\operatorname{sech}^{-1} s - \sqrt{1 - s^2}) \tag{9.24}$$

The second shock-wave condition (9.19d) is automatically satisfied, which is the reason that no term of order ε^2 is required in (9.22).

Terms of order ε^4 in the differential equation now give for the second approximation

$$(1 - s^2)f_2'' + \frac{f_2'}{s} = G\frac{\operatorname{sech}^{-1} s}{\sqrt{1 - s^2}} \tag{9.25a}$$

where

$$G = \frac{\gamma + 1}{M^2 - 1} \tag{9.25b}$$

Integrating and imposing the tangency condition and the first shock-wave condition yields

$$f_2(s) = \tfrac{1}{2}G(\operatorname{sech}^{-1} s - \sqrt{1 - s^2}\operatorname{sech}^{-1} s - \sqrt{1 - s^2}) \tag{9.26}$$

This is the transonic small-disturbance form of the second-order solution (Van Dyke, 1952), expressed in terms of a strained variable that is about to be determined.

Terms of order ε^6 in the differential equation now give for the third approximation

$$\begin{aligned}(1 - s^2)f_3'' + \frac{f_3'}{s} = G^2\Big[&\frac{\operatorname{sech}^{-1} s}{1 - s^2} - \frac{\operatorname{sech}^{-1} s}{\sqrt{1 - s^2}} - \frac{1}{2}\frac{1}{\sqrt{1 - s^2}} \\ &- \frac{1}{2}\frac{s^2(\operatorname{sech}^{-1} s)^2}{(1 - s^2)^{3/2}}\Big] + \frac{(1 - s^2)^{3/2}}{s}r_3'' - \frac{\sqrt{1 - s^2}}{s^2}r_3' \\ &+ \frac{1 - 3s^2}{s^3\sqrt{1 - s^2}}r_3\end{aligned} \tag{9.27}$$

It is at this stage that insurmountable difficulties arise in the absence of straining. The first term on the right is singular like $G^2(1 - s^2)^{-1/2}$ at $s = 1$, which would lead to a similar singularity in the velocity. This defect is removed by proper choice of the straining function $r_3(s)$.

The simplest choice, constant straining:

$$r_3(s) = \tfrac{1}{2}G^2 \tag{9.28a}$$

was successfully employed by Lighthill (1949b) to find the position of the shock wave, which is as far as he carried the solution. However, this eliminates the nonuniformity near the shock wave only to introduce another on the axis, which would make it impossible to impose the tangency condition there in the next approximation. This difficulty is avoided by choosing instead the linear straining

$$r_3(s) = \tfrac{1}{2}G^2 s \tag{9.28b}$$

The second shock-wave condition can now be used to find the departure of the shock wave from the free-stream Mach cone. At the shock wave, according to (9.21b), (9.22), and (9.28b)

$$s = 1 + \varepsilon^4[k_3 - r_3(s)] + \cdots = 1 + \varepsilon^4(k_3 - \tfrac{1}{2}G^2) + \cdots \tag{9.29}$$

and substituting into (9.19d) yields

$$\sqrt{2(\tfrac{1}{2}G^2 - k_3)} + G = \frac{4}{G}k_3 \tag{9.30}$$

The solution is

$$k_3 = \tfrac{3}{8}G^2 \tag{9.31}$$

which is the transonic small-disturbance form of the result found by Lighthill (1949b) and Bulakh (1961). This is the extent to which they carried their solution, which applies to a slender cone of any cross section. The following section covers new ground.

9.8. Third Approximation for Pressure on Cone

With the above straining, Eq. (9.27) for the third approximation simplifies to

$$(1-s^2)f_3'' - \frac{f_3'}{s} = G^2\left[\frac{\operatorname{sech}^{-1}s}{1-s^2} - \frac{\operatorname{sech}^{-1}s}{\sqrt{1-s^2}} - \frac{1}{2}\frac{1}{\sqrt{1-s^2}} - \frac{1}{2}\frac{s^2(\operatorname{sech}^{-1}s)^2}{(1-s^2)^{3/2}}\right] \tag{9.32}$$

Integrating and imposing the tangency condition and first shock-wave condition gives

$$f_3(s) = \tfrac{1}{2}G^2\Big[\left(\frac{5}{4} - \log 2\right)\sqrt{1-s^2} + (\log 2 - 1)\operatorname{sech}^{-1}s + \sqrt{1-s^2}\operatorname{sech}^{-1}s - \frac{1}{4}\left(\sqrt{1-s^2} + \frac{1}{\sqrt{1-s^2}}\right)(\operatorname{sech}^{-1}s)^2 + \int_s^1 \frac{\sqrt{1-t^2}}{t}\log\frac{\sqrt{1-t^2}}{t}\,dt\Big] \tag{9.33}$$

The integral appearing here has the properties

$$\int_s^1 \frac{\sqrt{1-t^2}}{t}\log\frac{\sqrt{1-t^2}}{t}\,dt \sim \tfrac{1}{2}\log^2 s - \left(\frac{\pi^2}{12} + \tfrac{1}{2}\log^2 2 - \log 2\right) - \tfrac{1}{4}s^2\log s + O(s^2) \tag{9.34a}$$

$$\sim \tfrac{1}{6}(1-s^2)^{3/2}\log(1-s^2) + O[(1-s^2)^{3/2}] \tag{9.34b}$$

Terms of order ε^8 give the equation for the fourth approximation which, with the right-hand approximated near $s = 1$, becomes

$$(1-s^2)f_4'' + \frac{f_4'}{s} \approx -G^3\left[\left(\frac{3}{4} + 2\frac{r_4}{G^3}\right)\frac{1}{\sqrt{1-s^2}} + \tfrac{1}{4}\log(1-s^2) + \cdots\right] \tag{9.35}$$

Singularities in the right-hand side and hence also in the fourth-order velocity are avoided by choosing the next term in the straining as

$$r_4(s) = -\tfrac{1}{8}G^3 s[3 + \sqrt{1-s^2}\log(1-s^2)] \tag{9.36}$$

The factor s again serves to prevent the introduction of a nonuniformity on the axis. At the shock wave these results give

$$s = 1 - \tfrac{1}{8}G^2\varepsilon^4 + (k_4 - \tfrac{3}{8}G^3)\varepsilon^6 + \cdots \tag{9.37}$$

Then substituting into the second shock-wave condition (9.19d) yields

$$k_4 = -\frac{1}{12}G^3 \tag{9.38}$$

Expressing the results in terms of the original parameters, we find that the shock wave lies at

$$\sqrt{M^2-1}\,\frac{r}{x} \sim 1 - \frac{3}{8}\left[\frac{(\gamma+1)\varepsilon^2}{M^2-1}\right]^2 - \frac{1}{12}\left[\frac{(\gamma+1)\varepsilon^2}{M^2-1}\right]^3 + \cdots \tag{9.39}$$

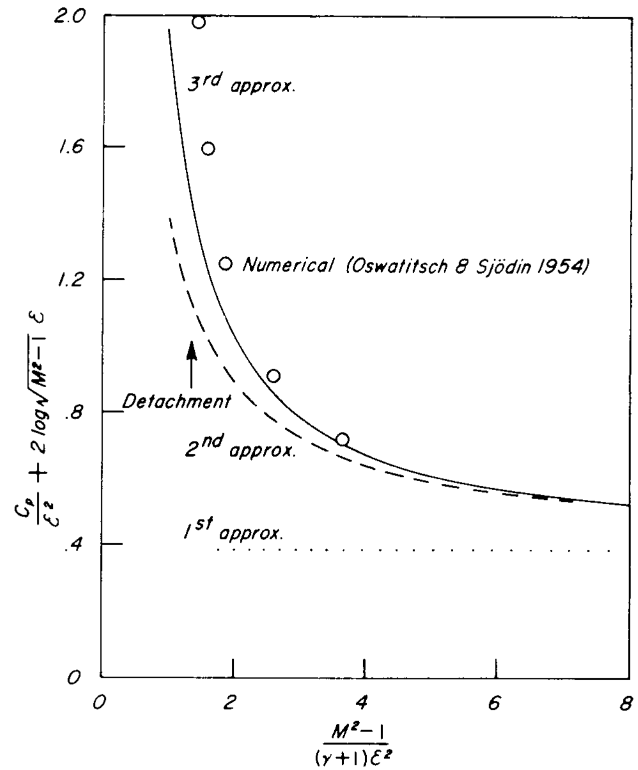

Fig. 9.7. Pressure on slender cone in transonic flow.

The surface pressure coefficient (9.20) can be written in accord with the transonic similarity rule of Oswatitsch and Berndt (1950) as

$$\frac{C_p}{\varepsilon^2} + 2 \log \sqrt{M^2 - 1}\, \varepsilon \sim (2 \log 2 - 1) + \frac{(\gamma + 1)\varepsilon^2}{M^2 - 1} + \left(\frac{\pi^2}{12} - \frac{1}{4}\right)\left[\frac{(\gamma + 1)\varepsilon^2}{M^2 - 1}\right]^2 + \cdots \quad (9.40)$$

As anticipated, these results are asymptotic expansions for large values of the transonic similarity parameter $(\gamma + 1)\varepsilon^2/(M^2 - 1)$. The first three approximations for surface pressure are compared in Fig. 9.7 with the numerical solution of Oswatitsch and Sjödin.

9.9. Hypersonic Flow past Thin Blunted Wedge

It was pointed out in Section 5.3 that slight blunting leads to nonuniformity downstream on a body in inviscid supersonic flow. Away from the nose, the flow is nearly that for the sharp body almost everywhere. At the surface, however, the entropy—because it is constant along streamlines—has the value for a normal rather than an oblique shock wave.

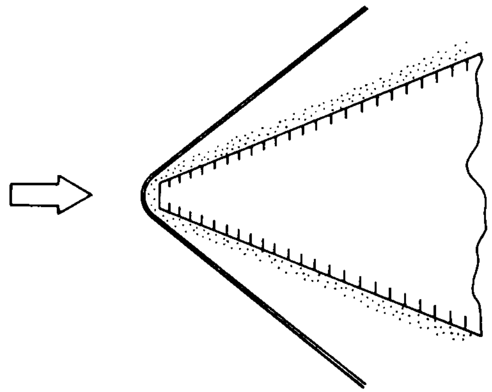

Fig. 9.8. Entropy layer on blunted wedge.

Certain other flow quantities are necessarily also different there. The changes take place across the *entropy layer* (Fig. 9.8), whose thickness is, for plane flow, of the order of the nose radius.

The effect of slight bluntness was first treated as a singular perturbation problem by Guiraud (1958). He considered the direct problem, where the body is given. The analysis is simpler for the inverse problem, where the shock wave is prescribed and the body sought. This approach was carried out for flow of a perfect gas at infinite Mach number by Yakura (1962) using the method of matched asymptotic expansions. We specialize his solution for a blunted wedge to the particular case when

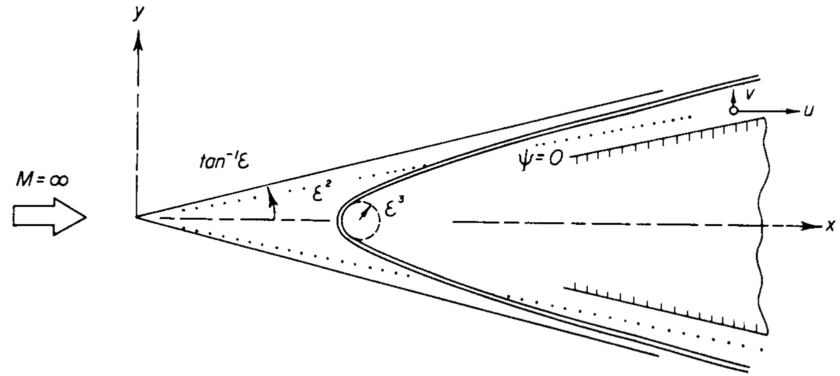

Fig. 9.9. Notation for thin hyperbolic shock wave.

the wedge is thin. Although this simplifies the analysis, it has the remarkable effect of splitting the entropy layer into two layers, so that we need an outer, middle, and inner expansion.

Consider the flow behind a hyperbolic shock wave (Fig. 9.9). Let its asymptotic slope ε be small. We take its nose radius to be ε^3, in order that the first approximation be that for the sharp wedge. Thus we carry out a parameter perturbation for small nose radius, whereas Yakura carried out a coordinate perturbation for large x. The shock wave is described by

$$y^2 = \varepsilon^2 x^2 - \varepsilon^4 \quad (9.41)$$

In an inverse problem the body is most conveniently found from the vanishing of the stream function ψ. We introduce it in the usual way for compressible flow by setting

$$d\psi = \rho u\, dy - \rho v\, dx \quad (9.42)$$

The conservation equations are

$$\begin{aligned} &\text{continuity:} && (\rho u)_x + (\rho v)_y = 0 && (9.43a)\\ &x\text{-momentum:} && \rho(u u_x + v u_y) + p_x = 0 && (9.43b)\\ &y\text{-momentum:} && \rho(u v_x + v v_y) + p_y = 0 && (9.43c)\\ &\text{entropy:} && u(p/\rho^\gamma)_x + v(p/\rho^\gamma)_y = 0 && (9.43d)\end{aligned}$$

The last of these expresses the fact that entropy is constant along streamlines between shock waves, which is equivalent to conservation of energy. It is useful to exploit this property by taking the stream function as an independent variable, reversing the roles of y and ψ by applying the von Mises transformation of boundary-layer theory. Then the differential equations (9.43) become

$$\text{streamline slope:} \qquad \frac{\partial y}{\partial x} = \frac{v}{u} \tag{9.44a}$$

$$\text{continuity:} \qquad \frac{\partial y}{\partial \psi} = \frac{1}{\rho u} \tag{9.44b}$$

$$\text{momentum normal to streamline:} \qquad \frac{\partial v}{\partial x} + \frac{\partial p}{\partial \psi} = 0 \tag{9.44c}$$

$$\text{Bernoulli integral:} \qquad u^2 + v^2 + \frac{2\gamma}{\gamma - 1}\frac{p}{\rho} = 1 \tag{9.44d}$$

$$\text{entropy integral:} \qquad \frac{p}{\rho^\gamma} = f(\psi) \tag{9.44e}$$

Let the flow variables be made dimensionless by referring velocities and density to their free-stream values U and ρ_∞, and pressure to $\rho_\infty U^2$. This leaves the preceding equations unchanged. Then because the slope of the shock wave is

$$\frac{dy}{dx} = \frac{\varepsilon x}{\sqrt{x^2 - \varepsilon^2}} \tag{9.45}$$

the Rankine-Hugoniot relations provide the initial conditions

$$\left.\begin{aligned} p &= \frac{2}{\gamma+1}\varepsilon^2 \frac{x^2}{(1+\varepsilon^2)x^2 - \varepsilon^2} \\ \rho &= \frac{\gamma+1}{\gamma-1} \\ u &= 1 - \frac{2}{\gamma+1}\varepsilon^2 \frac{x^2}{(1+\varepsilon^2)x^2 - \varepsilon^2} \\ v &= \frac{2}{\gamma+1}\varepsilon \frac{x\sqrt{x^2-\varepsilon^2}}{(1+\varepsilon^2)x^2 - \varepsilon^2} \\ y &= \varepsilon\sqrt{x^2 - \varepsilon^2} \end{aligned}\right\} \quad \text{at} \quad \psi = \varepsilon\sqrt{x^2 - \varepsilon^2} \tag{9.46}$$

Hence the entropy integral (9.44e) is evaluated at the shock wave as

$$\frac{p}{\rho^\gamma} = \frac{2}{\gamma+1}\left(\frac{\gamma-1}{\gamma+1}\right)^\gamma \varepsilon^2 \frac{\psi^2 + \varepsilon^4}{(1+\varepsilon^2)\psi^2 + \varepsilon^6} \tag{9.44e$'$}$$

9.10. Small-Disturbance Solution for Blunted Wedge

As the perturbation parameter ε vanishes, the above problem reduces to the hypersonic small-disturbance problem for a sharp wedge (Hayes and Probstein, 1959, p. 47). The initial conditions (9.46) suggest improving upon that basic solution by expanding in powers of ε^2. We therefore make the conventional expansion of hypersonic small-disturbance theory (Hayes and Probstein, 1959, Chapter II), setting

$$u \sim 1 + \varepsilon^2 u_1(x, \psi_1) + \varepsilon^4 u_2(x, \psi_1) + \cdots \tag{9.47a}$$

$$v \sim \varepsilon v_1(x, \psi_1) + \varepsilon^3 v_2(x, \psi_1) + \cdots \tag{9.47b}$$

$$p \sim \varepsilon^2 p_1(x, \psi_1) + \varepsilon^4 p_2(x, \psi_1) + \cdots \tag{9.47c}$$

$$\rho \sim \rho_1(x, \psi_1) + \varepsilon^2 \rho_2(x, \psi_1) + \cdots \tag{9.47d}$$

$$y \sim \varepsilon y_1(x, \psi_1) + \varepsilon^3 y_2(x, \psi_1) + \cdots \tag{9.47e}$$

Here

$$\psi_1 \equiv \frac{\psi}{\varepsilon} \tag{9.48}$$

is the stream function referred to a typical thickness of the shock layer for $x = O(1)$.

Substituting these expansions into the full problem (9.44) and (9.46) and equating like powers of ε gives for the first approximation a nonlinear system whose solution is simply that for the sharp wedge:

$$\begin{gathered} p_1 = -u_1 = v_1 = \frac{2}{\gamma+1}, \\ \rho_1 = \frac{\gamma+1}{\gamma-1}, \qquad y_1 = \frac{2x + (\gamma-1)\psi_1}{\gamma+1} \end{gathered} \tag{9.49}$$

The linear equations for the second approximation can also be solved in closed form. Our present purpose is served, however, by noting that the entropy integral (9.44e$'$) gives for the second approximation

$$\frac{p_2}{p_1} - \gamma\frac{\rho_2}{\rho_1} = \frac{1}{\psi_1^2} - 1 \tag{9.50}$$

Thus there is a singularity at $\psi_1 = 0$. One finds that the pressure is regular there, so that the density is singular at the surface of the body like $1/\psi_1^2$. Likewise v is regular, but y is singular like $1/\psi_1$ and u like $1/\psi_1^2$. These nonuniformities are compounded in the third and higher approximations.

9.11. Middle Expansion for Entropy Layer

The straightforward small-disturbance expansion breaks down near the surface because the solution for the sharp wedge is not a valid first approximation in the entropy layer. We treat the nonuniformity by the method of matched asymptotic expansions.

Because the nonuniformity occurs along a line, as in boundary-layer theory, only the normal coordinate ψ_1 is to be magnified. According to (9.47d), (9.49), and (9.50) the outer expansion of the density behaves for small ψ_1 like

$$\rho \approx \frac{\gamma+1}{\gamma-1}\left(1 - \frac{\varepsilon^2}{\gamma\psi_1^{\,2}} + \cdots\right) \tag{9.51}$$

This suggests introducing the new independent variable

$$\bar{\psi} \equiv \frac{\psi_1}{\varepsilon} = \frac{\psi}{\varepsilon^2} \tag{9.52}$$

We call this the *middle variable*, because still another magnification will be required to reach the surface of the body.

Comparison with the outer expansion suggests a middle expansion of the form

$$u \sim 1 + \varepsilon^2\bar{u}_1(x,\bar{\psi}) + \varepsilon^4\bar{u}_2(x,\bar{\psi}) + \cdots \tag{9.53a}$$

$$v \sim \varepsilon\bar{v}_1(x,\bar{\psi}) + \varepsilon^3\bar{v}_2(x,\bar{\psi}) + \cdots \tag{9.53b}$$

$$p \sim \varepsilon^2\bar{p}_1(x,\bar{\psi}) + \varepsilon^4\bar{p}_2(x,\bar{\psi}) + \cdots \tag{9.53c}$$

$$\rho \sim \bar{\rho}_1(x,\bar{\psi}) + \varepsilon^2\bar{\rho}_2(x,\bar{\psi}) + \cdots \tag{9.53d}$$

$$y \sim \varepsilon\bar{y}_0(x,\bar{\psi}) + \varepsilon^2\bar{y}_1(x,\bar{\psi}) + \varepsilon^3\bar{y}_2(x,\bar{\psi}) + \cdots \tag{9.53e}$$

Substituting into the full equations (9.44), and matching with the leading terms of the outer expansion (9.47) according to the asymptotic matching principle (5.24) gives, for the first approximation,

$$\frac{\partial\bar{y}_0}{\partial\bar{\psi}} = 0, \qquad \bar{y}_0(x,\infty) = \frac{2}{\gamma+1}x \tag{9.54a}$$

$$\bar{v}_1 = \frac{\partial\bar{y}_0}{\partial x}, \qquad \bar{v}_1(x,\infty) = \frac{2}{\gamma+1} \tag{9.54b}$$

$$\frac{\partial\bar{p}_1}{\partial\bar{\psi}} = 0, \qquad \bar{p}_1(x,\infty) = \frac{2}{\gamma+1} \tag{9.54c}$$

$$\frac{\bar{p}_1}{\bar{\rho}_1^{\,\gamma}} = \frac{2}{\gamma+1}\left(\frac{\gamma-1}{\gamma+1}\right)^{\gamma}\frac{1+\bar{\psi}^2}{\bar{\psi}^2}, \qquad \bar{\rho}_1(x,\infty) = \frac{\gamma+1}{\gamma-1} \tag{9.54d}$$

$$2\bar{u}_1 + \bar{v}_1^{\,2} + \frac{2\gamma}{\gamma-1}\frac{\bar{p}_1}{\bar{\rho}_1} = 0, \qquad \bar{u}_1(x,\infty) = -\frac{2}{\gamma+1} \tag{9.54e}$$

$$\frac{\partial\bar{y}_1}{\partial\bar{\psi}} = \frac{1}{\bar{\rho}_1}, \qquad \bar{y}_1(x,\bar{\psi}) = \frac{\gamma-1}{\gamma+1}\bar{\psi} \quad \text{as} \quad \bar{\psi}\to\infty \tag{9.54f}$$

These can be solved in succession, giving

$$\begin{aligned}
\bar{y}_0 &= \frac{2}{\gamma+1}x, \qquad \bar{v}_1 = \frac{2}{\gamma+1} \\
\bar{p}_1 &= \frac{2}{\gamma+1}, \qquad \bar{\rho}_1 = \frac{\gamma+1}{\gamma-1}\left(\frac{\bar{\psi}^2}{1+\bar{\psi}^2}\right)^{1/\gamma} \\
\bar{u}_1 &= -\frac{2}{(\gamma+1)^2} - \frac{2\gamma}{(\gamma+1)^2}\left(\frac{1+\bar{\psi}^2}{\bar{\psi}^2}\right)^{1/\gamma} \\
\bar{y}_1 &= \frac{\gamma-1}{\gamma+1}\left\{\bar{\psi} - \int_{\bar{\psi}}^{\infty}\left[\left(\frac{1+t^2}{t^2}\right)^{1/\gamma} - 1\right]dt\right\}
\end{aligned} \tag{9.55}$$

This expansion too is invalid at the surface of the body, where the velocity component u becomes infinite and the density is zero in the first approximation. For the second approximation the entropy integral (9.44e′) gives

$$\gamma\frac{\bar{\rho}_2}{\bar{\rho}_1} = \frac{1}{\bar{\psi}^2} + 1 + \frac{\bar{p}_2}{\bar{p}_1} \tag{9.56}$$

Again it can be shown that $\bar{p}_2$ is regular; hence, in view of (9.55), $\bar{\rho}_2$ is singular like $\bar{\psi}^{-(2-2/\gamma)}$.

9.12. Inner Expansion for Entropy Layer

The nonuniformity of the middle expansion shows that a third asymptotic expansion is required to complete the solution. According to (9.53d), (9.55), and (9.56), the middle expansion of the density behaves for small $\bar{\psi}$ like

$$\rho \sim \frac{\gamma+1}{\gamma-1}\bar{\psi}^{2/\gamma}\left(1 + \frac{\varepsilon^2}{\gamma\bar{\psi}^2} + \cdots\right) \tag{9.57}$$

This suggests introducing the new *inner variable*

$$\Psi \equiv \frac{\bar{\psi}}{\varepsilon} = \frac{\psi}{\varepsilon^3} \tag{9.58}$$

which is the stream function normalized with respect to the nose radius of the shock wave.

Comparison with the middle expansion suggests an inner expansion of the form

$$u \sim 1 + \varepsilon^{2-2/\gamma} U_1(x, \Psi) + \cdots \tag{9.59a}$$

$$v \sim \varepsilon V_1(x, \Psi) + \cdots \tag{9.59b}$$

$$p \sim \varepsilon^2 P_1(x, \Psi) + \cdots \tag{9.59c}$$

$$\rho \sim \varepsilon^{2/\gamma} R_1(x, \Psi) + \cdots \tag{9.59d}$$

$$y \sim \varepsilon Y_0(x, \Psi) + \varepsilon^{3-2/\gamma} Y_1(x, \Psi) + \cdots \tag{9.59e}$$

Substituting into the full equations and matching with the middle expansion yields

$$\frac{\partial Y_0}{\partial \Psi} = 0, \qquad Y_0(x, \infty) = \frac{2}{\gamma + 1} x \tag{9.60a}$$

$$\frac{\partial P_1}{\partial \Psi} = 0, \qquad P_1(x, \infty) = \frac{2}{\gamma + 1} \tag{9.60b}$$

$$\frac{P_1}{R_1^{\gamma}} = \frac{2}{\gamma + 1}\left(\frac{\gamma - 1}{\gamma + 1}\right)^{\gamma} \frac{1}{1 + \Psi^2}, \qquad R_1(x, \Psi) \sim \frac{\gamma + 1}{\gamma - 1} \Psi^{2/\gamma} \tag{9.60c}$$

$$U_1 = -\frac{\gamma}{\gamma - 1} \frac{P_1}{R_1}, \qquad U_1(x, \Psi) \sim -\frac{2\gamma}{(\gamma + 1)^2} \Psi^{-2/\gamma} \tag{9.60d}$$

$$\frac{\partial Y_1}{\partial \Psi} = \frac{1}{R_1}, \qquad Y_1(x, \Psi) \sim -\frac{\gamma - 1}{\gamma + 1} \int_{\Psi}^{\infty} \frac{dt}{t^{2/\gamma}} \tag{9.60e}$$

These equations can be integrated in succession to find

$$Y_0 = \frac{2}{\gamma + 1} x, \qquad R_1 = \frac{\gamma + 1}{\gamma - 1}(1 + \Psi^2)^{1/\gamma}$$

$$P_1 = \frac{2}{\gamma + 1}, \qquad U_1 = -\frac{2\gamma}{(\gamma + 1)^2} \frac{1}{(1 + \Psi^2)^{1/\gamma}} \tag{9.61}$$

$$Y_1 = -\frac{\gamma - 1}{\gamma + 1} \int_{\Psi}^{\infty} \frac{dt}{(1 + t^2)^{1/\gamma}}$$

This last expansion is valid at the surface of the body. In particular, it gives the asymptotic shape of the body that supports the hyperbolic shock wave as

$$y \sim \varepsilon\left[\frac{2}{\gamma + 1} x - \frac{\gamma - 1}{\gamma + 1} \varepsilon^{2-2/\gamma} \int_0^{\infty} \frac{dt}{(1 + t^2)^{1/\gamma}} + \cdots\right]$$

$$= \varepsilon\left[\frac{2}{\gamma + 1} x - \frac{\gamma - 1}{\gamma + 1} \frac{\sqrt{\pi}}{2} \frac{\Gamma(\gamma^{-1} - \frac{1}{2})}{\Gamma(\gamma^{-1})} \varepsilon^{2-2/\gamma} + \cdots\right] \tag{9.62}$$

where Γ is the gamma function. The first term is the result for the sharp wedge, indicated by a dotted line in Fig. 9.9. The second term is the asymptotic value of the displacement thickness of the entropy layer. As in a viscous boundary layer, the mass flux is reduced because the entropy, and hence the temperature, is increased by blunting, and the density correspondingly reduced. Hence in the direct problem (Fig. 9.10a) the shock wave is forced away from the body downstream

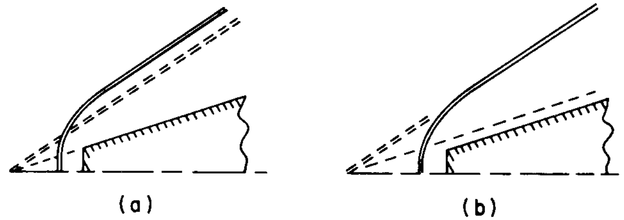

Fig. 9.10. Displacement effect of blunting. (a) Direct problem. (b) Inverse problem.

even though it moves closer near the nose; in the inverse problem (Fig. 9.10b) the body must move instead. Another similarity between entropy layers and viscous boundary layers is evident from (9.54c) and (9.60b): To a first approximation the pressure is constant across the layer.

In analyzing the nonslender wedge, Yakura (1962) has calculated the next approximation, which adds a term in x^{-1} to (9.62). This suffices to describe the body accurately up to within a few radii of its nose. His analysis requires only the outer and inner expansions. Our middle expansion is introduced by the double limit process (cf. Section 5.3) in which the slope and nose radius vanish simultaneously. Fig. 9.11 indicates how this produces the three disparate lengths that characterize the three expansions, where we have tacitly assumed L to be of order unity.

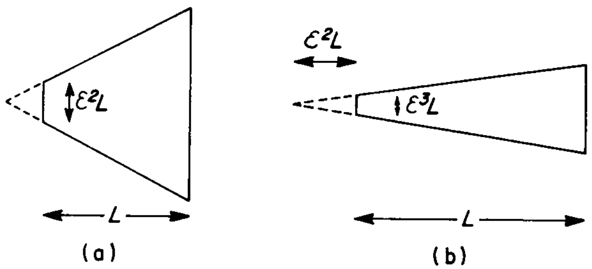

Fig. 9.11. Disparate reference lengths for blunted wedges. (a) Thick wedge. (b) Thin wedge.

9.13. Composite Expansions for Blunted Wedge

In order to display the variation of flow quantities throughout the disturbed region between the shock wave and body, we want to combine the separate expansions into a single composite expansion. This provides a useful illustration of the technique of forming a composite expansion from more than two components (cf. Exercise 5.4).

Consider first the density. Applying the multiplicative rule (5.34) to the middle and inner solutions yields

$$\rho \sim \frac{\gamma+1}{\gamma-1}\left(\frac{\psi^2+\varepsilon^6}{\psi^2+\varepsilon^4}\right)^{1/\gamma} \tag{9.63}$$

which is valid in both subdivisions of the entropy layer. It is clear how this expression assumes different forms in the middle and inner limits. Repeating the process to combine this with the outer solution leaves the result unchanged. It is therefore the desired uniform approximation, valid in all three regions.

If instead we apply the additive rule (5.32), the uniform approximation is found as

$$\rho \sim \frac{\gamma+1}{\gamma-1}\left[\left(\frac{\psi^2}{\psi^2+\varepsilon^4}\right)^{1/\gamma} + \left(\frac{\psi^2+\varepsilon^6}{\varepsilon^4}\right)^{1/\gamma} - \left(\frac{\psi^2}{\varepsilon^4}\right)^{1/\gamma}\right] \tag{9.64}$$

Although this is equivalent, the previous form would be preferred for its simplicity. It also corresponds to the result of Yakura for the thick wedge.

For the ordinate y, our three approximations may be written as

outer: $$y \sim \frac{2}{\gamma+1}\varepsilon x + \frac{\gamma-1}{\gamma+1}\psi \tag{9.65a}$$

middle: $$y \sim \frac{2}{\gamma+1}\varepsilon x + \frac{\gamma-1}{\gamma+1}\left\{\psi - \int_\psi^\infty \left[\left(\frac{t^2+\varepsilon^4}{t^2}\right)^{1/\gamma} - 1\right] dt\right\} \tag{9.65b}$$

inner: $$y \sim \frac{2}{\gamma+1}\varepsilon x - \frac{\gamma-1}{\gamma+1}\int_\psi^\infty \left(\frac{\varepsilon^4}{t^2+\varepsilon^6}\right)^{1/\gamma} dt \tag{9.65c}$$

The result of either additive or multiplicative composition is unnecessarily complicated. A simpler form is found by inspection as

See Note 6

$$y \sim \frac{2}{\gamma+1}\varepsilon x + \frac{\gamma-1}{\gamma+1}\left\{\psi - \int_\psi^\infty \left[\left(\frac{t^2+\varepsilon^4}{t^2+\varepsilon^6}\right)^{1/\gamma} - 1\right] dt\right\} \tag{9.66}$$

and this corresponds to the result that Yakura found by additive composition of his two expansions.

Figure 9.12 shows the distribution of density between the shock wave and body given by (9.63) and (9.66) at 24.5 radii downstream from the nose of a hyperbolic shock wave with $\varepsilon = 0.437$, corresponding to a wedge

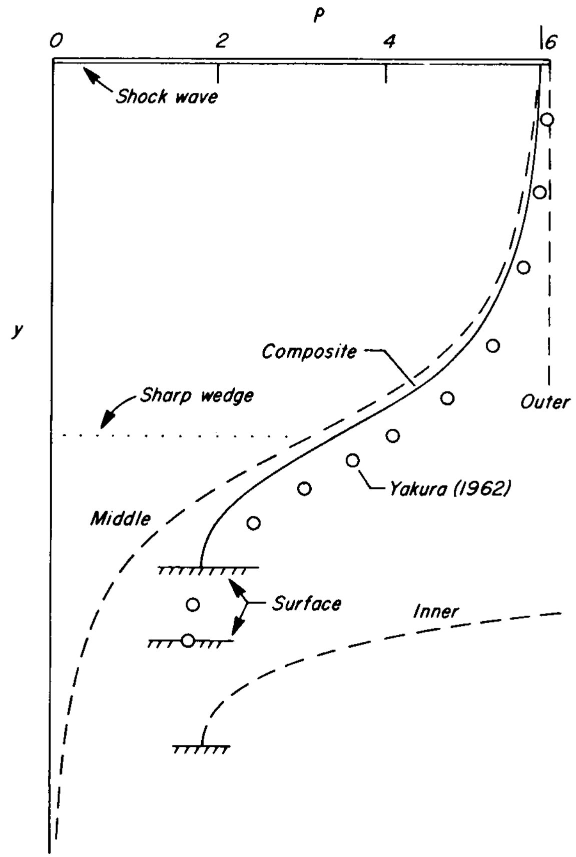

Fig. 9.12. Density distribution at 24.5 shock radii downstream on 20° wedge, $M = \infty$, $\gamma = 7/5$.

of 20-degree semivertex angle. Also shown are the outer, middle, and inner approximations, and the result of Yakura in which the wedge is not assumed to be thin. The discrepancies in surface location indicate the inaccuracy arising from such a large value of ε.

Yakura (1962) has applied the method of matched asymptotic expansions also to the axisymmetric problems of the blunted cone that supports a hyperboloidal shock wave, and the body that produces a paraboloidal shock wave at $M = \infty$. The latter problem has been treated with equal success by Sychev (1962) using the method of strained coordinates. However, it appears that the solution for the blunted wedge cannot be found by straining the coordinates.

EXERCISES

9.1. *Elongated nonlifting body.* As a model of thickness effects for a wing of high aspect ratio, consider incompressible potential flow normal to the axis of a slender smooth body of revolution (Fig. 9.13). Show that to a first approxi-

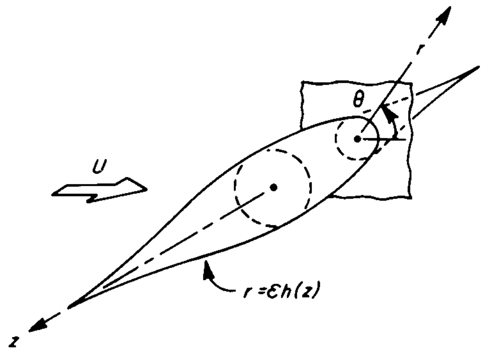

Fig. 9.13. Flow normal to slender body of revolution.

mation the flow is plane at each section, but that straightforward iteration leads to a difficulty analogous to Whitehead's (Chapter VIII). Find the next approximation using the method of matched asymptotic expansions. Apply your solution to the ellipsoid of revolution, checking with the rule of Munk (1929) that the surface speed on any ellipsoid is the projection of the maximum velocity onto the tangent plane. Apply your solution also to the pointed parabolic spindle. Explain why no correction is necessary at the tips of the ellipsoid. Devise and apply a correction for the tips of the spindle.

9.2. *Lifting wing with sharp tips.* Calculate from (9.15) and (9.16) the second-order spanwise loading and lift-curve slope for the wing of lenticular planform bounded by two parabolic arcs. Devise a correction that renders the solution uniformly valid near the tips. Discuss the corresponding correction for the middle of a diamond planform.

9.3. *Near-equilibrium flow over a wavy wall.* Consider steady plane flow of an inviscid gas in vibrational or chemical nonequilibrium. At an equilibrium

Mach number of $\sqrt{2}$, the linearized equation for the perturbation velocity potential is (Vincenti, 1959) See Note 3

$$\frac{\partial^2\phi}{\partial y^2} - \frac{\partial^2\phi}{\partial x^2} + \varepsilon \frac{\partial}{dx}\left(\frac{\partial^2\phi}{\partial y^2} - A\frac{\partial^2\phi}{dx^2}\right) = 0$$

where $0 < A < 1$, and ε is proportional to the relaxation time. Iterate upon the familiar result for equilibrium flow ($\varepsilon = 0$) over the wavy wall $y = \tau \sin x$ to find the correction of order $\varepsilon\tau$. It is helpful to use the oblique coordinates $\xi = x - y$ and $\eta = y$ (cf. Section 6.4). Correct the result in its region of nonuniformity far above the wall. Form a uniformly valid first approximation. Compare with Vincenti's solution.

Chapter X

OTHER ASPECTS OF PERTURBATION THEORY

10.1. Introduction

This last chapter is devoted to various special topics in perturbation theory. We first consider several methods, other than the two standard ones employed in previous chapters, for dealing with singular perturbation problems. Next, we discuss the curious role of logarithms in perturbation expansions. We then examine in some detail the fascinating question of extracting accurate results from a divergent or slowly convergent series. Finally, we describe ways of joining two different perturbation expansions in cases where they cannot be matched in the sense of the method of matched asymptotic expansions.

10.2. The Method of Composite Equations

We saw in Chapter VIII how Oseen corrected the nonuniformity in Stokes' approximation for flow at low Reynolds numbers by partially including the neglected convective terms. The same idea can be applied to any singular perturbation problem in which the nonuniformity arises from the differential equations. One would proceed as follows:

(a) Identify the terms in the differential equations whose neglect in the straightforward approximation is responsible for the nonuniformity.

(b) Approximate those terms insofar as possible while retaining their essential character in the region of nonuniformity.

(c) Try to solve the resulting *composite equations*.

This *ad hoc* procedure has been successfully applied also to the position of shock waves by Lighthill (1948), and to the vortical layer on an inclined cone by Cheng (1962).

However, the method of composite equations seems always to be inferior to the two more systematic methods discussed earlier. Its disadvantages are apparent in flow at low Reynolds numbers (Chapter VIII), where the inner and outer expansions are relatively simple compared with the composite solution of the Oseen equations. Thus it has been superseded in the shock-wave problem by the method of strained coordinates (Section 9.6; Lighthill, 1949b), and in the vortical-layer problem by the method of matched asymptotic expansions (Munson, 1964).

The shortcomings of the method of composite equations may be illustrated by reconsidering the boundary layer on a semi-infinite flat plate (Chapter VII). We profit from experience (Section 7.14) and use parabolic coordinates. The Navier-Stokes equations give for the stream function the equation of Exercise 8.1. The straightforward approximation consists in setting $\nu = 0$, which yields

$$\left(\psi_\xi \frac{\partial}{\partial\eta} - \psi_\eta \frac{\partial}{\partial\xi}\right) \frac{\psi_{\xi\xi} + \psi_{\eta\eta}}{\xi^2 + \eta^2} = 0 \tag{10.1}$$

This is invalid in the boundary layer, where applying Prandtl's procedure to the full equation yields instead

$$\frac{1}{\xi^2}\left[\nu\psi_{\eta\eta\eta\eta} + \psi_\xi\psi_{\eta\eta\eta} - \psi_\eta\psi_{\xi\eta\eta} + \frac{2}{\xi}\psi_\eta\psi_{\eta\eta}\right] = 0 \tag{10.2}$$

We now seek a composite equation that includes both of these approximations. Only the first term in (10.2) is absent from (10.1). Adding it to (10.1) yields as a composite equation

$$\frac{\nu}{\xi^2}\psi_{\eta\eta\eta\eta} + \left(\psi_\xi \frac{\partial}{\partial\eta} - \psi_\eta \frac{\partial}{\partial\xi}\right) \frac{\psi_{\xi\xi} + \psi_{\eta\eta}}{\xi^2 + \eta^2} = 0 \tag{10.3}$$

Because our coordinates are optimal for this problem (Section 7.13), we might suppose that the appropriate solution of this equation is Blasius' solution expressed in parabolic coordinates:

$$\psi(\xi, \eta; \nu) = \sqrt{\nu}\xi f\left(\frac{\eta}{\sqrt{\nu}}\right) \tag{10.4}$$

However, trial shows that this is is not a solution. In fact, no simple solution exists. In tackling simultaneously the difficulties of the inner and outer regions, we have set ourselves an intractable problem.

Of course, the composite equation is not unique. To our form (10.3) may be added any of the neglected terms in the full equation, and any

multiple of the potential equation. Thus, knowing the solution (10.4), we can construct an unlimited number of alternative composite equations that it does satisfy, one of the simplest being

$$\nu\left[\xi^2\psi_{\eta\eta\eta\eta} - 2\eta\frac{\partial}{\partial\eta}(\psi_{\xi\xi} + \psi_{\eta\eta})\right] + \left[\xi^2\left(\psi_\xi\frac{\partial}{\partial\eta} - \psi_\eta\frac{\partial}{\partial\xi}\right)\right.$$
$$\left. + 2(\xi\psi_\eta - \eta\psi_\xi)\right](\psi_{\xi\xi} + \psi_{\eta\eta}) = 0 \tag{10.5}$$

But surely no amount of insight would have suggested this choice.

10.3. The Method of Composite Expansions

A more promising method of directly obtaining a uniformly valid solution is to substitute an assumed composite expansion (cf. Section 5.4). Latta (1951) has shown that one can often deduce the required form of the expansion from an examination of the inner ("boundary-layer") solution. This provides a finite number of special functions, which are taken as the basis for the expansion.

We illustrate this method for Friedrichs' model problem (5.1). The inner solution (5.6b) is found to involve the function $e^{-x/\varepsilon}$. Because this reproduces itself upon differentiation, no other special functions are required. Latta therefore assumes a composite expansion in the form

$$f(x; \varepsilon) \sim [f_1(x) + \varepsilon f_2(x) + \cdots] + e^{-x/\varepsilon}[h_1(x) + \varepsilon h_2(x) + \cdots] \tag{10.6}$$

Substituting into (5.1) and collecting like powers of ε and factors of $e^{-x/\varepsilon}$ yields

$$f_1' = a, \qquad h_1' = 0, \qquad f_1(0) + h_1(0) = 0, \qquad f_1(1) = 1 \tag{10.7a}$$

$$f_m' = -f_{m-1}'' = 0, \qquad h_m' = h_{m-1}'' = 0, \qquad f_m(0) + h_m(0) = 0, \qquad f_m(1) = 0, \qquad m \geqslant 2 \tag{10.7b}$$

Solving these gives $f_1 = (1 - a) + ax$, $h_1 = -(1 - a)$, and $f_m = h_m = 0$. Hence the solution is

$$f(x; \varepsilon) \sim (1 - a)(1 - e^{-x/\varepsilon}) + ax \tag{10.8}$$

This result is supposed to be uniformly valid in the interval of interest $0 \leqslant x \leqslant 1$, with an error smaller than any power of ε. This is seen to be true by comparison with the exact solution (5.2).

In more complicated problems the inner solution, together with its derivatives, may suggest more than one rapidly varying special function. For example, if we consider the linearized Oseen equation (8.16) in Cartesian coordinates for a semi-infinite flat plate, the boundary-layer solution contains the complementary error function $\operatorname{erfc}(y/2R^{-1/2}x^{1/2})$; and we must also include its derivative $\exp(-y^2/4R^{-1}x)$, higher derivatives giving nothing new. Also, it may be necessary to generalize the argument of the special functions, allowing it to be a smooth function of all the coordinates that is to be determined in the course of the analysis. As a result of these two modifications, the composite expansion for the stream function in Oseen flow past the flat plate is taken in the form

$$\begin{aligned}\psi(x, y; R) \sim &[f_1(x, y) + R^{-1/2}f_2(x, y) + \cdots] \\ &+ \operatorname{erfc}[g(x, y)/R^{-1}]^{1/2}[h_1(x, y) + R^{-1/2}h_2(x, y) + \cdots] \\ &+ \exp[g(x, y)/R^{-1}][k_1(x, y) + R^{-1/2}k_2(x, y) + \cdots] \end{aligned} \tag{10.9}$$

The change of argument permitted by the function g is essential in this case, whereas it was unnecessary in the previous example. In fact, one finds that $g(x, y)$ must be $\frac{1}{2}[(x^2 + y^2)^{1/2} - x]$, $\frac{1}{2}$ the square of the parabolic coordinate η, which leads naturally to the optimal coordinates of Kaplun (Section 7.13). The reader can complete the solution, or see Latta (1951) for details.

Further complications may arise, particularly in nonlinear problems. In the model problem of Section 6.2, the rapidly varying functions suggested by the inner solution (6.18) and its derivatives are infinite in number. Also, examination of the inner solution does not always indicate the correct form of the special functions.

10.4. The Method of Multiple Scales

See Note 14

The difficulties just mentioned can be avoided by assuming a more general form for the composite expansion. As discussed in Section 5.3, a perturbation solution is singular because it involves two disparate length scales for one of the coordinates. Accordingly, Cochran (1962) and Mahony (1962) suppose that the solution depends upon that coordinate separately in each of its two scales. That is, the sensitive coordinate is replaced by a pair of coordinates, thus increasing the number of independent variables. One can then assume a conventional asymptotic expansion. A similar idea has been advanced by Cole and Kevorkian (1963).

We again use Friedrichs' model (5.1) for illustration. It is clear from the inner solution or other considerations that the solution depends upon

x/ε as well as x itself. We therefore assume an asymptotic expansion of the form

$$f(x; \varepsilon) \sim f_1(x, X) + \varepsilon f_2(x, X) + \varepsilon^2 f_3(x, X) + \cdots \tag{10.10a}$$

where

$$X \equiv x/\varepsilon \tag{10.10b}$$

This expansion is intended to hold uniformly not only for $0 \leqslant x \leqslant 1$ but also for $0 \leqslant X \leqslant \infty$. Certain restrictions will have to be imposed to assure uniformity for $X \to \infty$, corresponding to $\varepsilon \to 0$ with $x > 0$; and this is in fact the crux of the method.

Of course we have replaced ordinary by partial differential equations, but it will be seen that no real complication has been introduced. Substituting into (5.1) and equating like powers of ε yields the system of equations

$$f_{1XX} + f_{1X} = 0 \tag{10.11a}$$

$$f_{2XX} + f_{2X} = a - 2f_{1xX} - f_{1x} \tag{10.11b}$$

$$f_{mXX} + f_{mX} = -2f_{(m-1)xX} - f_{(m-1)x} - f_{(m-2)xx}, \qquad m \geqslant 3 \tag{10.11c}$$

Although these are nominally partial differential equations, the first is formally identical with the first inner equation [(5.5) with $\varepsilon = 1$], and this is always the case. Its solution is

$$f_1(x, X) = c_1(x) + d_1(x)e^{-X} \tag{10.12}$$

where the functions of integration $c_1(x)$ and $d_1(x)$ are still arbitrary.

At this point the argument assumes a striking resemblance to that of Lighthill's method of strained coordinates (Chapter VI). If our composite expansion (10.10) is to be uniformly valid, the ratios f_2/f_1, f_3/f_2, and so on, must remain of order unity as $\varepsilon \to 0$. We therefore require that

> Each approximation shall be no more singular than its predecessor—or vanish no more slowly—as $\varepsilon \to 0$ for arbitrary values of the independent variables. The same shall be true of all derivatives. (10.13)

The analogy with Lighthill's principle (6.1) is evident.

Just as in the method of strained coordinates, it is possible to achieve a uniform first approximation by examining the second-order equation, without solving it. In our example, the second-order equation (10.11b) becomes

$$f_{2XX} + f_{2X} = a - c_1'(x) + d_1'(x)e^{-X} \tag{10.14}$$

Any particular integral will include a term $(a - c_1')X$. This would make the second approximation more singular than the first as $X \to \infty$, and will therefore be removed by choosing $c_1'(x) = a$. Similarly, the remaining particular integral will include a term $-d_1'Xe^{-X}$, which would make the derivative f' vanish more slowly in the second approximation than the first as $X \to \infty$. We therefore annihilate the right-hand side by choosing also $d_1'(x) = 0$. The values of the constants c_1 and d_1 can now be found by replacing X with x/ε in (10.12) and imposing the boundary conditions in (5.1). The result is just (10.8), which was found by Latta's method.

At least one generalization is required in more complicated problems. As in the preceding method, it may be necessary to generalize the magnified coordinate (10.10b) by setting

$$X \equiv \frac{g(x)}{\varepsilon}, \qquad g(0) = 0 \tag{10.15}$$

where g is a smooth function that is positive when its argument is positive, and is determined in the course of the analysis. The reader can verify that in the present example the principle (10.13) requires that $g'(x) = 1$. In general, of course, g must vanish at the location of the nonuniformity, ε may be replaced by some other power or function of the perturbation parameter, and the asymptotic sequence may involve other functions of ε than integral powers. Partial differential equations are increased in degree by only one as a result of introducing the new variable X, but the function g must depend upon all the original independent variables. Some illuminating examples are given by Cochran (1962).

This method and the one discussed in the previous section are seen to convert the inner solution of the method of matched asymptotic expansions into a uniformly valid approximation. They therefore apparently provide an answer to the question of how to generalize the concept of optimal coordinates (Section 7.15). It is the role of the function g to provide the freedom necessary to make the coordinates optimal. It is possible that, with further development, one of these methods will replace those used previously as the most versatile and reliable technique for treating singular perturbation problems.

10.5. The Prevalence of Logarithms

The devotee of perturbation methods is continually being surprised by the appearance of logarithmic terms where none could reasonably have been anticipated. The recent history of fluid mechanics records a number of well-known investigators who fell victim to the plausible

assumption that their expansion proceded by powers of the small parameter. As suggested in Chapter III, one must be ready to suspect the presence of logarithms at the first hint of difficulty. Their presence in both parameter and coordinate perturbations has been amply illustrated by examples in previous chapters. See, for example, (1.2), (1.4), (1.6), (3.24), (3.27), (7.47), (8.38), (8.48), (9.18), and (9.40). Although Stewartson (1957, 1961) has encountered loglog's in various viscous flow problems, they are blessedly rare.

Logarithmic terms arise from a variety of sources. In some problems they appear naturally as a result of cylindrical symmetry. This is true, for example, of slender-body theory (Section 9.8), where logarithms describe the essential singular nature near the axis of such functions as the Bessel function K_0 and the inverse hyperbolic function sech^{-1} that occur in more complete theories.

Another common source of logarithms is a small exponent. This is exemplified by (4.50), which shows how the expansion is nonuniform. This situation always arises at a slight corner where the equations are elliptic, as for the biconvex airfoil of Section 4.7. When one is confident that this is the correct diagnosis, it may be possible to render the solution uniformly valid simply by replacing the logarithms with near-integral powers (Exercise 9.1; Munson, 1964).

In inverse coordinate expansions for viscous flow, logarithms seem often to be required to ensure exponential decay of vorticity (Section 7.11). In other problems their source is even more obscure. Many of these are singular perturbation problems. One can only philosophize that description by fractional powers fails to exhaust the myriad phenomena in the universe, and logarithms are the next simplest function.

Expansions in this latter group typically begin with simple powers of the perturbation quantity, its logarithm entering linearly only in the second, third, or even fifth term. Thereafter logarithms appear regularly to integral powers that increase successively, though often only at alternate steps. In a singular perturbation problem the appearance of logarithms in, say, the inner expansion forces them into the outer expansion at a later stage through the shift in order of terms that takes place in changing from inner to outer variables.

When a logarithm thus makes its first appearance in a higher-order term, it is accompanied by an algebraic term containing the same power of the perturbation quantity. The logarithmic term is much easier to calculate than its algebraic companion, because it satisfies a homogeneous differential equation. Nevertheless, the two terms must be regarded as together constituting a single step in the process of successive approximation. That the two terms are intimately related is evident from the fact that modifying the perturbation quantity (Section 3.1) transfers a constant from the logarithmic term to its algebraic companion.

For practical values of the perturbation quantity, its logarithm does not differ greatly from unity, so that the algebraic term—though of smaller mathematical order—may actually have the greater magnitude. Moreover, experience suggests that the two terms are invariably of opposite sign, and that their sum is often much smaller than either of them alone, so that retaining only the logarithmic term may worsen the accuracy. An example is the expansion (1.6) for the lift of an elliptic wing. For $A = 6.37$ it gives

$$\frac{dC_L}{d\alpha} = 2\pi(1 - 0.314 - 0.074 + 0.088 + \cdots) \tag{10.16}$$

whereas Krienes (1940) calculates the exact value as 4.55. Two terms give 6 per cent error, the logarithmic term increases that to 15 per cent, but its algebraic companion reduces it again to 3 per cent. Thus it appears that the final terms in such series as (1.2) and (1.4), though of theoretical interest, have no practical value until the next term is calculated. Similar remarks apply to the Nth power of the logarithm, which must be grouped as a single term with its N companions containing lower powers of the logarithm.

We saw in Section 8.6 that the occurrence of logarithmic terms can severely limit the range of applicability of a perturbation series. We return to this question later, in Section 10.7.

10.6. Improvement of Series; Natural Coordinates

See Note 15

One can calculate only a few terms of a perturbation expansion, usually no more than two or three, and almost never more than seven. The resulting series is often slowly convergent, or even divergent. Yet those few terms contain a remarkable amount of information, which the investigator should do his best to extract.

This viewpoint has been persuasively set forth in a delightful paper by Shanks (1955), who displays a number of amazing examples, including several from fluid mechanics. A simple one is the numerical series

$$\pi = 4\left(1 - \frac{1}{3} + \frac{1}{5} - \frac{1}{7} + \frac{1}{9} - \frac{1}{11} + \frac{1}{13} - \cdots\right) \tag{10.17}$$

which converges, but with painful slowness. The seventh partial sum, shown below in the second column, is correct to only one figure, and 400,000 terms would be required for six-figure accuracy. Nevertheless,

the first seven terms actually *contain* π to more than six significant figures, as is shown by forming the following array:

n	S_n	$e_1(S_n)$	$e_1^2(S_n)$	$e_1^3(S_n)$
1	4.0000000			
2	2.6666667	3.1666667		
3	3.4666667	3.1333333	3.1421053	
4	2.8952381	3.1452381	3.1414502	3.1415993
5	3.3396825	3.1396825	3.1416433	
6	2.9760462	3.1427129		
7	3.2837385			

(10.18)

Here the third column has been formed from the second by applying the nonlinear transformation

$$e_1(S_n) = \frac{S_{n+1}S_{n-1} - S_n^2}{S_{n+1} + S_{n-1} - 2S_n} \tag{10.19}$$

Repeating the process yields the subsequent columns, the last of which is correct to six figures. Applying the transformation once more along the lower diagonal improves the accuracy further. These and related transformation are discussed in detail by Shanks.

An important preliminary consideration in a perturbation problem is the proper choice of the expansion quantity (cf. Section 3.1). For coordinate expansions, this means using a system of *natural coordinates.* This is by no means as precise a concept as that of optimal coordinates. However, some problems are clearly adapted to a particular coordinate system, which is generally found to yield the most satisfactory results. A good example is the superiority of parabolic to Cartesian or other coordinates in problems involving parabolic boundaries. For the limiting case of a semi-infinite flat plate, the role of parabolic coordinates in boundary-layer theory was discussed in Chapter VII.

A second example is the inverse blunt-body problem (Fig. 3.5) for a paraboloidal shock wave. We introduce parabolic coordinates ξ, η according to

$$x + iy = \tfrac{1}{2}b[(\xi + i\eta)^2 + 1] \tag{10.20}$$

so that a shock wave of nose radius b is described by $\eta = 1$. Then Cabannes' series (3.25) for the stream function near the axis, with its erratic changes of sign, is recast (Van Dyke, 1958b) into one that alternates smoothly after the first two terms:

$$\frac{\psi}{\xi^2} = \frac{1}{2} - \frac{8}{3}(1-\eta) - \frac{1}{18}(1-\eta)^2 + \frac{155}{54}(1-\eta)^3 - \frac{15{,}235}{648}(1-\eta)^4 + \frac{35{,}416}{243}(1-\eta)^5 - \frac{5{,}656{,}651}{5832}(1-\eta)^6 + \cdots \tag{10.21}$$

Figure 10.1 shows that among the advantages of this form is a clear indication that the expansion diverges at the nose of the body, though less wildly than its Cartesian counterpart. Further improvement of this series is discussed in the next section.

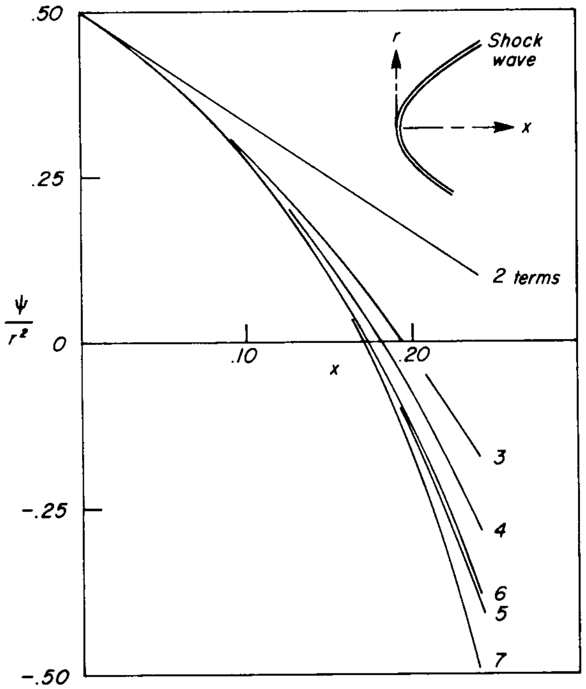

(a)

Fig. 10.1. Series expansion for stream function on axis behind paraboloidal shock wave at $M = 2$, $\gamma = 7/5$. (a) Cartesian coordinates.

A third example is the Blasius series (1.5) for the skin friction on a parabola. Recasting it into parabolic coordinates [with b in (10.20) replaced by a] yields (Van Dyke, 1964a)

See Note 12

$$\tfrac{1}{2}\sqrt{R}\,c_f = 1.23259\xi - 1.72643\xi^3 + 2.11376\xi^5 - 2.44192\xi^7 + 2.73149\xi^9 - 2.99343\xi^{11} + \cdots \tag{10.22}$$

Numerical tests (Exercise 10.3) tend to confirm a conjecture, based on theoretical arguments, that the radius of convergence has been increased by almost 50 per cent.

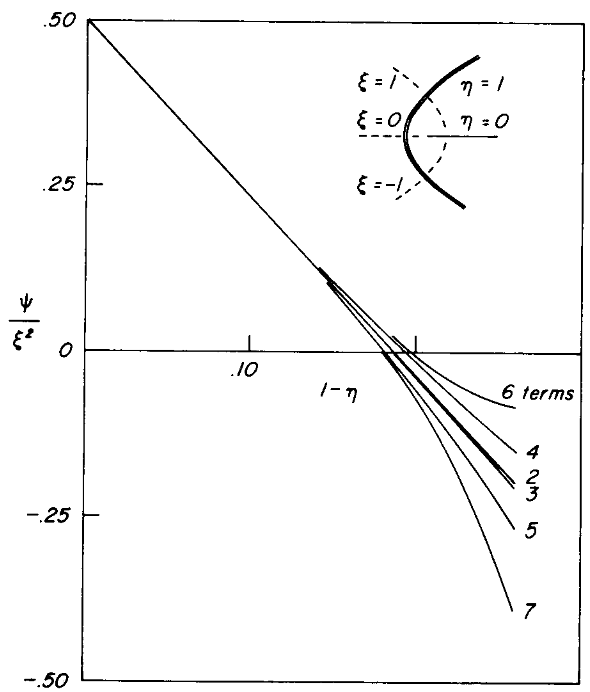

(b)

Fig. 10.1. (b) Parabolic coordinates.

10.7. Rational Fractions

Applying Shanks' nonlinear transformation (10.19) to the first three terms of a power series $1 + a\varepsilon + b\varepsilon^2 + \ldots$ yields a simple *rational fraction*:

$$\frac{a + (a^2 - b)\varepsilon}{a - b\varepsilon} \tag{10.23}$$

This is often a more accurate approximation to the sum of the series than the original three terms. For example, it yields the exact sum if the original is a geometric series, whether convergent or divergent. This fact tends to explain the success of Shanks' transformation with a series such as (10.17), which is evidently "nearly geometric."

When more than three terms of a power series are known, Shanks (1955) suggests forming rational fractions of higher order. Thus from the first five terms of Goldstein's series (1.3) for the drag of a sphere in the Oseen approximation, he obtains

$$\frac{R}{6\pi} C_D \approx \frac{73,920 + 66,600R + 10,880R^2}{73,920 + 38,880R + 689R^2} \tag{10.24}$$

See Note 15

Here R is the Reynolds number based on radius. This agrees well with more exact calculations out to $R = 10$, whereas the original series is useless for computation above $R = 1$. The denominator of the rational fraction (10.24) vanishes at $R = -1.97$ and -54.4. Although the second of these is too large to be significant, the first suggests that the convergence of the original series (1.3) is limited by a singularity at $R = -2$. This is plausible because, as is evident from (8.17) and (8.18), the natural parameter for Oseen flow is $\frac{1}{2}R$, in terms of which the singularity would lie at -1 in the complex plane (cf. Section 3.5).

See Note 2

In the same way, Van Tuyl (1960) has formed rational fractions from Cabannes' series (3.25) for the flow behind a paraboloidal shock wave at $M = 2$, and its counterpart (10.21) in parabolic coordinates. The latter gives

$$\frac{2\psi}{\xi^2} \approx \frac{1 - 0.73878(1-\eta) - 37.827(1-\eta)^2 + 72.098(1-\eta)^3}{1 + 4.5946(1-\eta) - 13.212(1-\eta)^2 - 3.5958(1-\eta)^3} \tag{10.25}$$

Whereas the original series diverges at the body (Fig. 10.1), this agrees well with numerical solutions, apparently giving the stand-off distance Δ correct to four significant figures. The superiority of parabolic coordinates is strikingly confirmed by the discovery that in Cartesian coordinates the corresponding rational fraction becomes infinite in the flow field between the shock wave and the body.

We can make a bolder application of the same technique to Cabannes' other attack on the blunt-body problem. From his two-term expansion (3.26) in powers of time for the stand-off distance following an impulsive start, we can form a rational fraction that remains bounded at infinite time, and so hope to estimate the steady-state value. This gives for $M = \infty$ and $\gamma = 7/5$:

$$\frac{\Delta}{a} \approx \frac{\frac{1}{5}\left(\frac{Ut}{a}\right)}{1 + (n-1)\frac{7}{15}\left(\frac{Ut}{a}\right)} \tag{10.26}$$

This approaches 0.429 for plane flow ($n = 1$), which is far closer than the original result to the accurate numerical calculation of 0.377 for a circular cylinder. This success makes it seem worthwhile to compute

further terms in the expansion. As suggested in Section 3.9, the agreement is poorer for axisymmetric flow, where the rational fraction (10.26) gives 0.214 compared with a numerical value of 0.128 for the sphere. Other tests of this technique of extrapolating a direct coordinate expansion to infinity are proposed in Exercises 10.7 and 10.8.

A technique analogous to that of rational fractions is needed to improve the utility of series containing logarithmic terms, such as (1.4). No striking results have yet been achieved. We give an example of partial success. The series (1.6) for the lift of an elliptic wing can, by analogy with Prandtl's result (9.1a), be rewritten as See Note 13

$$\frac{dC_L}{dx} \approx \frac{2\pi}{1 + \frac{2}{A} + \frac{16}{\pi^2}\left(\log \pi A - \frac{7}{8}\right)\frac{1}{A^2}} \tag{10.27}$$

This is, in fact, of the form that arose naturally (with different, incorrect, constants) in the analysis of Krienes (1940). The accuracy is considerably improved, the error being reduced from 11 to 1 per cent at $A = 2.55$, for example. However, this modification has the defect of still becoming infinite (Fig. 9.4), though at a smaller value of A than the original series. There is evidently room here for further improvement.

10.8. The Euler Transformation

The transformations used in the previous section suffer—despite their evident utility—from the objection that they must usually be applied arbitrarily and blindly, with no understanding of the mechanism involved. This is inevitable when one knows neither the nature nor the location of the singularity that limits convergence. It also goes without saying that one does not always achieve such remarkable improvement as in the preceding examples.

With further insight into the source of divergence, one can proceed more rationally and hence more successfully. Thus one may know the location of the singularity, though not its character. As discussed in Section 3.5, it often happens in applied mechanics that a power-series expansion having physical significance only for positive real values of the perturbation quantity is restricted by a singularity elsewhere in the complex plane, usually on the negative axis, and at -1 if the variables have been chosen in the most natural way. That this situation exists may be known from fundamental considerations, or be suggested by a rational fraction as in (10.24), or merely be suspected.

It was suggested in Section 3.5 that under these circumstances it is usually possible to improve the series by recasting it in powers of the new parameter

$$\bar{\varepsilon} = \frac{\varepsilon}{1+\varepsilon} \tag{10.28}$$

The result is a special case of a rational fractions. The purpose of this *Euler transformation* is to transfer the singularity from $\varepsilon = -1$ to the point at infinity. If there are no other singularities in the complex plane, the radius of convergence is thereby made infinite. Various applications in applied mechanics have been discussed by Bellman (1955). We give three examples drawn from Chapter I.

First, consider once more the Blasius series (1.5) for skin friction on a
See Note 12 parabola, which was improved somewhat by transforming to the more natural parabolic coordinates (10.22). The latter form clearly has unit radius of convergence, no doubt as a consequence of the singularity at $\xi = i$ in the conformal mapping for the parabola. The appropriate Euler transformation is therefore an expansion in powers of $\xi^2/(1+\xi^2)$, after extraction of a factor ξ because the skin friction is an odd function of ξ. This yields (Van Dyke, 1964a)

$$\begin{aligned}\tfrac{1}{2}\,\xi\,\sqrt{R}\,c_f \sim{}& 1.23259\Big(\frac{\xi^2}{1+\xi^2}\Big) - 0.49384\Big(\frac{\xi^2}{1+\xi^2}\Big)^2 \\ &- 0.10650\Big(\frac{\xi^2}{1+\xi^2}\Big)^3 - 0.04733\Big(\frac{\xi^2}{1+\xi^2}\Big)^4 \\ &- 0.02675\Big(\frac{\xi^2}{1+\xi^2}\Big)^5 - 0.0172\Big(\frac{\xi^2}{1+\xi^2}\Big)^6 - \cdots\end{aligned} \tag{10.29}$$

The coefficients now decrease more rapidly than $1/n^2$, suggesting that even far downstream the series converges faster than $\sum 1/n^2 = \pi^2/6$. If so, it should at $\xi = \infty$ reproduce Blasius' value of 0.664 for the flat plate (Section 7.10). The successive partial sums are

$$1.743, \quad 1.045, \quad 0.894, \quad 0.827, \quad 0.789, \quad 0.765, \quad \cdots \tag{10.30}$$

and closer examination leaves little doubt that these are indeed converging to the Blasius value. Thus the radius of convergence of the Blasius series has been extended to infinity.

As a second example, we undertake to improve Chester's Newtonian series (1.7) for the stand-off distance of the blunt body that produces a paraboloidal shock wave at $M = \infty$. There is reason to believe (Van Dyke, 1958b) that this promising method yields an expansion that converges for $\gamma < 11/5$, a value not attainable in reality. However, the

rate of convergence is discouragingly slow. At $\gamma = 7/5$, where the perturbation parameter $(\gamma - 1)/(\gamma + 1)$ is only $\frac{1}{6}$, the series gives

$$\frac{\Delta}{b} = \tfrac{1}{6}(1 - 0.667 + 0.433 - 0.306 + \cdots) \tag{10.31}$$

which is useless for computation.

Following our recommendation of natural coordinates (Section 10.6), we first recast this in parabolic coordinates (10.20). The value of η at the nose of the body is then given by

$$1 - \eta_0 = \frac{3}{8}\varepsilon^2\Big(1 - \varepsilon + \frac{93}{80}\varepsilon^2 - \frac{631}{448}\varepsilon^3 + \cdots\Big), \qquad \varepsilon = \sqrt{\frac{8}{3}\,\frac{\gamma-1}{\gamma+1}} \tag{10.32}$$

There are various indications that this choice of ε is the most natural one, including the fact that the series now oscillates almost like a geometric one with a singularity at $\varepsilon = -1$. Making the appropriate Euler transformation (10.28) then yields

$$1 - \eta_0 = \frac{3}{8}\varepsilon\Big[\frac{\varepsilon}{1+\varepsilon} + \frac{13}{80}\Big(\frac{\varepsilon}{1+\varepsilon}\Big)^3 + \frac{177}{2240}\Big(\frac{\varepsilon}{1+\varepsilon}\Big)^4 + \cdots\Big] \tag{10.33}$$

This result is an unqualified success. The coefficients of the last two terms decrease faster than the inverse square of their exponents, suggesting rapid convergence even at $\varepsilon = \infty$. However, even $\gamma = \infty$ would correspond only to $\varepsilon = 1.633$; and for actual gases γ cannot exceed $5/3$, so that ε is less than 0.817, and $\varepsilon/(1+\varepsilon)$ less than 0.450.

For $\gamma = 7/5$, the successive partial sums of (10.33) give the stand-off distance as

$$\frac{\Delta}{b} = 0.0950, \quad 0.0973, \quad 0.0978, \quad \cdots \tag{10.34}$$

Applying Shanks' transformation (10.19) to these yields 0.0979. Various numerical calculations have given values between 0.0980 and 0.0990. It is interesting to observe that this approximation, though based on the assumption that γ is close to 1, can now be used at $\gamma = \infty$, where it predicts a stand-off distance about three times as great as at $\gamma = 7/5$. Previous less successful attempts to improve Chester's series, using rational approximations, are given by Van Dyke (1958b) and Van Tuyl (1959).

As a third example, we reconsider Goldstein's series (1.3) for the Oseen drag of a sphere. As discussed in Section 10.7, both theoretical and numerical considerations suggest that there is a singularity at $R = -2$. The appropriate Euler transformation then yields

$$C_D \sim 3\pi\left(\frac{R}{2+R}\right)^{-1}\left[1 - \frac{1}{4}\left(\frac{R}{2+R}\right) - \frac{19}{80}\left(\frac{R}{2+R}\right)^2 - \frac{1}{64}\left(\frac{R}{2+R}\right)^3 - \frac{2459}{134{,}400}\left(\frac{R}{2+R}\right)^4 - \frac{9469}{537{,}600}\left(\frac{R}{2+R}\right)^5 - \cdots\right] \qquad (10.35)$$

This has the appearance of converging for all R, though less spectacularly than the previous two examples. The result is less accurate than the rational fraction (10.24) at $R = 20$, but has the advantage of remaining useful at $R = \infty$, where (10.24) gives $C_D = 0$ but the next rational fraction, with a cubic numerator, predicts negative drag. At $R = \infty$ the successive partial sums of (10.35) give

See Note 2

$$C_D \approx 9.42, \quad 7.07, \quad 4.83, \quad 4.68, \quad 4.51, \quad 4.34, \quad \cdots \qquad (10.36)$$

Although these decrease somewhat irregularly, it is not unlikely that they are approaching from above the value 3.33 calculated by Stewartson (1956).

10.9. Joining of Coordinate Expansions

Matching, as it is used in the method of matched asymptotic expansions, connects two parameter expansions for the same limit process that are valid in adjacent regions of space-time. Occasionally it is possible to join other kinds of expansions in analogous fashion. We discuss in this and the last section two kinds of problems where this is possible.

Different coordinate expansions for the same problem can sometimes be joined. If they are both convergent power series, the process is that of analytic continuation, which is simple in principle. The practical complications are illustrated by Cabannes' expansion for the stream function behind a paraboloidal shock wave, recast in parabolic coordinates (10.21). That series converges only about three-quarters of the way to the body (Fig. 10.1), because of a limit line in the physically nonexistent upstream continuation of the flow field (Van Dyke, 1958b). The series can be used to calculate, say, halfway to the body, and a new series from there will reach the body. However, the new series cannot be obtained directly from the original truncated series, because it would be equivalent to it and so have the same limit of convergence. A remedy (Lewis, 1959) is to use the original series only to obtain new initial data at the intermediate station, and to calculate further coefficients using the differential equation.

More often one makes a direct and an inverse expansion for small and large values of a coordinate. The latter is usually not convergent, but only asymptotic, and contains logarithmic terms and undetermined constants (Section 3.10). Nevertheless, the two series can be joined—and the constants thereby found—if the direct series has an infinite radius of convergence. We demonstrate this for the boundary layer on a parabola.

Recasting the inverse expansion (3.27) into parabolic coordinates (10.20) and transferring the logarithmic term to the left side gives

$$\left(\frac{Ux}{\nu}\right)^{1/2} c_f - 0.399\,\frac{\log(1+\xi^2)}{1+\xi^2} \sim 0.664\left(1 + \frac{C_1 - 1}{1+\xi^2} + \cdots\right) \qquad (10.37)$$

We now evaluate this same quantity from the direct expansion (10.29), using the fact that the series

$$\frac{\log(1+\xi^2)}{1+\xi^2} = \frac{\xi^2}{1+\xi^2} - \frac{1}{2}\left(\frac{\xi^2}{1+\xi^2}\right)^2 - \frac{1}{6}\left(\frac{\xi^2}{1+\xi^2}\right)^3 - \cdots \qquad (10.38)$$

converges for $\xi^2 \leqslant \infty$. Together with the fact that $\xi^2 = 2x$ on the parabola, this gives

$$\begin{aligned}\left(\frac{Ux}{\nu}\right)^{1/2} c_f - 0.399\,\frac{\log(1+\xi^2)}{1+\xi^2} = {} & 1.34\left(\frac{\xi^2}{1+\xi^2}\right) - 0.499\left(\frac{\xi^2}{1+\xi^2}\right)^2 \\ & - 0.084\left(\frac{\xi^2}{1+\xi^2}\right)^3 - 0.034\left(\frac{\xi^2}{1+\xi^2}\right)^4 \\ & - 0.018\left(\frac{\xi^2}{1+\xi^2}\right)^5 \\ & - 0.011\left(\frac{\xi^2}{1+\xi^2}\right)^6 - \cdots \end{aligned} \qquad (10.39)$$

for all $\xi^2 \leqslant \infty$. Then expanding formally for small $1/(1+\xi^2)$ and comparing with (10.37) yields the undetermined constant C_1 as (Van Dyke, 1964a)

$$\begin{aligned} C_1 = 1 + (&-1.34 + 1.00 + 0.25 + 0.13 + 0.09 \\ &+ 0.07 + \cdots)/0.664 \approx 1.90 \end{aligned} \qquad (10.40)$$

To be sure, the result is found only approximately as the partial sum of an infinite series; but it is obtained by asymptotic joining rather than numerical patching at some large finite value of ξ. Patching with a numerical integration from the nose at $\xi = 6.8$ gives $C_1 = 1.83$.

This sort of joining is not possible when the direct series has only a finite radius of convergence, or is merely asymptotic. In the latter category, for example, is the approximation (3.24) of Carrier and Lin (1948) for viscous flow near the leading edge of a semi-infinite flat plate, which cannot logically be joined with the higher-order boundary-layer expansion (Section 7.11). Imai (1957a) has patched the skin friction at $Ux/\nu = 1$, but the validity of this step is questionable.

10.10. Joining of Different Parameter Expansions

Expansions for different limits of a single parameter (e.g., for small and large Reynolds number) could be joined as in the preceding section if one of them were convergent over the whole range. No examples are known, although (10.35) comes close to providing one.

Expansions for two different parameters can be joined in finite terms only if one obeys an appropriate similarity rule. Thus the thin-airfoil or slender-body expansion for subsonic compressible flow can be extracted from the Janzen-Rayleigh expansion in powers of M^2, but the converse is not possible.

Consider the simplest example, plane flow past the parabola $y = \pm\,\varepsilon(2x)^{1/2}$, having nose radius ε^2. The expansion of the velocity potential in powers of M^2 has been carried out by Imai (1952) including terms in $(\gamma+1)M^4$. Expanding that complicated result formally for small ε yields

$$\begin{aligned}\phi \sim x + \varepsilon\eta + \tfrac{1}{2}M^2\varepsilon\eta^2\,\frac{\eta - 2\varepsilon}{\xi^2+\eta^2} - \tfrac{1}{4}M^2\varepsilon^2\log\frac{\xi^2+\eta^2}{4\varepsilon^2}\\ - \frac{\gamma+1}{16}M^4\varepsilon^2\Big[4\frac{\eta^4}{(\xi^2+\eta^2)^2} + \log\frac{\xi^2+\eta^2}{4\varepsilon^2}\Big] + O[M^4, (\gamma+1)M^6, \varepsilon^3]\end{aligned} \qquad (10.41a)$$

where [cf. (10.20)]

$$\begin{aligned}\xi^2 &= \sqrt{x^2+y^2} + x + O(\varepsilon^2)\\ \eta^2 &= \sqrt{x^2+y^2} - x + O(\varepsilon^2)\end{aligned} \qquad (10.41b)$$

To convert this double expansion for small ε and M^2 into a single expansion for small ε, we must sum the series in M^2. This unlikely task is accomplished simply by appealing to the second-order similarity rule for subsonic small-disturbance theory (Van Dyke, 1958a), according to which

$$\phi(x, y; M, \gamma, \varepsilon) \sim x + \varepsilon^2 f_1(x, \beta y; \beta\varepsilon) + \varepsilon^4\Big[f_{21}(\ \ ) + M^2 f_{22}(\ \ ) + (\gamma+1)\frac{M^4}{\beta^2}f_{23}(\ \ )\Big] + O(\varepsilon^6) \qquad (10.42)$$

where $\beta \equiv (1 - M^2)^{1/2}$ and each function has the same arguments as the first. The previous double expansion (10.41) is compatible with this rule only if it can be replaced by

$$\begin{aligned}\phi \sim x + \frac{\varepsilon}{\beta}\bar\eta - \frac{1}{4}\frac{M^2}{\beta^2}\varepsilon^2\Big(4\frac{\bar\eta^2}{\bar\xi^2+\bar\eta^2} + \log\frac{\bar\xi^2+\bar\eta^2}{4\beta^2\varepsilon^2}\Big)\\ - \frac{\gamma+1}{16}\frac{M^4}{\beta^4}\varepsilon^2\Big[4\frac{\bar\eta^4}{(\bar\xi^2+\bar\eta^2)^2} + \log\frac{\bar\xi^2+\bar\eta^2}{4\beta^2\varepsilon^2}\Big] + O(\varepsilon^3)\end{aligned} \qquad (10.43a)$$

where

$$\begin{aligned}\bar\xi^2 &= \sqrt{x^2+\beta^2y^2} + x\\ \bar\eta^2 &= \sqrt{x^2+\beta^2y^2} - x\end{aligned} \qquad (10.43b)$$

and this is the second-order thin-airfoil solution. The corresponding joining for the paraboloid of revolution is given by Van Dyke (1958c).

EXERCISES

10.1. *Lighthill's equation by multiple scales.* Solve the problem (6.3) using the method of multiple scales, showing that the result is not (6.12c) but an equally acceptable alternative. Try solving also by Latta's method of composite expansions.

10.2. *Unmatchable problem.* Show that the method of multiple scales is successful for the problem

$$\varepsilon f'' + f = 1, \qquad f(0) = f'(0) = 1$$

whereas the method of matched asymptotic expansions breaks down.

10.3. *Estimate of radius of convergence.* Estimate the radii of convergence of the series (1.5) and (10.22) using Cauchy's ratio test, and compare with the values $(s/a) = \pi/4$ and $\xi^2 = 1$ suggested by the conformal mapping for the potential flow. Do the same for (1.7) and (10.21), and compare with the singularities of successive rational approximations. See Note 3

10.4. *Lift of elliptic wing.* Calculate the first three approximations from (1.6) and (10.27) for $A = 8/\pi$ (axis ratio of 2 : 1). Estimate the complete sum, and compare with Krienes' value of 2.99. See Note 3

10.5. *Rational approximations for friction on parabola.* Form rational approximations to (1.5) and (10.22), and thereby try to extract the limiting value far downstream.

10.6. *Critical Mach number for circle.* The critical Mach number (where local sonic speed is first attained) is approximated by successive partial sums of Simasaki's series (1.1) as

See Note 3

$$0.4659, \quad 0.4206, \quad 0.4090, \quad 0.4043, \quad 0.4020, \quad 0.4008, \quad \cdots$$

Estimate the true value, and compare with Simasaki's own estimate of 0.40. Estimate the radius of convergence of (1.1), compare with Simasaki's 0.50, and contrast with the critical Mach number. Consider the possibility of applying an Euler transformation to (1.1).

See Note 3

10.7. *Friction at nose of impulsively started cylinder.* Try to extrapolate (3.23) to infinite time, and compare with Hiemenz' value for steady flow (Schlichting, 1960, p. 78).

See Note 3

10.8. *Separation on impulsively started circle.* On a circular cylinder of radius a started moving impulsively through viscous fluid with speed U, the skin friction varies initially with time in proportion to (Goldstein and Rosenhead, 1936)

$$1 + 2.8488 \cos \theta\left(\frac{Ut}{a}\right) - [0.8795 \cos^2 \theta - 0.2390 \sin^2 \theta]\left(\frac{Ut}{a}\right)^2$$

where θ is the angle from the forward stagnation point. Find the location of the separation point as a function of time. Extrapolate to infinite time, and compare with the known value of $\theta = 109$ degrees (Schlichting, 1960, p. 154).

NOTES

Note 1. Introduction

These Notes have been added to bring the text of 1964 up to date. They briefly describe significant advances in the subject, and add relevant references to the literature through mid-1975. Further lists of references, for applications to fluid mechanics and other fields, can be found in the book of Nayfeh (1973).

Each note is keyed to one or more sections of the main text, where an indicator of the form shown here at the right appears in the margin of the page. Whenever possible, related comments have been combined into a single Note, with the aim of making this section less fragmentary.

See Note 1

Note 2. Computer Extension of Regular Perturbations

Since the late 1950s it has been feasible to delegate to an electronic digital computer the rapidly mounting arithmetic labor involved in extending a regular perturbation series to high order. This procedure has been applied to a variety of problems in fluid mechanics, including several discussed in this book. The history of the idea, practical details, and a number of applications have been surveyed by Van Dyke (1975, 1976).

The Janzen-Rayleigh expansion (Section 1.3) has been extended to order M^{12} by Hoffman (1974a) and to order M^{16} by W. C. Reynolds (unpublished). The result for maximum surface speed, with $\gamma = \frac{7}{5}$, is

$$\begin{aligned}\frac{q_{\max}}{U} = {} & 2.00000 + 1.16667\,M^2 + 2.57833\,M^4 + 7.51465\,M^6 \\ & + 25.59041\,M^8 + 96.26329\,M^{10} + 387.92345\,M^{12} \\ & + 1646\,M^{14} + 7450\,M^{16} + \cdots \end{aligned} \qquad \text{(N.1)}$$

Here the coefficients of M^4 through M^{10} differ slightly from those of Simasaki in Equation (1.1) because the value of γ is different. The last two coefficients are relatively inaccurate because they were computed only in single-precision arithmetic. Calculating the successive approximations to the critical Mach number (Exercise 10.6) and then repeatedly applying the nonlinear transformation of Shanks (Eq. 10.19), Hoffman estimates the critical Mach number as 0.3983 $\pm$ 0.0002. This agrees with the value 0.39852 $\pm$ 0.0002 calculated numerically by Melnik and Ives (1971).

Goldstein's series (1.3) for the Oseen drag of a sphere in powers of Reynolds number has been extended by Van Dyke (1970). Terms through order R^{23} were calculated in one minute of computer time. The graphical ratio test of Domb and Sykes (Note 15) shows that the nearest singularity, which was conjectured on the basis of rational fractions (p. 206) to lie at $R = -2$, is actually located at $R = -2.09086$. Applying the Euler transformation (Section 10.8) that maps that singularity away to infinity yields a new series that converges out to infinite R and, with some further manipulation, reproduces Stewartson's value (p. 210) of $C_D = 3.33$ at $R = \infty$.

A noteworthy application of this technique is to plane periodic water waves. Early in his career Stokes expanded the solution in powers of the coefficient a of the linearized approximation, calculating the second approximation for constant depth and the third approximation for deep water. Thus he found the surface of the wave in deep water described, for an observer moving with the wave, by

$$y = a \cos x - \frac{1}{2}a^2 \cos 2x + \frac{3}{8}a^3 \cos 3x + \cdots \tag{N.2}$$

More than thirty years later Stokes added two more terms, and conjectured that the expansion converges for the highest wave, which has sharp peaks of 120-degree angle. Subsequently Wilton carried the calculation for deep water to tenth order, but made errors at eighth order. Using the computer, Schwartz (1974) has extended the series to 117th order. Analyzing the coefficients, he showed that Stokes's expansion fails to converge to the highest wave because the coefficient a is not a monotonic function of the wave height. He eliminated this defect by reverting the series to give an expansion in powers of wave height, and was then able to calculate the maximum wave height to five figures.

Some other computer extensions at low Reynolds number are described in Note 10.

Note 3. Comments on the Exercises

It was mentioned in the original Preface that the Exercises at the end of each chapter contain much additional information in concise form. We point out here that some of them have been subsequently solved in the literature or otherwise extended, that several can be better posed, and that it is interesting to try alternative techniques on a few.

Exercise 2.2. *Slightly porous circle.* It is better to ask for the velocity potential, because for it the effect of slight compressibility can be deduced from Equation (2.2), whereas it is tedious to extract from it the corresponding result for the stream function.

Exercise 2.3. *Corrugated quasi cylinder.* Davey (1961) has used this solution to illustrate how a stagnation point can be a saddle point of attachment in inviscid flow.

Exercise 2.4. *Circle in parabolic shear.* As preparation for the modification of Exercise 5.7 described below, it would be useful to consider also the parallel stream with profile $u = U \cosh(\varepsilon^{1/2} y/a)$.

Exercise 4.5. *Exact solution for biconvex airfoil.* The discrepancy pointed out in the last two sentences is discussed in Note 4 below and in the reference given there.

Exercise 5.7. *Circle in parabolic shear.* The problem as posed is unnecessarily complicated by nonlinearity. The essentials are exhibited more simply if, in the parallel flow far upstream, the parabolic profile is replaced by the hyperbolic-cosine profile $u = U \cosh(\varepsilon^{1/2} y/a)$, which is almost the same near the cylinder.

Exercise 6.2. *A problem of Carrier.* The factor multiplying the exponential in the expression given for x can be simplified to a linear form if we weaken Lighthill's principle as described in Exercise 6.1. Another way of treating the problem is to interchange the roles of the independent and dependent variables, which transforms it into a regular perturbation problem for $x(f)$. The solution using matched asymptotic expansions, discussed by Carrier, is more complicated.

Exercise 6.4. *Pritulo's method.* Pritulo's idea of introducing the straining of coordinates a posteriori has several times been discovered anew (Martin 1967, Usher 1968). Crocco (1972) illustrates its effectiveness for several problems in gas dynamics.

Pritulo (1969) points out that a parameter can be treated similarly. The idea of slightly straining a parameter so as to suppress nonuniformity was invented by Lindstedt (1882) to avoid secular terms in celestial mechanics and, as mentioned on page 100, was generalized by Poincaré. Nayfeh (1973) has called this the *method of strained parameters.* Pritulo shows how parameter straining can be introduced a posteriori in the example of the fourth-order thin-airfoil expansion of Donov (1939) for plane supersonic flow. Divergence of the approximation as the free-stream Mach number M becomes large can be suppressed by straining the compressibility factor $(M^2 - 1)^{1/2}$ so that each term in the expansion for the pressure coefficient remains bounded for large M.

Exercise 8.2. *Viscous flow past slender paraboloid.* The first step of the solution was given by Veldman (1973). As discussed in Note 4, the second step involves a failure of the asymptotic matching principle because of a "forbidden region," which is avoided by proceeding to the third step, matching two terms of the Oseen expansion to two terms of the Stokes expansion.

Exercise 8.3. *Wake of axisymmetric body.* This problem is the first step in the solution of Viviand and Berger (1964). In the second approximation, the failure of the vorticity to decay exponentially (p. 131) was shown by Berger (1968) to require, much as for the boundary layer on a semi-infinite plate (Section 7.11), introduction of a logarithmic term; and then its algebraic companion term is undetermined. Berger also deduces the form of the third and higher terms. This solution, and much other work on laminar wakes, is discussed in the book by Berger (1971).

Exercise 8.5. *Transcendentally small terms for circle.* As described in Notes 10 and 11, the solution of this exercise is included in the work of Skinner (1975).

Exercise 9.3. *Near-equilibrium flow over a wavy wall.* It is instructive also to show that the method of strained coordinates leads very simply to a definite result, but it is erroneous because the solution does not decay at infinity. See Note 7; also Note 6.

Exercise 10.3. *Estimate of radius of convergence.* The graphical ratio test of Domb and Sykes, described in Note 15, is the best technique for making these estimates.

Exercise 10.4. *Lift of elliptic wing.* As pointed out in Note 13, the fraction $\frac{7}{2}$ in Equation (1.6) should be $\frac{9}{2}$, and the $\frac{7}{8}$ in (10.27) should

be $\frac{9}{8}$. Krienes's value has been improved to 2.944 ± 0.004 by Medan (unpublished calculations using the method of Medan, 1974).

Exercise 10.6. *Critical Mach number for circle.* As discussed in Note 2, Simasaki's series (1.1) has been extended by computer, and the critical Mach number (for $\gamma = \frac{7}{5}$) estimated accurately from that as well as other methods.

Exercise 10.7. *Friction at nose of impulsively started cylinder.* The expansion in powers of time has been extended by Collins and Dennis (1973a). The boundary-layer approximation (3.23) for the friction near the front stagnation point is

$$\tau \sim \rho\nu^{1/2}U^{3/2}\, x \frac{1}{\sqrt{\pi U_1 t}}[1 + 1.42442(U_1t) - 0.21987(U_1t)^2 - 0.0127(U_1t)^3 + 0.0254(U_1t)^4 - 0.00566(U_1t)^5 - 0.00134(U_1t)^6 + 0.00095(U_1t)^7 + \cdots] \quad \text{(N.3)}$$

Exercise 10.8. *Separation on impulsively started circle.* The extension of Collins and Dennis (1973a) gives, in the first-order boundary-layer approximation, the friction proportional to

$$\begin{aligned} &1 + 2.8488 \cos\theta(Ut/a) - (0.3202 + 0.5592\cos 2\theta)(Ut/a)^2 \\ &- (0.0767\cos\theta + 0.0246\cos 3\theta)(Ut/a)^3 \\ &+ (0.0661 + 0.1982\cos 2\theta + 0.1427\cos 4\theta)(Ut/a)^4 \\ &- (0.0332\cos\theta + 0.0722\cos 3\theta + 0.0755\cos 5\theta)(Ut/a)^5 \\ &- (0.0105 + 0.0285\cos 2\theta + 0.0414\cos 4\theta + 0.0052\cos 6\theta)(Ut/a)^6 \\ &+ (0.0117\cos\theta + 0.0207\cos 3\theta + 0.0560\cos 5\theta \\ &+ 0.0335\cos 7\theta)(Ut/a)^7 + \cdots \qquad \text{(N.4)} \end{aligned}$$

Collins and Dennis (1973b) also computed the time-dependent flow numerically, using a method of series truncation, and found that they could not continue the integration beyond $(Ut/a) = 1.25$. Telionis and Tsahalis (1973; see also Sears and Telionis, 1975) have also integrated the boundary-layer equations numerically, using a finite-difference scheme, and at about $(Ut/a) = 0.65$ discern a singularity in the interior of the boundary layer that has the properties of the square-root singularity at the surface in steady separation (Goldstein, 1948, Stewartson, 1958).

Note 4. The Asymptotic Matching Principle

Occasionally the counting involved in the asymptotic matching principle (4.36, 5.24) may seem ambiguous; then an alternative version of the rule is useful. One may feel uncertain how to count terms, for example, in the following four situations: (i) if the asymptotic sequence has gaps (e.g., the series proceeds by integral powers of ε except that the coefficient of ε^3 vanishes identically); (ii) if the asymptotic sequences are essentially different for the inner and outer expansions (e.g., one expansion proceeds by powers of ε, the other by half-powers); (iii) if logarithmic terms arise (e.g., $\varepsilon^n \log \varepsilon$ appears as well as ε^n); or (iv) if eigensolutions exist.

In all such cases, uncertainty is avoided by adopting the following unambiguous version of the rule:

The inner expansion to order Δ of (the outer expansion to order δ) = the outer expansion to order δ of (the inner expansion to order Δ). (N.5)

Here $\Delta(\varepsilon)$ and $\delta(\varepsilon)$ are any two gauge functions (not necessarily the same), which may or may not actually appear in the asymptotic sequences for the outer and inner expansions. Of course this alternative is equivalent to the original version (5.24) whenever it is clear how to count terms. Similar alternative rules based on orders rather than counting have been introduced by Fraenkel (1969b, c, pp. 246, 265) and Crighton and Leppington (1973, p. 317).

In proposing the asymptotic matching principle the author intended merely to provide a specific procedure embodying Kaplun's ideas, and supposed that it was equivalent to the *intermediate* matching principle (5.29). However, in an important study of the matching procedure Fraenkel (1969a, b, c) has shown that the two rules are significantly different. He points out that the asymptotic rule is easier to use than the intermediate one, which requires a search for the range of the intermediate variable and the order of overlap in that range. Moreover, the asymptotic rule is more economical, because in certain problems where the overlapping is weak a constant in the inner expansion can be found by matching with fewer terms of the outer expansion than are required with the intermediate rule. Thus Fraenkel has demonstrated with several examples (Fraenkel, 1969b, c, pp. 251, 269) that, contrary to what was widely believed, the asymptotic matching principle can be applied to inner and outer expansions that contain too few terms to overlap to the order of the terms being matched. However, Lagerstrom (1975) points out that this shortcoming can be circumvented by working with the *correction* boundary layer—the inner expansion of the difference between the full solution and its outer expansion.

Unfortunately, the asymptotic rule can fail when the series contain logarithms. This has been analyzed by Fraenkel, who has discovered two restrictions, one or the other of which is to be imposed on the asymptotic matching principle, depending on how the logarithms appear. These are no mere mathematical quibbles, for in each case we now know that ignoring the restriction has led to error in a realistic problem in fluid mechanics. A majority of the many solutions of physical problems carried out in the last decade using the method of matched asymptotic expansions are based on the asymptotic rule. It is therefore of practical importance to recognize these two restrictions:

1. Don't cut between logarithms. Fraenkel insists on normalizing ε as the ratio of the inner and outer scales. (We have not always adhered to this convention; for example, we took the ratio as ε^2 in Eq. (4.34) for the round-nosed airfoil, and even as $e^{-1/\varepsilon}$ in Eq. (4.48) for the sharp-edged airfoil.) Then condition (iii) of his Theorem I (Fraenkel, 1969a, p. 223) serves as a warning that the asymptotic matching principle may fail if applied to an expansion truncated by separating terms that differ by less than any power of ε. In particular, when the series proceeds in powers of ε and of its logarithm, all the powers of $\log \varepsilon$ multiplying a given power of ε should be treated as a single term.

This warning was violated by Proudman and Pearson (1957) who, as described on page 160, calculated the term of order $R^2 \log R$ in the Stokes expansion for the sphere while disregarding its companion term of order R^2. Apparently no harm was done in this case, however, because Chester and Breach (1969) have confirmed that term by extending the series to one higher power of R (and in so doing have themselves violated Fraenkel's warning at the next stage).

On the other hand, Crighton and Leppington (1973) have found that violating the restriction leads to an erroneous result for the diffraction of long waves by a semi-infinite plate of finite thickness. The outer expansion has the form

$$\phi \sim \phi_0 + \varepsilon \log \varepsilon\, \phi_1 + \varepsilon\, \phi_2 + \varepsilon^2 \log^2 \varepsilon\, \phi_3 + \varepsilon^2 \log \varepsilon\, \phi_4 + \varepsilon^2 \phi_5 + \cdots \tag{N.6}$$

where ε is the ratio of plate thickness to wave length, and hence of the inner to outer scales. Matching to order $\varepsilon \log \varepsilon$ as well as to order ε gives the correct result; but matching to order $\varepsilon^2 \log^2 \varepsilon$ yields a ϕ_3 that is recognized as being incorrect only because this linear problem possesses a reciprocal theorem that is violated. This trouble is avoided by matching the three terms in ε^2 as a block. Crighton and Leppington discuss the mechanics of this restricted matching principle.

2. Forbidden regions in the purely logarithmic case. The restriction just discussed cannot be met when, as for the circle at low Reynolds number (Sec. 8.7), the outer and inner expansions proceed in inverse powers of $\log \varepsilon$ (or, equivalently, of $\log \varepsilon + k$). Fraenkel (1969a, p. 226) finds that in this case the asymptotic matching principle (5.24) is valid unless m and n fall within a certain "forbidden region" whose shape in the mn-plane can be calculated in the course of solution.

It is convenient to uniformize the counting by agreeing that for both the inner and the outer expansions the kth term is of order $(\log \varepsilon)^{-k}$ (so that typically the "zeroth-order" term is absent from the inner expansion). Then in the common case that the inner expansion of the outer expansion is a polynomial in $\log x$ of degree N, the matching holds for $|m - n| \geqslant N$. Fraenkel (1969c, p. 276) illustrates this restriction with a one-dimensional model of the circle at low Reynolds number. The forbidden region is just the line $m = n$, so that matching can be carried out successfully by choosing, for example, $n = m + 1$ (or $n = m - 1$).

A more realistic example is the problem in Exercise 8.2 of axisymmetric viscous flow past a slender paraboloid. For the paraboloid of nose radius a, separation of variables yields the Stokes approximation

$$\psi \sim \frac{1}{2} Ua^2\, \Delta_1(R)\, \bar{\xi}^2(\bar{\eta}^2 \log \bar{\eta}^2 - \bar{\eta}^2 + 1) \tag{N.7}$$

where the Stokes variables are $\bar{\xi} = \xi/a^{1/2}$ and $\bar{\eta} = \eta/a^{1/2}$. The first term of the Oseen expansion is just the uniform stream, with

$$\psi \sim \frac{1}{2}\frac{\nu^2}{U^2}\tilde{\xi}^2\tilde{\eta}^2 \tag{N.8}$$

where $\tilde{\xi} = \xi/(\nu/U)^{1/2}$ and $\tilde{\eta} = \eta/(\nu/U)^{1/2}$. Matching these determines the multiplier in the Stokes approximation as $\Delta_1 = (\log 1/R)^{-1}$, where the Reynolds number is $R = Ua/\nu$. The solution has been carried to this stage by Veldman (1973). (This result, with an incorrect factor Δ_1 independent of Reynolds number, was first obtained by Sampson (1891) by taking the limit of the Stokes solution for an ellipsoid of revolution.)

The next term can then be calculated in the Oseen expansion, giving

$$\psi \sim \frac{1}{2}\frac{\nu^2}{U^2}\tilde{\xi}^2\left(\tilde{\eta}^2 + \Delta_1\{A[\tilde{\eta}^2 E_1(-\tilde{\eta}^2/2) - 2(1 - e^{-\tilde{\eta}^2/2})] + B\}\right) \tag{N.9}$$

where E_1 is the exponential integral. (Veldman also gives this result, but he imposes the surface boundary condition to find the Oseen approximation, rather than matching.) This can almost be matched to (N.7) with $A = 1$ and $B = 0$, but the secondary terms give the mismatch $\log \bar{\eta} = \frac{1}{2}$. Since $\log \eta$ appears only linearly, the asymptotic matching principle is valid for $|m - n| \geqslant 1$. Thus we are at this stage in the forbidden region, which is again just the line $m = n$.

As in the case of the circle (p. 163), the higher terms in the Stokes expansion are multiples of the first, so that the two-term expansion has the form

$$\psi \sim \frac{1}{2}Ua^2[\Delta_1 + c\Delta_1^2 + \cdots]\bar{\xi}^2(\bar{\eta}^2 \log \bar{\eta}^2 - \bar{\eta}^2 + 1) \tag{N.10}$$

We have now moved out of the forbidden region, and this matches perfectly with (N.9), giving $A = 1$, $B = 0$, and $c = \gamma - \log 2$.

Davis and Werle (1972) have calculated an approximation to the third term of the Stokes expansion that becomes correct far downstream, as $\xi \to \infty$. They suggest that it is nearly correct for all ξ, and confirm this by comparing their numerical solutions with the resulting expansion for the local skin friction:

$$[R(1 + \bar{\xi}^2)/\bar{\xi}](\tau/\rho U^2) = \Delta_1 - (\log 2 - \gamma)\Delta_1^2 - [2 \log 2 + \pi^2/12 - (\log 2 - \gamma)^2]\Delta_1^3 + \cdots \tag{N.11}$$

We would expect that, just as for the circular cylinder (Note 15), the accuracy of the Stokes expansion could be improved by telescoping the first two terms into one. This means changing the definition of the gauge function to $\Delta_1' = (\log 2/R - \gamma)^{-1}$, so that $c = 0$ in (N.10). Then Davis and Werle's approximation (N.11) assumes the simpler form

$$[R(1 + \bar{\xi}^2)/\bar{\xi}](\tau/\rho U^2) = \Delta_1' - (2 \log 2 + \pi^2/12)\Delta_1'^3 + \cdots \quad \text{(N.12)}$$

which was given by Mark (1954). This modification does improve the agreement with numerical results somewhat, but not so dramatically as for the circle (Fig. N.4).

In the problem of the circular cylinder the log ρ in Eq. (8.47) means that the 1-term Stokes expansion and the 2-term Oseen expansion (the inner and outer expansions to order Δ_1) lie in the forbidden region, which is again the line $m = n$. Nevertheless, we were able to match them correctly on page 163, much as Proudman and Pearson (1957) did, using the asymptotic matching principle. This means that, just as in the case of powers of ε and log ε discussed above, violating Fraenkel's warnings will not invariably lead to error. (On the other hand, the Stokes and Oseen expansions to order unity, which are 0 and 1 respectively, obviously do not match.)

Are Poincaré expansions necessary? Fraenkel's proof of the restricted asymptotic matching principle is based on the assumption that both the outer and the inner expansion are of Poincaré form—that is, of the form (3.10a), where the coefficients c_n ordinarily depend on space or time variables but are independent of ε, for example,

$$f(x;\, \varepsilon) \sim \sum_{n=1}^{N} c_n(x)\, \delta_n(\varepsilon) \quad \text{(N.13)}$$

Sheer (1971) points out that for a sharp-edged airfoil the inner solution (4.49) is not of this form. He attributes to this fact the apparent failure of the matching pointed out in Exercise 4.5 when the final comparison is made in inner rather than outer variables. His remedy is to work with the logarithm of the velocity, which converts the inner solution to Poincaré form without significantly changing the outer expansion. He goes on to show that putting all of the unbounded part into the first approximation leads to a uniform expansion, so that the method of matched asymptotic expansions, having served its purpose, is unnecessary.

Sheer does not discuss the remarkable fact that matching the velocity itself gives the correct second-order result (4.53) if the final comparison is made in outer variables, as on page 70. Is this related to the fact that the outer expansion does have Poincaré form? We examine the next approximation, matching three terms each of the outer (4.24) and inner (4.49) expansions. (However in (4.49) we must, for the semi-vertex angle, replace the thin-airfoil approximation $\tan^{-1} 2\varepsilon$ by its exact value $2 \tan^{-1} \varepsilon$ for the circular-arc airfoil because the difference, though only of order ε^3, makes a change of order ε^2 through the factor $e^{-1/\varepsilon}$.) Making the final comparison again in outer variables yields

$$U_i = e^{-2/\pi} U \left\{ 1 + \frac{2}{\pi}\varepsilon\left(2 - \log 2 - \frac{2}{\pi}\right) + \frac{2}{\pi^2}\varepsilon^2\left[\log^2 2 + \left(\frac{4}{\pi} - 6\right)\log 2 + 6 - \frac{12}{\pi} + \frac{4}{\pi^2} + \frac{\pi}{3}\right] + \cdots \right\} \quad \text{(N.14)}$$

That this is correct is confirmed by expanding the exact solution quoted in Exercise 4.5. This might tempt us to conjecture that the asymptotic matching principle remains valid when only one or the other of the inner and outer expansions is of Poincaré form, provided the final matching is carried out in the corresponding variables.

It seems, however, that the resolution of the difficulty is much simpler. We did not in fact properly apply our matching rule on page 70. The matching principle requires the inner expansion to be expanded for small ε and truncated while it is written in outer variables. We did not carry out that expansion and truncation completely, because the form of U_i was not prescribed at the stage of Eqs. (4.52c) and (4.52d). Consequently, (4.52d) contains some third-order terms in ε^2 that should have been eliminated.

The remedy is to work with a specific expansion for U_i, which (4.51d) shows to be $U_i = A + B\varepsilon + \cdots$. Then the rule can be applied properly, and the discrepancy mentioned in Exercise 4.5 disappears. Similarly, in the next approximation using $U_i = A + B\varepsilon + C\varepsilon^2 + \cdots$ leads to the correct result (N.14) whether the final matching is made in outer or inner variables. Thus it appears that, at least in this example, the expansions need not both be of Poincaré form. However, Note 5 deals with examples where the asymptotic rule fails unless the expansions are cast into Poincaré form.

Note 5. The Theory of Matching

For practical application of the method of matched asymptotic expansions to specific problems, it is ordinarily most efficient to work with limit-process expansions, and to match using the asymptotic matching principle (Note 4). That is the method followed in this book, and in most of the examples in the literature. The choice of technique is certainly a matter of personal taste, however, and Cole (1968), while using limit-process expansions, always matches them by taking intermediate limits (Section 5.8). However, it is clear that these approaches gloss over many subtleties, some of which have practical implications.

For a deeper understanding of the ideas underlying matching, expansions characterized by their domains of validity are more fundamental than limit-process expansions. They may also be essential for constructing the expansions in some cases. That is, the idea of applying limits to the equation and then finding solutions of the resulting approximate equations is more basic than looking for limits of the solution. This view, originating in the work of Kaplun and Lagerstrom (Kaplun and Lagerstrom, 1957, Kaplun, 1957, Kaplun, 1967), has been set forth fully by Lagerstrom and Casten (1972). The reader will find there a detailed discussion of the heuristic ideas underlying the method of matched asymptotic expansions.

In particular, Lagerstrom (1961, pp. 87, 109) has proposed a model problem (different from that of Fraenkel mentioned in Note 4) that illustrates the mathematical structure of viscous flow past the circle and sphere at low Reynolds number:

$$\frac{d^2u}{dr^2} + \frac{n-1}{r}\frac{du}{dr} + u\frac{du}{dr} + \delta\left(\frac{du}{dr}\right)^2 = 0, \qquad u(\varepsilon) = 1, \qquad u(\infty) = 0 \tag{N.15}$$

Here n corresponds to the number of space dimensions (2 for the circle, 3 for the sphere), and the factor δ is zero for the model of incompressible flow and unity for compressible flow. This problem has been analyzed by Lagerstrom (1961, 1970), Cole (1968, p. 61), Bush (1971), and Lagerstrom and Casten (1972).

The incompressible model, like the actual incompressible problem (Chapter 8), can be treated using limit-process expansions. The Oseen expansion is a regular perturbation (cf. Note 7). In the compressible model, on the other hand, the Stokes equation is nonlinear, and is not contained in the Oseen equation. This is the situation in the actual flow problem as well (Lagerstrom, 1964).

Nonlinearity of the Stokes equation has the further consequence that the solution cannot be found using limit-process expansions based on the outer variable r and inner variable r/ε, for they do not match at all. Instead, one must use an inner expansion characterized by its domain of validity, with the inner variable $r/\eta(\varepsilon)$, where $\eta \ll 1$. Alternatively, Bush (1971) shows that one can use an inner-limit expansion with the inner variable changed to $(\log 1/r)/(\log 1/\varepsilon)$.

The same situation arises in a turbulent boundary layer. Millikan (1939) deduced from physical arguments that there are two different regions, a thin layer near the wall where viscous stresses are important, and a thicker outer layer where only Reynolds stresses are significant. For incompressible flow, this idea has been formalized as an asymptotic theory for Reynolds number tending to infinity by Yajnik (1970) and Mellor (1972). Bush and Fendell (1972) have extended the analysis to higher approximations using eddy-viscosity models. For compressible flow, however, Melnik and Grossman (1974) and Adamson and Feo (1975) find that limit-function expansions do not match. Again the remedy is either to consider domains of validity or to make a change of variable that leads to matching.

Note 6. Alternative Rules for Composite Expansions

J. Ellinwood (unpublished) has observed that the additive rule (5.32) for composition is the basic one. It can be used to generate a very general family of alternative rules. If $F(f)$ is any sufficiently smooth functional (generally without poles) that has an inverse $F^{-1}(f)$, then a composite is given by

$$f_c^{(m,n)} = F^{-1}\{F(f_i^{(m)}) + F(f_o^{(n)}) - F[(f_i^{(m)})_o^{(n)}]\} \tag{N.16}$$

The additive rule corresponds to $F(f) = f$ and the multiplicative rule (5.34) to $F(f) = \log f$.

The rules corresponding to $F(f) = f^2, f, \log f, 1/f$, and $1/f^2$ yield a monotonic sequence, approximately evenly spaced, at any fixed argument; and this variation might be exploited to improve the agreement with exact or experimental results. The composite solution (9.66) that was formed by inspection for hypersonic flow past a blunted wedge corresponds to $F(f) = \log(\partial f/\partial\psi)$, where only the constant of integration need be fixed by inspection.

Schneider (1973) has pointed out that the multiplicative rule involves the risk of dividing by zero, in which case the result—far from being uniformly valid—becomes infinite within the region of interest. In fact, he shows that this happens in just the example treated on page 96, the thin elliptic airfoil. The multiplicative composite (5.36) is valid on the surface, but ahead of (or behind) the airfoil it breaks down even on the dividing streamline.

In the notation of Section 4.9 (with s the distance downstream from the leading edge of an ellipse of chord 2 and thickness ratio ε), the exact speed on the x-axis is found by conformal mapping as

$$\frac{u}{U} = \frac{1}{1-\varepsilon}\left(1 - \varepsilon\frac{1-s}{\sqrt{-2s+s^2+\varepsilon^2}}\right), \qquad s < 0 \qquad \text{(N.17)}$$

The outer and inner expansions can be extracted from this by expanding for small ε in terms of s and $S = \varepsilon^2 s$, respectively. Thus it is seen that the denominator of the multiplicative rule vanishes at about half a nose radius ahead of the edge. For example, the 2-term outer expansion of the 1-term inner expansion is $1 - \varepsilon(-2s)^{-1/2}$, which vanishes at $s = -\varepsilon^2/2$.

Similarly, W. Reddall (unpublished) found in working Exercise 9.3 that the multiplicative composite formed from two terms of the outer and one term of the inner expansion has a denominator that vanishes at $(1 - A)\varepsilon y = 2$. To avoid this danger, the additive rule (5.32) should ordinarily be preferred, as it largely has been in the literature, despite some attractive features of the multiplicative rule.

At the stagnation point of the ellipse, with two terms of the outer expansion and one of the inner, Ellinwood's alternative composites based on f^2, f, and $\log f$ give velocities of order $\varepsilon^{1/2}$, ε, and 0, respectively. This illustrates that different composite expansions may have different accuracies, and that the error may exceed that of either of the constituent expansions.

Note 7. Utility of the Method of Strained Coordinates

Although the method of strained coordinates (Chapter 6) has now been applied to a considerable variety of problems in fluid mechanics (and a few in other fields), the question of when it can be relied upon is not settled. Mathematicians have studied the method only for ordinary differential equations (e.g., Comstock, 1972), which provides scant guidance for partial differential equations. From time to time a solution previously calculated by straining is found to be erroneous by a worker using a more pedestrian but reliable method (e.g., Jischke, 1970).

It seems amply confirmed that no difficulties arise if the governing equations are hyperbolic, as they are in the majority of applications. The generalization of Lin (p. 100) that consists in successively refining two families of characteristic lines has been further developed by Oswatitsch (1962a, b) as the *analytic method of characteristics,* and applied by him and his colleagues to a number of problems in gas dynamics (cf. Stuff, 1972).

The straining must, however, be carried out for the physical ("primitive") variables—velocity, pressure, temperature, etc.—rather than for such constructs as the velocity potential or stream function. For example, treating the problem of supersonic flow past a thin airfoil using the perturbation velocity potential (6.28) rather than the streamwise velocity increment (6.30) yields only half the correct straining function in Eq. (6.35).

Strained coordinates cannot generally be applied to parabolic equations, as in boundary-layer theory. However, they prove effective in a wake. Crane (1959) showed that straining provides an attractive alternative to the logarithmic terms that Stewartson (1957) had to introduce into Goldstein's (1933) expansion for the laminar wake far behind a flat plate in order to maintain exponential decay of vorticity. (This requirement, discussed on page 131, would appear to be different from Lighthill's principle of Eq. (6.1), but non-exponential decay leads to singularities at the next step.) Berger (1968) shows that straining succeeds in the same way for the axisymmetric far wake.

The situation is similarly unclear for elliptic equations. The criticism (p. 119) that Lighthill's success with a round-nosed airfoil in incompressible flow cannot be extended to higher order has been refuted by Bollheimer and Weissinger (1968) and Hoogstraten (1967), who show that it is only necessary to strain both coordinates slightly, or in fact the single complex variable $x + iy$. However, Hoogstraten finds that difficulties persist for other nose shapes.

Although the equations of supersonic flow are hyperbolic, they become elliptic inside the Mach cone in conical flow. Lighthill (1949b) found the conical shock wave using strained coordinates; but Melnik (1965b) emphasizes that the method fails near the triple point where the plane shock wave from a supersonic edge meets the nearly circular conical wave from the vertex. There he shows that the method of matched expansions can be used to join five different boundary layers (which were studied earlier by Bulakh, 1961).

Melnik also shows how the vortical layer on a cone in supersonic flow can be matched directly to the outer flow. (He gives a useful comparison with other less accurate solutions, including that of Munson, 1964.) However, in the hypersonic thin-shock-layer approximation he finds (Melnik 1965a) that there is no overlap until the method of strained coordinates is applied to minimize the nonuniformity of the outer solution near the surface (as an alternative to introducing an intermediate third region). This idea of combining the method of strained coordinates with the method of matched asymptotic expansions has been applied also to two problems in gas dynamics by Crocco (1972) and to a hypersonic boundary layer by Matveeva and Sychev (1965).

Note 8. Flat Plate at High Reynolds Number; Triple Decks

Much effort has been devoted in the past decade to improving the solutions for viscous flow past the semi-infinite flat plate and the finite plate at large Reynolds number.

The eigensolutions discussed in Section 7.6 have been studied further by Murray (1965, 1967), Brown (1968), and Ting (1968). A solution for the semi-infinite plate can be evaluated by how well it predicts the coefficient C_1 of the first of these eigensolutions in the expansions (7.46), (7.47) for skin friction far downstream, as well as the undetermined constants in the Stokes expansion (3.24) near the leading edge, which (with those constants redefined) gives the local skin friction as

$$c_f = A\ R_x^{-1/2} + B\ R_x^{1/2} - \frac{\pi}{32}A^2\ R_x + \cdots \qquad \text{(N.18)}$$

The most reliable values are given by Botta and Dijkstra (1970) who, refining the procedure of van de Vooren and Dijkstra (1970), carried out a careful finite-difference solution of the Navier-Stokes equations in parabolic coordinates, using three different mesh sizes, and being guided by all that is known of the analytical structure of the solution. They were only able to estimate $2.2 < C_1 < 2.5$, but found $A = 0.75475 \pm 0.00005$ and $B = 0.041$. [A less detailed finite-difference solution (Yoshizawa, 1970) gave $C_1 = 1.6$, $A = 0.748$, and $B = 0.044$.] This value of A means that the skin friction near the leading edge is 14 per cent higher than the Blasius value.

Finite plate. Our understanding of viscous flow past a finite flat plate (Section 7.9) has been revolutionized by the simultaneous discovery of Stewartson (1969) and Messiter (1970) that at high Reynolds number the flow near the trailing edge has a compound structure that Stewartson calls the *triple deck.* It comprises a region around the trailing edge whose extent is of order $R^{-3/8}$ times the length of the plate, and which matches upstream with the classical Blasius solution and its associated outer flow and downstream with the two-layered wake analyzed by Goldstein (1930). It consists of three layers, in each of which the Navier-Stokes equations can be approximated in a different

way, as shown in Fig. N.1 (which is a composite of the drawings of Messiter and Stewartson). There is also a small circular core in which,

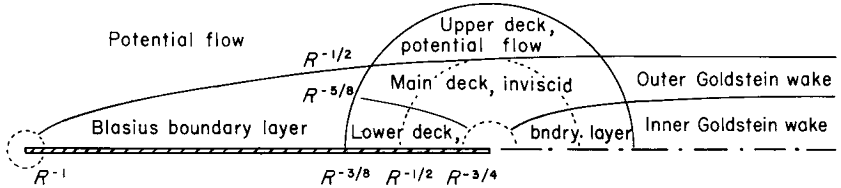

Fig. N.1. Schematic picture of matching regions for flow past finite flat plate at high Reynolds number; primary regions shown by solid lines and secondary regions by dashed lines.

just as in the corresponding vicinity of the leading edge, the full equations apply. (These, and another circular region of size $R^{-1/2}$ about the trailing edge, are shown dashed because they affect only higher approximations.)

This structure contributes a correction to the Blasius drag that is of order $R^{-7/8}$, and hence slightly more important than the displacement effects of order R^{-1} calculated by Kuo (p. 136) and Imai (p. 138). Thus Equation (7.40) is corrected to

$$c_F = \frac{1.328}{R^{1/2}} + \frac{2.661}{R^{7/8}} + O\left(\frac{1}{R}, \frac{1}{R^{7/6}}, \frac{1}{R^{5/4}}\right) \qquad \text{(N.19)}$$

The coefficient 2.661 was evaluated numerically by Melnik and Chow (1975); Jobe and Burggraf give instead 2.694, and Veldman and van de Vooren (1974) find 2.651 ± 0.003. Of the subsequent terms, that of order R^{-1} arises from the trailing-edge region of size $R^{-3/8}$ as well as from the displacement effects, that of order $R^{-7/6}$ from the region of size $R^{-1/2}$, and that of order $R^{-5/4}$ from the region of size $R^{-3/4}$.

That last small region was treated approximately by Stewartson (1968), and later Dijkstra (1974) solved the full Navier-Stokes equations numerically. They both found that the Stokes solution (3.24) of Carrier and Lin (1948) applies locally at the trailing as well as the leading edge. Dijkstra evaluated the coefficient of that square-root singularity in local skin friction, but was unable to find the coefficient of the term in the drag (N.19) of order $R^{-5/4}$.

Jobe and Burggraf find that the two-term approximation (N.19) agrees unexpectedly well with both experimental measurements (Janour, 1947) and numerical solutions of the Navier-Stokes equations (Dennis and Dunwoody, 1966, Dennis and Chang, 1969). This means that the subsequent terms must either have much smaller coefficients than the first two, or tend to cancel one another.

The triple-deck structure has been extended to a plate at an angle of attack of order $R^{-1/16}$ by Brown and Stewartson (1970), to an airfoil with a finite trailing-edge angle of order $R^{-1/4}$ by Riley and Stewartson (1969), and to a three-dimensional wing with a pair of eddies at the trailing edge by Guiraud (1974).

Separated flow. The multistructured boundary layer that Stewartson calls the triple deck was discovered at the same time for the flat plate and for the region of free interaction near a separation point in supersonic flow. The latter problem was analyzed independently by Stewartson and Williams (1969) and by Neiland (1969), who show that the primary regions have the same dimensions as in Fig. N.1. Neiland (1971) later matched that local solution to a four-layered region of separated flow farther downstream, and found agreement with experimental measurements of the "plateau" pressure.

The same structure persists near separation at hypersonic speeds if the hypersonic interaction parameter $\chi = M/R^{1/2}$ is small; but otherwise Neiland (1970) has shown that the region of free interaction is of the order of the length of the body. It depends on an eigensolution that grows from the leading edge as a high power of distance. Kozlova and Mikhailov (1970) show that a similar non-uniqueness arises for an infinite yawed wing, and in the case of an infinite triangular wing permits the flows on the two halves to meet smoothly on the centerline.

Sychev (1972) has explained how the structure of Fig. N.1 applies also to separation from a smooth body in incompressible flow. An adverse pressure gradient of magnitude $R^{1/8}$ acts over the interaction region of length $R^{-3/8}$, and in the limit the local pattern is the inviscid free-streamline flow that has bounded curvature. Sychev shows that this structure is compatible with flows upstream and downstream, which have also been studied by Messiter and Enlow (1973). Messiter (1975) discusses how this model, though formally self-consistent, is not yet complete because of our ignorance of the global structure of the recirculating wake, which could, for example, induce an infinite sequence of vortices below the separation streamline.

All these problems, and others involving multistructured boundary layers, have been comprehensively surveyed by Stewartson (1974).

Note 9. Extension of the Idea of Optimal Coordinates

Kaplun (1954) limited his study of the role of coordinate systems in boundary-layer theory to incompressible, steady, plane flow past a solid body without separation, and with an irrotational oncoming stream. He promised to remove those restrictions in a later paper, but did not live to write it.

Legner (1971) has shown that Kaplun's rule (7.56b) for constructing optimal coordinates applies unchanged to axisymmetric flows, to oncoming streams containing vorticity, to boundary layers with no adjacent walls, such as jets and wakes, to free-convection boundary layers, to compressible fluids, and to uncoupled and coupled thermal boundary layers. It is implicit in his reasoning that Kaplun's correlation theorem (7.50b) also applies to all those flows. In addition, Legner has extended the rule for constructing optimal coordinates to unsteady boundary layers, and to three-dimensional ones in terms of Clebsch's pair of stream functions. He gives examples for many of these situations.

Kaplun also limited consideration to the first-order boundary layer plus the resulting outer flow due to displacement. We have given the second-order correlation theorem in Exercise 7.4, and it clearly applies also to the first group of problems just mentioned, and could no doubt be extended to the second group.

Legner has also extended Kaplun's rule for optimal coordinates to arbitrarily high order. Let the solution be carried out in any convenient coordinate system x, y. The outer expansion will be a continuation of the form (7.48a):

$$\psi \sim \psi_1(x, y) + R^{-1/2}\,\psi_2(x, y) + R^{-1}\,\psi_3(x, y) + R^{-3/2}\,\psi_4(x, y) + \cdots \tag{N.20}$$

Then optimal coordinates are given by the generalization of (7.56b)

$$\begin{aligned} \xi_{\text{opt}}(x, y) &= F_1[\psi_2(x, y) + R^{-1/2}\,\psi_3(x, y) + R^{-1}\,\psi_4(x, y) + \cdots] \\ \eta_{\text{opt}}(x, y) &= \psi_1(x, y)\, F_2[\psi_2(x, y) + R^{-1/2}\,\psi_3(x, y) + \cdots] \end{aligned} \tag{N.21}$$

If logarithms of R appear in the outer expansion, they are simply to be included here in the obvious way.

Legner has verified this rule to second or higher order in a number of specific examples. Davis (1974) points out that, in contrast to Kaplun's result, this rule is not completely general. However, he adopts it in showing how optimal coordinates can prove advantageous in numerical solution of the Navier-Stokes equations. On the other hand, L. E. Fraenkel (unpublished) has questioned the demonstration that (N.21) yields optimal coordinates. Thus the extension to second and higher order remains to be resolved.

The "shrinking rectangular" coordinates of Fig. 7.8 are an unnecessarily artificial choice to illustrate that the boundary layer may not contain even the basic outer flow. Polar coordinates, which are an attractive system for the semi-infinite plate, also display this total lack of optimality.

Note 10. The Sphere and Circle at Low Reynolds Number

Chester and Breach (1969) have, in a difficult computation, continued the analysis of Proudman and Pearson (1957) to include one higher power of Reynolds number. Thus they extend the series (1.4) for the drag coefficient of a sphere by two terms to find

$$C_D = \frac{6\pi}{R}\left[1 + \frac{3}{8}R + \frac{9}{40}R^2 \log R + \frac{9}{40}\left(\gamma + \frac{5}{3}\log 2 - \frac{323}{360}\right)R^2 + \frac{27}{80}R^3 \log R + O(R^3)\right] \tag{N.22}$$

Here $\gamma = 0.5722 \ldots$ is Euler's constant.

This result is disappointing, because comparison with experiment suggests that the range of applicability has scarcely been increased. Chester and Breach conclude that "the expansion is of practical value only in the limited range $0 \leqslant R \leqslant 0.5$ and that in this range there is little point in continuing the expansion further." Below $R = 0.3$, however, Dennis and Walker (1971) find that it gives a better approximation than any other asymptotic solution to the drag that they calculate numerically.

This limited utility contrasts with that of regular perturbation expansions, which have recently been found actually to converge for Reynolds numbers considerably larger than unity. For example, Kuwahara and Imai (1969) have calculated by computer (cf. Note 2) eight terms of a power series in R for the steady plane flow produced inside a circle by tangential motion of the boundary, and estimate convergence up to about $R = 32$ in three different cases. Again, Hoffman (1974b) has computed 17 terms for the self-similar flow between infinite concentric rotating disks, and finds convergence up to $R = 15$ for the case of one disk fixed and $R = 42$ for equal contra-rotation.

In an appendix to the paper of Chester and Breach, Proudman suggests that the limited utility of their series is due to the unsuitability of the drag for expansion in terms of Reynolds number, and attempts to recast it into more appropriate form. Clearly some such reinterpretation of the terms containing log R is necessary in order that the result be useful for R greater than unity. (Cf. Note 15.)

We may ask whether Chester and Breach's last term is correct, since they have violated the warning of Fraenkel (1969a), discussed in Note 4, against separating like powers of R that differ only by powers of log R. To be sure, their solution itself shows that Proudman and Pearson happened to escape unscathed in calculating the term in R^2 log R while neglecting that in R^2. However, it is just at the next stage that ignoring Fraenkel's warning is known (Note 4) to lead to error in the simpler problem of diffraction by a thin semi-infinite plate.

It was mentioned on page 155 that whereas the Stokes approximation is a singular perturbation, the Oseen expansion appears to be a regular one. [Kaplun (1957) observed that this is a coincidence that disappears in compressible flow, where the Stokes approximation is nonlinear (Lagerstrom, 1964).] The second approximation for a sphere was calculated by C. R. Illingworth in 1947 (unpublished), who found for the drag coefficient

$$C_D = \frac{6\pi}{R}\left(1 + \frac{3}{8}R + \frac{9}{40}R^2 \log R + 0.1333\,R^2 + \frac{81}{320}R^3 \log R - 0.0034\,R^3 + \cdots\right) \tag{N.23}$$

Thus iterating on the solution of the Oseen equations extends the agreement with the Navier-Stokes drag from relative order R to R^2 log R, and subsequent iterations would no doubt produce further agreement.

Separated flow. Dorrepaal, Ranger, and O'Neill (1975) have discovered that the Stokes approximation is rich enough to predict separation on a finite body, provided it is concave. Furthermore, Ranger (1972) shows that in the diverging Jeffery-Hamel flow between plane walls the Reynolds number for separation is predicted within three per cent by two terms of the Stokes expansion, and for the channel of 45-degree half angle to within one and one-half per cent by four terms. In that problem the Stokes expansion is a regular perturbation, proceeding in powers of Reynolds number.

This suggests that it is no coincidence that in the singular perturbation problem of the sphere the standing eddy is described well by the two-term Stokes expansion, as shown in Figs. 8.3 and 8.4. [The

Reynolds number of 8 (based on radius) that it gives for the onset of separation may also be compared with the recent values of 10 from finite-difference solution of the Navier-Stokes equations (Pruppacher, Le Clair, and Hamielec, 1970), 10.25 from series truncation (Dennis and Walker, 1971), and 8.5 from flow visualization (Payard and Coutanceau, 1971).] However, Eq. (8.38) for the Reynolds number at separation can be extended, using the solution of Chester and Breach (1969), to give

$$1 - \frac{1}{8}R + \frac{9}{40}R^2\left(\log R + \frac{5}{3}\log 2 + \gamma + \frac{83}{840}\right) + O(R^3 \log R) = 0 \tag{N.24}$$

and Ranger (1972) points out that this again has no real root, nor does the result of including the term in $R^3 \log R$. Once more it seems that the logarithm needs reinterpretation.

The solution of Skinner (1975) provides a corresponding equation for the circular cylinder:

$$\begin{aligned}(\Delta_1 - 0.87\,\Delta_1^3 + \cdots) &- \frac{1}{2}R\left(1 - \frac{1}{2}\,\Delta_1 + \cdots\right)\\ &- \frac{7}{96}R^2\left(1 - \frac{3}{14}\Delta_1 + \cdots\right) + O(R^3) = 0 \end{aligned}\tag{N.25}$$

where $\Delta_1 = (\log 4/R - \gamma + \frac{1}{2})^{-1}$. Two terms give separation at $R = 1.12$, and three terms at $R = 1.0$, which may be compared with the value 2.88 computed by Underwood (1969) using series truncation (and Yamada's value, quoted on page 156, of 1.51 for the Oseen approximation). This rough agreement seems satisfactory, since the quantity Δ_1 that is assumed small is then equal to 0.8.

Note 11. Transcendentally Small Terms

A perturbation solution that yields a formal series in powers of ε will never include such exponentially small terms as $e^{-1/\varepsilon}$. An example showing how they may be numerically important is the asymptotic expansion (Olver, 1964)

$$\begin{aligned}\int_0^\pi \frac{\cos nt}{t^2+1}dt \sim \frac{\pi}{2}e^{-n} + (-)^{n-1}\Bigg[&\frac{2\pi}{(\pi^2+1)^2}\frac{1}{n^2}\\ &- 24\pi\frac{\pi^2-1}{(\pi^2+1)^4}\frac{1}{n^4} + \cdots\Bigg] \quad \text{as } n\to\infty\end{aligned}\tag{N.26}$$

Even at $n = 10$ the exponentially small term contributes 15 per cent of the total. Dingle (1973) has persuasively argued the case for seeking a "complete asymptotic expansion," including any sets of exponentially small terms that may be present.

Regular perturbations seem usually to be free of such terms. For example, each of the series discussed in Notes 2 and 10 that has been extended to high order by computer appears to represent an analytic function of the perturbation quantity, having a finite radius of convergence in the complex plane. On the other hand, Terrill (1973) has shown that in the singular perturbation problem of laminar flow through a porous pipe at high Reynolds number, the first set of exponentially small terms is needed to explain the nature of the solution. A numerical computation showed that there are dual solutions for $R > 9.1$ and none for $2.3 < R < 9.1$. Matching a boundary layer to the inviscid core in conventional fashion gave only a single solution in powers of R^{-1}. However, including terms in e^{-R} yields dual solutions for $R > 9.1$ and none for $3.3 < R < 9.1$, in remarkable agreement with the numerical results. Likewise, Adamson and Richey (1973) found exponentially small terms essential for treating transonic flow through a nozzle with shock waves.

Bulakh (1964) has included exponentially small terms in the outer expansion of the boundary-layer solution for converging flow between plane walls, and checked with the exact Jeffery-Hamel solution. He shows that such terms will arise also in the higher-order boundary-layer solution at a plane or axisymmetric stagnation point, and in other problems.

In the "purely logarithmic case," where straightforward matching yields outer and inner expansions in powers of $(\log 1/\varepsilon)^{-1}$ or $(\log K/\varepsilon)^{-1}$, terms of order ε and higher powers often appear. As mentioned on page 165 (see also Exercise 8.5), such transcendentally small terms were discussed tentatively by Proudman and Pearson (1957) for flow past a circle at low Reynolds number. Skinner (1975) has systematically examined the first two sets of transcendentally small terms in that problem. He finds that terms in R affect the symmetry of the flow pattern significantly even at $R = 0.025$, but do not contribute to the drag. Terms in R^2 extend Kaplun's result (8.49) for the drag coefficient to

$$\begin{aligned}C_D \sim \frac{4\pi}{R}\Bigg\{&\Delta_1 - 0.87\,\Delta_1^3 + O(\Delta_1^4)\\ &- \frac{1}{32}R^2\left[1 - \frac{1}{2}\Delta_1 + O(\Delta_1^2)\right] + O(R^4)\Bigg\}\end{aligned}\tag{N.27}$$

However, it is clear from Fig. 8.5 that at least for $R > 0.4$ this correction is in the wrong direction, no doubt because it is smaller than the unknown term of order Δ_1^4 in Kaplun's expansion.

Note 12. Viscous Flow Past Paraboloids

Paraboloids enjoy many simple and remarkable properties in fluid mechanics, in both potential and viscous flows. We have seen in Sections 4.6, 4.8, 4.9, 10.6, 10.8, and 10.9 how they serve as models for more complicated flows, or as elements in their solution.

Laminar flow along the axis of a parabolic cylinder has been calculated numerically, as a generalization of the flow past a semi-infinite plate, by several of the groups of workers cited in Note 8. Dennis and Walsh (1971), Davis (1972), and Botta, Dijkstra, and Veldman (1972) independently solved the Navier-Stokes equations in parabolic coordinates by finite-difference methods over the range of Reynolds number from zero, corresponding to the flat plate, to infinity, corresponding to Prandtl's boundary-layer approximation. The three solutions give the same local skin friction to within a fraction of a per cent. A striking conclusion is that second-order boundary-layer theory, as represented by the friction near the leading edge (Fig. N.2), is of little practical utility, for it departs rapidly from the exact solution as the Reynolds number decreases.

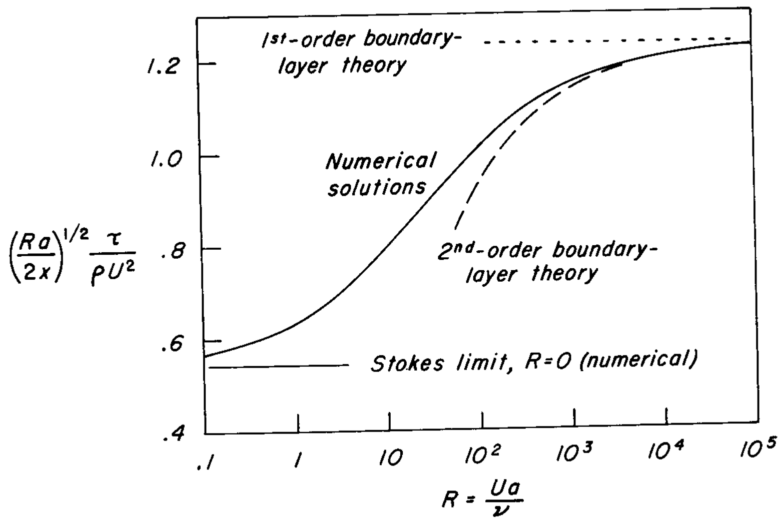

Fig. N.2. Skin friction at leading edge of parabolic cylinder.

Werle and Davis (1972) have calculated numerically the boundary layer on a parabola in asymmetric flow. They inevitably encounter the square-root singularity of Goldstein (1948) whenever the skin friction vanishes.

The expansion at low Reynolds number for axisymmetric flow past a paraboloid of revolution is discussed in Note 4. Davis and Werle (1972) and Veldman (1973) have solved the Navier-Stokes equations numerically over the whole range of Reynolds number.

Note 13. Lifting Wing of High Aspect Ratio

Kerney (1972) has discovered that the integrals in Eq. (9.15) were evaluated incorrectly by Van Dyke (1964b) for the elliptic wing. The expression (9.18) for the circulation is to be replaced by

$$\frac{\Gamma}{\Gamma_\infty} = 1 - \frac{2}{A} - \frac{4}{\pi^2}\frac{\log A}{A^2}\frac{3-2z^2}{1-z^2} + \frac{4}{\pi^2}\frac{1}{A^2}\left[\frac{5}{2} + \pi^2 + \frac{2z^2}{1-z^2} - \log(1-z^2) - \frac{\log 2(1-z^2)}{1-z^2} - \frac{3-2z^2}{1-z^2}\log\frac{\pi}{\sqrt{1-z^2}}\right] + \cdots \tag{N.28}$$

Integrating this changes the result (1.6) for the lift-curve slope to

$$\frac{dC_L}{d\alpha} = 2\pi\left[1 - \frac{2}{A} - \frac{16}{\pi^2}\frac{\log A}{A^2} + \frac{4}{\pi^2}\left(\frac{9}{2} + \pi^2 - 4\log\pi\right)\frac{1}{A^2} + \cdots\right] \tag{N.29}$$

Correspondingly, when this is recast by analogy with Prandtl's result (9.1a) it gives, in place of (10.27),

$$\frac{dC_L}{d\alpha} \approx \frac{2\pi}{1 + \dfrac{2}{A} + \dfrac{16}{\pi^2}\left(\log \pi A - \dfrac{9}{8}\right)\dfrac{1}{A^2}} \tag{N.30}$$

These corrected results are compared with lifting-surface theory in Fig. N.3, which replaces Fig. 9.4. Krienes's results from lifting-surface theory have been replaced by the following refined values calculated by R. T. Medan using the method of Medan (1974):

A:	$1/\pi$	$2/\pi$	$8/\pi$	$16/\pi$
$dC_L/d\alpha$:	0.496 ± 0.002	0.969 ± 0.006	2.944 ± 0.004	4.151 ± 0.004

together with the value 1.7900230 found by Jordan (1971) for the circular wing ($A = 4/\pi$). Correcting the error has slightly improved the agreement at high aspect ratio, while worsening it at low values.

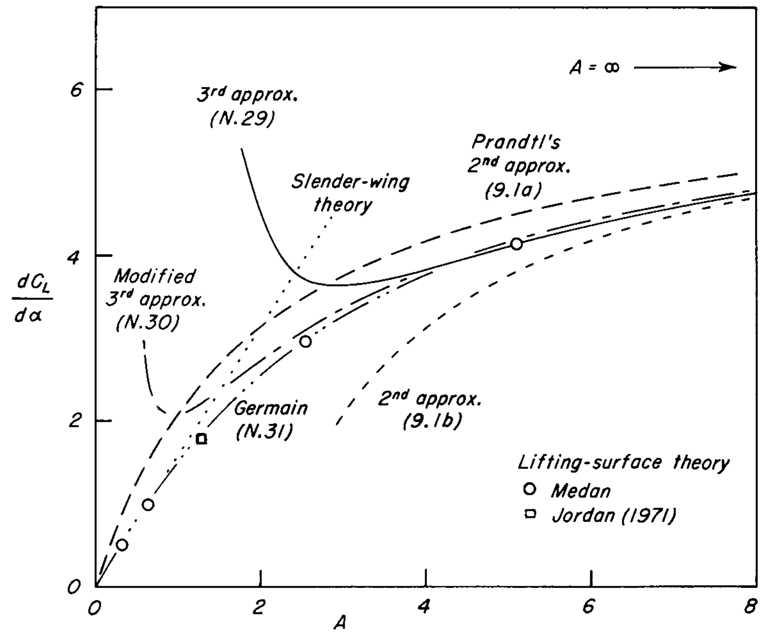

Fig. N.3. Lift-curve slope of elliptic wing (correction of Fig. 9.4).

Germain (1967) has suggested an alternative recasting of (1.6) that is better for small aspect ratio A. When corrected for the error in (1.6) it becomes

$$\frac{dC_L}{d\alpha} \approx \frac{2\pi}{1 + \frac{2}{A} + \frac{16}{\pi^2}\frac{1}{A^2}\log(1 + \pi e^{-9/8}A)} \qquad \text{N.31)}$$

Fig. N.3 shows that this version provides a very close approximation over the whole range of A. For small values it gives $1.72\,A$, compared with the exact limit of $(\pi/2)A = 1.57\,A$ from slender-wing theory.

Thurber (1965) has treated the more general case of a wing of smooth symmetrical swept-back planform, and finds that the logarithm of the aspect ratio then appears in the second rather than the third approximation. Thus the circulation has, instead of (9.15), the form

$$\frac{\Gamma}{\Gamma_\infty} = 1 + \frac{\log A}{A}f_1(z) + \frac{1}{A}f_2(z) + \cdots \qquad (\text{N.32})$$

and Thurber gives expressions for evaluating the functions f_1 and f_2 in terms of the geometry of the planform.

Kerney (1971) and Tokuda (1971) independently analyzed the straight wing with a jet flap. However, their results differ, and the discrepancies have not yet all been resolved.

Note 14. The Method of Multiple Scales

This book is relatively strong on the method of matched asymptotic expansions, but weak on the method of multiple scales (Sec. 10.4). The reason is that multiple scales were just being developed when it was written. That technique has flourished in the last decade, so as to be second in importance only to matched expansions for fluid mechanics. It is not possible to redress the balance in these Notes; we must refer the reader elsewhere.

Cole (1968) devotes a chapter to what he calls "two-variable expansion procedures," but gives no applications to partial differential equations, and the same is true of the useful article by Kevorkian (1966). The most complete account is Chapter 6 of Nayfeh (1973). He distinguishes three variants of the method:

1. The *many-variable* or *derivative-expansion method.* One works with (the first few of) an unlimited number of successively slower simple scales, for example,

$$X_1 = x, \qquad X_2 = \varepsilon x, \qquad X_3 = \varepsilon^2 x, \qquad \cdots \qquad (\text{N.33})$$

2. The *two-variable expansion method.* The slower scale is simple, and the faster scale slightly stretched (linearly), for example,

$$X_1 = x(1 + c_2\varepsilon^2 + c_3\varepsilon^3 + \cdots), \qquad X_2 = \varepsilon x \qquad (\text{N.34})$$

No term in $c_1\varepsilon$ is ordinarily needed in X_1 because it is accounted for by X_2.

3. The *generalized method.* The slower scale is simple, and the faster scale strained nonlinearly, for example,

$$X_1 = \frac{g_1(x)}{\varepsilon} + g_2(x) + \varepsilon g_3(x) + \cdots, \qquad X_2 = x \tag{N.35}$$

Here again examples suggest that the term $g_2(x)$ could be omitted.

As a matter of fact, most of the problems in fluid mechanics that have been solved using the method of multiple scales require only the primitive version with just two simple scales, say x and εx, either strictly or because the expansion has been carried only to low order. Some typical recent examples are Hinch and Leal (1973), Grimshaw (1974), and Nayfeh and Tsai (1974).

Still other variants are encountered in the literature. Levey and Mahony (1968) slightly stretch the slower rather than the faster scale:

$$X_1 = x, \qquad X_2 = \varepsilon x(1 + d_1\varepsilon + d_2\varepsilon^2 + \cdots) \tag{N.36}$$

and Peyret (1970) slightly stretches both:

$$X_1 = x(1 + c_1\varepsilon + c_2\varepsilon^2 + \cdots),$$
$$X_2 = \varepsilon x(1 + d_1\varepsilon + d_2\varepsilon^2 + \cdots) \tag{N.37}$$

Any problem that can be solved by matched expansions can also be solved by multiple scales, though less efficiently. The method of multiple scales is therefore reserved for problems where matched expansions do not apply, typically problems involving slowly modulated oscillations or waves.

Some writers mistakenly suggest that the method of multiple scales yields results valid over an indefinitely long range. In general, the solution is valid only to $x = O(\varepsilon^{-1})$ if the short and long scales are x and εx. An example is the "aging spring" (Cheng and Wu, 1970), governed by the equation

$$\ddot{x} + e^{-\varepsilon t}\, x = 0 \tag{N.38}$$

where the solution by multiple scales holds only for $\varepsilon e^{\varepsilon t/2} \ll 1$.

Note 15. Analysis and Improvement of Series

Since this book was written the author has learned several ways, in addition to those discussed in Sections 10.6–10.8, for improving the utility of a perturbation series. These apply mostly to regular perturbations, where the solution is found (aside perhaps from a multiplicative function) as a formal power series in the perturbation quantity. Then the power of complex analysis can be brought to bear by considering the perturbation quantity in the complex plane, even though it usually has physical significance only for positive real values.

For power series we thus have a battery of devices that can be used (Van Dyke, 1974) to unveil in part the analytic structure of the solution, and then exploit that knowledge to increase the accuracy of the series or extend its range of validity. Together with the growing use of the computer to calculate many terms (Note 2), this process of analysis and improvement provides a three-step program for treating regular perturbations (Van Dyke, 1976):

i. Extend the series to high order by delegating the routine arithmetic labor to the digital computer.
ii. Examine the coefficients to reveal the analytic structure of the solution in the complex plane of the perturbation quantity.
iii. Transform the series as suggested by that structure.

This semi-numerical program represents, at least for certain simple problems, a more effective use of the computer than finite-difference or other purely numerical schemes. Greater accuracy can be achieved in shorter computing times, and the solution is found as a function of the perturbation quantity, rather than for just a few fixed values. Complete success consists in starting with an expansion predicated on vanishingly small values of a perturbation quantity, and recasting the series to yield accurate results over the entire range of physical interest. Two such triumphs are discussed in Note 2: Schwartz's (1974) recasting of Stokes's series to render it convergent for the highest water wave, and Van Dyke's (1970) transformation of Goldstein's series for the Oseen drag of a sphere at low Reynolds number, giving three-figure accuracy at infinite Reynolds number.

Singular perturbation series, especially those involving logarithms of the perturbation quantity, often seem to cry out for improvement, but no general approach is known. In the "purely logarithmic" case, where the expansion has the form

$$f(\varepsilon) = \frac{A}{\log(1/\varepsilon)} + \frac{B}{(\log 1/\varepsilon)^2} + \frac{C}{(\log 1/\varepsilon)^3} + \cdots \qquad \text{(N.39)}$$

the first two terms can be telescoped into one, giving

$$f(\varepsilon) = \frac{A}{\log K/\varepsilon} + \frac{C_2}{(\log K/\varepsilon)^3} + \cdots \qquad \text{(N.40)}$$

with $K = e^{-B/A}$. As mentioned on page 163, Kaplun chose this form (Eq. 8.49) for the drag of a circular cylinder at low Reynolds number, whereas Proudman and Pearson (1957) used the first form. Figure N.4 (which should be compared with Fig. 8.5) shows that this modification

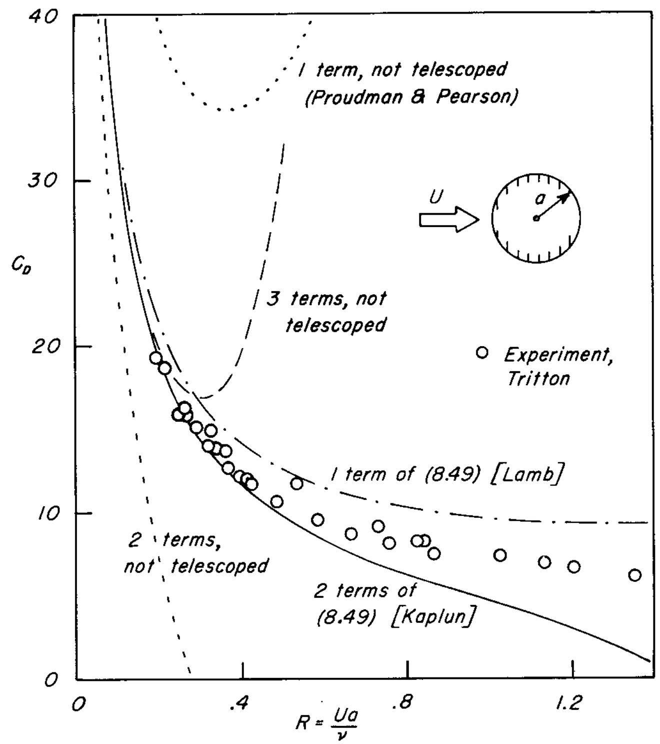

Fig. N.4. Effect of telescoping terms for drag of circular cylinder at low Reynolds number.

greatly improves the accuracy at any stage. In certain linear problems, and for special geometries, an infinite number of terms can in this way be telescoped into one, as Batchelor (1970) has pointed out for Stokes flow past a slender particle.

In the case of products of powers of ε and its logarithm, we know of only two attempts at improvement: our recasting (N.30) of the series (N.29) for the lift-curve slope of an elliptic wing by analogy with Prandtl's first-order result (9.1a), which was further recast by Germain into the form (N.31); and Proudman's proposed reinterpretation (Note 10) of the series (N.22) for the drag of a sphere at low Reynolds number.

The nearest singularity; Domb-Sykes plots. The most useful way of analyzing the structure of a power series through its coefficients is to investigate the nature of the nearest singularity in the complex plane of the perturbation quantity. First, the direction of the nearest singularity is revealed by the pattern of signs. If the terms of the series sooner or later settle down to a fixed sign—all positive or all negative—as appears to be the case in Eqs. (1.1) and (10.29), the singularity lies on the positive real axis. A particularly well behaved example displaying this pattern is the series of Howarth (1938) for the skin friction in a laminar boundary layer with decreasing external speed given by $U = U_0(1 - x/8l)$:

$$c_f = \frac{1}{4}R_x^{-1/2}[1.328242 - 1.02054(x/l) - 0.06926(x/l)^2 - 0.0560(x/l)^3 - 0.0372(x/l)^4 - 0.0272(x/l)^5 - 0.0212(x/l)^6 - 0.0174(x/l)^7 - 0.0147(x/l)^8 - \cdots] \qquad \text{(N.41)}$$

More often the signs alternate, as in Eqs. (1.3), (1.5), (1.7), (10.21), and (10.22), and this means that the singularity lies on the negative real axis. Other more complicated patterns are occasionally encountered, and can be interpreted similarly.

The distance to the nearest singularity—that is, the radius of convergence—can be estimated by graphical application of the d'Alembert ratio test, according to which the power series

$$f(\varepsilon) = \sum^{\infty} c_n \varepsilon^n \qquad \text{(N.42a)}$$

has radius of convergence

$$\varepsilon_0 = \lim_{n\to\infty}\left|\frac{c_n - 1}{c_n}\right| \qquad \text{(N.42b)}$$

A straightforward plot of $|c_{n-1}/c_n|$ versus n is ineffective, as illustrated for Howarth's series (N.41) in Fig. N.5a. Instead, Domb and Sykes

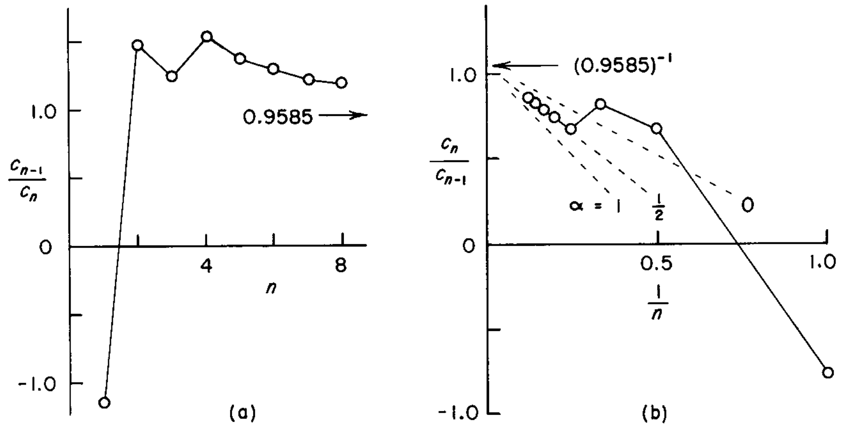

Fig. N.5. Graphical ratio test for Howarth's series (N.41). (a) Straightforward plot. (b) Domb-Sykes plot.

(1957) recommend inverting both scales, plotting $|c_n/c_{n-1}|$ versus $1/n$. This has the obvious advantage of requiring extrapolation to the origin rather than infinity. More important, the extrapolation is often nearly linear, as in Fig. N.5b. The reason for this is that if

$$f(\varepsilon) = \text{const} \times \begin{cases} (\varepsilon_0 \pm \varepsilon)^\alpha, & \alpha \neq 0, 1, 2, \cdots \\ (\varepsilon_0 \pm \varepsilon)^\alpha \log(\varepsilon_0 \pm \varepsilon), & \alpha = 0, 1, 2, \cdots \end{cases} \tag{N.43a}$$

then

$$\frac{c_n}{c_{n-1}} = \mp\frac{1}{\varepsilon_0}\left(1 - \frac{1+\alpha}{n}\right) \tag{N.43b}$$

so that the Domb-Sykes plot is straight. It seems that in many physical problems the nearest singularity starts with this algebraico-logarithmic form, so that the plot is asymptotically straight. Then the radius of convergence is readily estimated as the reciprocal of the intercept at $1/n = 0$. In Fig. N.5b that value clearly corresponds to the singularity at the separation point, which is known from numerical calculations (Leigh, 1955) to lie at $x/l = 0.9585$. At the same time the nature of the nearest singularity is revealed by the slope of

the asymptote. Thus Fig. N.5b clearly shows a slope corresponding to $\alpha = \frac{1}{2}$, and this agrees with the local analysis of Goldstein (1948) and Stewartson (1958), which shows a multiple singularity at the separation point dominated by a square root.

The Domb-Sykes plot is seldom so straight as in this example. Other weaker or more distant singularities can make it curved, kinked, oscillatory, zig-zag, sluggish, or irregular. Examples of these possibilities, drawn from problems in viscous flow, are shown in Van Dyke (1974), together with examples of zero and infinite radius of convergence. Some useful modifications and refinements are described by Gaunt and Guttmann (1974) in the context of the thermodynamics of lattice models of crystals (the subject from which we have borrowed the Domb-Sykes plot).

A quite different alternative way of investigating the nature of the nearest singularity, and others in the complex plane, is to form rational fractions (Section 10.7), more commonly called *Padé approximants,* and examine the zeros of the denominator (p. 206). The use of Padé approximants for improving series has become very popular among physicists. Useful references are Baker (1965, 1975), Hunter and Baker (1973), and Gaunt and Guttmann (1974).

Note 16. The Resolution of Paradoxes

The method of matched asymptotic expansions is most striking when it resolves a long-standing paradox. D'Alembert's paradox was effectively resolved by Prandtl's boundary-layer theory. At the other extreme of low Reynolds number, the paradoxes of Stokes and Whitehead, clarified by Oseen, were resolved by Kaplun (1957) using matched expansions (Chapter 8). Without straining the definition, we may assert that each of the three problems sketched below stood as a paradox, "exhibiting an apparently contradictory nature," until resolved by the same method. Like the paradoxes of Stokes and Whitehead, each involves logarithmic divergence at infinity in a plane problem.

Filon's paradox. Filon (1928) studied steady viscous flow far from a cylinder using the Oseen approximation. In the second approximation he found the moment on an asymmetric shape as an angular-momentum integral that tended logarithmically to infinity as the contour increased. This difficulty was resolved by Imai (1951), who showed that the singularity in the second-order wake solution is cancelled by the third-order inviscid solution outside the wake. (The reasoning is analogous to that later used by Imai for the drag of a semi-infinite plate, discussed on page 138.) Chang (1961) has simplified this resolution of Filon's paradox by systematically applying the method of matched asymptotic expansions.

Planing at high Froude number. Green (1936) calculated the plane inviscid free-streamline flow for a flat plate of chord L planing on the surface of deep water at high Froude number $F = (Ug/L)^{1/2} = 1/\varepsilon^2$. His approximation suffers the defect that, because gravity was neglected, the free surface drops off logarithmically to infinity with distance. Rispin (1966) has resolved this defect by embedding Green's approximation into a systematic perturbation scheme as the first term of a local expansion, and matching to a distant expansion based on linear wave theory. The expansion near the plate is found to involve the logarithm of the Froude number from the second step, having just the form of the expansion (N.6) for diffraction near a semi-infinite plate. Ting and Keller (1974) have improved the solution by including the impact on the free surface of the jet thrown up by the plate.

Vortex rings. Whereas rectilinear vortices are conveniently idealized as having concentrated cores, a curved vortex induces upon itself a velocity that increases logarithmically with the inverse of its core radius. Some cut-off device therefore has to be introduced to simulate a vortex ring (Batchelor, 1967, p. 253). This difficulty was resolved by Tung and Ting (1967), who match the outer solution for a concentrated ring vortex to the inner solution for a diffusing rectilinear viscous vortex. As a result they find that as its core diffuses with the square root of time, the speed of the vortex ring decreases logarithmically with time. Saffman (1970) has corrected some algebraic errors.

Laminar mixing. In contrast to these successes, we note that "the riddle of the course of the viscous shear layer between two streams of different speeds" has apparently not, as stated on page 77, been solved by the matching of Ting (1959). Klemp and Acrivos (1972) show that when all higher-order effects are considered the lateral position of the mixing zone remains indeterminate by an amount of the order of its own width.

REFERENCES AND AUTHOR INDEX

The numbers in square brackets show the pages on which the references appear, so that this list serves as an author index.

ACRIVOS, A. *See* Klemp and Acrivos.

ABBOTT, I. H., and VON DOENHOFF, A. E. (1959). *Theory of Wing Sections.* Dover, New York. [47]

ADAMSON, T. C., JR., and FEO, A. (1975). Interaction between a shock wave and a turbulent boundary layer in transonic flow. *SIAM J. Appl. Math.* **29,** 121–145. [227]

ADAMSON, T. C., and RICHEY, G. K. (1973). Unsteady transonic flows with shock waves in two-dimensional channels. *J. Fluid Mech.* **60,** 363–382. [237]

ALDEN, H. L. (1948). Second approximation to the laminar boundary layer flow over a flat plate. *J. Math. and Phys.* **27,** 91–104. [139]

AOI, T. *See* Tomotika and Aoi.

BAKER, G. A., JR. (1965). The theory and application of the Padé approximant method. *Advances in Theoretical Physics,* (K. A. Brueckner, ed.), pp. 1–58. Academic Press, New York and London. [247]

BAKER, G. A., JR. (1975). *Essentials of Padé Approximants.* Academic Press, New York. [247]

BAKER, G. A., JR. *See* Hunter and Baker.

BATCHELOR, G. K. (1956). A proposal concerning laminar wakes behind bluff bodies at large Reynolds number. *J. Fluid Mech.* **1,** 388–398. [122]

BATCHELOR, G. K., (1967). *An Introduction to Fluid Dynamics.* Cambridge Univ. Press, London and New York. [248]

BATCHELOR, G. K., (1970). Slender-body theory for particles of arbitrary cross-section in Stokes flow. *J. Fluid Mech.* **44,** 419–440. [244]

BELLMAN, R. (1955). Perturbation methods applied to nonlinear dynamics. *J. Appl. Mech.* **22,** 500–502. [208]

BELLMAN, R. (1964). *Perturbation Techniques in Mathematics, Physics, and Engineering.* Holt, Rinehart & Winston, New York; Dover, New York, 1972. [xi]

BERGER, S. A. (1968). The incompressible laminar axisymmetric far wake. *J. Math. and Phys.* **47,** 292–309. [218, 229]

BERGER, S. A. (1971). *Laminar Wakes.* American Elsevier, New York. [218]

BERGER, S. A. *See* Viviand and Berger.

BERNDT, S. B. *See* Oswatitsch and Berndt.

BOLLHEIMER, L., and WEISSINGER, J. (1968). An application of the "PLK method" to conformal mapping and thin airfoil theory. *Zeit. Flugwiss.* **16,** 6–12. [229]

BOTTA, E. F. F., and DIJKSTRA, D. (1970). An improved numerical solution of the Navier-Stokes equations for laminar flow past a semi-infinite flat plate. *Rept. Math. Inst. Univ. Groningen* No. TW-80. [230]

BOTTA, E. F. F., DIJKSTRA, D., and VELDMAN, A. E. P. (1972). The numerical solution of the Navier-Stokes equations for laminar, incompressible flow past a parabolic cylinder. *J. Eng. Math,* **6,** 63–81. [238]

BREACH, D. R. (1961). Slow flow past ellipsoids of revolution. *J. Fluid Mech.* **10,** 306–314. [78]

BREACH, D. R. *See* Chester and Breach.

BRETHERTON, F. P. (1962). Slow viscous motion round a cylinder in a simple shear. *J. Fluid Mech.* **12,** 591–613. [77, 78]

Broderick, J. B. (1949). Supersonic flow round pointed bodies of revolution. *Quart. J. Mech. Appl. Math.* **2,** 98–120. [29]
Brown, S. N. (1968). An asymptotic expansion for the eigenvalues arising in perturbations about the Blasius solution. *Appl. Sci. Res.* **19,** 111–119. [230]
Brown, S. N., and Stewartson, K. (1970). Trailing-edge stall. *J. Fluid Mech.* **42,** 561–584. [232]
Bulakh, B. M. (1961). On some properties of supersonic conical gas flow. *J. Appl. Math. Mech.* **25,** 708–717. [78, 177, 180, 229]
Bulakh, B. M. (1964). On higher approximations in the boundary-layer theory. *J. Appl. Math. Mech.* **28,** 675–681. [237]
Burgers, J. M. *See* von Kármán and Burgers.
Burggraf, O. R. *See* Jobe and Burggraf.
Burns, J. C. (1951). Airscrews at supersonic forward speeds. *Aero. Quart.* **3,** 23–50. [36]
Bush, W. B. (1971). On the Lagerstrom mathematical model for viscous flow at low Reynolds number. *SIAM J. Appl. Math.* **20,** 279–287. [226, 227]
Bush, W. B., and Fendell, F. E. (1972). Asymptotic analysis of turbulent channel and boundary-layer flow. *J. Fluid Mech.* **56,** 657–681. [227]
Cabannes, H. (1951). Étude de l'onde de choc attachée dans les écoulements de révolution. *Rech. Aéro.* No. 24, pp. 17–23. [9, 39]
Cabannes, H. (1953). Études du départ d'un obstacle dans un fluide au repos. *Rech. Aéro.* No. 36, pp. 7–12. [40]
Cabannes, H. (1956). Tables pour la détermination des ondes de choc détachées. *Rech. Aéro.* No. 49, pp. 11–15. [39]
Carrier, G. F. (1954). Boundary layer problems in applied mathematics. *Comm. Pure Appl. Math.* **7,** 11–17. [119]
Carrier, G. F. *See* Lewis and Carrier.
Carrier, G. F., and Lin, C. C. (1948). On the nature of the boundary layer near the leading edge of a flat plate. *Quart. Appl. Math.* **6,** 63–68. [39, 212, 231]
Casten, R. G. *See* Lagerstrom and Casten.
Chang, G.-Z. *See* Dennis and Chang.
Chang, I. D. (1961). Navier-Stokes solutions at large distances from a finite body. *J. Math. Mech.* **10,** 811–876. [38, 41, 41, 75, 78, 131, 132, 165, 248]
Cheng, H., and Wu, T. T. (1970). An aging spring. *Studies Appl. Math.* **49,** 183–185. [242]
Cheng, H. K. (1962). Hypersonic flows past a yawed circular cone and other pointed bodies. *J. Fluid Mech.* **12,** 169–191. [195]
Chester, W. (1956a). Supersonic flow past a bluff body with a detached shock. Part I. Two-dimensional body. *J. Fluid Mech.* **1,** 353–365. [29]
Chester, W. (1956b). Supersonic flow past a bluff body with a detached shock. Part II. Axisymmetrical body. *J. Fluid Mech.* **1,** 490–496. [6]
Chester, W. (1960). The propagation of shock waves along ducts of varying cross section. *Advances in Appl. Mech.* **6,** 119–152. [3]
Chester, W. (1962). On Oseen's approximation. *J. Fluid Mech.* **13,** 557–569. [161]
Chester, W., and Breach, D. R. (1969). On the flow past a sphere at low Reynolds number. *J. Fluid Mech.* **37,** 751–760. [221, 234, 236]
Chow, R. R., and Ting, L. (1961). Higher order theory of curved shock. *J. Aerospace Sci.* **28,** 428–430. [78]
Chow, R. *See* Melnik and Chow.
Cochran, J. (1962). *A New Approach to Singular Perturbation Problems.* Ph.D. Dissertation. Stanford Univ. [198, 200]
Cohen, D. *See* Jones and Cohen.

Cole, J. D. (1957). Newtonian flow theory for slender bodies. *J. Aeronaut. Sci.* **24,** 448–455. [22, 22]
Cole, J. D. (1968). *Perturbation Methods in Applied Mathematics.* Blaisedell, Waltham, Mass. [xi, 226, 226, 241]
Cole, J. D. *See* Lagerstrom and Cole.
Cole, J. D., and Kevorkian, J. (1963). Uniformly valid asymptotic approximations for certain non-linear differential equations. *Nonlinear Differential Equations and Nonlinear Mechanics,* (J. P. LaSalle and S. Lefschetz, eds.), pp. 113–120. Academic Press, New York. [198]
Cole, J. D. and Messiter, A. F. (1957). Expansion procedures and similarity laws for transonic flow. I. Slender bodies at zero incidence. *Z. Angew. Math. Phys.* **8,** 1–25. [78]
Coles, D. (1957). The laminar boundary layer near a sonic throat. *Preprints. Heat Transfer Fluid Mech. Inst.,* 1957, pp. 119–137. Stanford Univ. Press, Stanford, California. [77]
Collins, W. M., and Dennis, S. C. R. (1973a). The initial flow past an impulsively started cylinder. *Quart. J. Mech. Appl. Math.* **26,** 53–75. [219, 219]
Collins, W. M., and Dennis, S. C. R. (1973b). Flow past an impulsively started circular cylinder. *J. Fluid Mech.* **60,** 105–127. [219]
Comstock, C. (1972). The Poincaré-Lighthill perturbation technique and its generalizations. *SIAM Rev.* **14,** 433–446. [228]
Coutanceau, M. *See* Payard and Coutanceau.
Crane, L. J. (1959). A note on Stewartson's paper "On asymptotic expansions in the theory of boundary layers." *J. Math. and Phys.* **38,** 172–174. [229]
Crighton, D. G., and Leppington, F. G. (1973). Singular perturbation methods in acoustics: diffraction by a plate of finite thickness. *Proc. Roy. Soc. Ser. A* **335,** 313–339. [220, 221]
Crocco, L. (1972). Coordinate perturbation and multiple scale in gasdynamics. *Phil. Trans. Roy. Soc. A* **272,** 275–301. [217, 230]
Curle, N. (1956). Unsteady two-dimensional flows with free boundaries. I. General theory. II. The incompressible inviscid jet. *Proc. Roy. Soc. Ser. A* **235,** 375–395. [41]
Davey, A. (1961). Boundary-layer flow at a saddle point of attachment. *J. Fluid Mech.* **10,** 593–610. [217]
Davis, R. T. (1972). Numerical solution of the Navier-Stokes equations for symmetric laminar incompressible flow past a parabola. *J. Fluid Mech.* **51,** 417–433. [238]
Davis, R. T. (1974). A study of the use of optimal coordinates in the solution of the Navier-Stokes equations. *Rept. Dept. Aerospace Eng. Univ. Cincinnati* No. AFL 74-12-14. [233]
Davis, R. T. *See* Werle and Davis.
Davis, R. T., and Werle, M. J. (1972). Numerical solutions for laminar incompressible flow past a paraboloid of revolution. *AIAA J.* **10,** 1224–1230. [223, 239]
Dennis, S. C. R. *See* Collins and Dennis.
Dennis, S. C. R., and Chang, G.-Z. (1969). Numerical integration of the Navier-Stokes equations for steady two-dimensional flow. *Phys. Fluids, Suppl. II,* **12,** 88–93. [231]
Dennis, S. C. R., and Dunwoody, J. (1966). The steady flow of a viscous fluid past a flat plate. *J. Fluid Mech.* **24,** 577–595. [231]
Dennis, S. C. R., and Walker, J. D. A. (1971). Calculation of the steady flow past a sphere at low and moderate Reynolds numbers. *J. Fluid Mech.* **48,** 771–789. [234, 236]
Dennis, S. C. R., and Walsh, J. D. (1971). Numerical solutions for steady symmetric viscous flow past a parabolic cylinder in a uniform stream. *J. Fluid Mech.* **50,** 801–814. [238]
Dijkstra, D. (1974). The solution of the Navier-Stokes equations near the trailing edge of a flat plate. Doctoral Dissertation. Univ. Groningen. Nova Press, Groningen. [231]
Dijkstra, D. *See* Botta and Dijkstra; Botta, Dijkstra, and Veldman; van de Vooren and Dijkstra.
Dingle, R. B. (1973). *Asymptotic Expansions: Their Derivation and Interpretation.* Academic Press, London and New York. [237]

Domb, C., and Sykes, M. F. (1957). On the susceptibility of a ferromagnetic above the Curie point. *Proc. Roy. Soc. Ser. A* **240,** 214–228. [246]

Donov, A. E. (1939). A flat wing with sharp edges in a supersonic stream. *N.A.C.A. Tech. Memo.* No. 1394 (1956); transl. from *Izv. Akad. Nauk SSSR,* 603–626. [218]

Dorrepaal, M., Ranger, K. B., and O'Neill, M. E. (1975). Stokes flow past a body with a re-entry region. To be published. [235]

Dunwoody, J. *See* Dennis and Dunwoody.

Eckhaus, W. (1973). *Matched Asymptotic Expansions and Singular Perturbations.* North Holland, Amsterdam and London; American Elsevier, New York. [xi]

Enlow, R. L. *See* Messiter and Enlow.

Erdélyi, A. (1956). *Asymptotic Expansions.* Dover, New York. [26, 33]

Erdélyi, A. (1961). An expansion procedure for singular perturbations. *Atti Accad. Sci. Torino Cl. Sci. Fis. Mat. Nat.* **95,** 651–672. [84]

Fendell, F. E. *See* Bush and Fendell.

Feo, A. *See* Adamson and Feo.

Ferri, A. (1950). Supersonic flow around circular cones at angles of attack. *Tech. Note N.A.C.A.* No. 2236. [83]

Ferri, A., Ness, N., and Kaplita, T. T. (1953). Supersonic flow over conical bodies without axial symmetry. *J. Aeronaut. Sci.* **20,** 563–571. [9]

Filon, L. G. N. (1928). On the second approximation to the "Oseen" solution for the motion of a viscous fluid. *Phil. Trans. Roy. Soc. A* **227,** 93–135. [247]

Fraenkel, L. E. (1969a). On the method of matched asymptotic expansions. Part I: A matching principle. *Proc. Camb. Phil. Soc.* **65,** 209–231. [220, 221, 222, 235]

Fraenkel, L. E. (1969b). On the method of matched asymptotic expansions. Part II: Some applications of the composite series. *Proc. Camb. Phil. Soc.* **65,** 233–261. [220, 220, 221]

Fraenkel, L. E. (1969c). On the method of matched asymptotic expansions. Part III: Two boundary-value problems. *Proc. Camb. Phil. Soc.* **65,** 263–284. [220, 220, 221, 222]

Fraenkel, L. E., and Watson, R. (1964). The formulation of a uniform approximation for thin conical wings with sonic leading edges. *Proc. Symp. Transsonicum* (K. Oswatitsch, ed.), pp. 249-263. Springer-Verlag, Berlin. [78]

Friedrichs, K. O. (1942). Theory of viscous fluids. *Fluid Dynamics,* Chapter 4. Brown Univ. [79]

Friedrichs, K. O. (1948). Formation and decay of shock waves. *Comm. Pure Appl. Math.* **1,** 211–245. [111]

Friedrichs, K. O. (1953). *Special Topics in Fluid Dynamics,* pp. 120–130. New York Univ. [77, 168]

Friedrichs, K. O. (1954). *Special Topics in Analysis.* New York Univ. [77]

Friedrichs, K. O. (1955). Asymptotic phenomena in mathematical physics. *Bull. Amer. Math. Soc.* **61,** 485–504. [45]

Garabedian, P. R. (1956). Calculation of axially symmetric cavities and jets. *Pacific J. Math.* **6,** 611–684. [3, 23]

Gaunt, D. S., and Guttmann, A. J. (1974). Series expansions: analysis of coefficients. *Phase Transitions and Critical Phenomena,* (C. Domb and M. S. Green, eds.) **3.** Academic Press, New York. [247, 247]

Germain, P. (1967). Recent evolution in problems and methods in aerodynamics. *J. Roy. Aeronaut. Soc.* **71,** 673–691. [240]

Germain, P., and Guiraud, J.-P. (1960). Conditions de choc dans un fluide doué de coefficients de viscosité et de conductibilité thermique faibles mais non nuls. *C. R. Acad. Sci. Paris* **250,** 1965–1967. [78]

Germain, P., and Guiraud, J.-P. (1962). Conditions de choc et structure des ondes de choc dans un écoulement stationnaire de fluide dissipatif. *O.N.E.R.A. Publ.* No. 105. [78]

Goldstein, S. (1929). The steady flow of viscous fluid past a fixed spherical obstacle at small Reynolds numbers. *Proc. Roy. Soc. Ser. A* **123,** 225–235. [5, 156]

Goldstein, S. (1930). Concerning some solutions of the boundary layer equations in hydrodynamics. *Proc. Camb. Phil. Soc.* **26,** 1–30. [230]

Goldstein, S. (1933). On the two-dimensional steady flow of a viscous fluid behind a solid body.—I. *Proc. Roy. Soc. Ser. A* **142,** 545–562. [229]

Goldstein, S., ed. (1938). *Modern Developments in Fluid Dynamics.* Oxford Univ. Press, London and New York. [122, 131, 153]

Goldstein, S. (1948). On laminar boundary-layer flow near a position of separation. *Quart. J. Mech. Appl. Math.* **1,** 43–69. [220, 239, 247]

Goldstein, S. (1956). Flow of an incompressible viscous fluid along a semi-infinite flat plate. *Tech. Rep. Eng. Res. Inst. Univ. Calif.* No. HE-150-144. [29, 77, 139]

Goldstein, S. (1960). *Lectures on Fluid Mechanics.* Wiley (Interscience), New York. [77, 121, 139, 140]

Goldstein, S., and Rosenhead, L. (1936). Boundary layer growth. *Proc. Cambridge Philos. Soc.* **32,** 392–401. [38, 214]

Green, A. E. (1936). The gliding of a plate on a stream of finite depth. Part II. *Proc. Camb. Phil. Soc.* **32,** 67–85. [248]

Grimshaw, R. (1974). Internal gravity waves in a slowly varying, dissipative medium. *Geophys. Fluid Dyn.* **6,** 131–148. [242]

Grossman, B. *See* Melnik and Grossman.

Guiraud, J.-P. (1958). Écoulement hypersonique d'un fluide parfait sur une plaque plane comportant un bord d'attaque d'épaisseur finie. *C. R. Acad. Sci. Paris* **246,** 2842–2845. [182]

Guiraud, J.-P. (1974). Écoulement décollé au voisinage du bord de fuite d'une aile mince tri-dimensionnelle. *J. Mécanique* **13,** 409–432. [232]

Guiraud, J.-P. *See* Germain and Guiraud.

Guttmann, A. J. *See* Gaunt and Guttmann.

Hall, I. M. (1956). The displacement effect of a sphere in a two-dimensional shear flow. *J. Fluid Mech.* **1,** 142–162. [13]

Hamielec, A. E. *See* Pruppacher, Le Clair, and Hamielec.

Hancock, G. J. (1953). The self-propulsion of microscopic organisms through liquids. *Proc. Roy. Soc. Ser. A* **217,** 96–121. [152]

Hantzsche, W. (1943). Die Prandtl-Glauertsche Näherung als Grundlage für ein Iterationsverfahren zur Berechnung Kompressibler Unterschallströmungen. *Z. Angew. Math. Mech.* **23,** 185–199. [5, 29]

Hantzsche, W., and Wendt, H. (1941). Die laminare Grenzschicht an einem mit Überschallgeschwindigkeit angeströmten nicht angestellten Kreiskegel. *Jahrbuch der deutschen Luftfahrtforschung* **1,** 76–77. The laminar boundary layer on a circular cone at zero incidence in a supersonic stream. *Rep. and Trans., British M.A.P. (English Transl.)* No. 276 [9]

Hayes, W. D. (1954). Pseudotransonic similitude and first-order wave structure. *J. Aeronaut. Sci.* **21,** 721–730. [106, 107, 108]

Hayes, W. D. (1955). Second-order pressure law for two-dimensional compressible flow. *J. Aeronaut. Sci.* **22,** 284–286. [76]

Hayes, W. D., and Probstein, R. F. (1959). *Hypersonic Flow Theory.* Academic Press, New York. [3, 22, 22, 123, 185, 185]

Hinch, E. J., and Leal, L. G. (1973). Time-dependent shear flows of a suspension of particles with weak Brownian rotations. *J. Fluid Mech.* **57,** 753–767. [242]

Hoffman, G. H. (1974a). Extension of perturbation series by computer: symmetric subsonic potential flow past a circle. *J. Mécanique* **13,** 433–447. [215]

HOFFMAN, G. H. (1974b). Extension of perturbation series by computer: viscous flow between two infinite rotating disks. *J. Comp. Phys.* **16,** 240–258. [234]
HOOGSTRATEN, H. W. (1967). Uniformly valid approximations in two-dimensional subsonic thin airfoil theory. *J. Eng. Math.* **1,** 51–65. [229]
HOWARTH, L. (1938). On the solution of the laminar boundary layer equations. *Proc. Roy. Soc. Ser. A* **164,** 547–579. [245]
HUNTER, D. L., and BAKER, G. A., JR. (1973). Methods of series analysis. I. Comparison of current methods used in the theory of critical phenomena. *Phys. Rev. B* **7,** 3346–3376. [247]
IMAI, I. (1951). On the asymptotic behaviour of viscous fluid flow at a great distance from a cylindrical body, with special reference to Filon's paradox. *Proc. Roy. Soc. Ser. A* **208,** 487–516. [165, 247]
IMAI, I. (1952). Application of the M^2-expansion method to the subsonic flow of a compressible fluid past a parabolic cylinder. *Proc. 1st Japan Nat. Cong. Appl. Mech.* pp. 349–352. [212]
IMAI, I. (1953). On the asymptotic behaviour of compressible fluid flow at a great distance from a cylinder in the absence of circulation. *J. Phys. Soc. Japan* **8,** 537–544. [41, 41]
IMAI, I. (1957a). Second approximation to the laminar boundary-layer flow over a flat plate. *J. Aeronaut. Sci.* **24,** 155–156. [29, 54, 77, 138, 139, 140, 140, 212]
IMAI, I. (1957b). Theory of bluff bodies. *Tech. Note Inst. Fluid Dynamics and Appl. Math., Univ. Maryland.* No. BN-104. [23]
IMAI, I. *See* Kuwahara and Imai.
IVES, D. C. *See* Melnik and Ives.
JANOUR, Z. (1947). Resistance of a plate in parallel flow at low Reynolds numbers (transl. from Czech.). *N.A.C.A. Tech. Memo.* No. 1316, 1951. [231]
JANSSEN, E. (1958). Flow past a flat plate at low Reynolds numbers. *J. Fluid Mech.* **3,** 329–343. [139]
JEFFREYS, H. (1926). On the relation to physics of the notion of convergence of series. *Philos. Mag.* [7] **2,** 241–244. [30]
JENSON, V. G. (1959). Viscous flow round a sphere at low Reynolds numbers (<40). *Proc. Roy. Soc. Ser. A* **249,** 346–366. [160]
JISCHKE, M. C. (1970). Asymptotic description of radiating flow near stagnation point. *AIAA J.* **8,** 96–101. [228]
JOBE, C. E., and BURGGRAF, O. R. (1974). The numerical solution of the asymptotic equations of trailing edge flow. *Proc. Roy. Soc. Ser. A* **340,** 91–111. [231]
JONES, R. T. (1950). Leading-edge singularities in thin-airfoil theory. *J. Aeronaut. Sci.* **17,** 307–310. [55]
JONES, R. T., and COHEN, D. (1960). *High Speed Wing Theory.* Princeton Univ. Press, Princeton, New Jersey. [46, 48, 168]
JORDAN, P. F. (1971). The parabolic wing tip in subsonic flow. *AIAA paper* No. 71–10; *Air Force Office Sci. Res. Rept.* No. AFOSR-TR-71-0075. [240]
KAPLITA, T. T. *See* Ferri, Ness, and Kaplita.
KAPLUN, S. (1954). The role of coordinate systems in boundary-layer theory. *Z. Angew. Math. Phys.* **5,** 111–135. [64, 77, 84, 140, 145, 232]
KAPLUN, S. (1957). Low Reynolds number flow past a circular cylinder. *J. Math. Mech.* **6,** 595–603. [23, 29, 77, 161, 163, 163, 226, 235, 247]
KAPLUN, S. (1967). *Fluid Mechanics and Singular Perturbations,* (P. A. Lagerstrom, L. N. Howard, and C. S. Liu, eds.) Academic Press, New York and London. [226]
KAPLUN, S., and LAGERSTROM, P. A. (1957). Asymptotic expansions of Navier-Stokes solutions for small Reynolds numbers. *J. Math. Mech.* **6,** 585–593. [77, 156, 161, 226]
KAWAMURA, R., and TSIEN, F. H. (1964). Aerodynamic stability derivatives of axisymmetric body moving at hypersonic speeds. *Proc. 3rd Intern. Cong. Aero. Sci.* Spartan Books, Baltimore. [9]

KELLER, J. B. *See* Rubinow and Keller; Ting and Keller.
KELLY, R. E. (1962). The final approach to steady, viscous flow near a stagnation point following a change in free stream velocity. *J. Fluid Mech.* **13,** 449–464. [41]
KERNEY, K. P. (1971). A theory of the high-aspect-ratio jet flap. *AIAA J.* **9,** 431–435. [241]
KERNEY, K. P. (1972). A correction to "Lifting-line theory as a singular perturbation problem." *AIAA J.* **10,** 1683–1684. [239]
KEVORKIAN, J. (1966). The two variable expansion procedure for the approximate solution of certain nonlinear differential equations. *Lectures in Appl. Math.* **7,** 206–275. Amer. Math. Soc., Providence, Rhode Island. [241]
KEVORKIAN, J. *See* Cole and Kevorkian.
KLEMP, J. B., and ACRIVOS, A. (1972). A note on the laminar mixing of two uniform parallel semi-infinite streams. *J. Fluid Mech.* **55,** 25–30. [248]
KOZLOVA, I. G., and MIKHAILOV, V. V. (1970). Strong viscous interaction on triangular and slipping [yawed] wings. *Mekh. Zhidk. Gaza,* No. 6, 94–99; English transl.: *Fluid Dyn.* **5,** 982–986. [232]
KRIENES, K. (1940). Die elliptische Tragfläche auf potentialtheoretischer Grundlage. *Z. Angew. Math. Mech.* **20,** 65–88. The elliptic wing based on the potential theory. *Tech. Memo. N.A.C.A. (English Transl.)* No. 971. [202, 207]
KUO, Y. H. (1953). On the flow of an incompressible viscous past a flat plate at moderate Reynolds numbers. *J. Math. and Phys.* **32,** 83–101. [100, 136]
KUO, Y. H. (1956). Viscous flow along a flat plate moving at high supersonic speeds. *J. Aeronaut. Sci.* **23,** 125–136. [100]
KUWAHARA, K., and IMAI, I. (1969). Steady, viscous flow within a circular boundary. *Phys. Fluids, Suppl. II,* **12,** 94–101. [234]
LAGERSTROM, P. A. (1957). Note on the preceding two papers. *J. Math. Mech.* **6,** 605–606. [77, 89]
LAGERSTROM, P. A. (1961). Méthodes asymptotiques pour l'étude des équations de Navier-Stokes. Lecture notes, Institut Henri Poincaré, Paris. [226, 226]
LAGERSTROM, P. A. (1964). *Laminar flow theory. High Speed Aerodynamics and Jet Propulsion* (F. K. Moore, ed.) **4,** 20–285. Princeton Univ. Press, Princeton, N.J. [226, 235]
LAGERSTROM, P. A. (1970). Some recent developments in the theory of singular perturbations. *Problems in Analysis: A Symposium in Honor of Salomon Bochner,* 261–271. Princeton Univ. Press, Princeton, N.J. [226]
LAGERSTROM, P. A. (1975). Forms of singular asymptotic expansions. Presented at Conf. on New Directions in Singular Perturbations, Flagstaff, Ariz. To be published in *Rocky Mtn. J. Math.* [221]
LAGERSTROM, P. A. *See* Kaplun and Lagerstrom.
LAGERSTROM, P. A., and CASTEN, R. G. (1972). Basic concepts underlying singular perturbation techniques. *SIAM Rev.* **14,** 63–120. [226, 226]
LAGERSTROM, P. A., and COLE, J. D. (1955). Examples illustrating expansion procedures for the Navier-Stokes equations. *J. Rat. Mech. Anal.* **4,** 817–882. [64, 77, 85, 121, 132, 161, 166]
LAMB, H. (1911). On the uniform motion of a sphere through a viscous fluid. *Philos. Mag.* [6] **21,** 112–121. [155, 164]
LAMB, H. (1932). *Hydrodynamics,* 6th ed. Cambridge Univ. Press, London and New York. [13, 164]
LATTA, G. E. (1951). Singular perturbation problems. Ph.D. Dissertation. Calif. Inst. Tech. [197, 198]
LEAL, L. G. *See* Hinch and Leal.
LE CLAIR, B. P. *See* Pruppacher, Le Clair, and Hamielec.
LEGNER, H. H. (1971). On optimal coordinates and boundary-layer theory. Ph.D. Dissertation. Stanford Univ. [233]

LEGRAS, J. (1951). Application de la méthode de Lighthill à un écoulement plan supersonique. *C. R. Acad. Sci. Paris* **233,** 1005–1008. [100]

LEGRAS, J. (1953). Nouvelles applications de la méthode de Lighthill à l'étude des ondes de choc. *O.N.E.R.A. Publ.* No. 66. [100]

LEIGH, D. C. F. (1955). The laminar boundary-layer equation: a method of solution by means of an automatic computer. *Proc. Camb. Phil. Soc.* **51,** 320–332. [246]

LEPPINGTON, F. G. *See* Crighton and Leppington.

LEVEY, H. C. (1959). The thickness of cylindrical shocks and the PLK method. *Quart. Appl. Math.* **17,** 77–93. [100, 118]

LEVEY, H. C., and MAHONY, J. J. (1968). Resonance in almost linear systems. *J. Inst. Math. Applic.* **4,** 282–294. [242]

LEVINSON, N. (1946). On the asymptotic shape of the cavity behind an axially symmetric nose moving through an ideal fluid. I. *Ann. of Math.* (2) **47,** 704–730. [42]

LEWIS, G. E. (1959). Two methods using power series for solving analytic initial value problems. Ph.D. Thesis. New York Univ. [210]

LEWIS, J. A., and CARRIER, G. F. (1949). Some remarks on the flat plate boundary layer. *Quart. Appl. Math.* **7,** 228–234. [165]

LIBBY, P. A. (1965). Eigenvalues and norms arising in perturbations about the Blasius solution. *AIAA J.* **3,** 2164–2165. [132]

LIBBY, P. A., and FOX, H. (1963). Some perturbation solutions in laminar boundary-layer theory. Part I. The momentum equation. *J. Fluid Mech.* **17,** 433–449. [131]

LIEPMANN, H. W., and PUCKETT, A. E. (1947). *Introduction to Aerodynamics of a Compressible Fluid.* Wiley, New York. [3]

LIGHTHILL, M. J. (1948). The position of the shock-wave in certain aerodynamic problems. *Quart. J. Mech. Appl. Math.* **1,** 309–318. [1, 195]

LIGHTHILL, M. J. (1949a). A technique for rendering approximate solutions to physical problems uniformly valid. *Philos. Mag.* [7] **40,** 1179–1201. [71, 99]

LIGHTHILL, M. J. (1949b). The shock strength in supersonic "conical fields." *Philos. Mag.* [7] **40,** 1202–1223. [100, 177, 179, 180, 196, 229]

LIGHTHILL, M. J. (1951). A new approach to thin aerofoil theory. *Aero. Quart.* **3,** 193–210. [46, 61, 73, 100, 119]

LIGHTHILL, M. J. (1958). On displacement thickness. *J. Fluid Mech.* **4,** 383–392. [134]

LIGHTHILL, M. J. (1961). A technique for rendering approximate solutions to physical problems uniformly valid. *Z. Flugwiss.* **9,** 267–275. [100, 101, 119]

LIN, C. C. (1954). On a perturbation theory based on the method of characteristics. *J. Math. and Phys.* **33,** 117–134. [100, 108]

LIN, C. C. *See* Carrier and Lin.

LIN, T. C., and SCHAAF, S. A. (1951). Effect of slip on flow near a stagnation point and in a boundary layer. *Tech. Note N.A.C.A.* No. 2568. [36]

LINDSTEDT, A. (1882). Beitrag zur Integration der Differentialgleichungen der Störungstheorie. *Abh. K. Akad. Wiss.,* St. Petersburg, **31,** No. 4. [218]

MAHONY, J. J. (1962). An expansion method for singular perturbation problems. *J. Austral. Math. Soc.* **2,** 440–463. [198]

MAHONY, J. J. *See* Levey and Mahony.

MARK, R. M. (1954). Laminar boundary layers on slender bodies of revolution in axial flow. *Tech. Memo. Guggenheim Aeronaut. Lab. Calif. Inst. Tech.* No. 21. [224]

MARTIN, E. D. (1967). Simplified application of Lighthill's uniformization technique using Lagrange expansion formulas. *J. Inst. Math. Applic.* **3,** 16–20. [217]

MATVEEVA, N. S., and SYCHEV, V. V. (1965). On the theory of strong interaction of the boundary layer with an inviscid hypersonic flow. *J. Appl. Math. Mech.* **29,** 770-784. [230]

MEDAN, R. T. (1974). Improvements to the kernel function method of steady, subsonic, lifting surface theory. *NASA TM* No. X-62,327. [219, 240]

MELLOR, G. L. (1972). The large Reynolds number, asymptotic theory of turbulent boundary layers. *Int. J. Eng. Sci.* **10,** 851–873. [227]

MELNIK, R. E. (1965a). A conical thin-shock-layer theory uniformly valid in the entropy layer. *Rep. Air Force Flight Dyn. Lab.* No. FDL-TDR-64-82. [229]

MELNIK, R. E. (1965b). A systematic study of some singular conical flow problems. Ph.D. Dissertation, Polytech. Inst. Brooklyn. [229]

MELNIK, R. E., and CHOW, R. (1975). Asymptotic theory of two-dimensional trailing edge flows. Aerodynamic Analyses Requiring Advanced Computers. *NASA SP* No. 347. [231]

MELNIK, R. E., and GROSSMAN, B. (1974). Analysis of the interaction of a weak normal shock wave with a turbulent boundary layer. *AIAA Paper* No. 74–598. [227]

MELNIK, R. E., and IVES, D. C. (1971). Subcritical flows over two-dimensional airfoils by a multistrip method of integral relations. *Proc. 2nd Internat. Conf. Numer. Methods Fluid Dyn., Berkeley, Calif.,* 1970, *Lecture Notes in Physics* **8,** 243–251. Springer-Verlag, Berlin and New York. [216]

MESSITER, A. F. (1970). Boundary-layer flow near the trailing edge of a flat plate. *SIAM J. Appl. Math.* **18,** 241–257. [230]

MESSITER, A. F. (1975). Laminar separation—a local asymptotic flow description for constant pressure downstream. AGARD Symposium on Separated Flows. To be published. [232]

MESSITER, A. F. *See* Cole and Messiter.

MESSITER, A. F., and ENLOW, R. L. (1973). A model for laminar boundary-layer flow near a separation point. *SIAM J. Appl. Math.* **25,** 655–670. [232]

MIKHAILOV, V. V. *See* Kozlova and Mikhailov.

MILLIKAN, C. B. (1939). A critical discussion of turbulent flows in channels and circular tubes. *Proc. 5th Internat. Cong. Appl. Mech.,* 386–392. Wiley, New York. [227]

MILNE-THOMPSON, L. M. (1960). *Theoretical Hydrodynamics,* 4th ed. Macmillan, New York. [73, 74]

MIYAGI, T. *See* Tamada and Miyagi.

MOTT-SMITH, H. M. (1951). The solution of the Boltzmann equation for a shock wave. *Phys. Rev.* **82,** 885–892. [3]

MUNK, M. M. (1922). General theory of thin wing sections. *Rep. N.A.C.A.* No. 142. [71]

MUNK, M. M. (1929). *Fluid Dynamics for Aircraft Designers.* Ronald Press, New York. [192]

MUNSON, A. G. (1964). The vortical layer on an inclined cone. *J. Fluid Mech.* **20,** 625–643. [87, 196, 201, 229]

MURRAY, J. D. (1961). The boundary layer on a flat plate in a stream with uniform shear. *J. Fluid Mech.* **11,** 309–316. [78, 147]

MURRAY, J. D. (1965). Incompressible viscous flow past a semi-infinite flat plate. *J. Fluid Mech.* **21,** 337–344. [230]

MURRAY, J. D. (1967). A simple method for determining asymptotic forms of Navier-Stokes solutions for a class of large Reynolds number flows. *J. Math. and Phys.* **46,** 1–20. [230]

NAYFEH, A. H. (1973). *Perturbation Methods.* Wiley, New York. [xi, 215, 218, 241]

NAYFEH, A. H., and TSAI, M.-S. (1974). Nonlinear acoustic propagation in two-dimensional ducts. *J. Acoust. Soc. Amer.* **55,** 1166–1172. [242]

NEILAND, V. YA. (1969). Theory of laminar boundary layer separation in supersonic flow. *Mekh. Zhidk. Gaza,* No. 4, 53–57; English transl.: *Fluid Dyn.* **4,** 33–35. [232]

NEILAND, V. YA. (1970). Propagation of perturbation upstream with interaction between a hypersonic flow and a boundary layer. *Mekh. Zhidk. Gaza,* No. 4, 40–49; English transl.: *Fluid Dyn.* **5,** 559–566. [232]

NEILAND, V. YA. (1971). Flow behind the boundary layer separation point in a supersonic stream. *Mekh. Zhidk. Gaza,* No. 3, 19–25; English transl.: *Fluid Dyn.* **6,** 378–384. [232]

NESS, N. *See* Ferri, Ness, and Kaplita.

Olver, F. W. J. (1964). Error bounds for asymptotic expansions, with an application to cylinder functions of large argument. *Asymptotic Solutions of Differential Equations and Their Applications,* (C. A. Wilcox, ed.), 163–183. Wiley, New York. [236]

O'Malley, R. E., Jr. (1968). Topics in Singular Perturbations. *Advances in Math.* **2,** fascicule 4, 365–470. Academic Press, New York and London. [xi]

O'Malley, R. E., Jr. (1974). *Introduction to Singular Perturbations.* Academic Press, New York. [xi]

O'Neill, M. E. *See* Dorrepaal, Ranger, and O'Neill.

Oseen, C. W. (1910). Ueber die Stokes'sche Formel, und über eine verwandte Aufgabe in der Hydrodynamik. *Ark. Math. Astronom. Fys.* **6,** No. 29. [154, 155]

Oswatitsch, K. (1956). *Gas Dynamics.* Academic Press, New York. [15]

Oswatitsch, K. (1962a). Die Wellenausbreitung in der Ebene bei kleinen Störungen. *Arch. Mech. Stos.* **14,** 621–637. [228]

Oswatitsch, K. (1962b). Das Ausbreiten von Wellen endlicher Amplitude. *Zeit. Flugwiss.* **10,** 130–138. [228]

Oswatitsch, K., and Berndt, S. B. (1950). Aerodynamic similarity at axisymmetric transonic flow around slender bodies. *KTH Aero TN 15.* Roy. Inst. Tech., Stockholm. [177, 182]

Oswatitsch, K., and Sjödin, L. (1954). Kegelige Überschallströmung in Schallnähe. *Österreich. Ing.- Arch.* **8,** 284–292. [178]

Payard, M., and Coutanceau, M. (1974). Sur l'étude expérimentale de la naissance et de l'évolution du tourbillon attaché à l'arrière d'une sphère qui se déplace, à vitesse uniforme, dans un fluide visqueux. *C. R. Acad. Sci.* Paris **278,** série B, 369–372. [236]

Pearson, J. R. A. *See* Proudman and Pearson.

Peyret, R. (1970). Étude de l'écoulement d'un fluide conducteur dans un canal par la méthode des échelles multiples. *J. Mécanique* **9,** 61–97. [242]

Poincaré, H. (1892). *Les méthodes nouvelles de la mécanique céleste,* Vol. 1, Chapter 3. Dover, New York. [100]

Prandtl, L. (1905). Über Flüssigkeiten bei sehr kleiner Reibung. *Verh. III Internat. Math. Kongr., Heidelberg,* pp. 484–491. Teubner, Leipzig. Reprinted: *Vier Abhandlungen zur Hydrodynamik und Aerodynamik* (L. Prandtl and A. Betz, eds.). Göttingen, 1927. Motion of fluids with very little viscosity. *Tech. Memo. N.A.C.A. (English Transl.)* No. 452, 1928. [77]

Prandtl, L. (1935). The mechanics of viscous fluids. Division G. *Aerodynamic Theory* (W. F. Durand, ed.), Vol. 3, pp. 34–208. Springer, Berlin. [122, 136]

Prandtl, L., and Tietjens, O. G. (1934). *Applied Hydro- and Aeromechanics.* McGraw-Hill, New York. [55]

Pritulo, M. F. (1962). On the determination of uniformly accurate solutions of differential equations by the method of perturbation of coordinates. *J. Appl. Math. Mech.* **26,** 661–667. [73, 120]

Pritulo, M. F. (1969). The flow past a yawed delta wing. *Fluid Dynamics Transactions,* (W. Fiszdon, P. Kucharcyzk, and W. J. Prosnak, eds.) **4,** 261–275. PWN—Polish Sci. Pubs., Warsaw. [218]

Probstein, R. F. *See* Hayes and Probstein.

Proudman, I., and Pearson, J. R. A. (1957). Expansions at small Reynolds numbers for the flow past a sphere and a circular cylinder. *J. Fluid Mech.* **2,** 237–262. [5, 29, 29, 77, 156, 160, 161, 162, 165, 221, 224, 234, 237, 244]

Pruppacher, H. R., Le Clair, B. P., and Hamielec, A. E. (1970). Some relations between drag and flow pattern of viscous flow past a sphere and a cylinder at low and intermediate Reynolds numbers. *J. Fluid Mech.* **44,** 781–790. [236]

Puckett, A. E. *See* Liepmann and Puckett.

Ranger, K. B. (1972). The applicability of Stokes expansions to reversed flow. *SIAM J. Appl. Math.* **23,** 325–333. [235, 236]

Ranger, K. B. *See* Dorrepaal, Ranger, and O'Neill.

Richey, G. K. *See* Adamson and Richey.

Riley, N., and Stewartson, K. (1969). Trailing edge flows. *J. Fluid Mech.* **39,** 193–207. [232]

Rispin, P. P. (1967). A singular perturbation method for non-linear water waves past an obstacle. Ph.D. Dissertation. Calif. Inst. Tech. [248]

Rao, P. S. (1956). Supersonic bangs. *Aero. Quart.* **7,** 21–44, 135–155. [100]

Rayleigh, Lord (1916). On the flow of a compressible fluid past an obstacle. *Philos. Mag.* [6] **32,** 1–6. [16]

Rosenhead, L., ed. (1963). *Laminar Boundary Layers.* Oxford Univ. Press, London and New York. [122, 130, 131, 131, 136, 162]

Rosenhead, L. *See* Goldstein and Rosenhead.

Rubinow, S. I., and Keller, J. B. (1961). The transverse force on a spinning sphere moving in a viscous fluid. *J. Fluid Mech.* **11,** 447–459. [78]

Saffman, P. G. (1970). The velocity of viscous vortex rings. *Studies Appl. Math.* **49,** 371–380. [248]

Sampson, R. A. (1891). On Stokes's current function. *Phil. Trans. Roy. Soc. Ser. A* **182,** 449–518 (esp. 504). [223]

Schaaf, S. A. *See* Lin and Schaaf.

Schlighting, H. (1960). *Boundary Layer Theory,* 2nd English ed. McGraw-Hill, New York. [1, 18, 19, 130, 214, 214]

Schneider, W. (1973). A note on a breakdown of the multiplicative composition of inner and outer expansions. *J. Fluid Mech.* **59,** 785–789. [227]

Schwartz, L. W. (1974). Computer extension and analytic continuation of Stokes' expansion for gravity waves. *J. Fluid Mech.* **62,** 553–578. [216, 243]

Sears, W. R., and Telionis, D. P. (1975). Boundary-layer separation in unsteady flow. *SIAM J. Appl. Math.* **28,** 215–235. [219]

Serbin, H. (1958). The high speed flow of gas around blunt bodies. *Aero. Quart.* **9,** 313–330. [23]

Shanks, D. (1955). Non-linear transformations of divergent and slowly convergent sequences. *J. Math. and Phys.* **34,** 1–42. [5, 202, 205]

Sheer, A. F. (1971). A uniformly asymptotic solution for incompressible flow past thin sharp-edged aerofoils at zero incidence. *Proc. Camb. Phil. Soc.* **70,** 135–155. [224]

Simasaki, T. (1956). On the flow of a compressible fluid past a circular cylinder. II. *Bull. Univ. Osaka Prefecture Ser. A.* **4,** 27–35. [4, 214]

Sjödin, L. *See* Oswatitsch and Sjödin.

Skinner, L. A. (1975). Generalized expansions for slow flow past a cylinder. *Quart. J. Mech. Appl. Math.* **28,** part 3. [218, 236, 237]

Spreiter, J. R. (1953). On the application of transonic similarity rules to wings of finite span. *Rep. N.A.C.A.* No. 1153. [22]

Spreiter, J. R. (1959). Aerodynamics of wings and bodies at transonic speeds. *J. Aerospace Sci.* **26,** 465–487. [3]

Stewartson, K. (1956). On the steady flow past a sphere at high Reynolds number using Oseen's approximation. *Philos. Mag.* [8] **1,** 345–354. [210]

Stewartson, K. (1957). On asymptotic expansions in the theory of boundary layers. *J. Math. and Phys.* **36,** 173–191. [29, 131, 131, 132, 201, 229]

Stewartson, K. (1958). On Goldstein's theory of laminar separation. *Quart. J. Mech. Appl. Math.* **11,** 399–410. [220, 247]

Stewartson, K. (1961). Viscous flow past a quarter-infinite plate. *J. Aerospace Sci.* **28,** 1–10. [201]

Stewartson, K. (1968). On the flow near the trailing edge of a flat plate. *Proc. Roy. Soc. Ser. A* **306,** 275–290. [231]

Stewartson, K. (1969). On the flow near the trailing edge of a flat plate II. *Mathematika* **16,** 106–121. [230]

Stewartson, K. (1974). Multistructured boundary layers on flat plates and related bodies. *Adv. Appl. Mech.* **14,** 145–239. [232]

STEWARTSON, K. *See* Brown and Stewartson; Riley and Stewartson.

STEWARTSON, K., and WILLIAMS, P. G. (1969). Self-induced separation. *Proc. Roy. Soc. Ser. A* **312,** 181–206. [232]

STOKER, J. J. (1957). *Water Waves.* Wiley (Interscience), New York. [42]

STOKES, G. G. (1851). On the effect of the internal friction of fluids on the motion of pendulums. *Trans. Camb. Phil. Soc.* **9,** Part II, 8–106. Reprinted: *Math. and Phys. Papers* **3,** 1–141. Cambridge Univ. Press. [152]

STONE, A. H. (1948). On supersonic flow past a slightly yawing cone. *J. Math. and Phys.* **27,** 67–81. [9]

STUFF, R. (1972). Closed form solution for the sonic boom in a polytropic atmosphere. *J. Aircraft* **9,** 556–562. [229]

SYCHEV, V. V. (1962). On the method of small disturbances in the problem of the hypersonic gas flow over thin blunted bodies (Russian). *Zh. Prikl. Mekh. i Tekh. Fiz.* No. 6, 50–59. Grumman Aircraft Eng. Corp., Res. Dept., English Transl. TR-25. [192]

SYCHEV, V. V. (1972). [On] laminar separation. *Mekh. Zhidk. Gaza,* No. 3, 47–59; English transl.: *Fluid Dyn.* **7,** 407–417. [232]

SYCHEV, V. V. *See* Matveeva and Sychev.

SYKES, M. F. *See* Domb and Sykes.

TAMADA, K. and MIYAGI, T. (1962). Laminar viscous flow past a flat plate set normal to the stream, with special reference to high Reynolds numbers. *J. Phys. Soc. Japan* **17,** 373–390. [29]

TANEDA, S. (1956). Studies on wake vortices (III). Experimental investigation of the wake behind a sphere at low Reynolds numbers. *Rep. Res. Inst. Appl. Mech. Kyushu Univ.* **4,** 99–105. [160]

TELIONIS, D. P. *See* Sears and Telionis.

TELIONIS, D. P., and TSAHALIS, D. TH. (1973). Unsteady laminar separation over cylinders started impulsively from rest. Presented at 24th Internat. Astronaut. Cong., Baku. To be published in *Acta Astronautica.* [219]

TERRILL, R. M. (1973). On some exponentially small terms arising in flow through a porous pipe. *Quart. J. Mech. Appl. Math.* **26,** 347–354. [237]

THURBER, J. K. (1961). An asymptotic method for determining the lift distribution of a swept-back wing of finite span. Ph.D. Dissertation. New York Univ.

THURBER, J. K. (1965). An asymptotic method for determining the lift distribution of a swept-back wing of finite span. *Comm. Pure Appl. Math.* **18,** 733–756. [241]

THWAITES, B., ed. (1960). *Incompressible Aerodynamics.* Oxford Univ. Press, London and New York. [46]

TIETJENS, O. G. *See* Prandtl and Tietjens.

TIFFORD, A. N. (1954). Heat transfer and frictional effects in laminar boundary layers. Part 4. Universal series solutions. *Tech. Rep., Wright Air Dev. Center* No. 53-288. [6, 18]

TING, L. (1959). On the mixing of two parallel streams. *J. Math. and Phys.* **38,** 153–165. [77, 248]

TING, L. (1960). Boundary layer over a flat plate in presence of shear flow. *Phys. Fluids* **3,** 78–81. [78]

TING, L. (1968). Asymptotic solutions of wakes and boundary layers. *J. Eng. Math.* **2,** 23–38. [230]

TING, L. *See* Chow and Ting; Tung and Ting.

TING, L. and KELLER, J. B. (1974). Planing of a flat plate at high Froude number. *Phys. Fluids* **17,** 1080–1086. [248]

TOKUDA, N. (1971). An asymptotic theory of the jet flap in three dimensions. *J. Fluid Mech.* **46,** 705–726. [241]

TOMOTIKA, S., and AOI, T. (1950). The steady flow of viscous fluid past a sphere and circular cylinder at small Reynolds numbers. *Quart. J. Mech. Appl. Math.* **3,** 140–161. [152, 156, 164, 165]

TRAUGOTT, S. C. (1962). Evaluation of indeterminate second-order effects for the Rayleigh problem. *Phys. Fluids* **5,** 1125–1126. [54]

TRITTON, D. J. (1959). Experiments on the flow past a circular cylinder at low Reynolds numbers. *J. Fluid Mech.* **6,** 547–567. [164]

TSAHALIS, D. T. *See* Telionis and Tsahalis.

TSAI, M.-S. *See* Nayfeh and Tsai.

TSIEN, F. H. *See* Kawamura and Tsien.

TSIEN, H. S. (1956). The Poincaré-Lighthill-Kuo method. *Advances in Appl. Mech.* **4,** 281–349. [100]

TUNG, C., and TING, L. (1967). Motion and decay of a vortex ring. *Phys. Fluids* **10,** 901–910. [248]

UNDERWOOD, R. L. (1969). Calculation of incompressible flow past a circular cylinder at moderate Reynolds numbers. *J. Fluid Mech.* **37,** 95–114. [236]

USHER, P. D. (1968). Coordinate stretching and interface location. II. A new PL expansion. *J. Comp. Phys.* **3,** 29–39. [217]

VAN DE VOOREN, A. I. *See* Veldman and van de Vooren.

VAN DE VOOREN, A. I., and DIJKSTRA, D. (1970). The Navier-Stokes solution for laminar flow past a semi-infinite flat plate. *J. Eng. Math.* **4,** 9–27. [230]

VAN DYKE, M. D. (1951). The combined supersonic-hypersonic similarity rule. *J. Aeronaut. Sci.* **18,** 499–500. [22]

VAN DYKE, M. D. (1952). A study of second-order supersonic flow theory. *Rep. N.A.C.A.* No. 1081. [36, 75, 107, 111, 179]

VAN DYKE, M. D. (1954). Subsonic edges in thin-wing and slender-body theory. *Tech. Note N.A.C.A.* No. 3343. [119]

VAN DYKE, M. D. (1956). Second-order subsonic airfoil theory including edge effects. *Rep. N.A.C.A.* No. 1274. [49]

VAN DYKE, M. D. (1958a). The similarity rules for second-order subsonic and supersonic flow. *Rep. N.A.C.A.* No. 1374. [212]

VAN DYKE, M. D. (1958b). A model of supersonic flow past blunt axisymmetric bodies with application to Chester's solution. *J. Fluid Mech.* **3,** 515–522. [203, 208, 209, 210]

VAN DYKE, M. D. (1958c). The paraboloid of revolution in subsonic flow. *J. Math. and Phys.* **37,** 38–51. [75, 213]

VAN DYKE, M. D. (1959). Second-order slender-body theory—axisymmetric flow. *Tech. Rep. N.A.S.A.* No. R-47. [74]

VAN DYKE, M. D. (1962a). Higher approximations in boundary-layer theory. Part. 1. General analysis. *J. Fluid Mech.* **14,** 161–177. [29, 135, 136]

VAN DYKE, M. D. (1962b). Higher approximations in boundary-layer theory. Part 2. Application to leading edges. *J. Fluid Mech.* **14,** 481–495. [124]

VAN DYKE, M. D. (1964a). Higher approximations in boundary-layer theory. Part 3. Parabola in uniform stream. *J. Fluid Mech.* **19,** 145–159. [6, 39, 204, 208, 211]

VAN DYKE, M. D. (1964b). Lifting-line theory as a singular perturbation problem. *Arch. Mech. Stos.* **16,** No. 3. [173]

VAN DYKE, M. (1970). Extension of Goldstein's series for the Oseen drag of a sphere. *J. Fluid Mech.* **44,** 365–372. [216, 243]

VAN DYKE, M. (1974). Analysis and improvement of perturbation series. *Quart. J. Mech. Appl. Math.* **27,** 423–450. [243, 247]

VAN DYKE, M. (1975). Computer extension of perturbation series in fluid mechanics. *SIAM J. Appl. Math.* **28,** 720–734. [215]

VAN DYKE, M. (1976). Extension, analysis, and improvement of perturbation series. *Proc. 10th Naval Hydrodynamics Symposium, 1974.* To be published. [215, 243]

VAN TUYL, A. (1959). The use of rational approximations in the calculation of flows with detached shocks. *Rep. U. S. Naval Ord. Lab.* No. 6679. [209]

VAN TUYL, A. (1960). The use of rational approximations in the calculation of flows with detached shocks. *J. Aerospace Sci.* **27,** 559–560. [206]

VELDMAN, A. E. P. (1973). The numerical solution of the Navier-Stokes equations for laminar incompressible flow past a paraboloid of revolution. *Computers and Fluids* **1**, 251–271. [218, 223, 239]
VELDMAN, A. E. P. *See* Botta, Dijkstra, and Veldman.
VELDMAN, A. E. P., and VAN DE VOOREN, A. I. (1974). Drag of a finite flat plate. *Proc. 4th Internat. Conf. Numer. Methods Fluid Dyn., Boulder, Colo., Lecture Notes in Physics* **35**, 423–430. Springer-Verlag, Berlin and New York. [231]
VINCENTI, W. G. (1959). Non-equilibrium flow over a wavy wall. *J. Fluid Mech.* **6**, 481–496. [193]
VIVIAND, H., and BERGER, S. A. (1964). Incompressible laminar axisymmetric near wake behind a very slender cylinder in axial flow. *Rep. Inst. Eng. Res. Univ. Calif.* No. As 64-5; *AIAA J.* **3** (1965) 1806–1812. [218]
VON DOENHOFF, A. E. *See* Abbott and von Doenhoff.
VON KÁRMÁN, T. (1947). The similarity law of transonic flow. *J. Math. and Phys.* **26**, 182–190. [21]
VON KÁRMÁN, T., and BURGERS, J. M. (1935). General aerodynamic theory—perfect fluids. Division E. *Aerodynamic Theory* (W. F. Durand, ed.), Vol. 2. Springer, Berlin. [56]
WALKER, J. D. A. *See* Dennis and Walker.
WALSH, J. D. *See* Dennis and Walsh.
WARD, G. N. (1955). *Linearized Theory of Steady High-Speed Flow.* Cambridge Univ. Press, London and New York. [42, 176]
WASOW, W. (1955). On the convergence of an approximation method of M. J. Lighthill. *J. Rat. Mech. Anal.* **4**, 751–767. [101]
WEISSINGER, J. *See* Bollheimer and Weissinger.
WENDT, H. (1948). Die Jansen-Rayleighsche Näherung zur Berechnung von Unterschallströmungen. *Sitzsber. Heidelberg. Akad. Wiss., Math.-Naturwiss. Kl.*, 1948 **7**, 147–170. [4]
WENDT, H. *See* Hantzsche and Wendt.
WERLE, M. J. *See* Davis and Werle.
WERLE, M. J., and DAVIS, R. T. (1972). Incompressible laminar boundary layers on a parabola at angle of attack: a study of the separation point. *J. Appl. Mech.* **39**, 7–12. [239]
WEYL, H. (1942). On the differential equations of the simplest boundary-layer problems. *Ann. of Math.* **43**, 381–407. [131]
WHITEHEAD, A. N. (1889). Second approximations to viscous fluid motion. *Quart. J. Math.* **23**, 143–152. [153]
WHITHAM, G. B. (1952). The flow pattern of a supersonic projectile. *Comm. Pure Appl. Math.* **5**, 301–348. [100, 111, 113, 116]
WHITHAM, G. B. (1953). The propagation of weak spherical shocks in stars. *Comm. Pure Appl. Math.* **6**, 397–414. [100]
WILKINSON, J. (1955). A note on the Oseen approximation for a paraboloid in a uniform stream parallel to its axis. *Quart. J. Mech. Appl. Math.* **8**, 415–421. [165]
WILLIAMS, P. G. *See* Stewartson and Williams.
WU, T. T. *See* Cheng and Wu.
WU, Y. T. (1956). Two dimensional sink flow of a viscous, heat-conducting, compressible fluid; cylindrical shock waves. *Quart. Appl. Math.* **13**, 393–418. [100]
YAJNIK, K. S. (1970). Asymptotic theory of turbulent shear flows. *J. Fluid Mech.* **42**, 411–427. [227]
YAKURA, J. K. (1962). Theory of entropy layers and nose bluntness in hypersonic flow. *Hypersonic Flow Research* (F. R. Riddell, ed.), pp. 421–470. Academic Press, New York, [9, 78, 183, 189, 191]
YAMADA, H. (1954). On the slow motion of viscous liquid past a circular cylinder. *Rep. Res. Inst. Appl. Mech. Kyushu Univ.* **3**, 11–23. [156]
YOSHIZAWA, A. (1970). Laminar viscous flow past a semi-infinite flat plate. *J. Phys. Soc. Japan* **28**, 776–779. [230]

SUBJECT INDEX

Corrections to Annotated Edition (1975) of

PERTURBATION METHODS IN FLUID MECHANICS

as of January 1977

Page	Line (*: from bottom)	Correction
xi	14*	Change "error" to "errors."
xii	3*	Change "Knuffmann" to "Kaufmann."
73 74	5* 5	Change "Milne-Thompson" to "Milne-Thomson."
75	1*	Add minus sign: $C_p = -2\varepsilon\phi_{1x} - \ldots$
103	2	Change to $(sf_2)' = -\left[\frac{(1+s)^2}{2s^2} + \ldots\right.$
208	4	Change "fractions" to "fraction."
240	1*	Add parenthesis to eq. number: (N.31)
245	1*	Change to subscript: $\left\vert\frac{c_{n-1}}{c_n}\right\vert$
248	13*	Change p. 253 to p. 523.
257	27	Change to MILNE-THOMSON.
259	1-3	Put references to RICHEY, RILEY, and RISPIN in correct alphabetical order following RAYLEIGH.
259	17	Change SCHLIGHTING to SCHLICHTING.
259	18*	After "part 3" add ", 333-340."
261	13*	After "Stos. 16, No. 3" add "; Appl. Math. & Mech. 28, 90-101."
262	20*	After "Quart. J." add "Pure Appl."

Please send other corrections, no matter how trivial, to Milton Van Dyke, Division of Applied Mechanics, Stanford University, Stanford, CA 94305, USA.